AN ABSTRACT OF THE THESIS OF

Paul Roland Carlson (Name of student) for the Ph. D. (Degree)

in Oceanography (Major) presented on June 2, 1967 (Date)

Title: Marine Geology of Astoria Submarine Canyon

Redacted for privacy

Abstract approved: John V. Byrne

Astoria Submarine Canyon begins nine miles west of the Columbia River at a depth of 55 fathoms and winds sinuously southwestward across the continental terrace for a distance of 65 miles to a depth of 1140 fathoms. At this depth the canyon hooks sharply to the left and the morphologic characteristics change to those of a deep-sea channel (Astoria Channel) which continues across Astoria Fan. Eight distributary-like channels radiate across the fan from the mouth of Astoria Canyon.

This canyon has U- to V-shaped transverse profiles, high, fairly steep walls with rock outcrops, a winding course and numerous tributaries entering the canyon from both sides. It is more like Willapa and Hudson Canyons in morphology and sediment type than any of the other submarine canyons that have been studied in any detail. Between the head of Astoria Canyon and the mouth of the Columbia River, several buried channels have been detected which

suggest the importance of the Columbia River in cutting or at least shaping the head of the canyon during lower stands of sea level.

Based on the estimated volume of sediments of Astoria Fan and the sediments contributed by the Columbia River and by littoral transport, an age of late Pliocene to early Pleistocene is hypothesized for the inception of the Astoria Canyon-Fan system. Turbidity currents, bottom currents, mass movements and the burrowing actions of benthic organisms were important agents of submarine erosion. Step-like offsets of the canyon's axial trend plus offset sedimentary basins north and south of the canyon suggest the influence of tectonic activity on the location and orientation of the canyon.

The sediments and semi-consolidated sediments of the canyon area are of late Pliocene to Recent age. Coarse layers which range in mean particle size from fine sand to medium silt are more abundant deep in the canyon floor sediments than at the surface, suggesting a greater influx of turbidity currents during the Pleistocene than in postglacial time. These coarse layers are poorly sorted, graded and contain displaced shallow water benthic foraminifers. The mineralogy of these coarse layers closely resembles the mineralogy of Columbia River sediments, a fact which emphasizes the importance of the sediment contributions of this river. The surface sediments in the canyon area range from sandy muds high in plant fragments near the canyon head to hemi-pelagic silty clays at the lower end of

the canyon. Along the rim of the canyon near the edge of the shelf, relict sands which have textural characteristics similar to inner shelf sands occur in patches at the surface. At the outer edge of the shelf and on the upper slope, glauconite makes up a significant part of the sediment.

Although Astoria Canyon was an important route for turbidity currents during the Pleistocene, it no longer functions in this role. Since the last rise of sea level when the zone of longshore transport moved eastward of the present canyon head, Astoria Canyon has been filling. Rates of deposition in the canyon area, based on radiocarbon dates, occurrence of Mazama volcanic glass, and changes in the ratio of radiolarians to planktonic foraminifers, range from 10 cm/1000 yrs in tributaries to more than 50 cm/1000 yrs in tributaries to more than 50 cm/1000 yrs on the canyon floor which, if unchanged, could fill the canyon in less than eight million years.

Canyon geometry, facies relationships and sediment characteristics of modern submarine canyons are criteria useful in the identification of canyons in the geologic record.

Marine Geology of Astoria Submarine Canyon

by

Paul Roland Carlson

A THESIS

submitted to

Oregon State University

in partial fulfillment of
the requirements for the
degree of

Doctor of Philosophy

June 1968

APPROVED:

Redacted for privacy

Professor of Oceanography
in charge of major

Redacted for privacy

Chairman of Department of Oceanography

Redacted for privacy

Dean of Graduate School

Date thesis is presented June 2, 1967

Typed by Opal Grossnicklaus for Paul Roland Carlson

ACKNOWLEDGEMENTS

This study was made possible through the financial support of the Office of Naval Research (Contract Nonr 1286 (10) and the laboratory and shipboard facilities of the Department of Oceanography, Oregon State University.

The author is indebted to his major professor, Dr. John V. Byrne for his guidance during research and his critical review of the manuscript.

Special thanks are due to Dr. L. D. Kulm for his criticism of portions of the manuscript, numerous enlightening discussions and supplying a radiocarbon date. Thanks also to Dr. K. S. Deffeyes for supplying the other radiocarbon date used in the preparation of this manuscript.

The writer is grateful to Dr. Gerald A. Fowler for his time and effort in identifying many foraminifers and his criticism of a portion of the manuscript. Thanks also to Dr. June G. Pattullo for critically reading a section of the dissertation.

Appreciation is extended to Mrs. Susan Borden who did the computer programming for sediment analyses and Eric Crecelius for running organic carbon and carbonate analyses.

John Galloway provided seven sediment samples from a preliminary drill hole made by the Standard Oil Company of California.

Paul Howell of the Corps of Engineers in Portland made available unpublished data from that office. For this assistance the author is grateful.

Informal discussions with fellow students have been very helpful in the analysing of data and preparing this report. Thanks especially to Hans Nelson, John Duncan, Douglas Manske, Gary Griggs, Richard Boettcher, Richard Couch and Christopher Mooers.

To the personnel of the RV Acona and RV Yaquina and the staff and students aiding in collecting data at sea a sincere thank you is extended.

TABLE OF CONTENTS

TABLE OF CONTENTS (CONTINUED)

TABLE OF CONTENTS (CONTINUED)

LIST OF FIGURES

LIST OF FIGURES (CONTINUED)

LIST OF FIGURES (CONTINUED)

LIST OF TABLES

MARINE GEOLOGY OF ASTORIA SUBMARINE CANYON

I. INTRODUCTION

Submarine canyons have long been a subject of great interest to marine geologists. The origin of these puzzling morphologic features has sparked innumerable controversies for more than 75 years. However, it has only been within the last two score years that man has undertaken detailed studies of these impressive incisions in the continental margin.

Astoria Canyon located off the mouth of the Columbia River is the only major submarine canyon cutting the continental margin off Oregon. The purpose of the investigation of this canyon is three fold: (1) to obtain a detailed morphologic picture of Astoria Canyon and establish its relationships to the Columbia River on the east and Astoria Fan and Channel on the west; (2) to determine the nature and origin of the sediments of the canyon; and (3) to use the bathymetric and sedimentologic data to interpret the origin and history of this significant submarine canyon.

Astoria Canyon heads approximately nine miles west of the Columbia River north jetty. From its inception in water less than 60 fathoms deep the canyon winds southwest across the shelf and slope for 65 nautical miles where it reaches Astoria Fan (Figure 1).

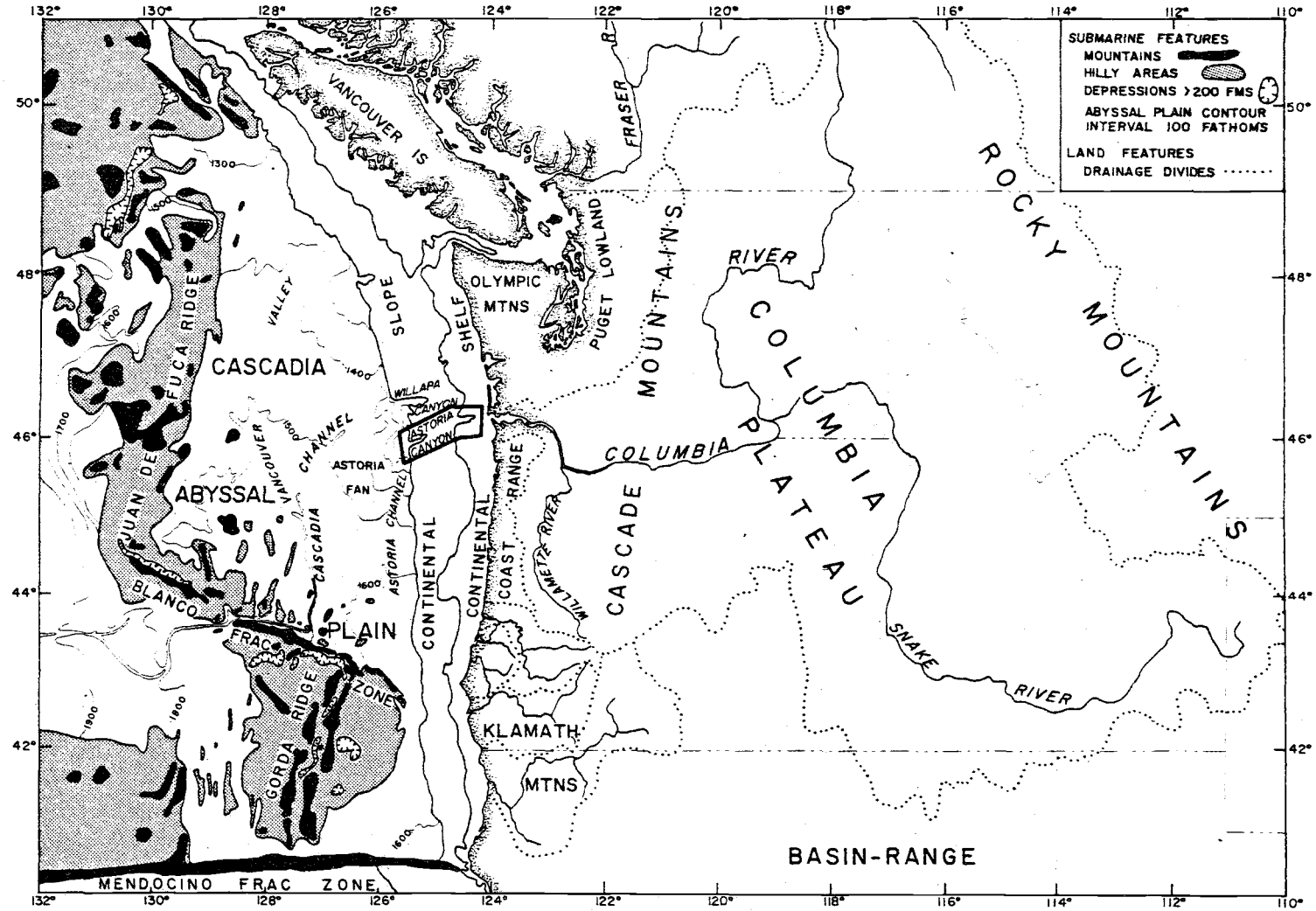

Figure 1. Submarine and continental physiographic features in the vicinity of Astoria Canyon. Area of study is outlined.

Previous Investigations

In 1938 the name Astoria Canyon was first used for this submarine canyon (U.S. Board on Geographic Names, 1938). At approximately the same time Shepard and Beard (1938) applied the name Columbia Canyon to this physiographic feature. Although this latter name seems more apropos to this writer, the name Astoria Canyon is the official name deeply engraved in the literature and on bathymetric charts.

Although unnamed at the time, the first contoured chart of Astoria Canyon was published in an article written by Shepard (1933). More than 40 years prior to this Le Conte (1891) wrote that nothing remarkable was to be found on the ocean floor off the Columbia River.

Bathymetric charts which include Astoria Canyon have been compiled by Hurley (1960), Byrne (1963) and Mc Manus (1964). None of these charts were based on sounding lines with great enough density to permit precise delineation of the terminal end of Astoria Canyon and its relationship to Astoria Channel.

No comprehensive studies of the sediments of Astoria Canyon have been previously undertaken. Runge (1966) analyzed the surface sediments of the continental shelf in the canyon area. Osterberg, Kulm, and Byrne (1963) reported on the radioactivity of surface sediments off the mouth of the Columbia River, and a similar study

was made by Gross and Nelson (1966).

The sediments of Willapa Canyon, a few miles north of Astoria Canyon, have been investigated by Royse (1964). It is the only canyon near Astoria Canyon that has been studied in detail. Numerous other canyons throughout the world have been investigated to various degrees. Shepard and Dill (1966) have summarized most of these investigations.

Regional Geology

The Columbia River drains four of the physiographic provinces outlined by Fenneman (1931). From west to east these are: the Pacific Border, the Sierra-Cascade, the Columbia Plateau, and the Rocky Mountain provinces (Figure 1). Erosional products from each of these areas contribute to the total sediment load of the Columbia River and eventually are carried to the sea.

Pacific Border Province

The northern part of this province is divided into the Coast Ranges on the west and the Puget Sound-Willamette Valley Trough on the east.

The Coast Range of Washington and Oregon extends from the Olympic Mountains in the north to the Klamath Mountains in the south, a distance of 300 miles. They are approximately 40 miles

wide and have a maximum elevation of 4097 feet (Marys Peak). According to Baldwin (1964) the average crestal elevation of this range is 1500 feet.

Snavely and Wagner (1964) reported that the Coast Range anticlinorium consists of some 25,000 feet of Tertiary volcanic and marine sedimentary rocks ranging in age from Eocene to Pliocene. The volcanic rocks are primarily basalt flows; some, as much as 1000 feet thick along the Columbia River, are correlative with Columbia River Basalt (Miocene). Gabbroic, basaltic and dioritic dikes and sills are especially numerous in the central Oregon portion of the Coast Range (Baldwin, 1964).

The Coast Range, which attained its present elevation by late Pliocene time (Snavely and Wagner, 1964), is bordered on the west by a narrow coastal fringe characterized by drowned rivers, sand dunes and elevated terraces. The Coast Range is drained westward by small streams that flow directly into the ocean. Many small streams draining the eastern side of this range empty eventually into the Columbia River.

The structural depression (Baldwin, 1964) referred to as the Puget Sound-Willamette Valley Trough is 350 miles long. It varies in width from more than 50 miles at the northern end occupied by Puget Sound to less than 20 miles for portions of the Willamette River Valley south of the Columbia River. Strata underlying this

depression are primarily Tertiary sedimentary and volcanic rocks. This trough is drained by two main rivers, the Willamette which flows north and the Cowlitz which flows south to intersect the Columbia River.

Sierra-Cascade Province

The Sierra-Cascade province is represented in the Columbia River drainage area by the rugged Cascade Mountains. This range is more than 600 miles long, extending from southern British Columbia to the Sierra Nevada Mountains of California; the average width is 50 to 60 miles. The average crestal elevation of the Cascades is 5000 feet (Baldwin, 1964), but numerous volcanic peaks rise above 10,000 feet with the maximum elevation attained by Mount Rainier (14,410 feet).

Baldwin has divided the Cascades into: (1) the Western Cascades, which consist largely of early Tertiary extrusives (flows and ash falls) and granitic intrusives, and (2) the High Cascades to the east, which contain the majestic composite volcanic cones made up of andesitic flows, ash and breccia. These volcanoes have been built upon flows which according to Turner and Verhoogen (1951) are primarily of basaltic and andesitic composition. Metamorphic rocks are plentiful in the northern Cascades of Washington as a result of folding of ancient sediments and intrusions by granites (Allison, 1962).

Uplift of the Cascade Mountain Range began during the Pliocene and may be continuing yet today (Mackin and Cary, 1965).

Drainage is greater to the west than the east of the Cascade Mountains because of the greater precipitation on the western flanks and the general asymmetric shape of the range. A large part of the Cascades' runoff eventually reaches the Columbia River, thus adding to the complex sediment load that this important river is transporting toward the sea.

Columbia Plateau Province

This region of vast outpourings of flood basalts, in places more than 10,000 feet thick, covers an area of approximately 200,000 square miles (Mackin and Cary, 1965).

The dominant rocks of the Columbia Plateau region are basalt flows primarily of Miocene age which Waters (1961) has divided into two main types: Yakima Basalt which is tholeiitic in composition and olivine basalts of the Picture Gorge type. According to Mackin and Cary (1965) the individual basalt flows vary in thickness from 100 to 800 feet.

The Columbia River and its largest tributary, the Snake River, are the major drainage routes of this province. Evidence of their erosional powers is best shown by the deep gorges they have cut through the basalt flows.

Rocky Mountain Provinces

The Snake River drains the western edge of the Middle Rockies and the Columbia River drains the Northern Rocky Mountain Province. Twenty thousand square miles of the Idaho Rockies are the exposed surface of an immense granitic batholith (Fenneman, 1931). Other major mountains in this province consist of folded and faulted metamorphic and sedimentary rocks.

Columbia River Drainage

This river, having the third largest flow of all rivers in the United States (Highsmith, 1962), drains an area of 259,000 square miles (Figure 1). It begins in the Canadian Rockies and flows south and west 1200 miles to the Pacific Ocean where it discharges annually approximately 180 million acre feet (7.8×10^{12} cubic feet) of water (Lockett, 1965a). June is the time of maximum discharge, sometimes reaching as much as 1,240,000 cfs (cubic feet per second). Peaks of >300,000 cfs occur sporadically during the period of high precipitation from December through March. Minimum discharge of less than 200,000 cfs occurs sporadically during the late summer and fall months (U.S. Army Engineers, 1961). Most of the runoff during late spring and early summer months is caused by the melting snow in the Rockies and Cascades. The tributaries west of the

Cascade Range contribute most of the fall and winter runoff. The U.S. Army Engineers (1962) report major flood conditions (>750,000 cfs) have occurred 20 times in the last 100 years. Twenty-five years is the average time span between floods with a stream flow of greater than 1,000,000 cfs.

The average amount of suspended sediment transported annually to the sea by the Columbia River is approximately 14,500,000 cubic yards (U.S. Army Engineers, 1962). Lockett (1965b) reported an average annual bed load of 4,000,000 tons (1,780,000 cubic yards) measured at the Vancouver, Washington, station. The median particle size of this bottom sediment decreases toward the mouth of the river with fine sand dominant in the lower estuary (Howell, 1966).

The present drainage pattern of the Columbia River began to take shape during the Miocene when outpourings of the Columbia River Basalts forced a consolidation of prior drainage (Mackin and Cary, 1965). Cascade andesitic lava, also of Miocene age, forced the river south to its present position. Following the establishment of the present drainage, Pliocene-Pleistocene uplift of the Cascade Mountains began. Downcutting by the river kept pace with uplift, resulting in the cutting of the picturesque Columbia River Gorge (Mackin and Cary, 1965).

According to Bretz et al. (1956), the Channeled Scablands of eastern Washington were scoured out by enormous Pleistocene

floods which carried huge quantities of water and sediment to the sea. Bretz et al. hypothesized that the cause of these floods was the bursting of ice dams which formed near the maxima of the glacial advances. The ice dam which formed glacial Lake Missoula broke at least three times resulting in catastrophic floods, the most recent of which took place during the last glaciation (Pinedale) approximately 18,000 years B. P. according to Richmond et al. (1965) Additional floods resulted from the failure of ice dams which blocked glacial lakes Columbia, Coeur d'Alene and Spokane (Richmond et al., 1965). Malde (1965) has reported evidence of a catastrophic flood that poured down the Snake River from ancient Lake Bonneville approximately 30,000 years B. P. These floods must have carried tremendous quantities of sediment to the ocean during glacial times.

Torrential bedding, poorly sorted gravels, and scour channels are cited by Lowry and Baldwin (1952) as evidence of Late Pleistocene flooding in the Portland area. Throughout the Pleistocene several episodes of renewed down-cutting have occurred in the lower Columbia River region as a result of complex interplays of regional uplift and lowering of sea level (Lowry and Baldwin, 1952). Since the last glaciation the rise in sea level has created a drowned valley with tidal influence extending 140 miles upstream during periods of low river flow (Lockett, 1965a).

Since the middle part of the nineteenth century man has been

influencing the sedimentation regime at the mouth of the Columbia River. In 1792 a single channel less than ten fathoms deep existed at the river entrance (Lockett, 1965a). Continued shoaling created navigational hazards which led to sporadic but ineffective dredging prior to 1885. According to Lockett, the hazards created by the shoaling resulted in the first of several phases of jetty construction south of the entrance which in turn led to the build-up of Clatsop Spit. Since that time the south jetty has been extended and a north jetty constructed. In spite of these developments a regular dredging program has been necessary to keep the channel mouth navigable.

From 1905, the beginning of a regular dredging program, until 1958 the dredging of "spoils" were dumped at a point southwest of the south jetty in water depths of 60 feet (Lockett, 1965b). This material seemed to be transported back into the mouth, Lockett reported. To counteract this, the dumping site was changed to a point due west of the south jetty in 120 feet of water. According to Lockett this reduced the net amount of annual dredging necessary. He concluded that the Lower Columbia Estuary is being filled not only by river transported sediment but also by salinity-induced movements of the north and southbound littoral current transported sediments.

For a 32 year period (1926-58), Lockett (1965a) reported that there had been a net accretion north of the jetties of 134,000,000 cubic yards of sediment. South of the jetties, however, 130,000,000

cubic yards of sediment have been eroded over the same time span. He attributed this change to interception of the southerly littoral current transported sediment. Livingston (1967), on the other hand, interprets this change as due to littoral drift to the north. Ballard (1964) and Gross (1966) also reported a northward net littoral drift in this area. Assuming that the 130, 000, 000 cubic yards of sediment represents net littoral transport over that 32 year period, the average annual volume of sediment transported by littoral drift would be 4, 070, 000 cubic yards (3.1×10^6 cu m/yr). This value is essentially the same as the volume given for long-shore transport off the California coast (Menard, 1960).

II. OCEANOGRAPHY

The oceanographic conditions off the Oregon and Washington coasts are of considerable importance in the total sedimentological picture of the Astoria Canyon region. The physical and chemical characteristics of the water masses and the velocities and types of currents play major roles in determining presence and distribution of plankton in the water and subsequently in the sediment. The currents are also important in the dispersal of fine terrigenous particles carried by the coastal streams and rivers. Although the sediments of Astoria Canyon are below the effective depths of present day wave action, these phenomena were of great importance during lower stands of sea level. Climatological variations affect the surface currents, upwelling patterns, and river runoff, and thus have a pronounced influence upon sediment dispersal.

Water Masses and Local Water Flow

The water off northern Oregon is transitional water with characteristics between those of Subarctic and Pacific Equatorial Water (Sverdrup, Johnson and Fleming, 1942). Rosenberg (1962) expanded upon this classification and defined three water masses: Modified Subarctic, Modified Equatorial Pacific, and Coastal Water. The Coastal Water, which essentially covers the

continental terrace, is a mixture of waters from the other two water masses and the fresh water influx from the coastal streams and rivers.

The Columbia River is the largest single source of fresh water in the area, contributing about 95% of the coastal drainage during its summer peak discharge (Duxbury, 1965). It dilutes the surface waters of the Pacific forming a low salinity belt of <32‰ near shore (Morse and McGary, 1965). The plume of the Columbia River has been traced some 350 kilometers to the southwest during the summer months (Osterberg, Cutshall and Cronin, 1965). The prevailing winds at this time are from the north (Lane, 1965) resulting not only in the displacement of the plume to the south, but also in a total net transport of surface water offshore accompanied by vigorous upwelling (Pattullo and McAlister, 1962; Park, Pattullo and Wyatt, 1962; Smith, Pattullo and Lane, 1966).

During the winter, winds from the south move the surface water northward (Lane, 1965). Pattullo and Denner (1965) report that rainfall is the dominant process affecting local water mass modification during the winter season. As this is the time of maximum discharge by coastal streams, it is difficult to distinguish the Columbia River contribution (Duxbury, 1965). Through the use of radionuclides, however, the effluent of the Columbia has been traced northward along the Washington Coast during the winter rainy season

(Osterberg, Cutshall and Cronin, 1965). Based on a study of radioactive marine sediments derived from the Columbia River, Gross (1966) concluded that the net movement of this sediment was northward on the shelf.

Major Currents

The Westwind Drift, which moves eastward across the Pacific Ocean, divides into two parts near latitude 45° North some 300 miles off the Oregon-Washington coast (Dodimead, Favorite and Hirano, 1963). Part swings north and part flows south as the California Current. Sverdrup, Johnson and Fleming (1942) reported that a northward flowing subsurface nearshore current breaks through to the surface along the California Coast during the winter months. This Davidson Current has been reported as far north as 50° North latitude during the winter (Burt and Wyatt, 1964). During the summer, however, they reported the movement of surface water to be southerly. Stevenson (1966) reported a mean longshore current, throughout the water column, as predominantly toward the south at ~80 km offshore with an average speed of 5 to 10 cm/sec. Maughan (1963) also indicated a seasonal change in the current directions along the Oregon Coast. He measured velocities as great as 25.8 cm/sec at a depth of ten meters over the continental slope region.

Very little quantitative information has been obtained about

current velocities at the sediment-water interface. Qualitative reports of strong bottom currents have been issued by various SCUBA divers and scientists viewing the bottom in deep submergence vehicles of various sorts (Shepard and Dill, 1966). Most of these observations have been reported off Southern California. However, maximum speeds up to 61 cm/sec have been measured some 20 to 30 meters above the bottom in water depths of about 60 fathoms off the Central Oregon Coast (Collins, Creech and Pattullo, 1966). They reported mean speeds of 27 cm/sec during a 25 day period in January, 1965. In the summer at the same station, however, these investigators obtained current speeds of about half of the winter speeds (maximum 29.5 cm/sec; mean 13.3 cm/sec). According to Sundborg (1956) a current velocity of 45 cm/sec ten meters above the bottom is capable of eroding unconsolidated fine sands and silts. While this velocity is occasionally attained by currents near the bottom in the mid-shelf areas, currents of the velocities reported by Collins et al. (1966) are not sufficient to erode the sediments in depths of water as great as 60 fathoms.

Waves

Deep Water Waves

During the winter the Northeast Pacific Ocean is a place of

frequent severe storms. According to the National Maritime Consultants (1961) extratropical cyclones generate winds up to hurricane force which approach the coast from directions ranging from southwest to west, sometimes producing waves with significant heights of 25 to 30 feet. The period for these waves ranges from 11 to 14 seconds. Maloney (1965) has calculated that waves 10 meters high with periods of 14 seconds traveling in water 130 meters deep attain maximum particle velocities of 31 cm/sec at the bottom. This speed according to Sundborg (1956) would be more than adequate to erode fine sand. Thus, it appears that during major storms even the fine sediments of the outer continental shelf might be stirred by wave action.

Shallow Water Waves

Tides along the Oregon-Washington coasts are mixed semidiurnal with a range varying from 6 to 10 feet (Pattullo and Burt, 1962). Mooers (1967) believes that a large portion of the current speed on the Oregon continental shelf is due to tidal influence. Although tidal current speeds determined by Mooers have been for the most part less than 8-10 cm/sec, the shear which results along the pycnocline may be sufficient to cause considerable dynamic instability in the frontal zone. According to Mooers these observed motions relate to the passage of internal waves, including internal tides.

Internal waves have been measured on the shelf off southern California which have large enough horizontal velocities to prevent deposition on high areas and possibly to cause erosion (Shepard, 1963). Not enough is presently known about these internal waves to be able to state what their effect is on the sediments of Astoria Canyon.

Seismic sea waves, or tsunamis, occasionally strike the Pacific Northwest shores. With wave lengths of hundreds of miles, seismic sea waves feel the bottom along their entire route. Schatz (1965) reported that five notable tsunamis have struck the shores of the Pacific Northwest in the last 20 years. The tsunami resulting from the March 27, 1964, Alaskan earthquake attained a speed of 280 knots before striking the Oregon Coast. A period of 40 minutes results in a calculated wave length of 294 nautical miles for this destructive shallow water type wave (Schatz, 1965). Assuming an amplitude of 0.5 meter for this wave, the particle velocity at a water depth of 1000 fathoms would be approximately 35 cm/sec. This velocity would be sufficient to erode unconsolidated medium sand to clay size sediments. Therefore, even though infrequent in the Astoria Canyon area, these seismic sea waves must be considered as contributors to the total sedimentation process.

III. PHYSIOGRAPHY

General Description

The major physiographic features of the Astoria Canyon region, in addition to the canyon, are the continental shelf and slope and Astoria Fan (Figure 1).

Continental Shelf

The shelf off the Columbia River is approximately 30 nautical miles wide. North of Astoria Canyon the shelf break is at 80 fathoms; south of the canyon, 90 fathoms. With the resulting inclination of 0° 11', the Oregon shelf is narrower, steeper and deeper than the average for the continental shelves of the world. Shepard (1963) reports these averages to be: width, 40 nautical miles; depth of shelf break, 72 fathoms; average slope, 0° 07'.

Continental Slope

In the vicinity of the canyon the continental slope is extremely irregular. The numerous ridges and troughs on the lower slope have a decided north-northwest orientation (Figure 2). The uniform alignment of these ridges suggests structural control. It has been hypothesized by Byrne (1966) that the ridges and troughs of this

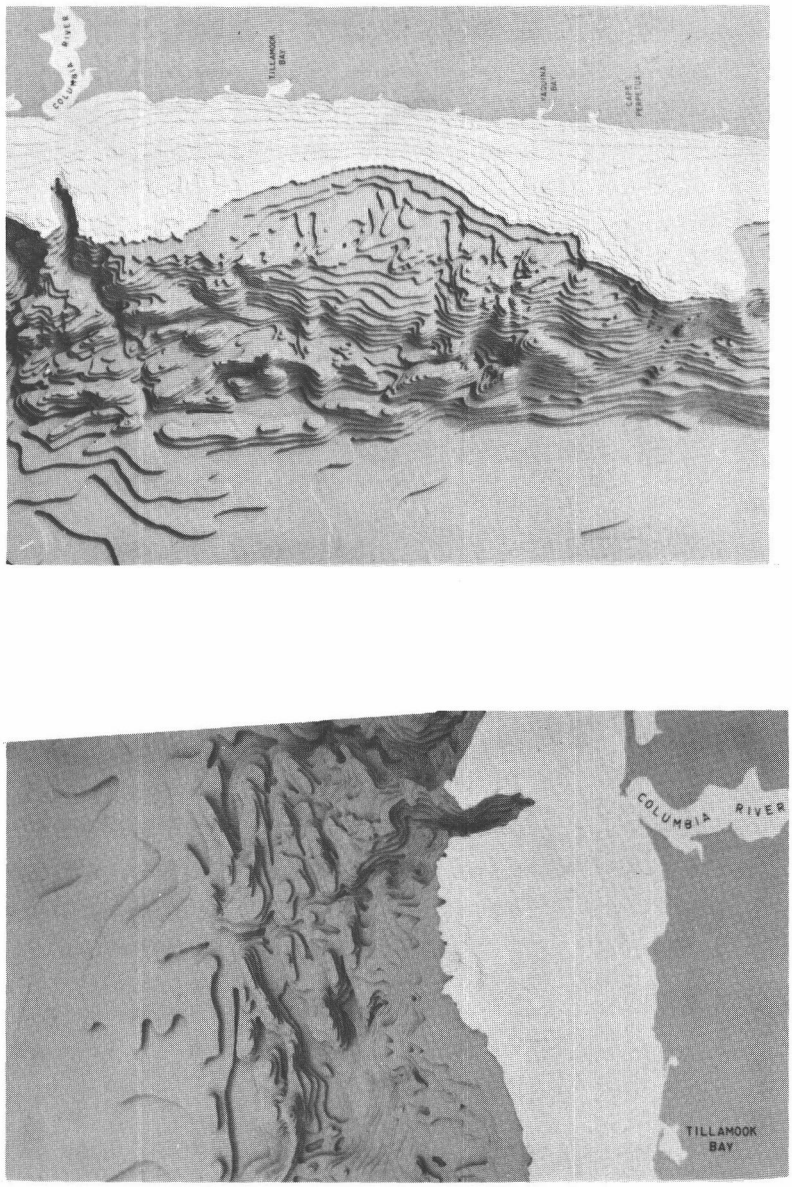

Figure 2. Three dimensional model on the Oregon continental terrace. The model was constructed by John Sheehy based on bathymetric charts by Byrne (1963).

region may be a consequence of compressional forces acting in a direction more or less normal to the continental margin. He further suggested that this force may result from sea-floor spreading originating from the crest of the East Pacific Rise (Figure 1).

The relief in this area reaches a maximum of 500 fathoms where the canyon cuts the upper part of the slope. Immediately north of the canyon mouth the relief is approximately 400 fathoms and throughout the lower part of the slope relief of several hundred fathoms is common.

Whereas the worldwide average inclination for continental slopes is 4°17' for the upper 1000 fathoms (Shepard, 1963), the average slope in the Astoria Canyon area is less than two degrees to the line of intersection of slope and fan. The base of the slope marking the break from slope to fan occurs at 1250 fathoms south of the canyon and 1100 fathoms north of the canyon. The width of the slope, from the shelf break to the beginning of Astoria Fan, is 37 nautical miles. The resulting average slope inclinations for these two areas are: north of the canyon, 1°33'; and 1°46' south of the canyon. Because of the ridge and valley nature of the slope, these average inclinations are deceiving (Figure 3). Byrne (1963) reported a somewhat steeper slope on the seaward side of the ridges, averaging 12 to 16 degrees with values of 8 to 11 degrees measured on the landward portions.

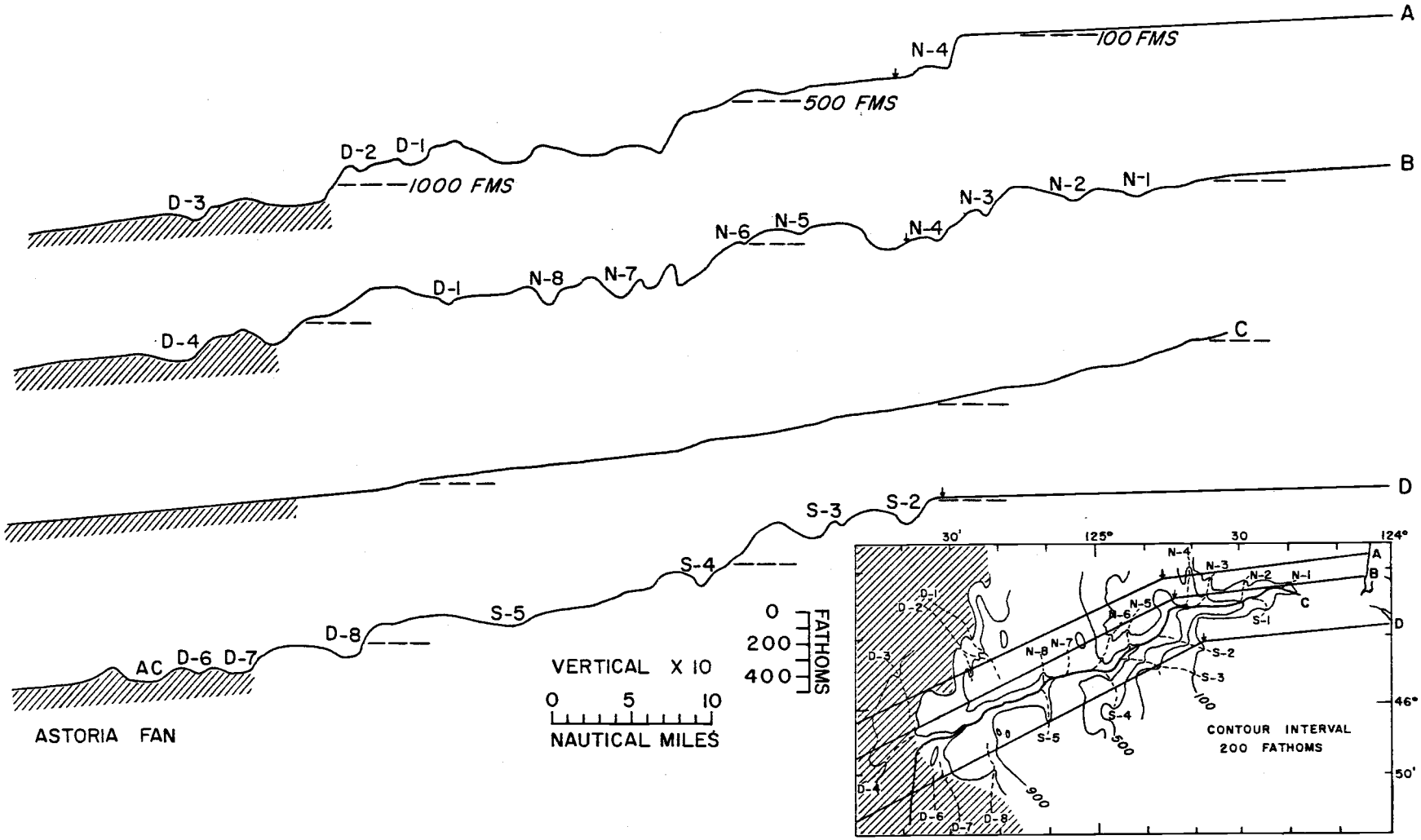

Figure 3. Continental terrace profiles paralleling Astoria Canyon.

Astoria Fan

The mouth of Astoria Canyon opens onto a depositional fan called Astoria Fan. This fan has an area of approximately 6,000 square miles to a depth of 1550 fathoms. Nelson (1967) has measured fan gradients ranging from 1/50 on the inner fan to less than 1/600 on the outer portions of the fan. Numerous channels radiate across the fan from the mouth of the canyon. Astoria Seachannel, first named by Menard in 1955, is the only one of these channels currently connected to Astoria Canyon (Figure 1). According to Hurley (1960) the apex of the fan is somewhat north of the canyon mouth and the crest of the fan is more than 100 fathoms higher than the floor of the canyon where it leaves the continental slope. Previous bathymetric surveys of this region, although pointing out the proximity of Astoria Canyon and Channel, were not sufficiently detailed to prove this connection. Soundings from Oregon State University cruises (See Figure 4 for track lines) have demonstrated the connection between Astoria Channel and Astoria Canyon. The bathymetric chart based on O.S.U. soundings shows this relationship (Figure 5).

Bathymetric Methods

Soundings upon which the bathymetric charts (Figures 5, 6, 7

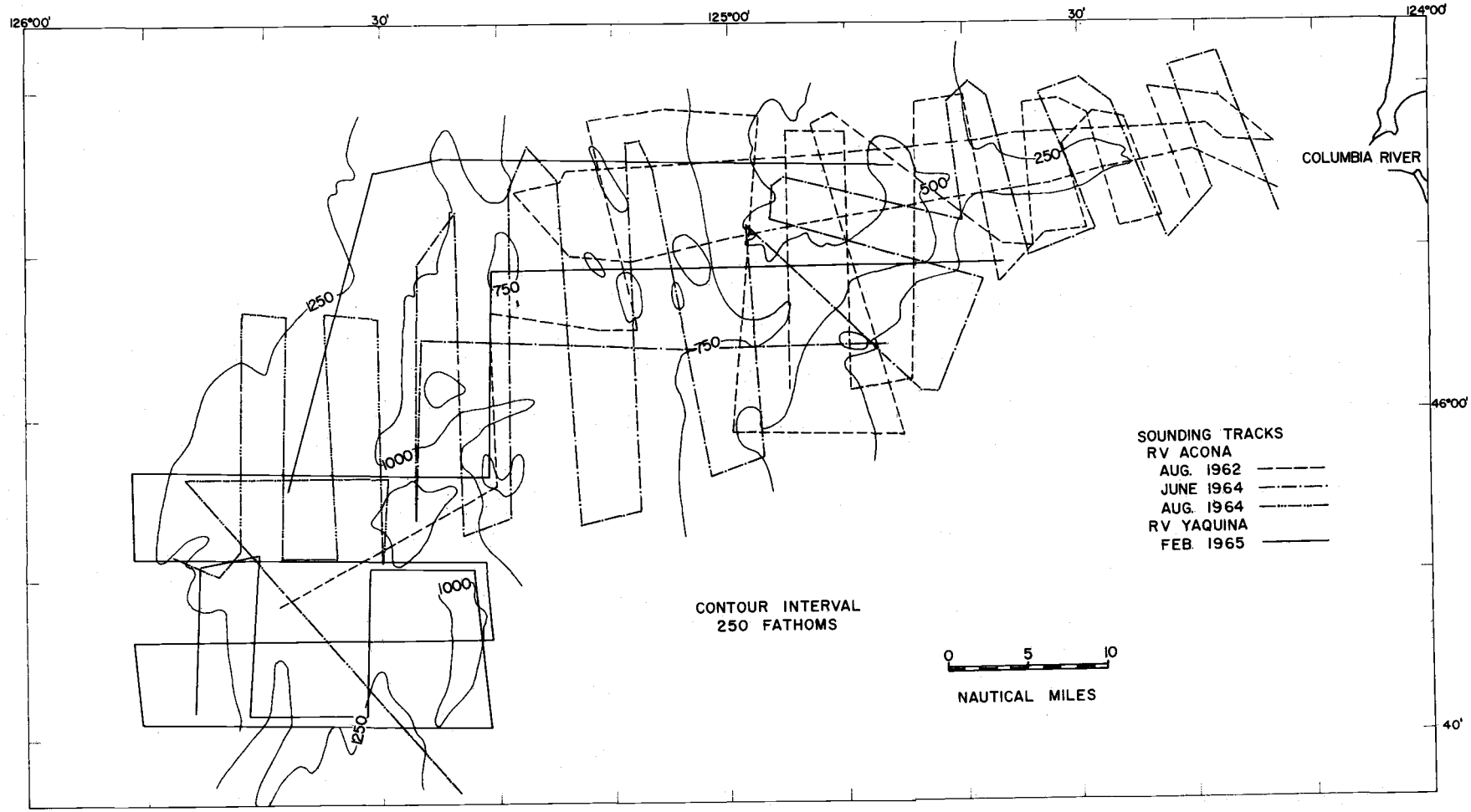

Figure 4. Sounding lines made by the Oregon State University research vessels.

FIGURE 5. BATHYMETRIC CHART OF ASTORIA SUBMARINE CANYON

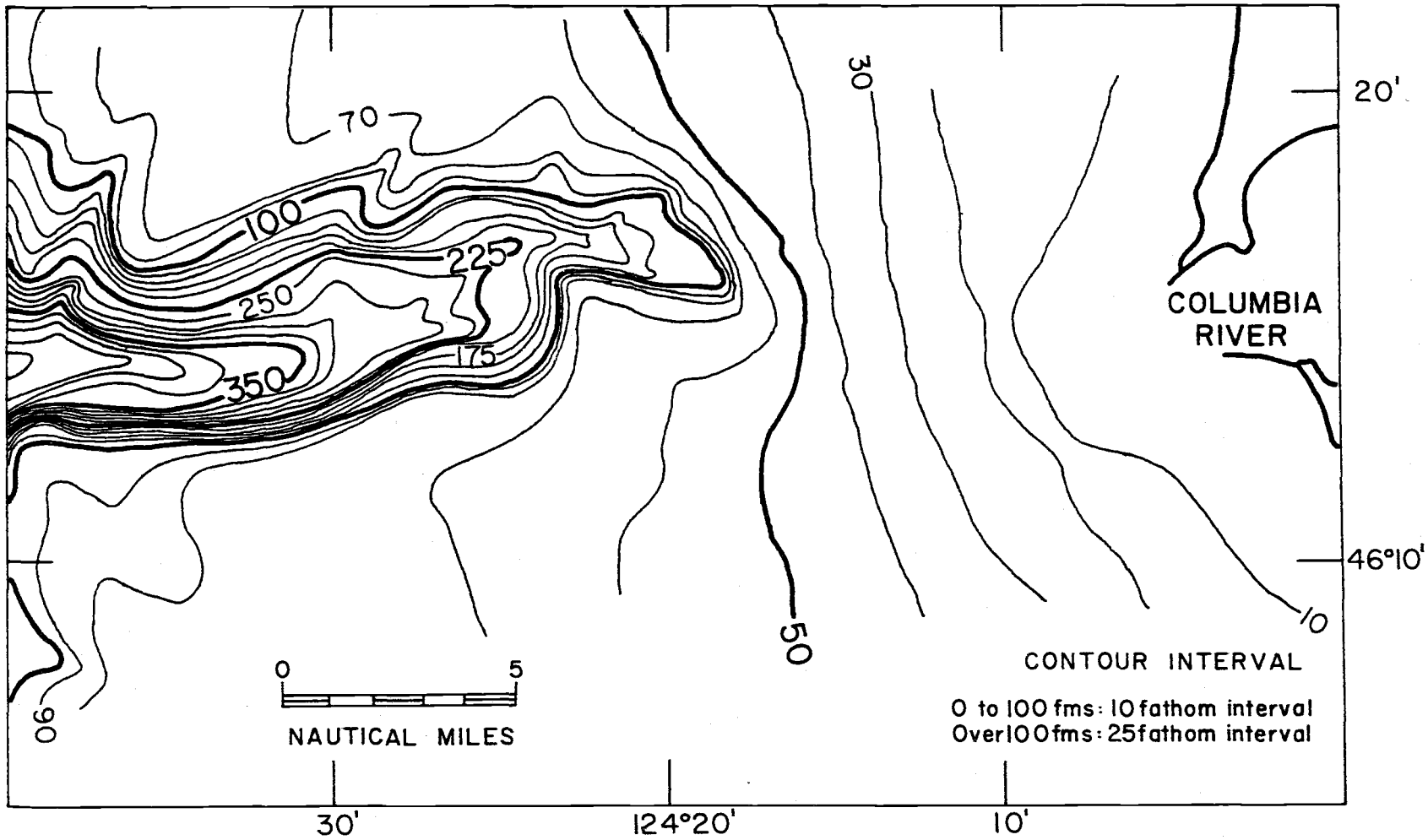

Figure 6. The head of Astoria Canyon and its relationship to the Columbia River. Contours based on OSU Oceanography Department soundings, supplemented with U. S. Coast and Geodetic Survey soundings.

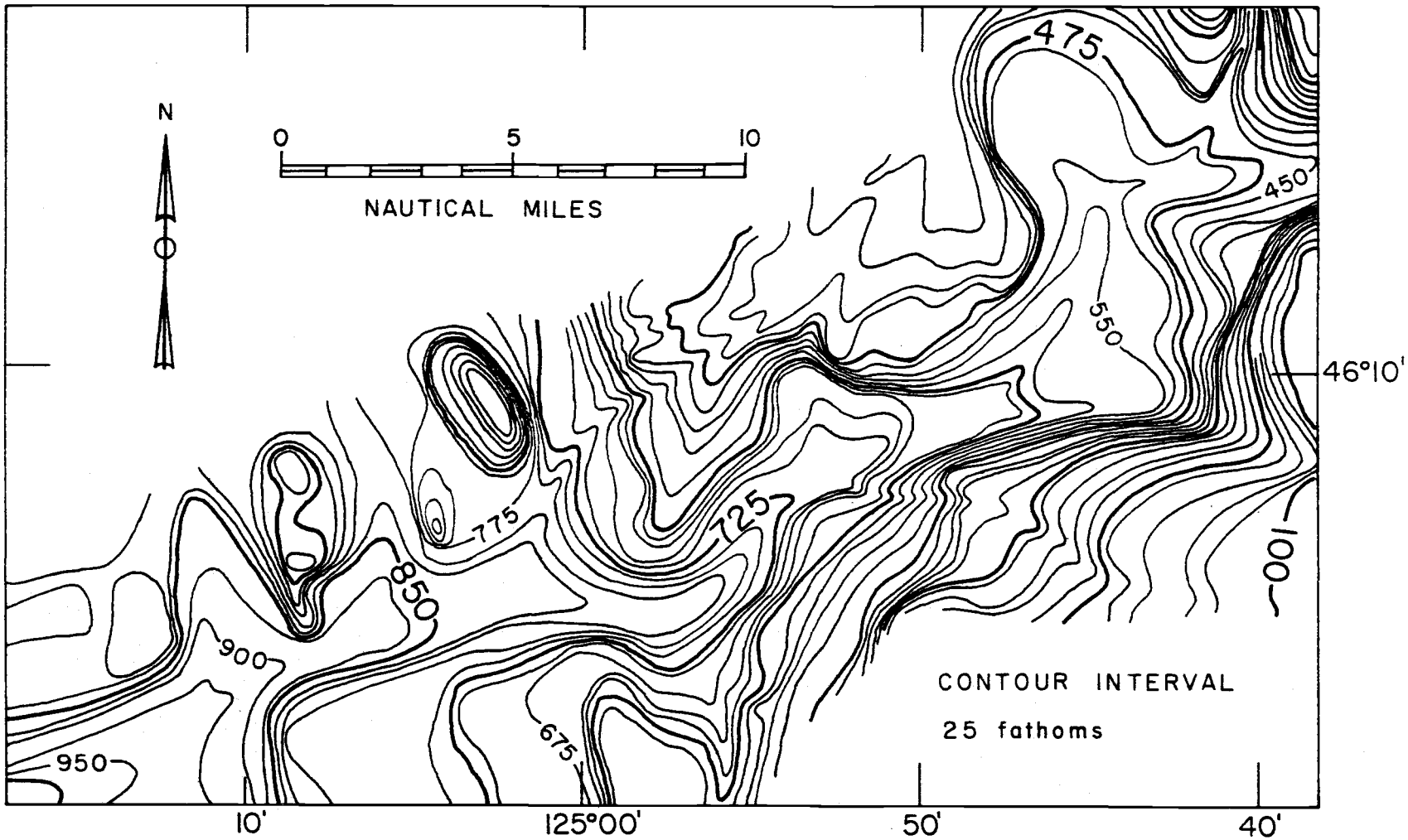

Figure 7. Bathymetric chart of the middle portion of Astoria Submarine Canyon. Contours based on OSU Oceanography Department soundings, supplemented with U.S. Coast and Geodetic Survey soundings.

and 8 are based, were collected on cruises of Oregon State University Oceanography Department vessels between 1961 and 1965. Figure 4 shows the cruise tracks. A Precision Depth Recorder (PDR, Mark V) couples with an Edo (185) echo sounder furnished the bathymetric data. Positioning was accomplished using either Loran A or radar to obtain "fixes" at intervals of 15 to 20 minutes.

A smooth sheet of the area was constructed with the aid of an IBM 1620 computer and an X-Y plotter. The uncorrected depths were plotted at a scale of 1:140,000.

Astoria Canyon Physiography

General Description

Shepard (1963) pointed out that there is a noticeable absence of major submarine canyons between the Eel Canyon off the coast of northern California and Astoria Canyon. North of Astoria Canyon several submarine canyons are incised into the continental terrace off the Washington coast. The most southerly of these is Willapa Canyon which, at the closest point, is about 10 miles from Astoria Canyon.

Astoria Canyon heads in water slightly less than 60 fathoms deep 9 miles west of the Columbia River north jetty. The canyon winds sinuously in a southwesterly direction across the continental

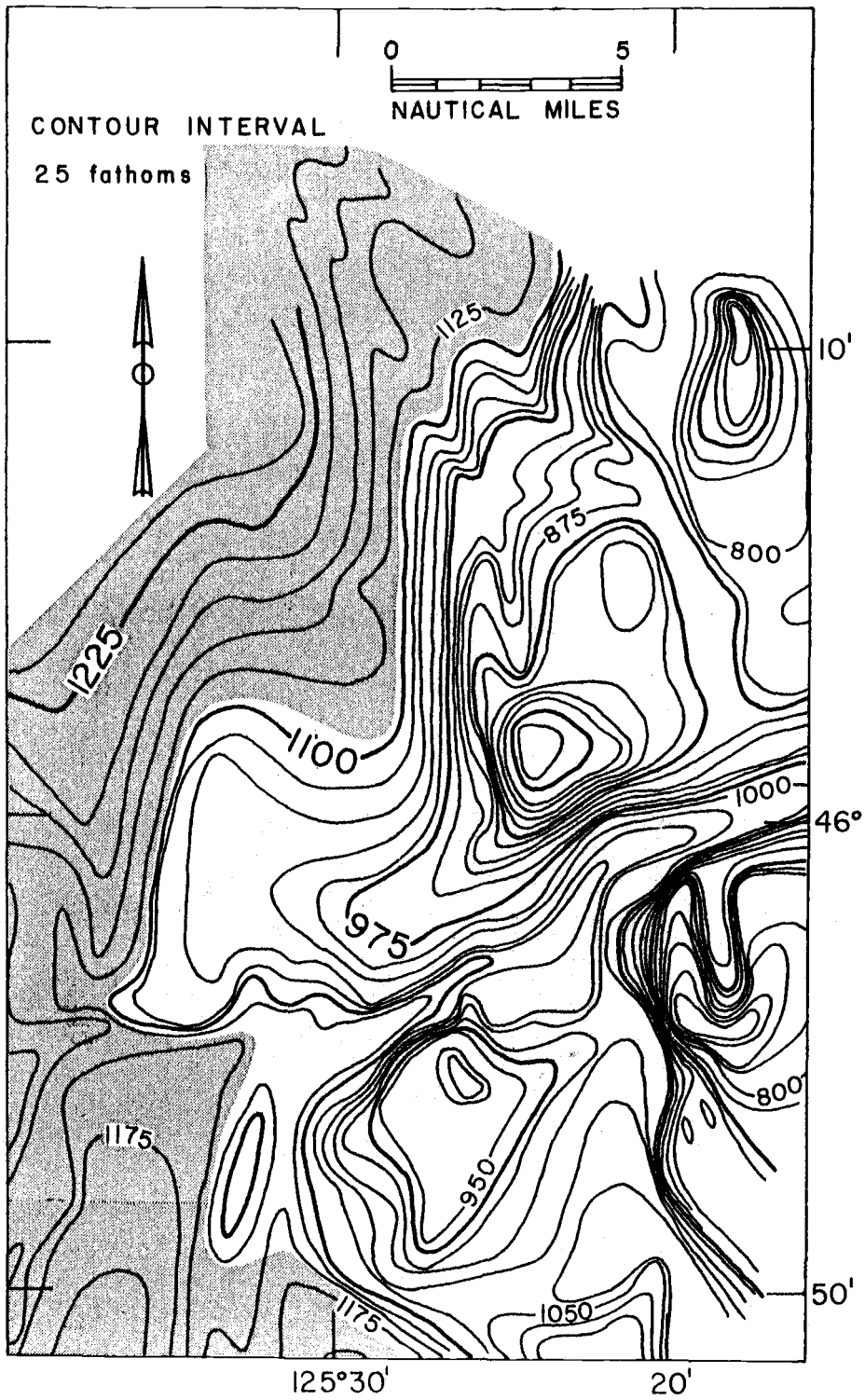

Figure 8. The mouth of Astoria Canyon showing the transition to Astoria Channel. Astoria Fan represented by stippled area. Contours based on OSU Oceanography Department soundings, supplemented with U.S. Coast and Geodetic Survey soundings.

shelf and down the slope to a depth of 1140 fathoms. At this depth it reaches Astoria Fan, and the profiles change from canyon to channel proportions.

As can be observed on the bathymetric chart (Figure 5) and the transverse profiles (Figure 9), Astoria Canyon varies greatly in width, both at the rim and across the canyon floor. The average width from edge to edge is 3.8 miles with a range from 1.3 to 7.2 miles. The average floor width is 1.2 miles; the maximum measured width is 3.3 miles, the minimum width, 0.3 miles. Table 1 which includes canyon profile widths indicates there is little consistency in width either across the canyon floor or from rim to rim. The extreme variations are probably due to slumping suggested by PDR traces, which narrows the floor and to entering tributary valleys which yield an anomalously high value for widths. There is, however, a consistency between edge and floor width of the canyon profiles. Figure 10, a plot of width versus distance down the canyon reveals similar trends in both rim and floor widths to a distance of 62 miles from the head. At this point, instead of parallel trends, the width of the floor increases and the width across the edge of the walls decreases. It is at this position, between profiles W and X (Figure 9), that the change from Astoria Canyon to Astoria Channel takes place.

The general shape of the canyon profiles (Figure 9) varies from

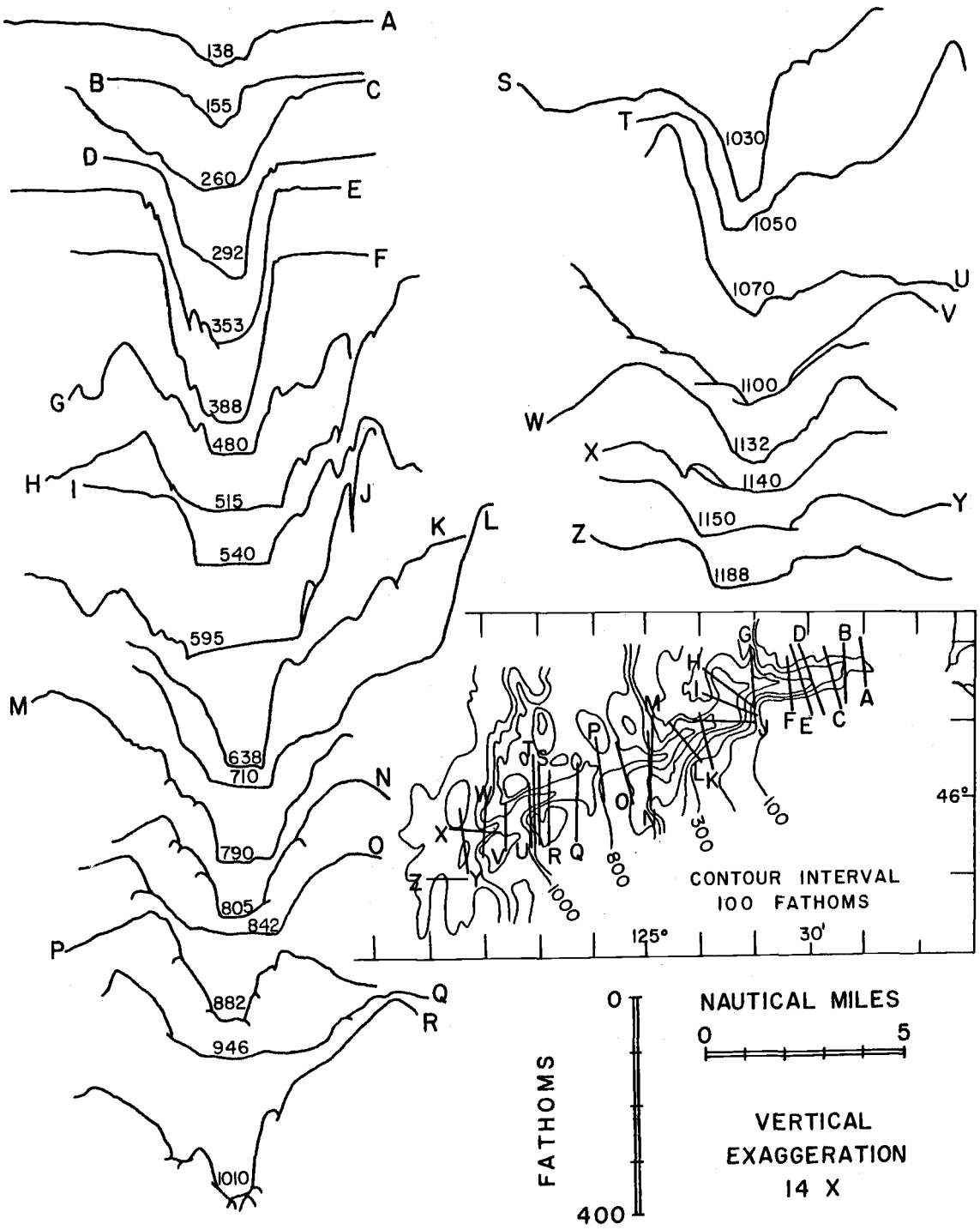

Figure 9. Transverse profiles of Astoria Submarine Canyon.

Table 1. Transverse profiles of Astoria Canyon (See Figure 9 for section locations)

Profile	Distance* (naut. mi.)	Axial Slope	Widths (naut. mi.) Top	Floor	Relief (fms) N. Wall	S. Wall	Average Slopes N. Wall	S. Wall
A	3+	1° 25'	2.0	0.3	60	60	3° 20'	3° 35'
B	4	1 59	1.3	0.3	85	85	2 16	4 06
C	8	1 01	5.2	1.0	200	200	3 11	5 00
D	10	1 01	2.8	0.5	210	210	6 06	11 42
E	11.5	2 02	3.2	1.0	280	280	6 27	8 35
F	13	1 25	3.1	1.0	310	310	13 14	17 01
G	18	1 42	3.0	1.0	200	225	6 12	5 31
H	19.5	0 51	3.4	1.8	130	270	6 01	7 28
I	21	0 51	4.0	2.5	140	425	14 20	6 03
J	25	0 54	4.5	3.3	230	425	4 34	13 07
K	27	1 25	3.2	1.0	220	415	5 10	5 12
L	30	0 41	5.8	1.7	220	520	6 34	5 39
M	33	1 59	5.6	1.4	190	250	4 32	6 20
N	34	0 34	3.5	1.2	320	220	9 05	6 23
O	38	0 31	4.5	2.3	145	150	5 17	4 42
P	42	0 37	2.5	0.8	210	125	6 54	9 12
Q	46.5	0 34	5.5	2.8	170	115	4 33	2 49
R	50	0 54	4.7	1.0	200	365	4 00	4 44
S	51.5	0 54	2.7	0.6	200	350	6 56	5 54
T	52.5	0 54	2.2	0.5	220	340	11 09	3 43
U	54	0 41	3.0	0.7	355	80	9 02	2 09
V	58	0 34	7.2	0.6	350	210	4 23	2 45
W	61.5	0 34	4.5	0.6	190	155	3 50	4 22
X**	62.5	0 34	4.5	2.6	100	100	2 20	3 20
Y**	63.5	0 27	4.1	2.4	100	75	4 46	3 04
Z**	68	0 27	2.3	2.0	95	75	5 04	1 42
Average		0 59	3.8	1.3	197	232	6 08	5 59

* Distance measured from head of the canyon

** Astoria Channel Profiles

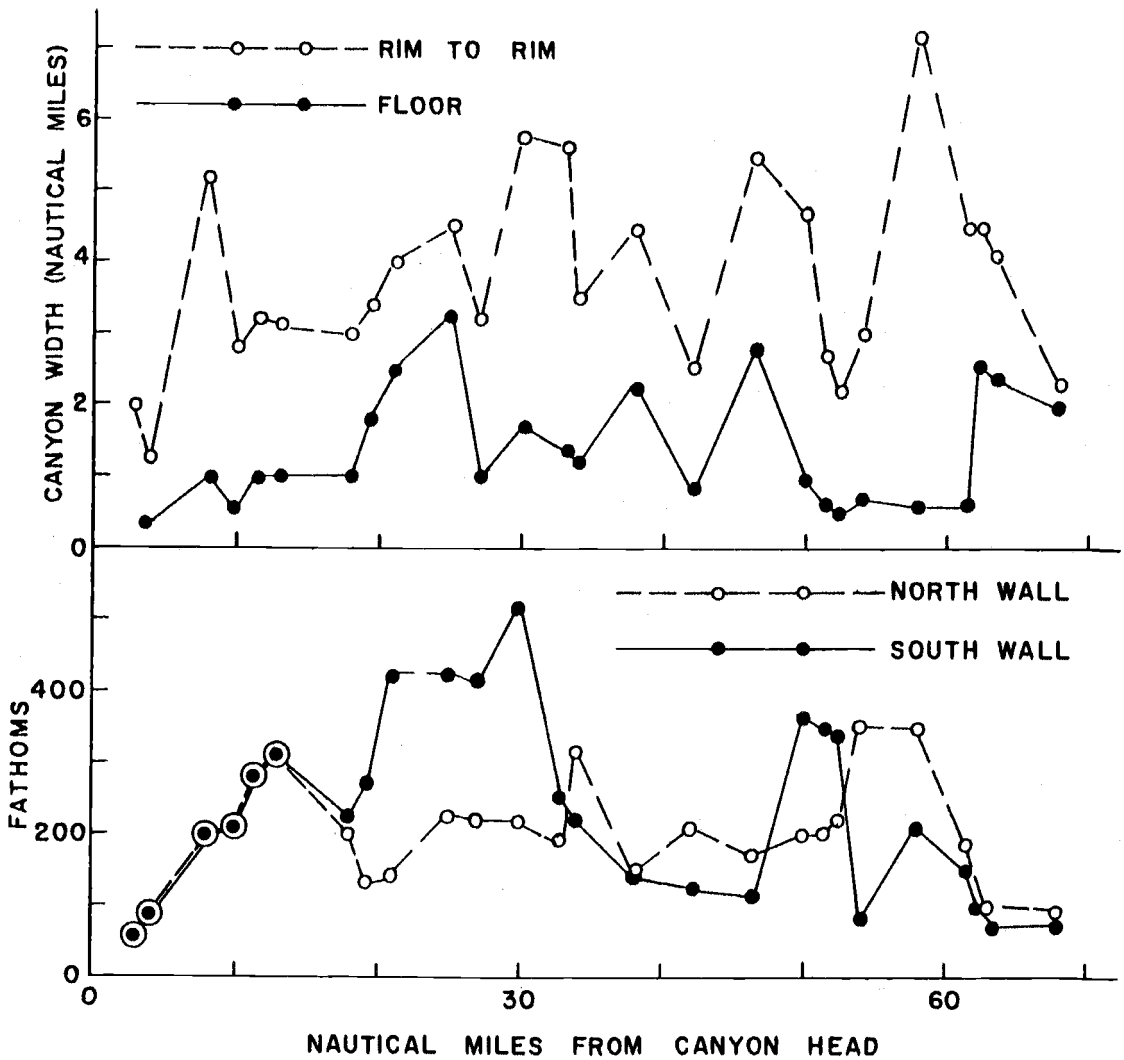

Figure 10. Changes in canyon width and wall relief with distance from the head.

U- to V-shaped at different places in the canyon. The upper portion of the canyon is characterized by a broad U-shaped profile. This changes to a steep-sided U-shaped to V-shaped canyon near the continental shelf break, as typified by profiles E and F (Figure 9). In the continental slope region, the profile becomes much more irregular and the tops of the two walls are seldom encountered at the same elevation.

Canyon Floor

The floor of Astoria Canyon is extremely variable in gradient, width, and degree of flatness. Table 1 contains a list of inclinations of the canyon floor calculated for the cross-profile areas from the head end to Astoria Channel. The maximum slope along the axis of the canyon is 3°57' at a thalweg depth of 325 fathoms. The slope generally decreases in a down-canyon direction resulting in a concave profile (Figure 11). However, numerous step-like terraces cause oscillations in axial slope. The gentlest slope on the canyon floor, at 840 fathoms, measures 0°31'. This low slope is not matched again until well into Astoria Channel, below a depth of 1140 fathoms.

The over-all average axial slope of Astoria Canyon is one degree. The upper portion is steepest where the canyon cuts the outer shelf. Just beyond the shelf-slope break, the canyon makes

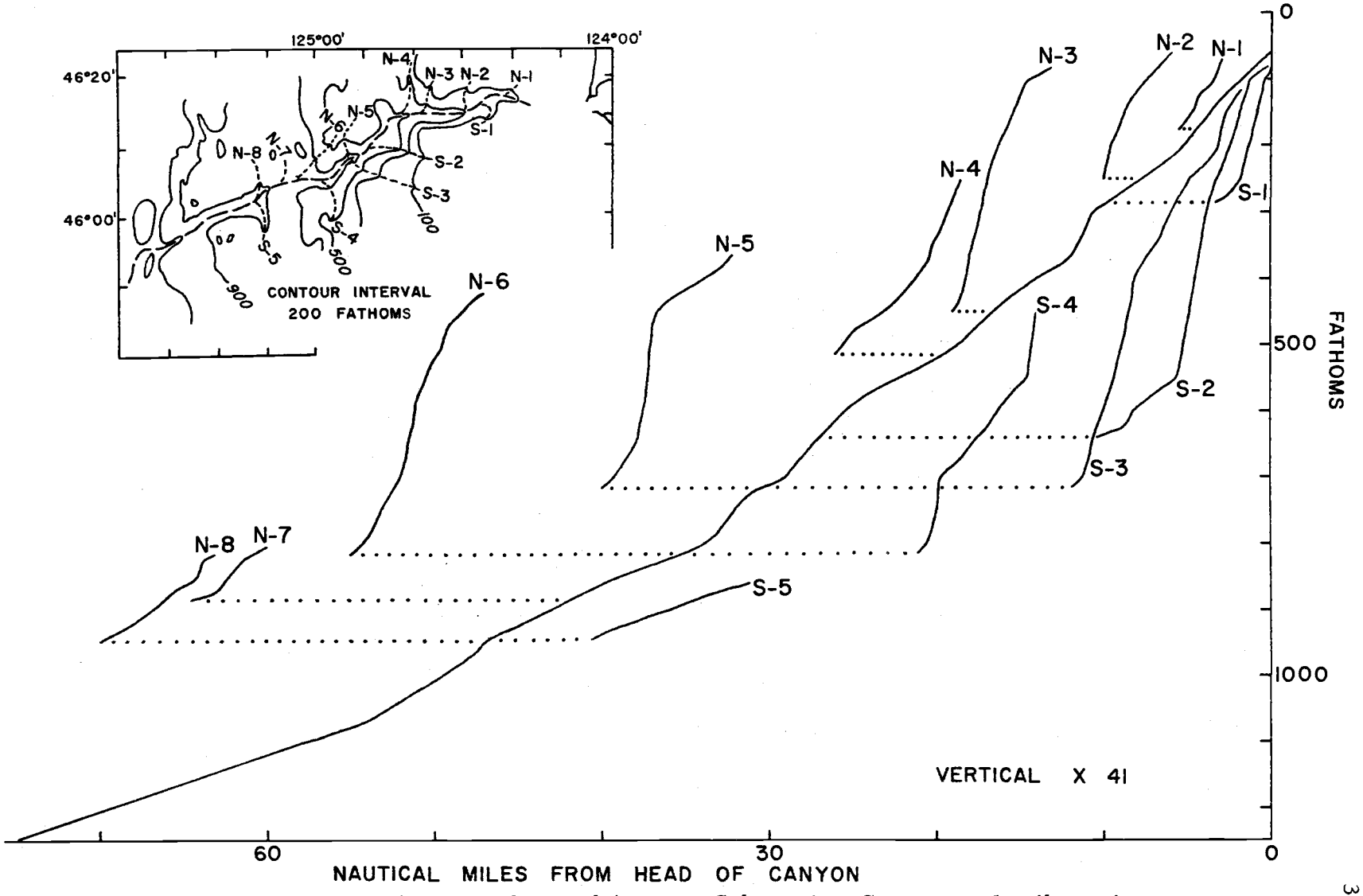

Figure 11. Longitudinal profiles of Astoria Submarine Canyon and tributaries.

an abrupt turn to the south and then southwest (Figure 5). Through this bend (Figure 7) the average axial slope of the canyon is diminished greatly, and the floor of the canyon becomes quite flat and much wider (Figure 9, profiles G-J). It is in this region that the PDR traces exhibit the most distinct sub-bottom reflections. As Hersey (1965) has suggested, the interface between a layer of clay and a layer of sand may be a reflector. Beyond this bend, in the area termed lower middle canyon, the slope again increases markedly to a maximum of almost two degrees at 775 fathoms, the canyon becomes narrower, and the floor more irregular. Below an axial depth of 800 fathoms, the axial slope variations diminish somewhat into rather subdued step-like terraces. A maximum slope of 1°25' occurs at 960 fathoms. No abrupt gradient change is found near the lower end of the longitudinal profile; Astoria Canyon merges smoothly with Astoria Channel (Figure 8). The canyon mouth appears to be located at a water depth of 1140 fathoms. Transverse profile W (Figure 9) marks the last canyon profile and profile X the beginning of Astoria Channel.

Canyon Walls

The walls of Astoria Canyon have an average steepness of slightly more than 6° (6°02'). The north wall averages 6°08' of slope, slightly greater than the south wall which has an average

declevity of 5°59'. The degrees of slope of the walls of the transverse profiles of Figure 9 are listed in Table 1. Along the upper part of the canyon to the shelf-slope break, the south wall is somewhat steeper than the north wall. Beyond the limits of the shelf, however, there is a lack of any consistency concerning wall steepness. From canyon head to shelf-slope break, a distance of approximately 15 miles, the angle of slope of both walls increases with increased water depth. Beyond the continental shelf, the slopes become much more irregular, but there is a general decrease in slope angle down canyon. The steepest wall angle measured on any of the profiles is 29°37', measured on the south wall of transverse section F (Figure 9). The north wall of the same profile was calculated to contain the second steepest angle of slope (29°33'). Even these maximum values are probably considerably below the true figures. Buffington (1964) and Shepard (1965a) emphasized that visual inspection of the walls of submarine canyons using manned submersibles have revealed vertical walls and even some overhangs. Slope angles obtained from these same canyons using depth recordings and wire line soundings have failed to indicate slope angles anywhere near as great.

Maximum relief of Astoria Canyon exceeds 500 fathoms at profile L where the axial depth is 710 fathoms. Seaward of the shelf edge the irregularity of topography which typifies the continental

slope in this region (Figures 2 and 3) causes great fluctuations in relief. Maximum values measured along the profiles of Figure 9 range from 150 to 520 fathoms (Table 1). In several places low spots coincide with the valleys or troughs which dissect the continental slope on both sides of Astoria Canyon.

The importance of slumping as a canyon shaping process is borne out especially well by the transverse profiles E and F (Figure 9). In both instances apparent slump blocks occur on the north wall. Although "slumping" is found on both sides, it appears to be somewhat more prevalent at the base of the north wall.

Canyon Head

The first sign on the continental shelf of a depression signalling the start of Astoria Canyon occurs at a water depth of approximately 55 fathoms. This very slight valley has a shallow U-shape and an initial relief of a few fathoms (Figure 6). The directional trend for the first 5.6 miles is west-northwest; the axial slope gradually increases from 1°25' to 1°59'. At a thalweg depth of approximately 200 fathoms, the canyon bends toward a south-southwest direction and the slope decreases to about a degree. This course is followed for a distance of 11 miles where the canyon trend gradually becomes due west. At this point the water depth in the axis of the canyon is 300 fathoms and the slope increases rather abruptly to a maximum

of 3°57'. From this position, the canyon axial slope undergoes a general but unsystematic decrease to the deep-sea fan.

One tributary valley (N-1, Figure 12) enters near the head of Astoria Canyon. It reaches the main canyon floor at a distance approximately four miles down canyon from the head and at a water depth of about 175 fathoms. From this point to the shelf-slope break, three more tributaries enter the canyon, two from the north and one from the south wall.

Profiles A-F (Figure 9) represent the upper portion of the canyon. According to Emery (1960), if the canyon was present before the shelf was bevelled, the depth of the canyon shelf break would be practically uniform along the canyon. The reasoning behind this is that the already cut embayment offers additional area for wave planation during lower stands of sea level. This condition is apparent in Figure 13. Therefore, it is concluded that the canyon may have already been partially incised into the shelf at the time of planation during the Pleistocene.

Between the head of Astoria Canyon at approximately 55 fathoms and the mouth of the Columbia River, a distance of nine miles, there are no surface manifestations of a channel detectable on Precision Depth Recordings. As can be seen in Figure 6, there is a significant outbowing of the ten fathom contour line adjacent to the mouth of the Columbia River. This bar would indicate a dumping

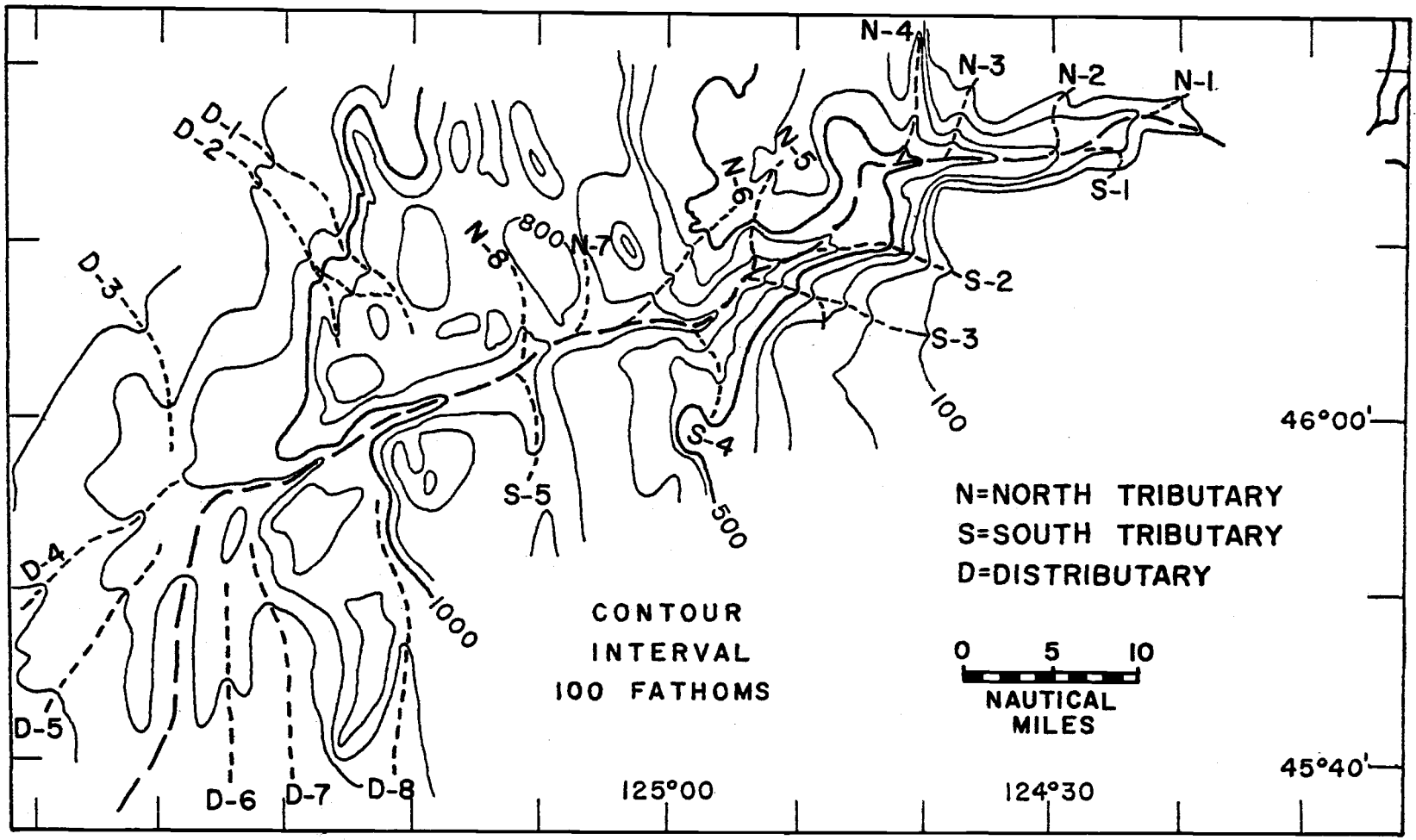

Figure 12. Tributaries and distributaries of Astoria Canyon.

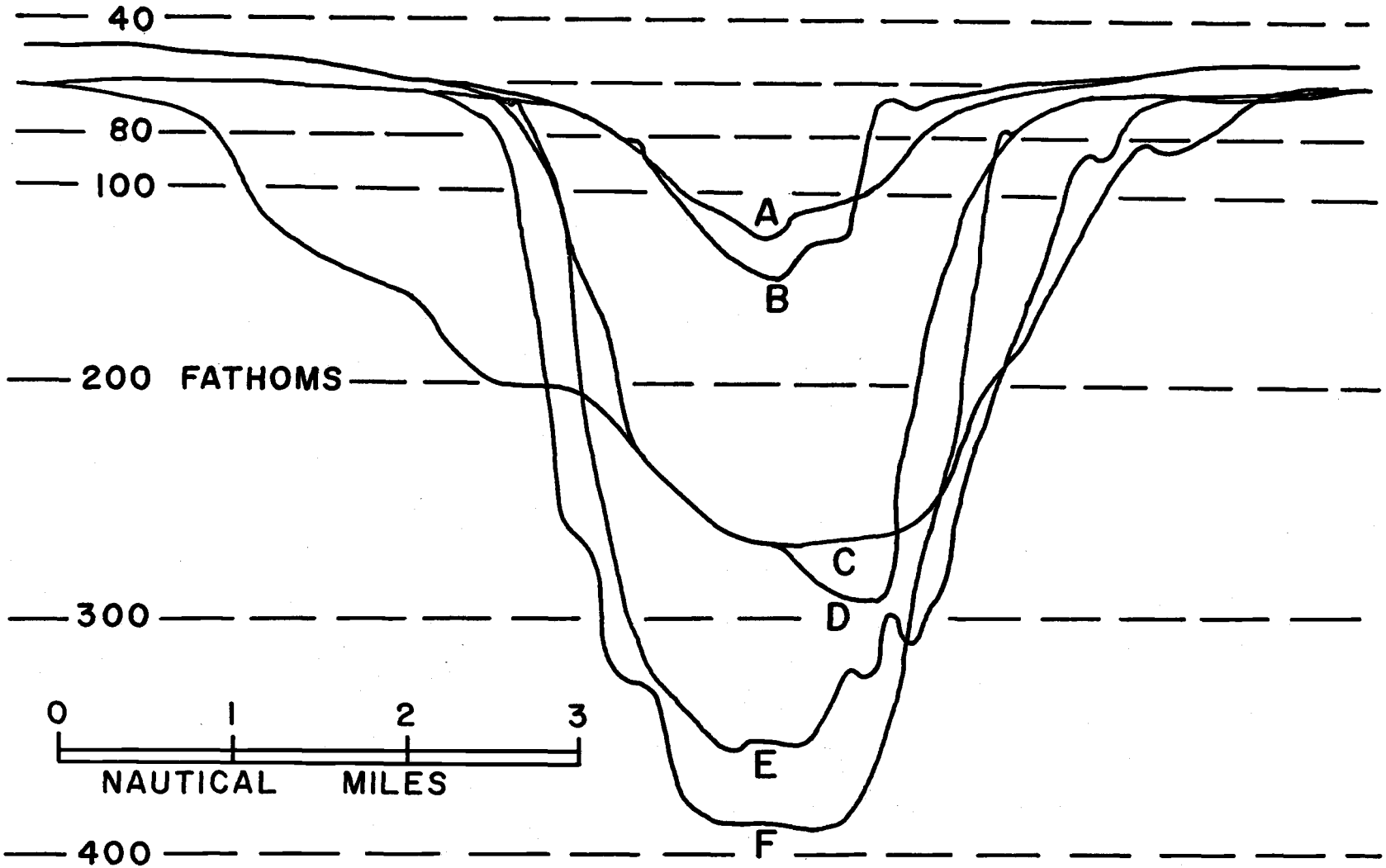

Figure 13. Transverse profiles of Astoria Canyon in the continental shelf region. Letters A-F indicate the location of the profiles in Figure 9.

of the sediments just outside the estuary. Sparker traces obtained between the mouth of the river and the head of the canyon reveal that channels were not always lacking. Two buried channels have been reported by Berg, King and Carlson (1966), indicating a connection between Astoria Canyon and the Columbia River during lower stages of sea level. On a subsequent cruise by the marine geophysicists of Oregon State University, additional buried channels were discovered in this area. Figure 14 shows the location of the channels. The apparent dimensions of these buried channels range from 0.2 to 2 miles in width, and wall relief may vary from 20 to 50 fathoms. There is approximately 30 to 40 fathoms of sediment covering this Pleistocene drainage network. Buried channels have also been discovered on the continental shelves shoreward of other submarine canyons such as Eel Canyon (Green and Conrey, 1966), several Georges Banks canyons (Roberson, 1964), and Hudson Canyon (Ewing, Le Pichon and Ewing, 1963).

Canyon Mouth

Astoria Canyon reaches Astoria Fan at a depth of 1140 fathoms (Figure 8). Beyond 1140 fathoms deep-sea fan valley characteristics predominate.

The deepest transverse profile of Astoria Canyon (Profile W, Figure 9) indicates a canyon width of 0.6 mile across the floor and

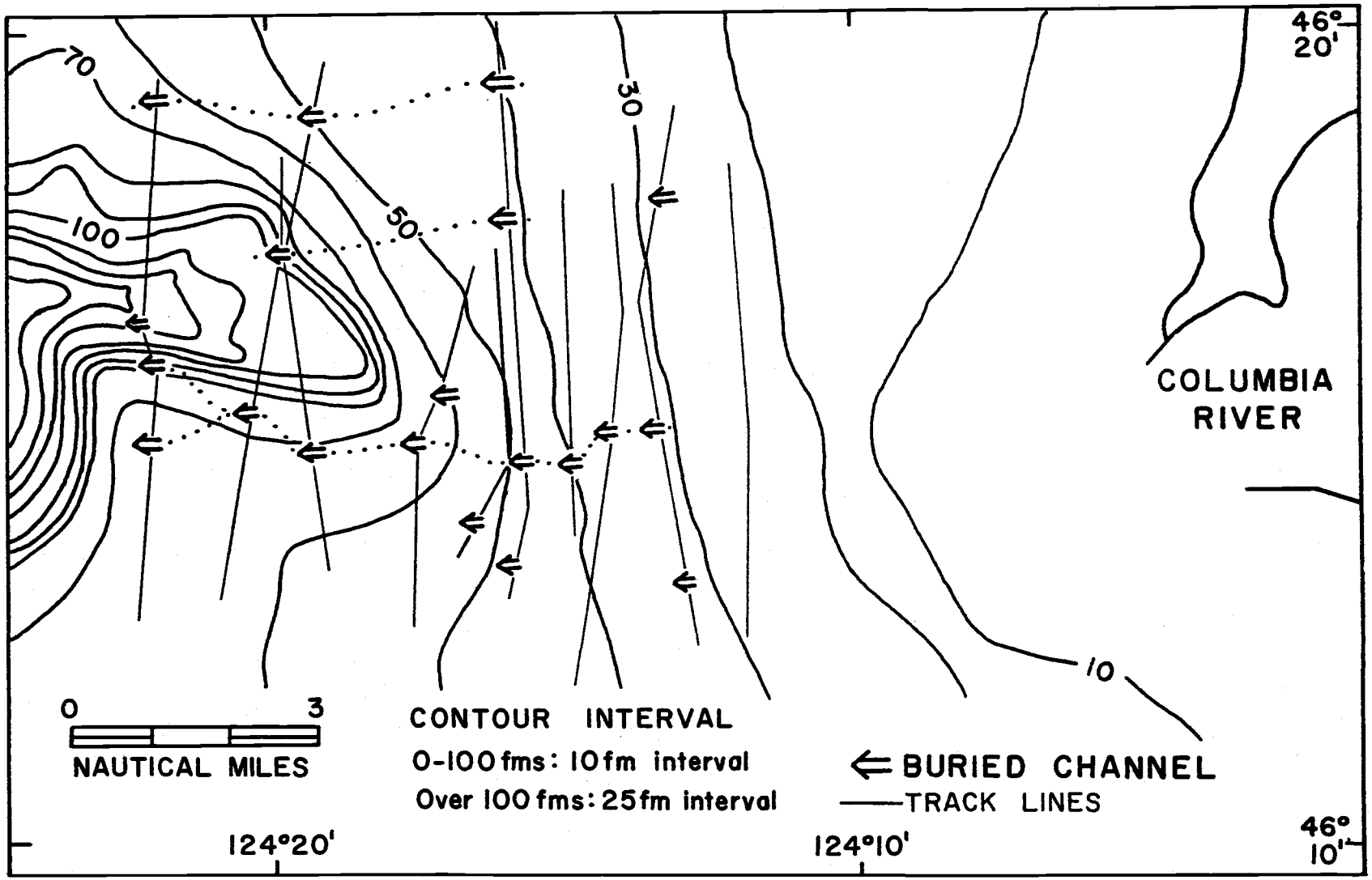

Figure 14. Location of the buried channels located between the head of Astoria Canyon and the mouth of the Columbia River.

4.5 miles across at the top of the walls. The two walls have close to the same relief, averaging 175 fathoms, and the axial slope at this point is 0°34'. This profile (W) and the first channel profile (X) have identical axial slopes and the same widths across the top of the profiles, but quite a marked change in other measurements. As illustrated in Figure 10, the channel floor becomes more than four times as wide as the canyon floor and the relief diminishes to 100 fathoms. The profiles of Astoria Channel show a distinctive levee system. According to Shepard (1965b) the best criteria for distinguishing between submarine canyons and fan-valleys are changes in transverse profile with a decrease in wall height and a development of levees.

Astoria Channel makes a sharp left hook just beyond the zone of transition from canyon to channel (Figure 8). This left hook was first reported by Menard (1955) and attributed to Coriolis forces. He suggested that greater buildup of the levees on the right side of the channel than on the left side would result in a migration of the fan channel from right to left across the fan. In addition to Astoria Channel, numerous other channels radiate from positions near the mouth of Astoria Canyon. Figure 15 shows the location of these channels which have all the appearances of distributary channels. Table 2 lists their dimensions. The northernmost of these eight distributaries is traced back to a break high on the north wall of

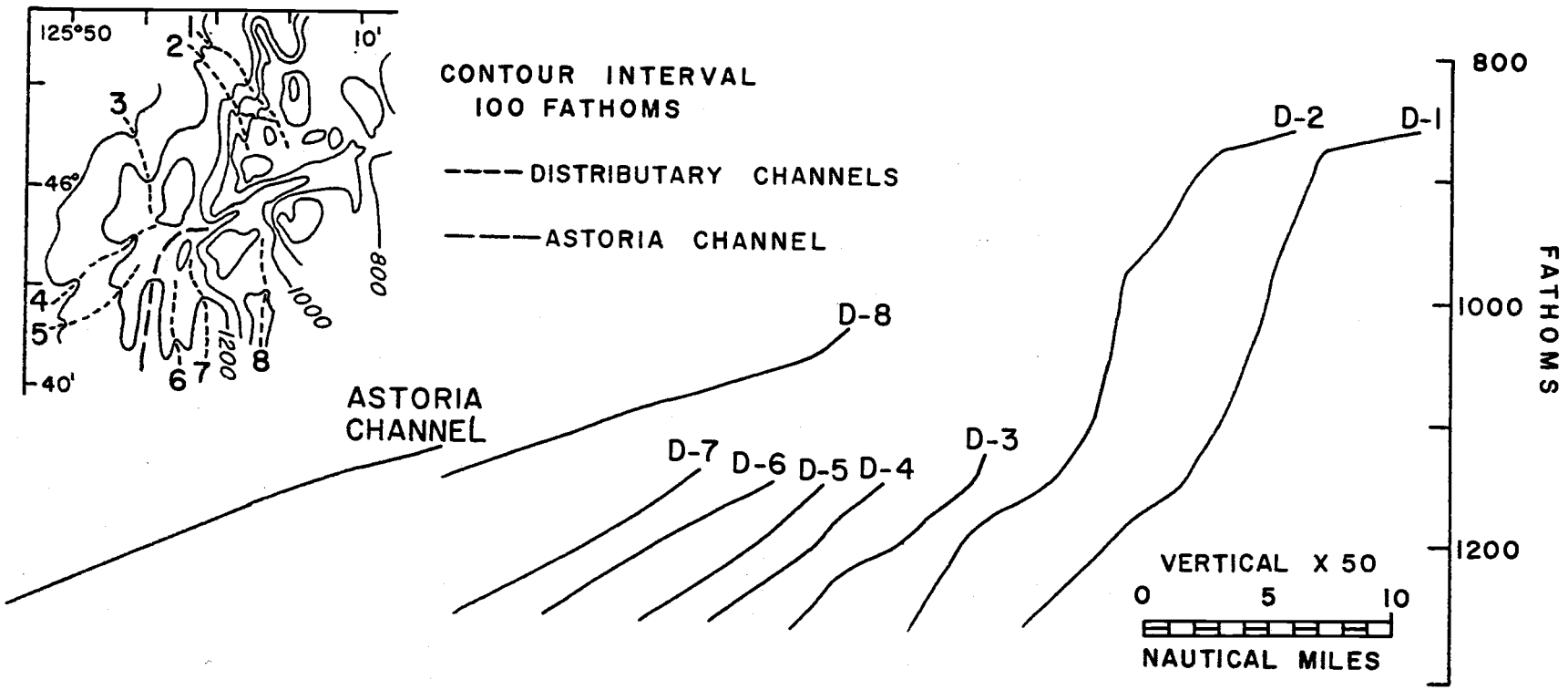

Figure 15. Longitudinal profiles of the distributaries of Astoria Submarine Canyon.

Astoria Canyon having a position of approximately 46°03'N, 125° 19'W. A PDR trace across the main axis of Astoria Canyon along this line of longitude (Figure 16, G) provides an oblique section across this distributary near its point of origin on the north wall of the canyon. Also shown in Figure 16 are additional cross sections of this and other distributary valleys. The decline in gradients, together with the position of these distributary valleys related to Astoria Channel, and the location of the apex of Astoria Fan above the mouth of Astoria Canyon, may be indicative of movement of the active channel from north to south during the Pleistocene as suggested by Menard (1955).

Table 2. Distributary valleys of the Astoria Canyon--Astoria Fan system to a depth of 1250 fms.

	Length (naut. miles)	Axial relief (fms)	Axial slope
D-1	16	390	1°24'
D-2	17	390	1 18
D-3	6.7	125	1 03
D-4	6	100	0 58
D-5	4.5	100	1 15
D-6	9	110	0 42
D-7	8.5	125	0 50
D-8	16.5	125	0 26
ave.	10.5	183	1°00'
Main channel (D-9)	16.3	125	0°26'

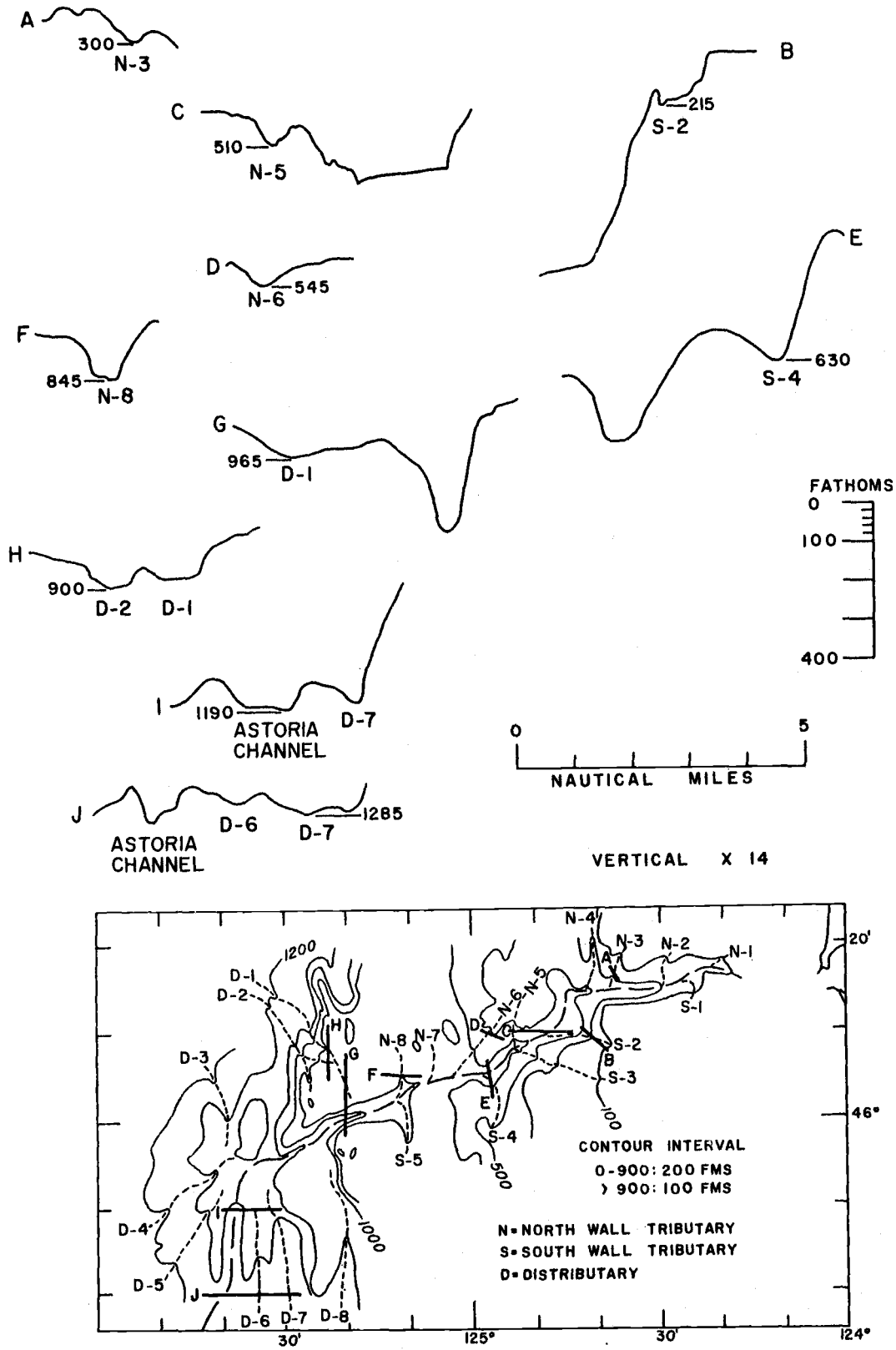

Figure 16. Astoria Canyon tributary and distributary profiles traced from precision depth recordings.

Tributary System

A total of 13 tributaries contribute to the drainage pattern of the Astoria Canyon system. Eight cut into the north and five into the south wall. The locations of these tributaries can be seen in Figure 12 and their lengths, depths and axial slopes are recorded in Table 3.

The tributaries on the north side of the canyon are shorter, averaging 6.1 miles, than those on the south side which average 7.6 miles in length. The lengths of the tributaries on the north are probably limited by the presence of Willapa Canyon which is approximately ten miles north of Astoria Canyon. Willapa also has a large network of tributaries, some of which head farther south than some of the northernmost tributaries of the Astoria Canyon system (Figure 5).

Although the north wall of the canyon is steeper than the south wall, the reverse is the case with the average tributary gradients. The axial slopes of the northern tributaries average 2°09'; whereas, those on the south wall average 2°56'. The maximum measured slope is 11°10' for a range of 100 fathoms near the upper end of tributary S-4. A comparison of the tributary axial slopes to the axial slope of Astoria Canyon is made in Figure 11. The slopes of the south wall tributaries, S-1 through S-4 are very similar, all

Table 3. Tributary valleys of Astoria Submarine Canyon.

Number	Length (naut. mi.)	Depth range (fms) Head to Mouth		Average axial slope	Maximum steepness Range (fms)	Maximum steepness axial slope
N-1	3.0	70	175	1° 58'	125-150	4° 43'
N-2	5.0	70	310	2 43	200-250	9 21
N-3	6.0	70	450	3 35	225-425	5 38
N-4	7.0	275	510	1 54	350-375	7 01
N-5	8.0	375	700	2 18	500-650	5 38
N-6	8.5	425	835	2 44	575-675	7 01
N-7	4.0	815	885	0 59	825-875	1 57
N-8	7.0	825	945	0 58	825-850	7 01
Average N. Wall	6.1			2 09		
S-1	3.0	80	280	3 49	100-250	5 38
S-2	8.8	80	640	3 35	350-550	8 24
S-3	9.0	125	715	3 36	400-550	7 18
S-4	7.0	425	815	3 09	450-550	11 10
S-5	10.0	860	950	0 31	875-950	0 48
Average S. Wall	7.6			2 56		

greater than three degrees, but S-5 has an average inclination that is even less than the canyon axial slope at the point where this tributary enters. The reason for this low inclination is the location of the tributary in one of the north-northwest trending troughs (Figure 12). A similar situation is encountered on the north side of the canyon for tributaries N-7 and N-8, although on this side the uppermost canyons are much more irregular in slope.

The lowermost canyons, those entering Astoria Canyon below an axial depth of 700 fathoms, tend to have a parallel alignment (Figure 12). The most logical explanation for this is the influence of the regionally oriented ridges and valleys dominating the slope in this area (Figures 2 and 5).

Summary and Discussion

Astoria Submarine Canyon begins nine miles west of the north jetty of the Columbia River at a water depth of 55 fathoms. It has cut a sinuous south-westerly path across the continental terrace for 62 nautical miles with an average axial slope of approximately one degree. At a water depth of 1140 fathoms the canyon hooks south onto Astoria Fan where it changes form and becomes known as Astoria Channel.

The average width of Astoria Canyon is 3.8 miles from rim to rim and 1.2 miles across the floor. Transverse profiles vary from

U- to V-shapes. The average slope of the walls is 6° with a maximum slope, measured from Precision Depth Recordings, of almost 30°. Slumping seems common and appears to be most prevalent at the base of the slightly steeper north wall.

Thirteen tributaries are incised into the walls of Astoria Canyon. They have an average axial slope of slightly more than 2° with a maximum of 11°. It appears that these tributaries enter the canyon at grade, although it is possible that some of the steeper tributaries may be of the hanging valley variety reported by Shepard and Dill (1966) to be so prevalent in some of the southern California canyons. In the lower canyon, the tributaries occupy north-northwest trending structural troughs. As a result, these tributaties show a similar alignment and enter the main canyon at a very low gradient.

Buried channels have been discovered between the head of the canyon and the mouth of the Columbia River. These channels, having dimensions of up to two miles in width and 50 fathoms in depth, are believed to represent Pleistocene drainage.

Radiating from the mouth of Astoria Canyon are a series of deep-sea fan channels. Astoria Channel, which is the most pronounced of these channels, is thought by Menard (1955) to have migrated from north to south across the fan during the Pleistocene.

Astoria Canyon is physically similar to most submarine

canyons. In Table 4 Astoria Canyon is compared to a variety of other canyons throughout the world. As can be expected, the dimensions vary greatly. Astoria Canyon more closely resembles its neighbor to the north, Willapa Canyon, than any of the others. It also bears a striking similarity to Hudson Canyon on the east coast of the United States.

In addition to the dimensional similarities of Astoria, Willapa and Hudson Canyons, several other features[1] common to these canyons are listed below:

(1) V-shaped transverse profiles,

(2) Numerous tributaries,

(3) High, steep canyon walls,

(4) Concave longitudinal profiles with local step-like steepening,

(5) Locations near river valleys which probably connected to canyons during lower stands of sea level,

(6) Canyon heads located in water depths beyond zone of longshore drift,

(7) Sediment supplies currently restricted but probably greater during Pleistocene,

(8) Definite connection to fan-valleys in the case of Astoria and

---

[1] Data for Willapa and Hudson Canyons taken from Shepard and Dill (1966), Royse (1964) and Heezen, Tharp and Ewing (1959).

Table 4. Dimensions of Astoria Canyon compared to submarine canyons in various parts of the world. Data for all but Astoria Canyon from Shepard and Dill (1966).

Canyon name and geographic area	Canyon length (naut. mi.)	Depth (fms) Canyon head	Depth (fms) Canyon mouth	Axial gradient (meters/km.)
U.S. West Coast				
Astoria	62.0	55	1140	17
Willapa	60.0	83	1166	24
Eel	27.0	42	1417	51
Monterey	60.0	9	1600	27
Redondo	8.0	5	320	39
Scripps	1.5	10	150	97
LaJolla	7.3	8	300	40
Ave. for Calif. Canyons	21.5	18	881	54
U.S. East Coast				
Oceanographer	17	100	1205	65
Hudson	50	50	1467	25
Ave. for East U.S. Canyons	26.2	66	1104	40
Western Europe				
Black Mud	30	150	2033	57
Cap Breton	135	67	2183	58
Aviles	65	10	1333	20
Ave. for Europe	52	89	1871	42
Mediterranean				
Grand Rhone	15	100	925	55
Nice	12	25	977	79
Ave. for Mediterranean	17	46	1060	61
Japan				
Tokyo	30	50	817	26
Kamogawa	25	33	1517	59
Ave. for Japan	29	50	789	60
Others				
Bering	220	100	1860	8
Great Bahama	125	600	2343	13
Congo	120	20	1167	10
Ave. for all	30	58	1158	58
Maximum range	1.5-220	5-600	150-2343	8-97

Hudson Canyons; connection probable for Willapa Canyon,

(9) Consolidated and/or semi-consolidated sedimentary rocks dredged from walls,

(10) Similarities in sediments in all three canyons.

Details of the sedimentological similarites will be presented in the next chapter.

IV. SEDIMENTOLOGY

Sampling

To obtain a picture of the environments of sedimentation in the Astoria Canyon region, samples were collected from the floor and walls of the canyon and from the adjacent shelf-slope region. The sample sites are shown in Figure 17 with latitudes, longitudes and water and core depths listed in Appendix 1. No cores were collected in the canyon mouth area because of the Navy Ammunition Dump located there. Samples were obtained using three different types of equipment; a modified Kullenberg piston corer, Phleger-type gravity corers, and a pipe dredge. The rotary core shown in Figure 17 (number 20) represents samples obtained from Standard Oil of California. These core samples were taken from an anchored barge. Samples from this hole represent the only deep samples obtained. The bottom-most of the seven samples is from 145 meters (435 feet) below the sediment-water interface. At the other sample sites the piston core samples were longest, up to 625 cm (20.5 feet), with an average core length of 415 cm (13.6 feet). The gravity cores averaged approximately 38 cm (15 in) in length.

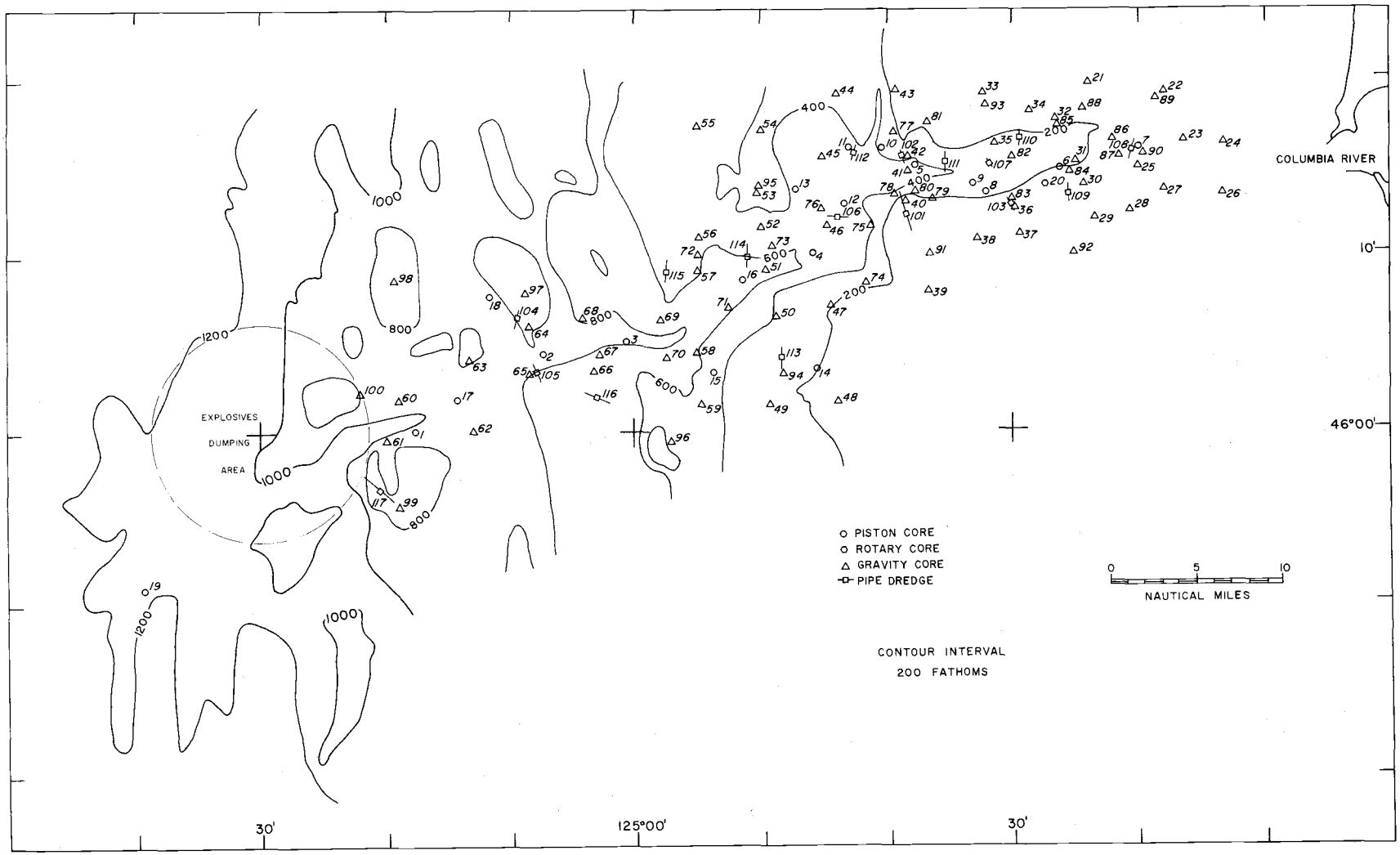

Figure 17. Sample location map of the Astoria Submarine Canyon region.

Core Processing

The cores, which were collected in plastic liners, were kept under refrigeration to prevent deterioration. The processing involved cutting the plastic liner with a circular saw, cutting the core lengthwise with a thin wire, photographing and describing the core. The sample increments were chosen on the basis of lithologic and color changes. Where lithology and color appeared homogeneous, samples were taken at 150 cm intervals. Because the samples were taken for several reasons (textural, mineralogical and micro-fossil studies), a sample up to 5 cm in length was collected where possible. This was not possible for many of the coarse layers, and in these cases the entire coarse layer was removed.

Analytical Procedures

The laboratory procedures used in analyzing the sediments are listed in Table 5. Some of the procedural modifications adopted are explained in Appendix 4.

An IBM 1410 computer was used to reduce the textural data to the statistical parameters of Inman (1952). Because of the fineness of the sediments, the 95th percentile was seldom obtained by the time the 24 hour hydrometer reading had been taken. As a result, an extrapolation technique was developed by Mrs. Susan Borden,

Table 5. Procedures of sediment analyses.

Procedure	Reference
Sea-water removal (millipore filters)	Krumbein and Pettijohn (1938)
Sediment dispersal (sodium hexametaphosphate) and hydrometer analysis	ASTM (1964)
Sieve analysis ($\sqrt[4]{2}$ series)	Krumbein and Pettijohn (1938), McManus (1965)
Modified Emery settling tube	Emery (1938), Poole (1957)
Description of color for moist sediments	G.S.A. (1963)
Coarse fraction analysis*	Shepard and Moore (1960)
Heavy mineral separations*	Fessenden (1959), Livingston (1964)
Magnetic separator	Appendix Four
Mounting of heavy minerals (Canada balsam)	Krumbein and Pettijohn (1938)
Mounting (Lakeside cement) and staining of light fraction	Bailey and Stevens (1960)
Organic and carbonate carbon	Curl (1962)

* Modifications of these techniques are explained in Appendix Four.

Oregon State University Oceanography Department statistician. The 95th percentile was obtained for clay-rich sediments by linear extrapolation using the last two points on the curve. The small number of samples coarse enough to give a direct reading for the 95th percentile makes the use of Folk and Ward (1957) parameters questionable. The parameters defined by Trask (1932) are quite inaccurate as approximations of the statistical moment measures (Folk, 1966). Because the statistical approximations proposed by Inman require the 86th percentile reading which is obtained in a large number of the samples and because the accuracies of these statistics are closer to the true moment measures than are Trask's statistical measures (Folk, 1966), all of the textural data included in this report have been computed using the statistics suggested by Inman (1952). Appendix 2 includes the values of Mdϕ (Median), Mϕ (Mean), $\sigma\phi$ (sorting or standard deviation), and $\alpha\phi$ (skewness) for all of the samples for which mechanical analyses have been run.[2] The coarse fraction analyses are listed in Appendix 3.

---

[2] Computed parameters using the equations of Folk and Ward (1957) and Trask (1932) are on file in the Oceanography Department, Oregon State University.

Texture and Coarse Fraction

Based on variations in texture, structure and color, the sediments of the Astoria Canyon area can be separated into six fairly distinct types. These sediment types are: olive gray silty clay, gray silty clay, laminated gray clayey silt, coarse layers, non-layered sandy sediment, and mixed or mottled sediment (Figure 18). Within these groups there are distinct characteristic coarse fractions (Figure 19).

The sediments can also be considered in the light of their physiographic position. Physiographically the canyon region consists of three main parts; canyon floor, canyon walls and tributaries, and adjacent continental terrace.

A very brief explanation of the stratigraphic relationships will set the stage for a discussion of the sediments. Draped over the entire canyon region is a blanket of olive-gray sediment of variable thickness. This layer represents sediment accumulation during postglacial time. Underlying the postglacial olive-gray sediment is an undetermined thickness of sticky gray silty clay which is somewhat finer than the postglacial sediment. The upper portion of this gray clay is considered to be Pleistocene. Substantiation of the Pleistocene age for the gray clay will be given in subsequent discussion. Within the Pleistocene sediments, coarse layers appear

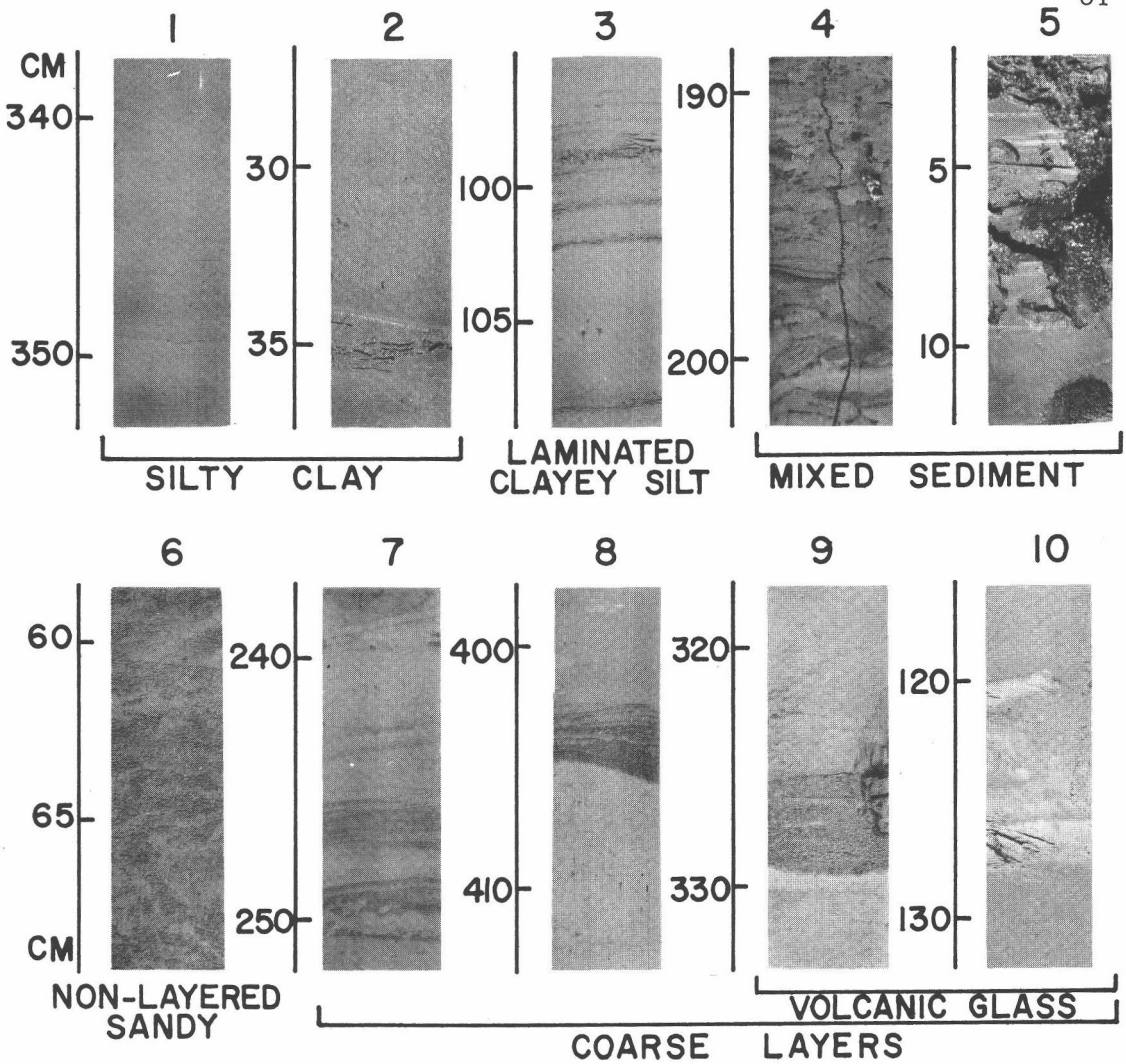

Figure 18. Sediment types in the Astoria Canyon region:
(1) olive gray silty clay, core 12;
(2) gray silty clay, core 61;
(3) laminated gray clayey silt, core 11;
(4) mixed sediment, possibly the result of slumping, core 6;
(5) mixed sediment, burrowing activity of benthic organisms, core 77;
(6) non-layered sandy sediment, core 84;
(7) coarse layers, mica-rich, core 19;
(8) coarse layer, quartz, feldspar and rock fragment rich, core 1;
(9) coarse layer, over 50% of coarse fraction is volcanic glass, but also high in quartz, feldspar and rock fragments, core 1;
(10) coarse layers, almost pure volcanic glass, core 18.
Sample locations in Figure 17.

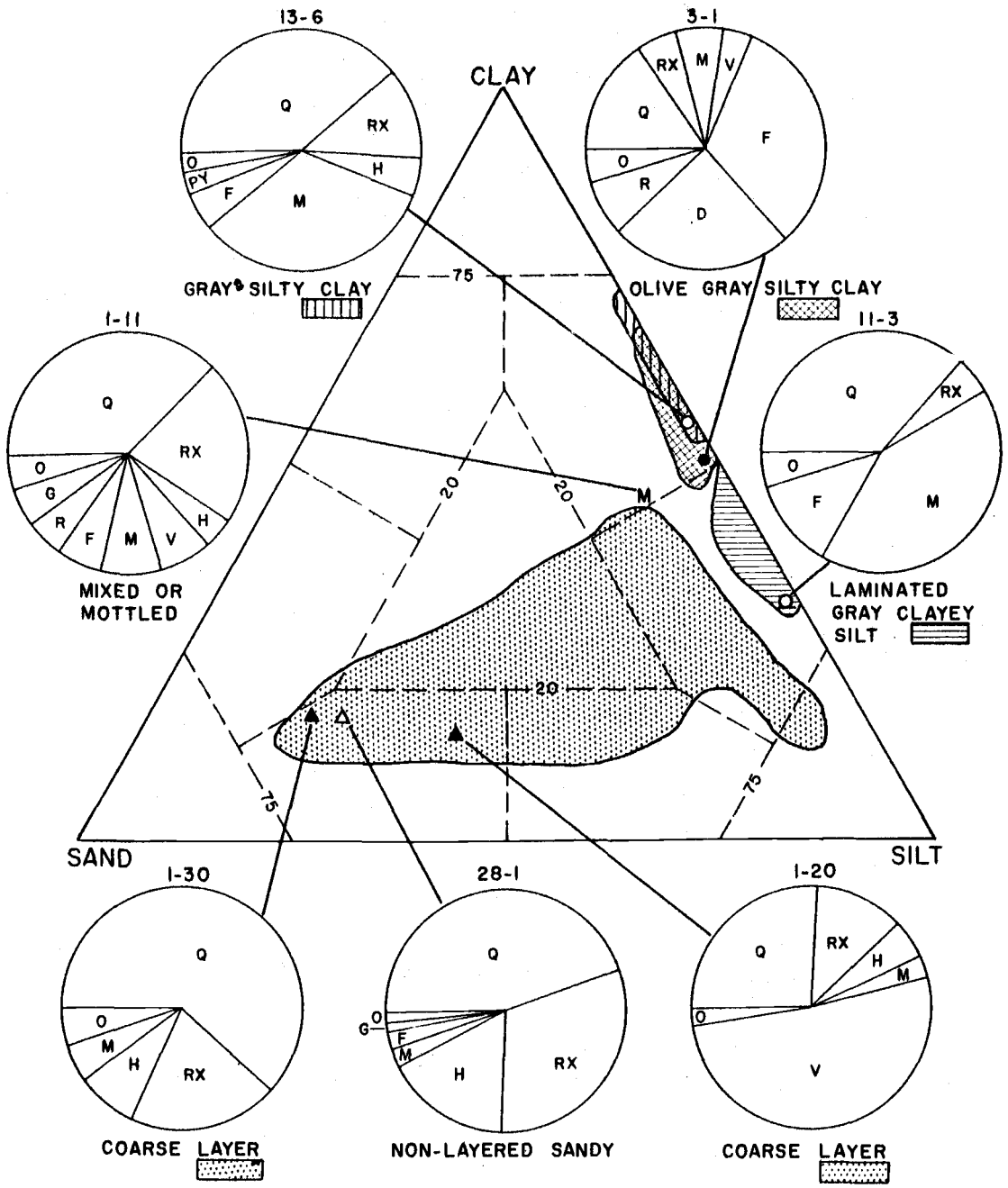

Figure 19. Coarse fraction compositions of the various sediment types. The number above each circle graph is the sample number chosen as representative of that type. Q = Quartz + Feldspar, RX = Rock fragments, H = Heavies, M = Mica, V = Volcanic glass, G = Glauconite, Py = Pyrite, O = Other. (Percentages of coarse fraction components listed in Appendix 3; sample locations in Figure 17.)

to be more prevalent than in the postglacial sediments.

In Table 6 the percentages of sediment type thickness based on centimeters of core length are listed according to physiographic areas. The olive gray silty clay is most prevalent on the canyon floor and in the tributary valleys. On the canyon walls the postglacial olive gray clay is much thinner. At some sample sites on the walls and adjacent shelf, the Pleistocene gray silty clay crops out within a very few centimeters of the surface. Some gray clay was cored in the tributary valleys, but was always found at least 100 centimeters below the sediment surface. Laminated gray clayey silt, although found in relatively minor amounts, appears to be a significant part of the Pleistocene canyon wall sediments. In addition to unconsolidated and semi-consolidated sediments, gray siltstones and shales of possible Pliocene to Pleistocene age were dredged from the canyon walls.

Olive Gray Silty Clay

The color of this sediment which mantles the surface of the entire area is olive gray (5 Y 3/2) based on a comparison of the damp sediment to the GSA color chart (1963). Table 7 lists ranges of the Inman textural parameters for this silty clay. It is very poorly sorted and primarily positively skewed. The coarse fraction ($> 62\mu$) composition is dominated by terrigenous materials, especially

Table 6. Percents of sediment types in cores from the different physiographic areas of the Astoria Canyon region. Percents are figured on centimeters of core length. (P = Piston core, G = Gravity core.)

Location	Canyon Floor		Walls		Tributaries	Adjacent shelf-slope	Totals	
Types of cores	P	G	P	G	P	G	P	G
Number of cores	11	7	4	40	3	23	18	70
Average length of cores (cm)	475	37	239	43	417	26	413	37
Sediment types	Percent of core length							
Olive gray silty clay	75	88	18	36	82	23	68	38
Gray silty clay	2	0	38	16	15	14	9	14
Laminated gray clayey silt	1	0	10	4	0	1	2	3
Coarse layers	9	1	21	7	3	2	10	5
Non-layered sandy sediment	9	9	12	31	0	54	8	34
Mixed or mottled	4	2	1	6	0	6	3	6

Table 7. Ranges in textural parameters of the sediment types in the three physiographic areas. Statistics calculated using equations developed by Inman (1952). (Values in phi units. Phi = $-\log_2$)

Physiographic area	Sediment type	Median	Mean	Sorting	Skewness
Canyon floor	Olive gray silty clay	7.6- 9.0	7.8- 9.2	1.8- 3.8	(-.1)- .4
	Coarse layers	3.2- 7.6	4.5- 7.8	1.4- 4.0	.0 - .7
	Non-layered sandy sediment	6.0- 7.9	5.7- 7.9	3.1- 5.5	(-.1)- .3
	Mixed or mottled	6.5- 9.8	8.2- 9.4	2.3- 4.4	(-.3)- .4
Canyon walls and tributaries	Olive gray silty clay	7.6- 9.2	8.2- 9.2	2.0- 3.4	(-.1)- .2
	Gary silty clay	8.2-10.1	8.6-10.1	2.0- 3.3	.0 - .2
	Laminated gray clayey silt	5.1- 7.9	5.9- 8.5	1.6- 3.0	.2 - .5
	Coarse layers	2.5- 8.3	3.1- 7.9	1.2- 5.3	(-.1)- .7
	Non-layered sandy sediment	3.3- 8.3	4.6- 8.3	0.8- 4.7	(-.3)- .7
	Mixed or mottled	6.1- 9.2	5.0- 9.7	2.2- 4.4	(-.3)- .3
Shelf and slope	Olive gray silty clay	8.0- 8.9	8.5- 8.9	2.3- 3.4	(-.1)- .1
	Non-layered sandy sediment	2.8- 7.6	3.1- 7.8	.8- 4.0	.1 - .8
	Relict sands	2.0- 3.1	3.1- 3.7	.8- 1.6	.6 - .7

quartz, feldspar, rock fragments and plant fragments. In addition, some of the olive gray clay contains abundant biogenic constituents. A typical coarse fraction composition is represented in Figure 19.

Canyon floor. Olive gray silty clay makes up > 75% of the sediment cored from the floor of Astoria Submarine Canyon. Comparing samples of this sediment type down the floor of the canyon, the following relationships can be observed with increasing water depth: particle size decreases; sorting becomes poorer; and skewness varies from positive and negative values above 600 fathoms to strictly positive values in the lower part of the canyon. A comparison of all the olive gray silty clay sediment to that sediment found only at the surface of the canyon floor shows great similarity of median, sorting and skewness (Figure 20). This indicates the fine nature of the sediment presently being deposited in the canyon, most of which is olive gray silty clay.

The coarse fraction components of the olive clay also undergo systematic changes down the canyon. Radiolarians and planktonic foraminifers become increasingly more abundant with distance down the canyon. Diatoms increase in abundance to mid-canyon depths, with an average of about 30% of the coarse fraction in the vicinity of the shelf-slope break, then decrease in relative abundance. In most of the samples of olive gray silty clay analyzed, the diatoms are most abundant (ave ~ 20%). The radiolarians are also abundant

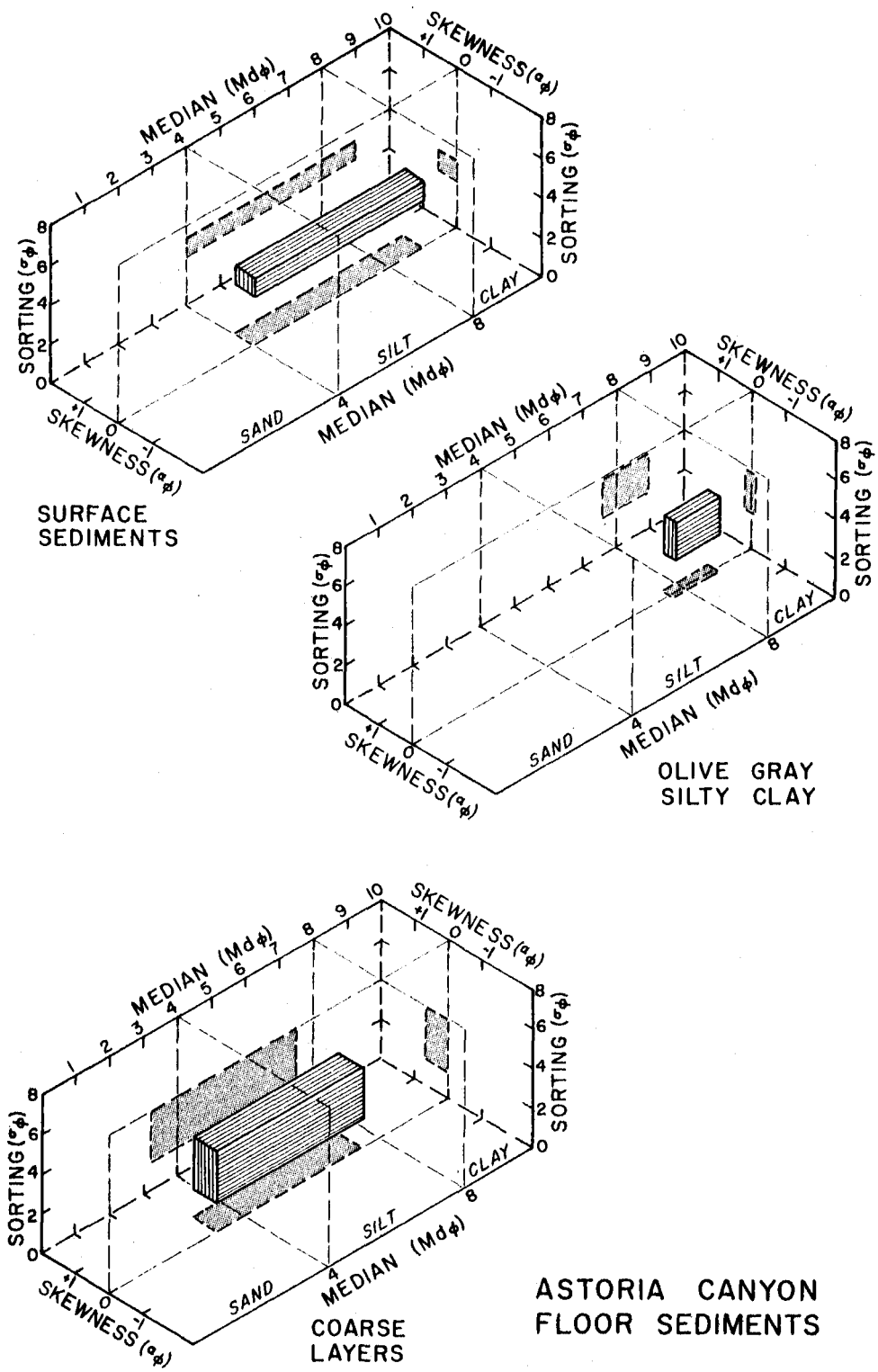

Figure 20. Canyon floor samples: Median (Mdφ), Sorting ($\sigma\,\phi$) and Skewness ($\alpha\,\phi$) variations. The prism in each 3-D graph represents the combined projections of the three areas enclosing the limits of the designated sediment type.

(ave > 5%), but the planktonic foraminifers only average about one percent of the coarse fraction.

Plant fragments are most common in the olive muds of the canyon floor. There is a general decrease in the relative abundance of these terrigenous organic components with distance down the canyon, from about 25% of the coarse fraction in the upper part of the canyon to < 10% near the terminal end.

Terrigenous components in general make up a smaller percentage of the coarse fraction in these olive gray muds than in the other sediment types. Mica increases with distance down canyon, whereas, as a coarse fraction component the more spherical mineral and rock fragments show a slight decrease in abundance down the canyon. This geographic sorting indicates the significance of shape as a hydrodynamic factor in sediment transport.

Canyon walls. The olive gray silty clay is much thinner on the walls of the canyon than in cores from the canyon axis (Table 6). However, if the three piston cores taken from tributary valleys are included with the wall sediments, this percentage increases.

A comparison of the textural parameters of the olive mud collected from the walls to that from the canyon floor reveals some marked differences (Figures 20 and 21). There is a greater range in size of the wall sediments; the sorting of the wall mud increases rather than decreases in a down canyon direction; and the skewness

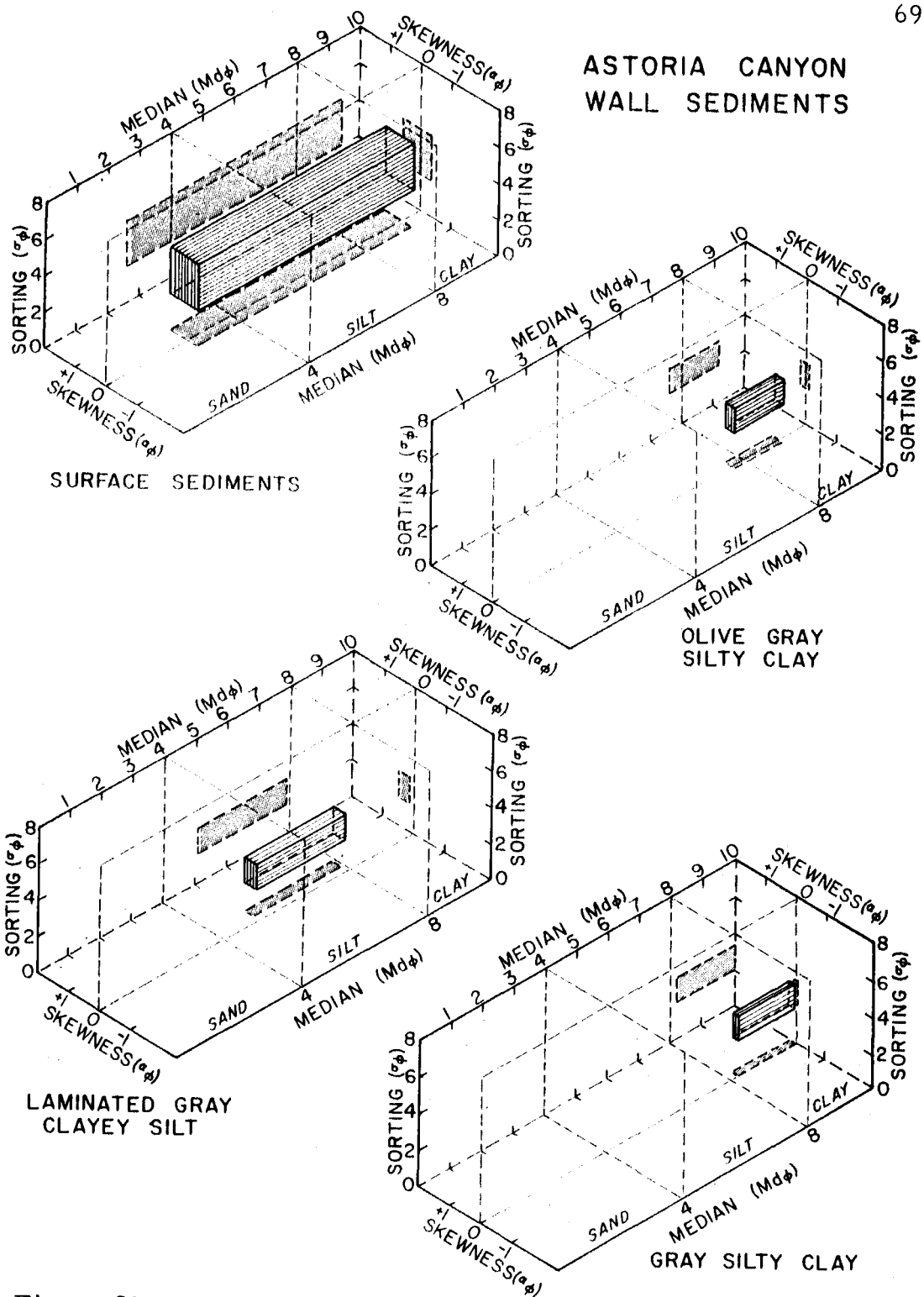

Figure 21. Comparisons of Median (Mdϕ), Sorting (σϕ) and Skewness (αϕ) of canyon wall samples. The prism in each 3-D graph represents the combined projections of the three areas enclosing the limits of the designated sediment type.

is quite different. The sediment is positively skewed in both the upper and lower portions of the canyon, but a negative skewness characterizes the olive gray silty clay wall samples in the middle part of the canyon.

The trends of planktonic organisms in the olive mud of the canyon walls is similar to that of the floor. Plant fragments, although not quite as abundant in the wall sediments as on the canyon floor, also decrease with distance from shore. The percentage of mica, however, is fairly constant in all the olive mud collected from the canyon walls.

Shelf-slope. The olive gray silty clay present in the cores taken on the continental terrace adjacent to the canyon has much the same character as other olive gray mud.

Gray Silty Clay

This gray (N-4)[3] clay appears to underlie the olive gray silty clay throughout the entire area of investigation. The ranges of textural parameters are listed in Table 7. The gray clay is somewhat finer grained than the overlying olive clay as illustrated by the frequency polygons of Figure 22. Figure 18 contains a photo of typical very poorly sorted, positively skewed, sticky gray clay.

---

[3] G. S. A. (1963).

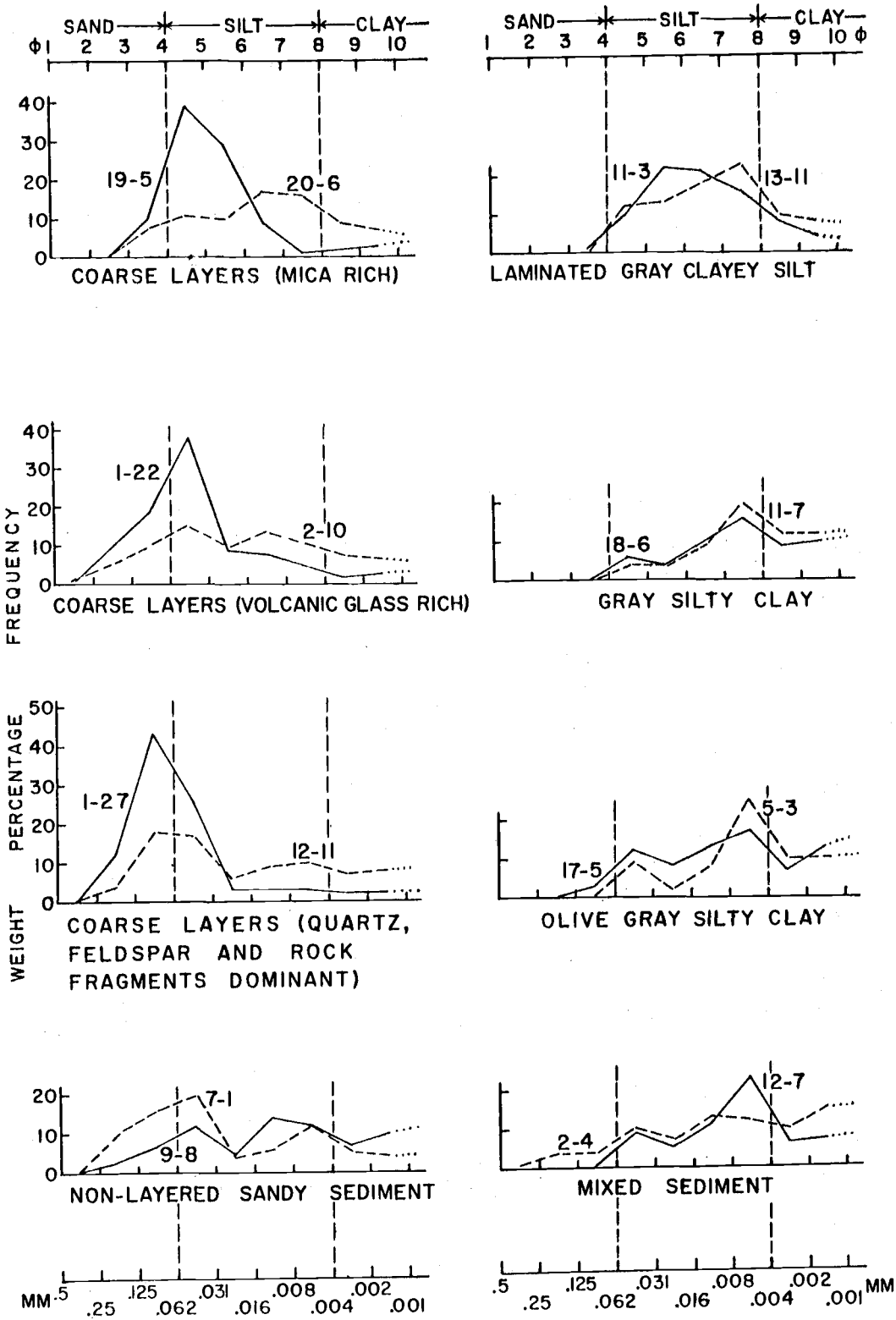

Figure 22. Frequency polygons of representative sediment types from Astoria Canyon. Sample locations shown in Figure 17.

This clay is considerably more consolidated than the olive mud as is borne out in a comparison of water contents. The water content of the gray clay ranges from 30 to 45 percent and that of the olive mud from 50 to 70 percent of the wet weight of the sediment.

Figure 19 reveals the marked difference of coarse fraction between the olive and gray clays. The sticky gray clay is typically high in mica and low in biogenous constituents. It also is much higher in quartz and rock fragments than is the olive mud. Several of the gray clay samples have a high pyrite content.

Canyon floor. Only one of the cores taken from the floor of Astoria Canyon penetrated the gray clay. This core, number one (Figure 17), was not taken in the axis of the canyon, but at the base of the south wall. At this location the sediment fill apparently was thin enough to permit penetration to the gray clay. The small amount of gray clay present in this core does not allow any trends to be determined. The clay, however, is very similar in texture and composition to the gray clay cored on the canyon walls.

Canyon walls. Gray sticky clay is the dominant sediment type obtained by piston corer from the walls of the canyon (Table 6). It also is abundant in the gravity cores taken, but because of the short length of cores obtained with this device, not all of these cores penetrated deep enough to pass through the cover of olive-gray sediment.

Figure 21 illustrates the differences in median diameter,

sorting, and skewness of the sediment of the canyon walls. The gray silty clay, with an average median phi diameter of about nine, is finer than the overlying olive mud. The sorting of the two sediment types is about the same, but all the gray clay of the walls is positively skewed compared to the both positive and negative skewness of the olive gray silty clay. Accumulations of sand-sized glauconite pellets contribute to the low median phi values attained by some of the surface sediments of the canyon walls.

Textural trends of the gray silty clay show a slight decrease of median particle size with increase of water depth. The poorest sorting of this very poorly sorted sediment occurs between 200 and 400 fathoms and at depths greater than 800 fathoms. The skewness values are quite constant and all positive.

The composition of the coarse fraction of the gray clay exhibits trends which differ from those of the overlying olive mud. Planktonic foraminifers are more abundant than radiolarians in the gray clay; the opposite is true of the olive mud. There is a slight increase in both planktonic foraminifer and radiolarian abundance with distance down the canyon. The diatoms are most prevalent in sediments of the middle portion of the canyon, near the shelf-slope break, and then decrease in a down-canyon direction. The detrital constituents of the gray silty clay make up more than 60% of the coarse fraction in most samples. The exceptions are those wall samples high in

authigenic constituents, especially pyrite. Quartz and feldspar are generally the most prevalent of the detrital components. The most distinctive component, however, is the mica. The mica and the other platy material of the coarse fraction, the plant fragments, decrease in percent in a down-canyon direction. The other detrital components are quite constant throughout the gray clay.

Shelf-slope. Very few of the shelf-slope cores contained gray silty clay, therefore no conclusions can be drawn regarding textural and compositional trends. The textural and compositional characteristics of this sediment, however, are very similar to the gray silty clay of the canyon walls.

Laminated Gray Clayey Silt

A typical section of this laminated sediment is shown in Figure 18. The gray clay is the same color as that previously discussed. It differs in that it contains fine laminae of micaceous silt. These silt laminae are generally found in groups as shown in the photograph. Occasionally a single layer of silt interrupts the homogeneous gray clay. A very high mica content accounts for the laminated character of this clayey silt. This preponderance of mica is clearly illustrated in Figure 19. It can be seen that the terrigenous elements of the coarse fraction are by far the most plentiful constituents. Plant fragments are also very abundant. Mica and plant fragments are

hydrodynamically equivalent to more equidimensional grains of much smaller diameter. The preponderance of these platy grains is an indication of low current velocity.

The walls of Astoria Canyon represent the only physiographic area of the three discussed to contain any significant amounts of laminated gray clayey silt. Even on the walls this sediment type is minor in amount (Table 6). Figure 21 shows a comparison of this sediment's textural parameters to those of the olive gray silty clay and the gray silty clay. The laminated silt is coarser, slightly better sorted, and more positively skewed than the other types. The frequency polygons in Figure 22 illustrate a typical particle size distribution. Compositionally this laminated clayey silt is much higher in detrital constituents than either the olive or gray clay.

The following trends in texture and composition characterize the laminated sediment:

(1) Particle size remains constant with water depth.

(2) Sorting becomes poorer with distance down the canyon.

(3) Skewness is positive with a slight increase down the canyon.

(4) Planktonic foarminifers are much more plentiful than either diatoms or radiolarians, but none show any noticeable trends with depth.

(5) Plant fragments are sporadic but fairly abundant.

(6) Mica is extremely abundant and exhibits an increase with

distance down the canyon.

Coarse Layers

Many of the cores penetrated very sandy sediment and frequently the sand was concentrated in distinct layers of different thickness. Many of these layers consist of sediment having a median diameter that is coarse silt size rather than sand size; therefore, the term coarse layer is used rather than sand layer. These coarse layers range in thickness from less than one centimeter to greater than ten centimeters. They are somewhat better sorted than the other sediment types, but still must be considered poorly sorted according to Folk and Ward's sorting ranks (1957). The ranges of textural parameters of the coarse layers are listed in Table 7.

The coarse layers are of several types. In each type the detrital element is supreme, but the particular detrital component varies. Some layers are very high in volcanic glass, up to 72% of the coarse fraction; others are primarily quartz, feldspar and rock fragments; and a third type consists of very large amounts of mica. Figure 18 contains photographs of the various types of coarse layers. A comparison of their compositions can be seen in Figure 19 and the particle size distributions can be compared in Figure 22, a plot of the frequency polygons of typical sediment types.

Canyon floor. The coarse layers contained in cores collected

from the floor of Astoria Submarine Canyon range in median diameter from very fine sand to very fine silt size. A comparison of the textural parameters, median, sorting and skewness, between the coarse sediments and the other sediment types of the area can be seen in Figures 20 and 21. The sediments of these coarse layers are poorly to very poorly sorted. There is a slight trend to better sorting with distance down the canyon. However, there is no apparent trend in sorting with depth in the core. The thickness of the layers and apparently their frequency increase with depth in the core (Figure 23).

The sediments that make up the coarse layers of the canyon floor are all positively skewed, but no significant trend is observed with distance. There is, however, a decrease in median diameter with distance down the canyon to a water depth of about 800 fathoms. Below this depth the particle size of the coarse layers undergoes an increase. This increase is continued a portion of the way down Astoria Channel where Nelson (1967) has found gravel in some of the coarse layers.

Several of the layers have a high volcanic glass content. The glass is found as angular shards, bubble shards, and pumice. It is believed to have been washed into the canyon, not deposited as a direct ash fall. The volcanic glass is most prevalent in the cores collected from the lower portion of the canyon, especially in cores

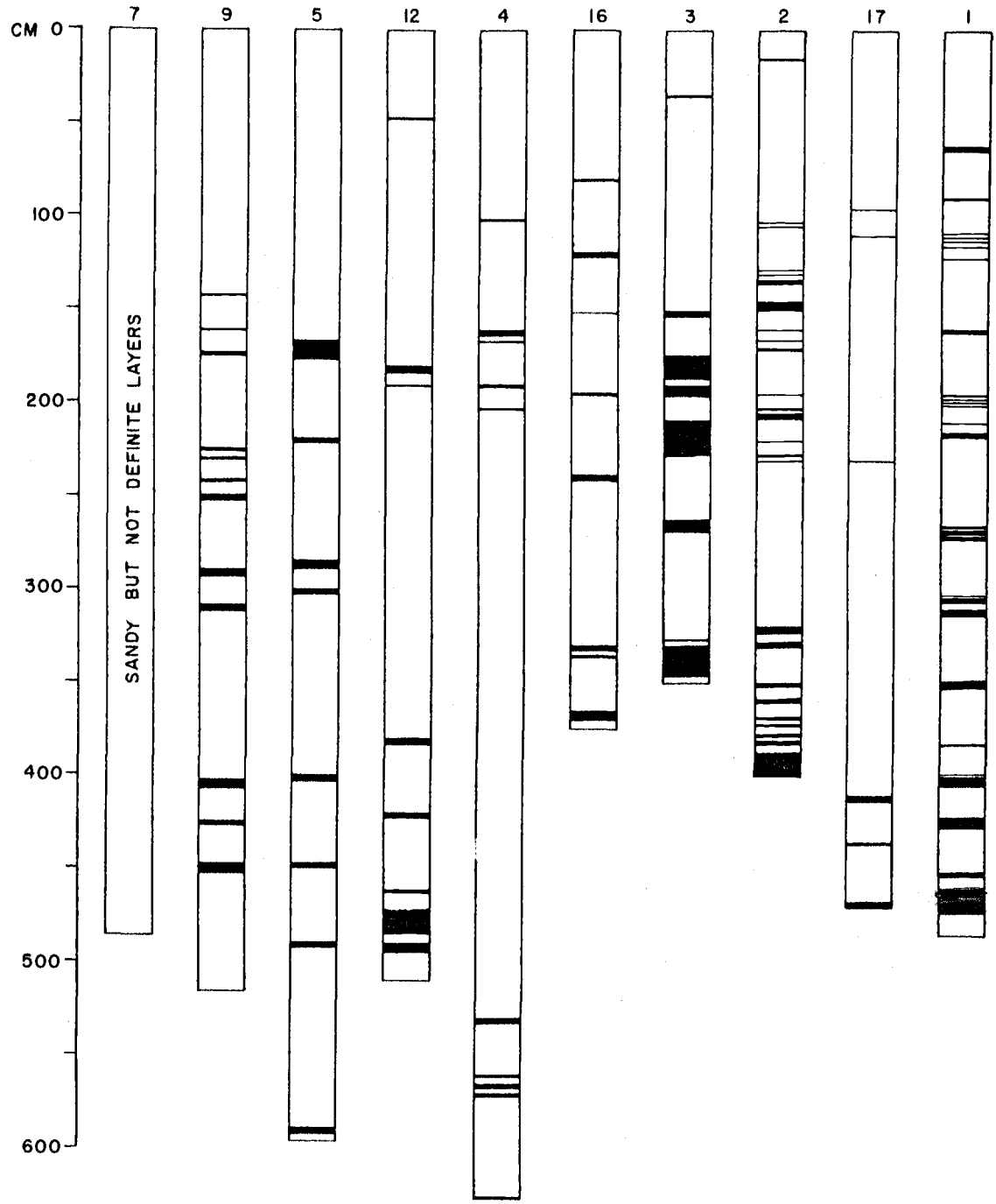

Figure 23. Cores from the floor of Astoria Canyon arranged in descending order from head of canyon at left. Identifiable coarse layers are marked. Core locations in Figure 17. Note the increased number of coarse layers near the mouth of the canyon and at depth in the core.

numbered one, two and three. In cores numbered two and three the glass content of the sediment increases from top to bottom reaching values of over 50% of the coarse fraction at the bottom of the core. In core number one, two distinct layers, each several centimeters thick, occur at a depth of 323 and 347 centimeters. Below this depth no ash is found. It may be that the ash is buried below the depth cored in the upper portions of the canyon. At the lower end of the canyon a lower sedimentation rate farther from the continental influence has not buried the glass-rich layers as deeply.

Quartz, feldspar and rock fragments are the principal constituents of most of the coarse layers. There does not seem to be any appreciable change in these quantities with distance down the canyon except for a decrease in quartz and feldspar in the volcanic glass-rich layers. Mica is much less plentiful in the canyon floor coarse layers than in the coarse layers cored on the canyon walls. Plant fragments, on the other hand, are relatively more abundant in the canyon floor layers. The tests of micro-organisms are minor constituents of the coarse layers of both canyon floor and walls. However, displaced shallow water benthic foraminifers occur in practically all of the coarse layers.

Canyon walls. There are very similar textural patterns of the coarse layers of canyon walls and floor (Figures 20 and 21). The layers of the walls have somewhat wider ranges of all three

parameters. The coarse layers of both environments show the following trends with distance down the canyon:

(1) Median diameter decreases to water depth of 700 fathoms, then increases.

(2) Sorting becomes better.

(3) Skewness remains constant and positive.

Although both wall and floor coarse fractions are largely terrigenous in composition, there are some key differences. Mica and authigenic minerals are characteristic of the wall coarse fractions. Mica is particularly dominant in some of the coarse layers, making up greater than 30% of the coarse fraction in some samples. There is an increase in the percentage of mica in an offshore direction and a corresponding decrease in percentage of heavy minerals. Most of the coarse layers in water depths of less than 100 fathoms have heavy mineral contents of greater than 10% of the coarse fraction.

Non-layered Sandy Sediments

As can be seen in Table 6 many of the cores contain sediment that has a high sand content, in some cases more than 80%, but the sand is not in distinct layers. A typical sample is shown in Figure 18. Some of the sediments in the stations near shore are moderately sorted but most of these sandy sediments are poorly to extremely poorly sorted. The median grain size of these muddy sands and

sandy muds range from fine sand to coarse clay sizes. The majority are positively skewed, but some of the deeper water samples are skewed negatively. Figure 22 shows a typical particle size distribution for this type of sediment.

Relatively high percentages of rock fragments and heavy minerals characterize the sandy sediments. A typical coarse fraction composition is illustrated in Figure 19.

Canyon floor. Sandy sediments collected from the region of the canyon floor decrease in median grain size with distance down the canyon. Most of these sediments are positively skewed, but at the lower end of the canyon some of the sediments become negatively skewed. This is in contrast to the coarse layers which are all positively skewed (Figures 20 and 21).

The chief differences in composition between the coarse layers and the non-layered sandy sediments of the canyon floor are the slightly higher contents of plant fragments, diatoms, and rock fragments in the non-layered sediments. The small differences in composition, the somewhat coarser mean grain size, and the slightly better sorting of the sediments of the coarse layers suggest that at least some of the non-layered sandy sediments may have been deposited as layers, but have since been mixed with the underlying mud by burrowing organisms.

Canyon walls. On the walls of the canyon, the non-layered

sandy sediment makes up the second largest sediment type (Table 6). It ranges in median particle size from that of very fine sand to coarse clay and is moderately to very poorly sorted. A comparison with the sandy floor sediments shows the sandy wall sediments to be generally coarser grained, better sorted and with a wider skewness range. The compositions of these sediment types on the walls and floor are quite similar. The chief differences are a lower percentage of plant fragments and slightly higher percentages of heavy minerals and rock fragments in the non-layered sandy sediments of the canyon walls.

Shelf-slope. Only gravity cores were collected from the adjacent shelf-slope region and most of these were obtained on the continental shelf. As would be expected, the sandy non-layered sediment is dominant (Table 6). It is coarser grained, better sorted and more positively skewed than either the floor or wall non-layered sands. Two compositional characteristics are the high percentages of heavy minerals and the relatively large amounts of rock fragments. Those sediments from water depths of less than 50 fathoms are high in plant fragments. Below a depth of 50 fathoms the majority of the plant fragment percentages drop to less than three percent. Glauconite content of these non-layered sandy sediments increases near the shelf-slope break.

Mixed or Mottled Sediments

The last of the sediment types from this area is termed "mixed sediment." The mixing may be the result of burrowing by benthic organisms as shown in Figure 18, or may be due to the slumping presumed to take place along the canyon walls. Slumping is best evidenced by cores from the canyon floor (Figure 18). Burrowing is the more widespread of these two phenomena.

Burrowed samples are of several types. Found most often in the canyon floor cores are burrowed coarse layers. Often the layer is almost totally destroyed by the activities of the burrowing organisms. On the canyon walls the contact between the olive mud and the underlying gray sticky clay is often disrupted by burrows. In places of slow deposition such as on high areas and in the region of the shelf break, organisms have burrowed into the glauconite forming on the surface and mixed it into the underlying gray clay. In addition to these burrowed sediments some of the homogeneous olive gray silty clay, which is so abundant in the canyon, may owe its homogeneity to the mixing activity of benthic organisms. It is difficult to determine how much of the olive gray silty clay has been disturbed by bottom feeding organisms, and for this reason this sediment is not included with the mixed sediment. There are great similarities in the textural parameters of all the mixed sediments (Table

7): they are fine grained, poorly sorted and practically all exhibit positive skewness.

Some differences exist in the composition of the mixed sediments of the different physiographic areas. The canyon floor sediments contain somewhat more plant fragments than the others, and the wall sediments contain more mica and pyrite. A constituent in common to almost all of these mixed sediments is the presence of several percent of benthic foraminifers. Some of the sand layers also have numerous benthic foraminifers, but many of them are displaced forms whereas, those in the mixed sediment are largely indigenous to the depth where found.

Sand-Silt-Clay Relationships

Surface sediments. The surface sediment distribution is shown in Figure 24. Olive gray silty clay blankets walls and floors alike in the deeper parts of the canyon. In the nearshore area the influence of sand contributed by the Columbia River and the longshore currents is evident. The map of sand percent, Figure 25, also shows high sand concentrations along the walls of the canyon on the outer shelf. These detrital sands range in median size from 2.0ϕ-3.1ϕ and sorting from 0.8ϕ-1.6ϕ. The surrounding sediments are finer (3.2ϕ-8.2ϕ) and much more poorly sorted (2.6ϕ-3.4ϕ). On the basis of these textural characteristics the sediments are interpreted as

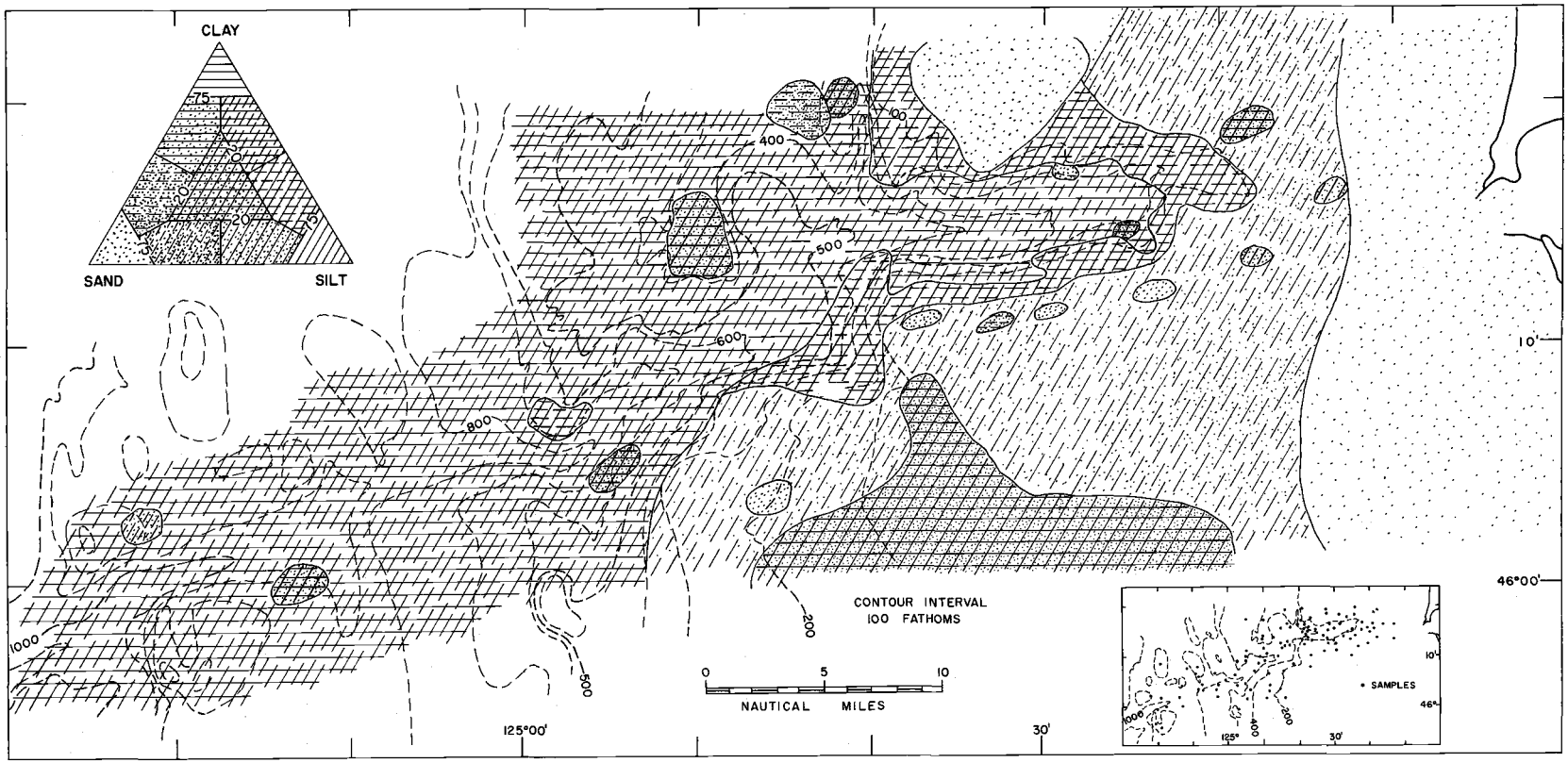

Figure 24. Surface distribution of sediment types in the Astoria Canyon area. (Classification after Shepard, 1954). Supplemental shelf data from Runge (1966).

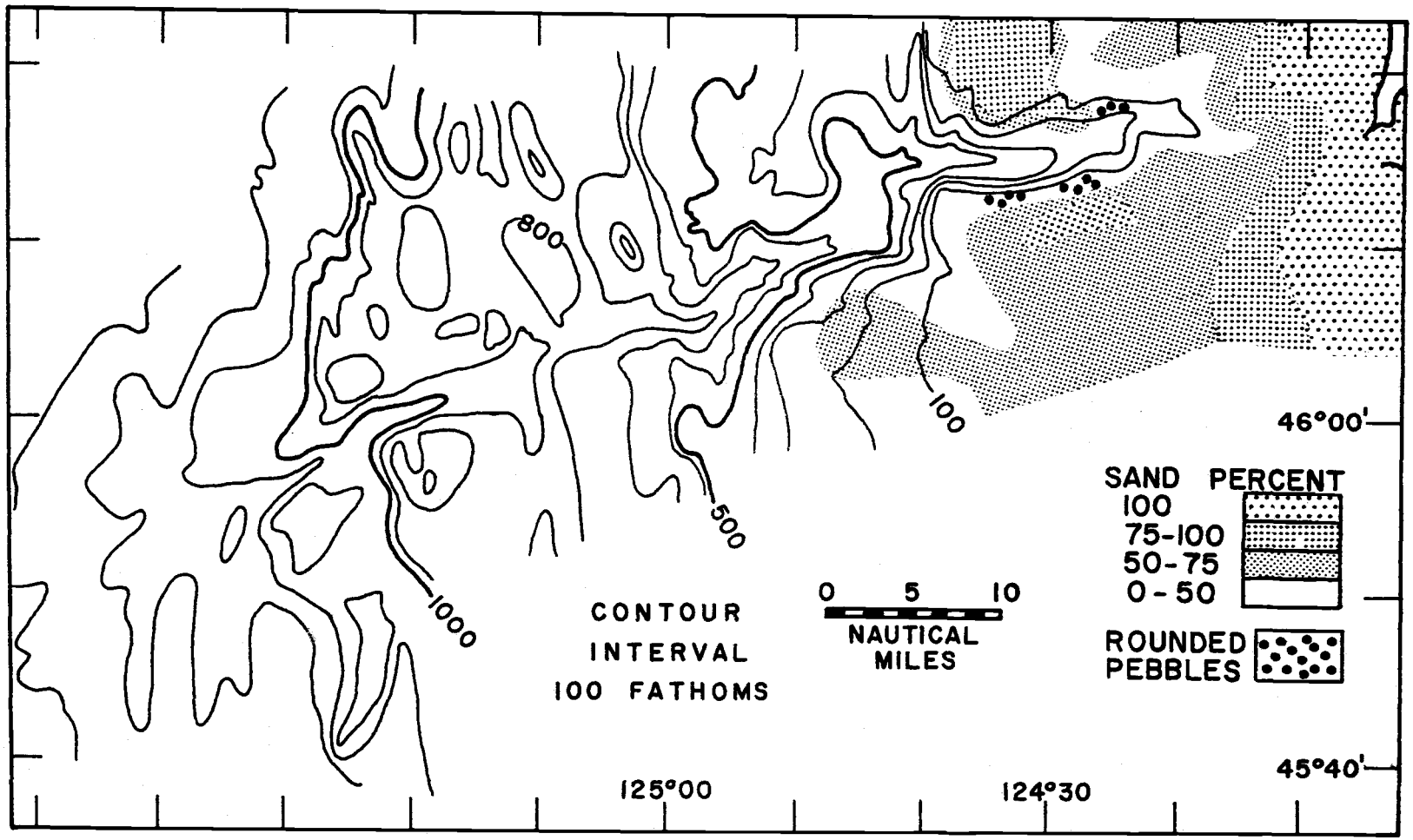

Figure 25. Distribution of surface sands in the Astoria Canyon region. Note the relict sands bordering the canyon on the outer shelf.

relict sands deposited when sea level was at its low point during one of the glacial stages. In addition, this map indicates places where rounded pebbles and cobbles were dredged. These coarse sediments were probably deposited by the Columbia River as it crossed the shelf to the low stand of sea level. A plot of the surface sediments according to the percentages of sand, silt and clay shows the textural similarity of the present day sediments of the physiographic areas of the canyon (Figure 26).

Subsurface sediments. The sediments of the Astoria Canyon area can be divided into postglacial and Pleistocene-Pliocene sediments based on the olive to gray color break. This color change is assumed to mark the change from glacial to postglacial time based on the C^{14} and radiolarian planktonic foraminiferal dates and changes in the benthic foraminifers. A comparison of the sand, silt, and clay contents of these sediments reveals some striking differences (Figure 26). The Pleistocene sediments from the canyon floor show a proportionately higher number of coarse layers than do the postglacial sediments. They are also somewhat coarser grained than the postglacial coarse layers. The clays of Plio-Pleistocene vintage on the other hand are finer than those of postglacial time. This last point is illustrated in the ternary diagrams of the wall sediments (Figure 26). Another major difference between the postglacial and Pleistocene sediments of the canyon walls is the prevalence of

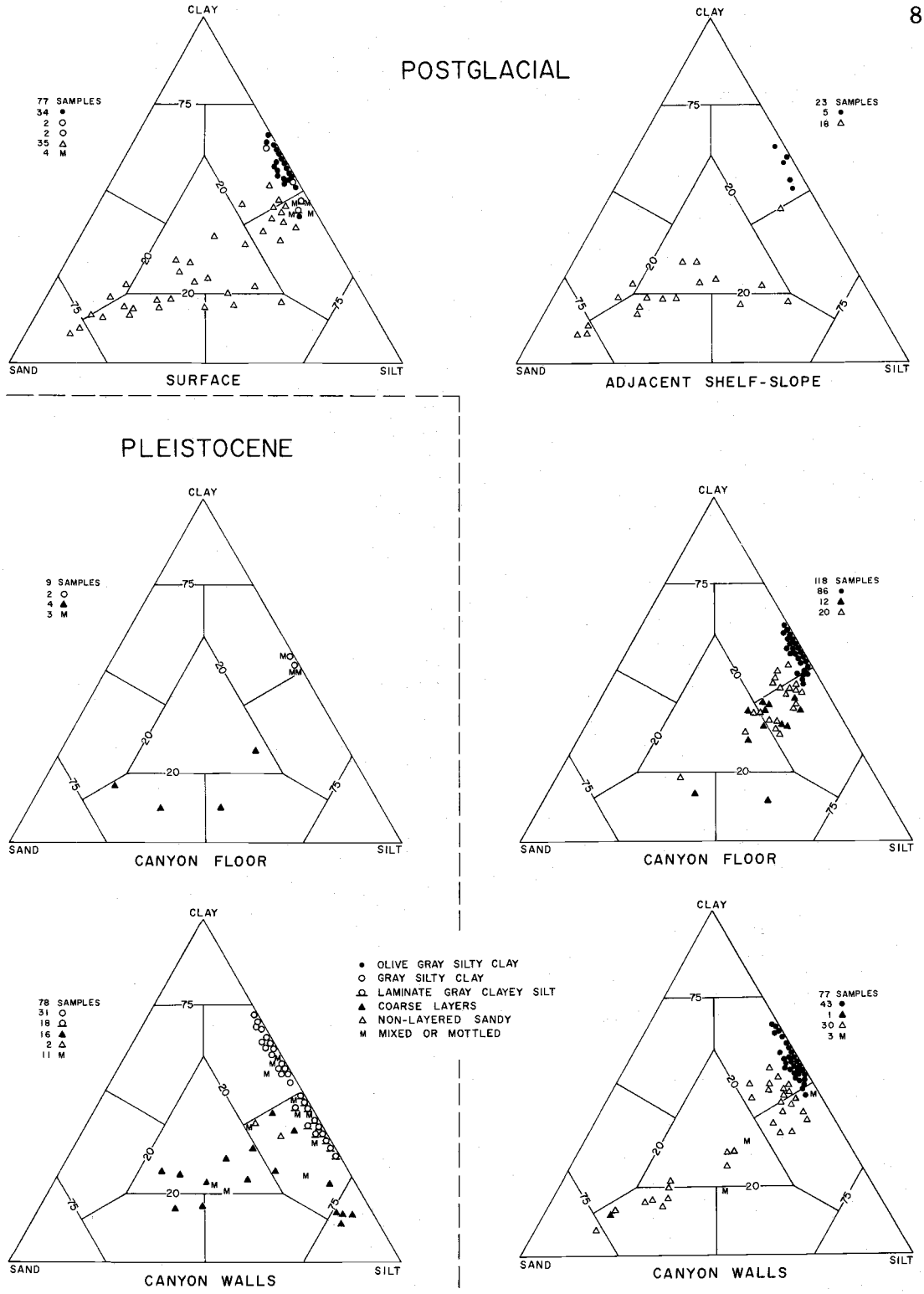

Figure 26. Sand-silt-clay contents of the various physiographic areas of the Astoria Canyon region for postglacial and Pleistocene sediments.

laminated gray clayey silt in Pleistocene sediments. A lack of deep cores on the adjacent shelf and slope makes a comparison of the postglacial to the Pleistocene of this region impossible. The decidedly coarser nature of the postglacial sediments of the shelf-slope region is primarily a function of water depth. Terrigenous sand predominates on the inner part of the shelf. On the outer shelf and upper slope the sand content is also quite high in spots. These high sand percentages may be due to the presence of abundant glauconite granules or in some instances to patches of relict sand.

Comparisons of Textural Parameters

In order to determine various sedimentary environments and sedimentary processes in the Astoria Canyon area, textural parameters of the sediments were plotted against one another in the manner of Folk and Ward (1957) and Passega (1957). These techniques enabled them and others (Inman and Chamberlain, 1955; Rusnak, 1960; Hubert, 1964; van Andel, 1964) to compare large numbers of samples and to draw conclusions about modes of transportation and environments of deposition.

The original plotting of the Astoria Canyon sediment parameters, mean vs. sorting, mean vs. skewness and silt/clay vs. water depth was done with an X-Y plotter coupled to an IBM 1620 computer.

Mean vs. sorting. The tendency for the data points to form a

sinusoidal pattern (Figure 27) is similar to that reported by Folk and Ward (1957). Hubert (1964) also showed a similar pattern for marine deep sea sands, but the sediments of Astoria Canyon are finer grained and generally poorer sorted than either of the other two.

Groupings of sediment types (Figure 27) are indicative of the various environments of deposition. Samples from the canyon floor are most abundant in the very fine silt to coarse clay range and the wall cores dominate in the medium clay size range. The best sorting of the samples is exhibited by the coarse layers which have median diameters of silt size. The best sorted sediments are those of the coarse layers from the lower end of the canyon. Even these, however, are poorly sorted at best. Some sediments from the shelf near the head of the canyon analyzed by Runge (1966) plot in much the same position on this mean vs. sorting diagram as do the Pleistocene coarse layers from the lower end of the canyon. This similarity of mean and sorting between the shelf sands and canyon floor coarse layers points to the shelf sands as the source of the sediments making up the coarse layers.

The sediment types based on groupings of points in Figure 27 have characteristic coarse fractions which reflect environmental variations. The coarse layers are most prevalent in the canyon floor environment, and consist largely of detrital minerals and

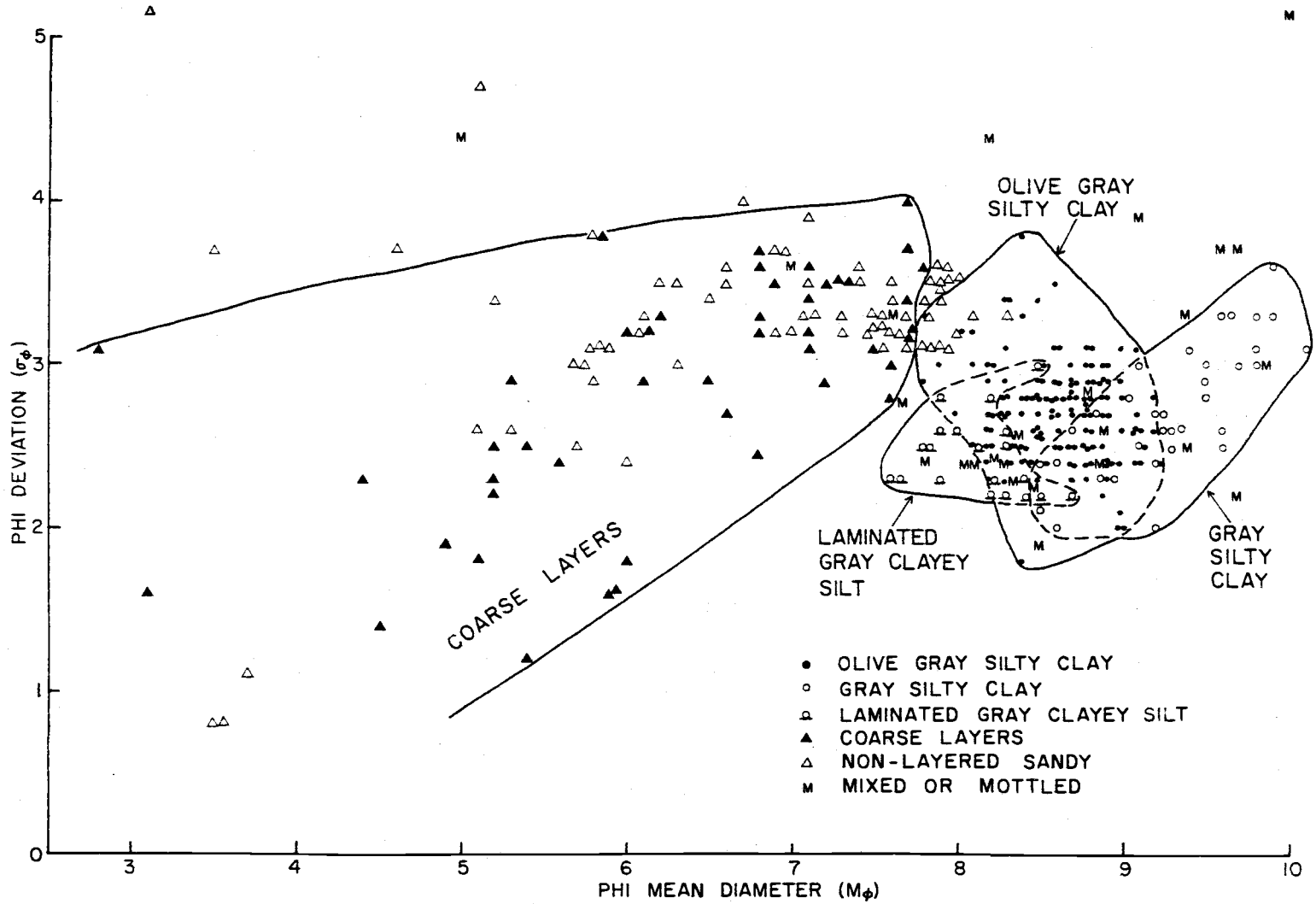

Figure 27. Sorting versus Mean of the various sediment groups.

rock fragments. In the more poorly sorted finer grained coarse layers plant fragments become more plentiful. The laminated silts and clayey silts are found almost exclusively on the canyon walls. They are also primarily of detrital composition, but more of a platey form. Mica is the most characteristic constituent. The olive gray silty clays are found covering the present surface of both floor and wall regions. In the Astoria Canyon area, however, this type is more representative of the floor because the postglacial sediment is a great deal thicker here than on the canyon walls. Plant fragments and tests of pelagic organisms make up a large part of the coarse fraction. The gray silty clays have sorting characteristics very similar to those of the overlying olive clays, but are finer, therefore offset somewhat on the mean vs. sorting graph. These gray clays are characterized by a higher percent of detrital components, especially mica, than the younger sediments. In addition, pyrite is an abundant constituent of many of these samples.

Skewness vs. mean. When skewness is plotted against mean, the sediment types tend to group in a manner similar to that of the graph of mean vs. sorting. The sediments are mainly positively skewed. Only about 10% are negatively skewed, and these are primarily olive muds of the canyon floor and sandy muds of the adjacent shelf. The canyon floor sediments are the closest to being perfectly symmetrical with respect to particle size distribution clustering

around zero skewness. Therefore, they show the closest textural relationship to the negatively skewed beach and inner shelf sediments (Byrne, Kulm and Maloney, 1966).

The highest values (> +0.70ϕ) of skewness are characteristic of the sediments with a mean phi in the medium silt size. The sediments of both coarser and finer mean phi have a more normal symmetry. The skewness values of the coarse layers range from +0.0ϕ to +0.7ϕ, values comparable to those obtained by Runge (1966) for the shelf samples near the canyon head. According to Duane (1964) negative skewness is the result of winnowing action by fluid media. It also can be due to a two component source, such as for foraminiferal clay. In the study area, however, this second alternative is unlikely because of the closeness to land and the resulting masking effect of these terrigenous sediments. The positive skewness of the coarse layer sediments of Astoria Canyon leads to the conclusion that winnowing was relatively unimportant in the sedimentologic history of these layers.

Silt/clay vs. water depth. The silt/clay ratio decreases with increased water depth for sediments of both the walls and shelf-slope. The silt/clay ratio for the canyon floor sediments, however, decreases only to the middle portion of the canyon (450-600 fathoms) and then increases. The concave pattern which such a plot of these canyon floor samples forms is due to the strong terrigenous

influence near shore and to the strong coarse layer influence near the canyon mouth. At depth in the piston cores this ratio also shows an increase. This, together with the increase in number and thickness of coarse layers at depth in the cores, suggests increased "turbidity current" activity during Pleistocene time.

Coarsest one percent vs. median diameter. According to Passega (1957), who first proposed the C M diagram, the coarse fraction is more representative of the agent of deposition than the fine fraction for many environments. Therefore, this technique was applied to the sediments of the Astoria Canyon region. This procedure involves the plotting of C, the coarsest grain as represented by the one percentile grain size, against M, the median grain size. Logarithmic graph paper is used with C plotted as the ordinate and M the abcissa.

The C M patterns for this area (Figure 28, a and b) show distinct groups of the various sediment types. The olive muds and gray clays, although falling in somewhat different patterns, nevertheless plot in the zone of the quiet water deposits referred to by Passega (1964) as pelagic suspension. The laminated gray silts of the canyon walls (Figure 29b) are slightly offset from the clays because of the interlayered mica laminae. These silts on the basis of their position on the C M diagram would also be considered quiet water deposits. However, the mica laminae may represent

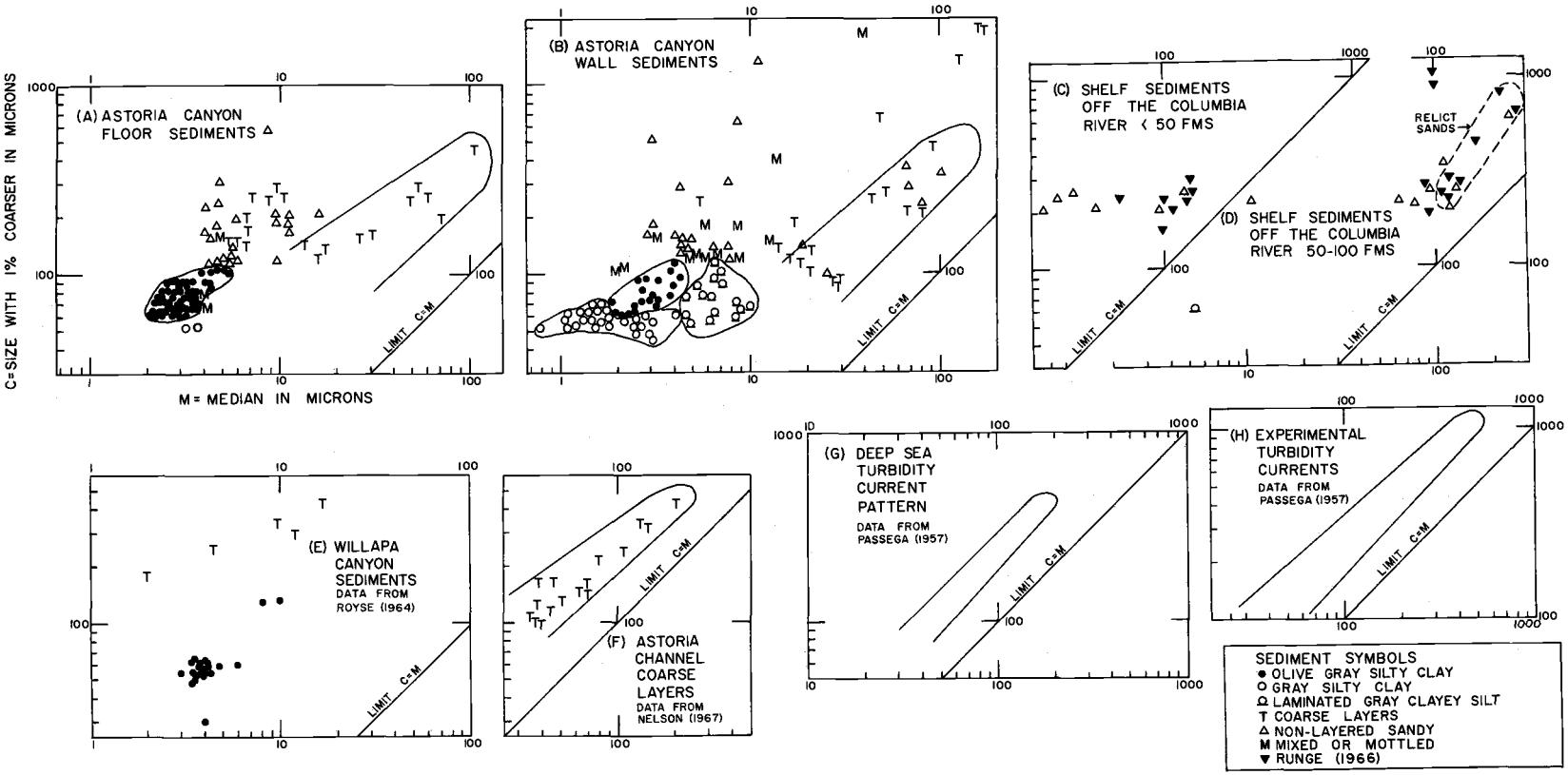

Figure 28. C M patterns of the Astoria Canyon area compared to C M patterns for sediments from other regions.

deposition along the outer edges of turbidity currents which flowed down the canyon floor. This laminated gray silt is a product of two agents of deposition.

The coarse layers are indicated in Figure 28 by a T. A comparison of the pattern of these coarse layers to that shown by Passega (1957) for turbidity current deposits (Figure 28, G and H) reveals a similarity in general trend. In some instances, such as those of the coarse layers found in core number one near the canyon mouth, the pattern is almost identical. This similarity of patterns is also evident in coarse layers from Astoria Fan (Figure 28 F). However, some of the canyon coarse layers plot a considerable distance away from the hypothetical pattern. According to Passega (1964) the distance from the limit line C = M measured along the abscissa varies from one to six phi units for different types of transport. The patterns as far away as six phi units from the limit line C = M are those formed by sediments deposited by mud flows. The turbidity current patterns are parallel to and less than three phi units from the limit line. Using these values as guides, the coarse layers of Astoria Canyon are hypothesized to be of two types, turbidity current and mudflow deposits (Figures 28, A and B). The pattern of coarse layers collected from Willapa Canyon (Figure 28E) is very similar to that formed by those sediments of Astoria Canyon attributed to possible slumping and consequent mud flow deposition.

In Figure 28, graphs C and D show the C M patterns for the shelf sediments adjacent to Astoria Canyon. The similarity in C and M values of these sandy sediments and the coarse layers found in the canyon points to these shelf sands as sources of the sediments of the coarse layers. Another explanation for the similarity of these sands could be that they both came from the same source.

The shelf sediments are divided into those collected from shallower (C) and deeper (D) than the 50 fathom contour line. Relict sands, encircled on graph D, occupy a position on this graph that is very similar to some of the sediments on graph C. This reinforces the suggestion that these are sands remaining from a Pleistocene low stand of sea level.

Additional Compositional Variations

The composition of the various sediment types has been discussed in previous sections. At this point the discussion will emphasize the regional compositional distribution both surficially and in the third dimension of authigenic and biogenic materials of the coarse fraction. Plant fragments are included with the biogenous group even though a large portion of them may have had a terrestrial origin.

Authigenic materials. The authigenic materials found in the sediments of the Astoria Canyon area are glauconite and pyrite. The surface distribution of glauconite is shown in Figure 29. The contours are based on percentage of the coarse fraction. The high

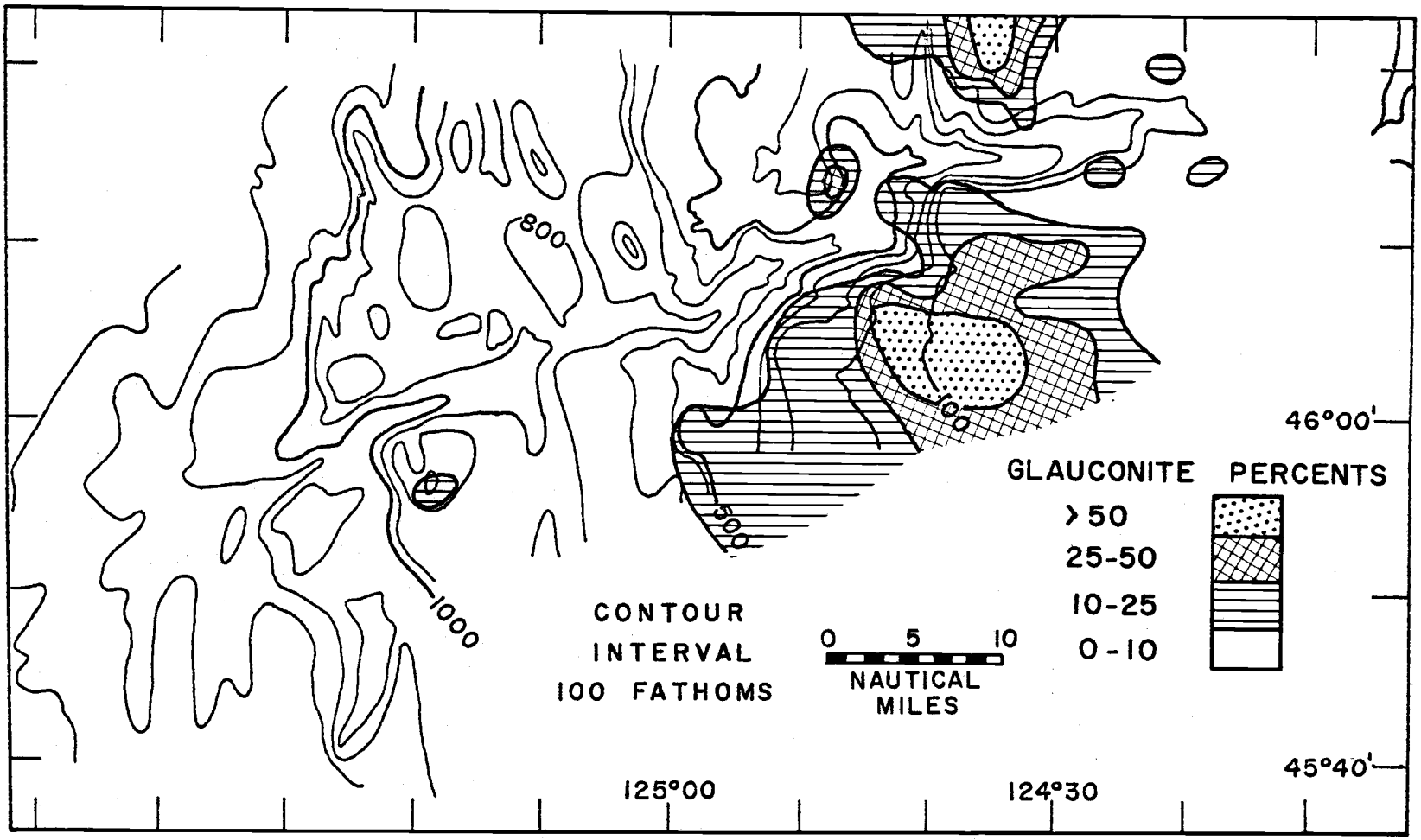

Figure 29. Distribution of glauconite in the surface sediments of the Astoria Canyon area. (Percentages are of the sand fraction.) Some of the shelf sediment data from Runge (1966).

percentages present in the surface samples suggests that glauconite is forming today. The most favorable environment for glauconite formation according to Cloud (1955) includes reducing conditions, source sediments (micaceous minerals or bottom muds with high iron content), and a low rate of sedimentation, but enough to supply the proper elements. Pratt (1963) suggested that reducing conditions exist in local micro-environments, but that over-all the environment may be one of oxidation. He further stressed the variable conditions under which glauconitization can take place and that glauconite can form by replacement and possibly even by direct precipitation. Whatever the origin on glauconite, these conditions are apparently best met in the vicinity of the shelf-slope break where glauconite values greater than 50% of the coarse fraction are found.

Glauconite of this area occurs in a variety of colors and forms. The colors range from yellowish-green to dark green. The glauconite takes the form of fecal pellets, foraminiferal fillings, irregular glauconitic sedimentary rock fragments, and mica-like, accordion-shaped blocks. Transitional shapes and colors were found to exist between these types. Triplehorn (1966) discussed the process of progressive glauconitization and concluded that the shapes of the pellets relate to the degree of glauconitization. The process must take place at the surface so he reasoned that the more highly glauconitized pellets should be more rounded than those at a

lower stage in the process because of the reworking and resulting abrasion needed to keep them at the surface. Evidence of reworking of the glauconite can clearly be seen in Figure 18.

The maximum percentages of glauconite in the sediments of the canyon floor are found at approximately the same longitude as the glauconite-rich sediments of the shelf-slope region. It is concluded, therefore, that much of the glauconite found on the floor of the canyon was not formed in situ but was transported from the adjacent shelf.

The distribution of glauconite at depth in the cores is variable, but high percentages were found only beneath present day surface areas rich in glauconite.

The second authigenic constituent found in some of the sediments is pyrite. Very little pyrite was found in the surface sediments; but at depth, particularly in the gray clay of the canyon walls, a fairly high incidence of pyrite was recorded for some samples. The form of pyrite ranges from clusters of spheres to perfect cubes. Sometimes it is found in small pod- or lens-shaped masses, but more frequently in the tests of foraminifers.

Biogenous constituents. A graph of coarse fraction composition of surface sediment plotted against water depth along the canyon floor (Figure 30) reveals three zones of different biogenic prevalence. At the upper end of the canyon, plant fragments are dominant; in the

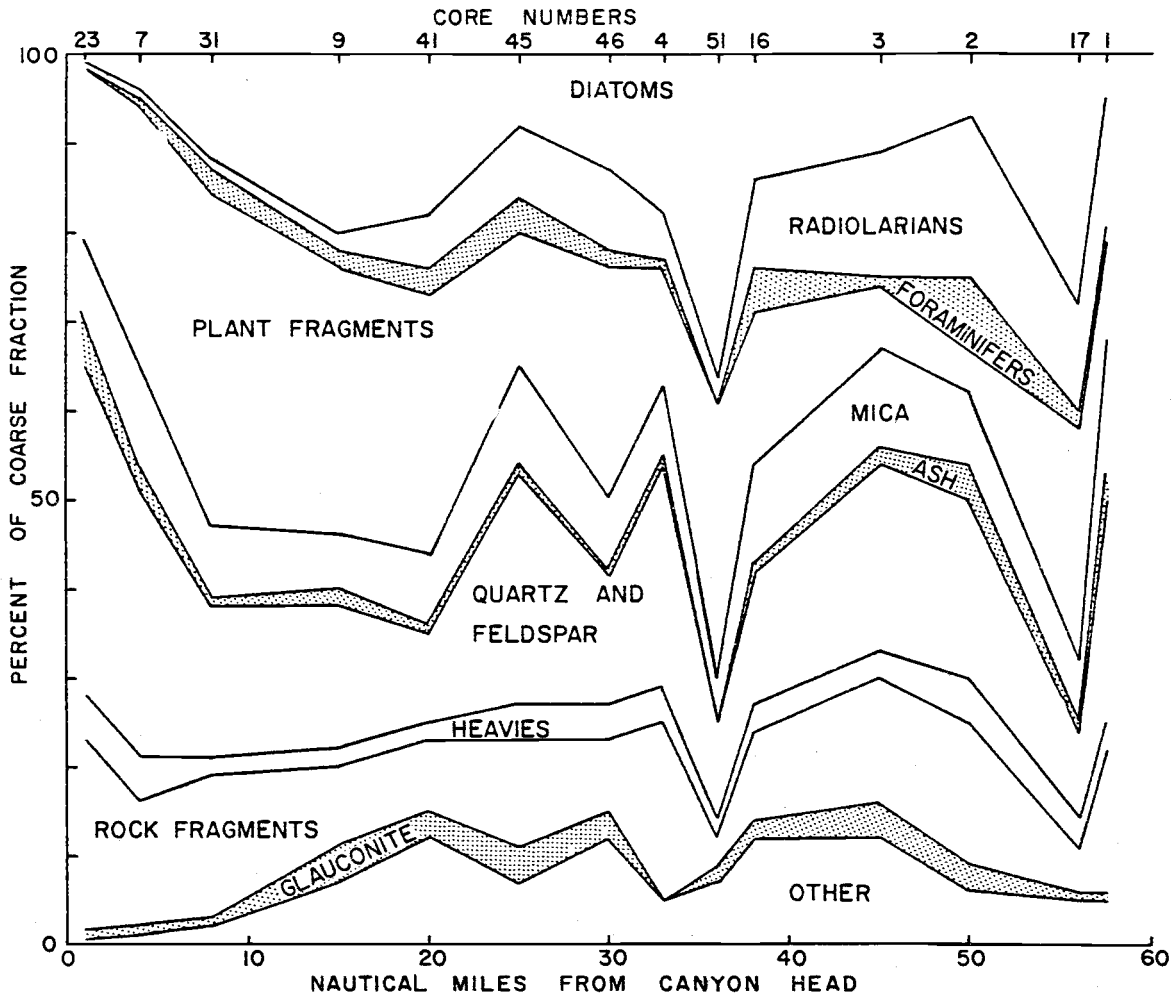

Figure 30. Distribution of coarse fraction components in surface samples from the floor of Astoria Canyon. The samples are arranged according to increasing distance from the head of the canyon.

middle portion, in the vicinity of the shelf-slope break, diatoms are the dominant biological constituent; and in the lower reaches of the canyon radiolarians predominate.

In the third dimension, the content of plant fragments and diatoms remain fairly constant with depth. Radiolarians are common to abundant in the olive muds, but are almost non-existent in the underlying gray clay. Conversely, the planktonic foraminifers, which are very minor in amount in the surface sediments, become much more abundant in the gray clay.

Summary and Discussion

The sediments of the Astoria Canyon region can be resolved into six types, olive-gray silty clay, gray silty clay, laminated gray clayey silt, coarse layers, non-layered sandy sediment, and mixed or mottled sediment, each with characteristic textural and compositional differences. Some of these sediment types are characteristic of certain of the three physiographic regions (canyon floor, canyon walls and shelf-slope); others are more ubiquitous.

The sediment being deposited in the Astoria Canyon area at this time ranges from a moderately sorted detrital sand, found shoreward of the canyon, to a hemipelagic, very poorly sorted silty clay, at the terminal end of the canyon. The particle size and sorting characteristics of these olive gray sediments are more

a function of distance from shore than of water depth.

Several differences may be noted between the olive muds and the underlying gray sediments. In the axis of the canyon, 20 foot piston cores do not penetrate beneath olive gray postglacial sediment. In places on the canyon walls, however, this olive sediment is only a few centimeters thick. Below this cover of olive gray sediment is an undetermined thickness of sticky gray clay of Pleistocene age and shale of probable Pliocene age. The olive mud is thicker in the tributaries than on the canyon walls.

Typically the canyon floor sediments consist of a very homogeneous olive gray silty clay near the surface with a high incidence of coarse layers deeper in the sediment fill. The olive muds of the canyon floor are probably most typified by abundant plant fragments and numerous diatoms (Figure 31). Near the mouth of the canyon radiolarians are the most abundant of the biogenic constituents. Coarse layers are often graded and most generally are high in percent of detrital minerals and rock fragments and contain some displaced benthic foraminifers. In addition to the graded bedding and displaced foraminifers, other evidence for a turbidity current origin of these coarse layers is a C M pattern similar to that of known turbidity currents.

The gray clays of the canyon walls have a composition that is high in mica (Figure 31) and pyrite. Planktonic foraminifers

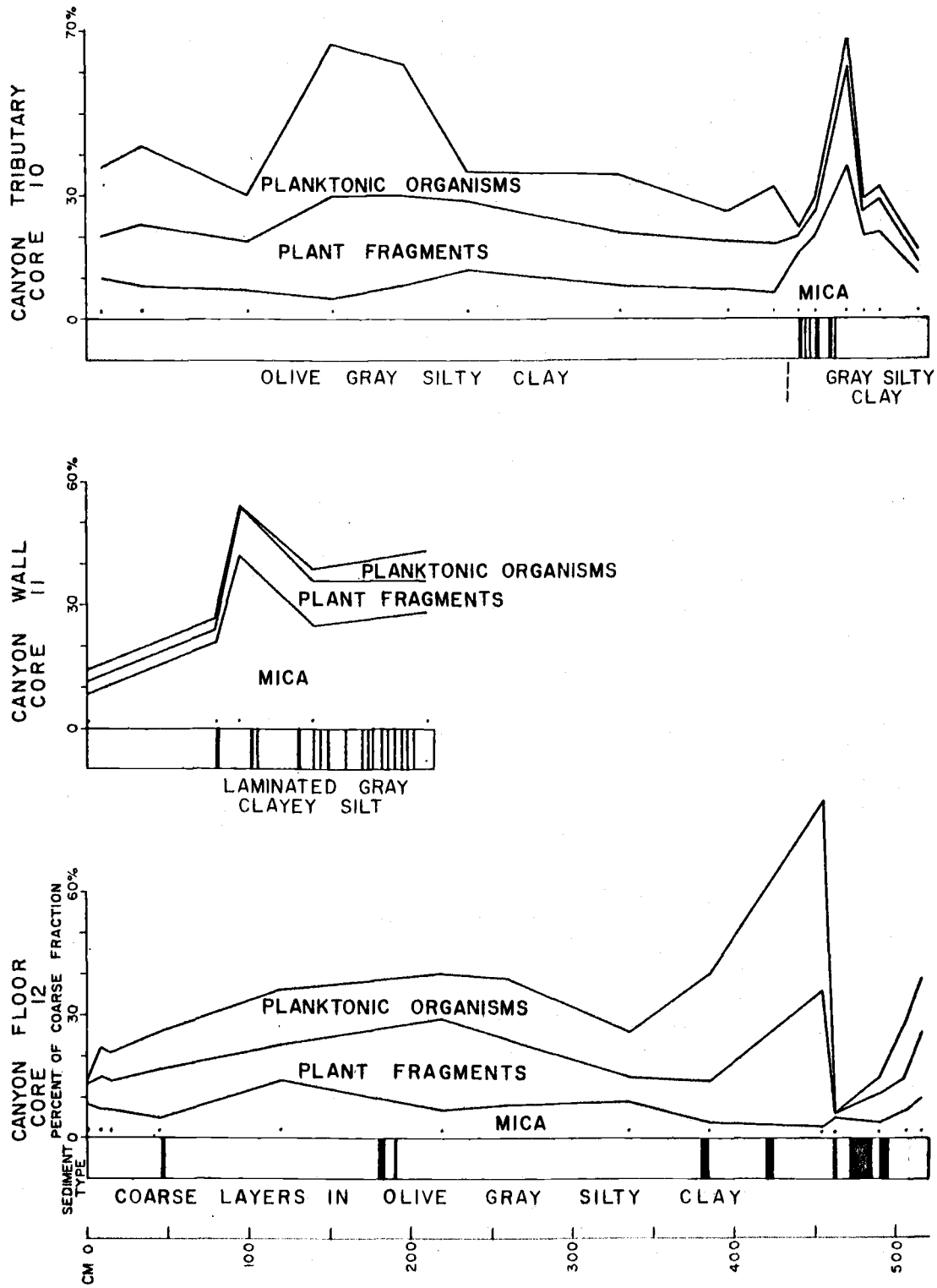

Figure 31. Comparison of percent of coarse fraction (>62μ) of mica, plant fragments and planktonic organisms in cores from floor (12), wall (11) and tributary (10) of Astoria Canyon. Dots adjacent to cores represent sample positions.

become the dominant biogenous constituent. Some of this gray clay is interlayered with thin laminae of micaceous silt. These mica laminae are probably the records left by the outer edges of turbidity currents which flowed down the canyon during Pleistocene time.

Relict sands related to lower stands of sea level are present on the continental shelf adjacent to Astoria Canyon. At the shelf-slope break some of the sediment contains large amounts of glauconite. The authigenic glauconite and the relict sands indicate a slow rate of deposition at present on the outer shelf in this area.

Mixed or mottled sediment is evidence for burrowing by bottom dwelling organisms and slumping from the canyon walls, two processes important in the ever changing sedimentation picture of Astoria Canyon. The well-preserved laminations in the gray clay of Pleistocene age, however, indicate an absence of burrowing activity by bottom dwelling organisms in the Astoria Canyon region during glacial time.

Mineralogy

Eight samples were chosen from the different environments of sedimentation for a study of the mineralogical variations of coarse layers. Analyses of these coarse layers were undertaken to determine the sources of the sediment. Four samples were selected from canyon floor core number one to determine: (1) the variability

of coarse layers in a given core and (2) the differences or similarities between coarse layers dominated by volcanic glass (1-20 and 1-22) and those free of glass (1-27 and 1-30). The other four samples were each chosen from different cores. Sample 12-11 was selected from a core also taken from the canyon floor, but nearer the middle of the canyon. Samples 13-9 and 14-8 were selected from wall cores, 14-8 from a glauconite-rich layer and 13-9 from a pyrite-rich layer. Number 18-12 came from a core collected in a tributary valley.

For each of the sands investigated, the entire coarse layer was sampled and a split was taken from this sample. This insured a proper representation of the various minerals even if selective sorting of mineral grains occurred during deposition. The sands ($> .062$ mm) were separated into light and heavy fractions by standard techniques (see Table 5 and Appendix 4).

Light Mineral Fraction

The various components of the light fraction differentiated in the count were quartz, K-feldspar, plagioclase feldspar, and rock fragments[4] (Table 8). The grains are primarily subangular to

[4] Includes glauconite and glauconitic sedimentary rock fragments.

Table 8. Light fraction mineralogy of selected coarse layers from the Astoria Canyon region and adjacent areas.

Astoria Canyon Sample No.	Light fraction constituents (% by count of 300 grains) *				Ratios		
		Feldspars		Rock	Quartz	K feldspars	Grain***
	Quartz	K	Plag.	Fragments**	Feldspar	Plag.	Matrix
1-20	13	5	8	74	1.0	0.6	3.2
1-22	10	4	6	80	1.0	0.7	2.8
1-27	28	16	25	31	0.7	0.6	4.9
1-30	35	10	26	29	1.0	0.4	2.8
12-11	26	9	26	39	0.7	0.4	0.7
13- 9	35	8	26	31	1.1	0.3	0.3
14- 8	7	3	7	83	0.7	0.4	3.2
18-12	34	12	29	25	0.8	0.4	2.3
Columbia River Reservoirs (Whetten, 1966)							
McNary	47	11	15	27	1,8	0,7	-
The Dalles	26	9	14	51	1.1	0.6	-
Bonneville	38	11	16	35	1.5	0.7	-
Astoria Fan (Nelson, 1967)							
Inner fan	30	13	12	47	1.2	1.1	1.7
Middle fan	30	13	20	37	0.9	0.7	9.0
Outer fan	33	14	19	34	1.0	0.7	3.8

* Grain count applies only to Astoria Canyon sediments.

** Includes glauconite and glauconitic rock fragments.

*** Grain (> 20)
Matrix (<20)

subrounded. Many of the quartz grains contain inclusions of magnetite. A large number of the feldspars are quite altered, and thus are difficult to distinguish from the rock fragments without staining. Based on albite twinning (Michel-Levy's method, Kerr, 1959, p. 258), the plagioclase compositions range from An_{52} to An_{72}. The average is about An_{68} (Labradorite). The lithic fragments are primarily basalt. There are, however, some fine-grained sedimentary rock fragments as well. Coarse layers 1-20 and 1-22 are largely pumiceous and 14-8 is primarily glauconitic.

The light fraction compositions of all of the sediments, with the exception of the three just mentioned, are very much alike. The percentages of quartz and rock fragments are similar, and the quartz to feldspar ratios range from 0.8 to 1.1. Plagioclase is more abundant than K-feldspar in all the coarse layers examined. For all except the glauconitic and glass-rich sediments, the ratios of quartz to feldspar plus rock fragments are almost the same (0.4 to 0.5).

One ratio that is very different in these sediments is that of grain to matrix which ranges from 0.3 to 4.9 (Table 8). In all the coarse layers, however, the matrix ($< 20\mu$) is plentiful enough that these coarse layers would be classified as graywackes according to Pettijohn's (1957) classification. Using the classification of Williams, Turner and Gilbert (1958), the sediments, if lithified, would be considered wackes (impure sandstones) and gritty mudstones. The

coarse layers are plotted on a ternary diagram in Figure 32 together with sediments from Astoria Fan (Nelson, 1967) and the Columbia River (Whetten, 1966). Sediments from all three areas have the following comparable features:

(1) quartz/feldspar ratios,

(2) quartz/feldspar + rock fragments ratios,

(3) K-feldspar/plagioclase ratios.

The similarity of canyon and fan sands to those of the Columbia River suggests that the Columbia River is a major source. The similarity of light fractions of the various canyon sands to each other and to the sands of Astoria Fan indicates that the canyon was an important path through which sediments were channeled to the deep-sea floor.

Heavy Mineral Fraction

The heavy minerals of these sand layers (Table 9) represent from 3.1 to 6.4 percent by weight of the sand fraction (> .062 mm). The dominant mineral groups are the pyroxenes and amphiboles. Pyroxenes make up a larger percentage of the total heavy fraction than do the amphiboles (average percentages: pyroxenes 23.5, amphiboles 19.1). Two samples, 13-9 and 14-8, contain anomalously low percentages of amphibole and 14-8 also has a low percentage of pyroxene. These low values are the result of extremely

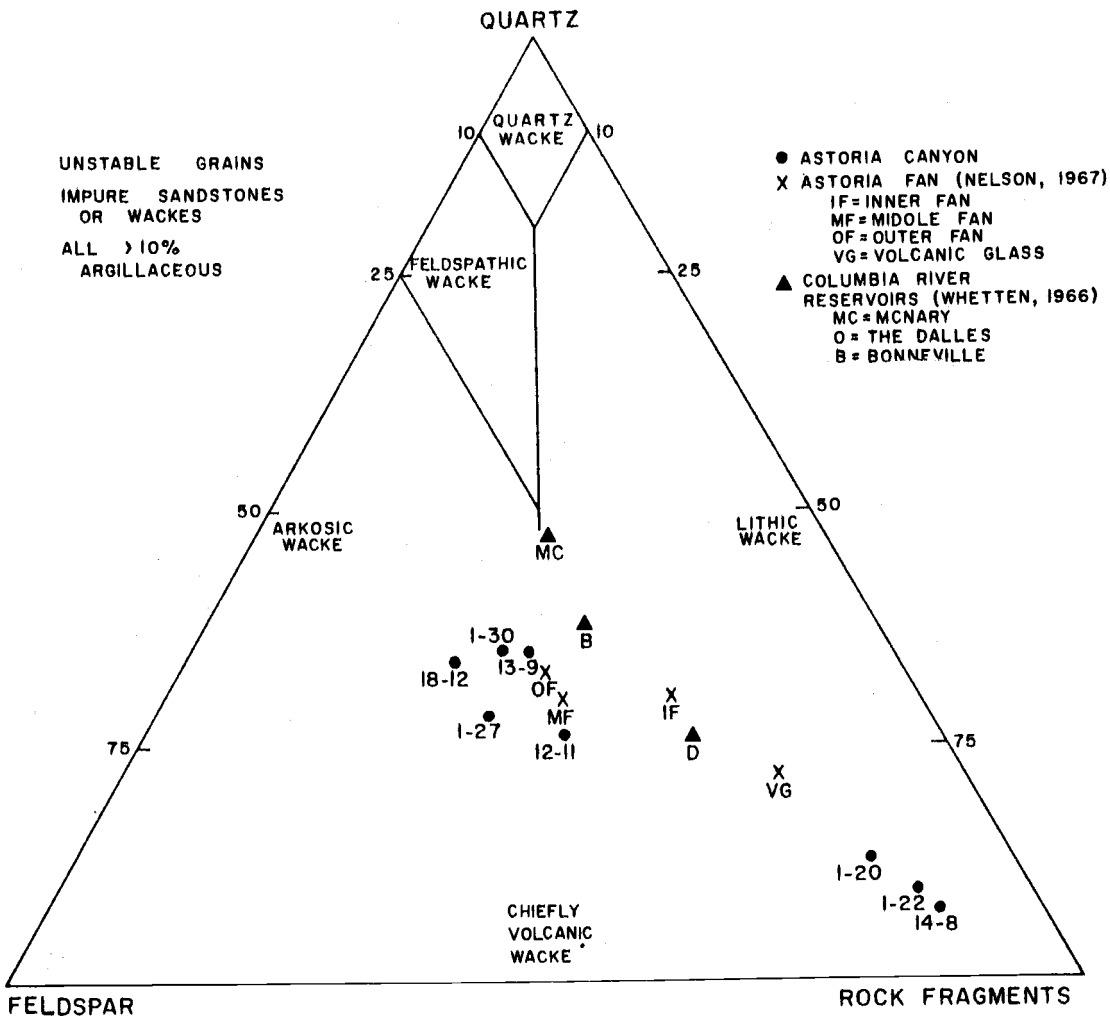

Figure 32. Ternary diagram comparing mineral and rock fragment compositions of sediment samples from Astoria Canyon, Astoria Fan and the Columbia River. (Classification after Williams, Turner and Gilbert, 1954.)

Table 9. Mineralogy of heavy fractions from selected coarse layers (Values are given in percent: minerals by count of >100 transparent grains; % heavies by weight of sand fraction; % sand by weight of total sample).

Minerals	Sample numbers							
	1-20	1-22	1-27	1-30	12-11	13-9	14-8	18-12
Amphibole group	21.0	21.5	20.0	21.2	23.2	10.4	5.9	29.4
Actinolite	1.7	0.5	1.2	1.3	0.5	1.0	-	-
Hornblende	19.6	21.0	18.3	19.8	22.6	9.4	5.9	28.8
Basaltic	2.0	1.6	1.2	2.6	1.6	0.7	0.5	-
Blue-green	2.6	1.6	1.8	3.3	2.2	0.7	0.2	3.4
Common	15.0	17.7	15.3	13.9	18.8	8.0	5.2	25.4
Apatite	1.7	0.5	2.4	2.6	1.6	-	-	-
Chlorite	1.0	0.5	1.8	0.7	1.6	0.7	0.7	3.4
Epidote group	1.5	-	4.2	3.3	5.5	1.0	0.9	3.9
Garnet	1.0	0.5	2.4	2.6	3.3	1.8	1.9	6.0
Hematite	1.7	1.6	2.4	2.6	-	-	-	-
Magnetite and Ilmenite	7.1	4.3	8.8	10.6	5.5	3.8	2.1	4.5
Mica	1.7	4.3	3.5	1.3	5.5	0.7	0.5	6.8
Monazite	0.5	-	-	0.7	-	0.7	1.2	0.6
Olivine	1.0	0.5	3.5	4.0	1.1	-	-	0.6
Pyrite	0.5	1.1	1.2	2.6	1.6	36.0	62.7	2.3
Pyroxene group	28.0	27.4	27.0	24.5	21.6	23.6	13.4	23.2
Clinopyroxene	15.3	17.7	19.4	15.9	14.4	13.9	5.6	14.7
Orthopyroxene	12.8	9.7	7.7	8.6	7.2	9.4	7.8	8.5
Enstatite	6.1	3.8	1.2	1.3	1.6	1.8	1.2	4.0
Hypersthene	6.6	5.9	6.5	7.3	5.5	7.6	6.6	4.5
Sillimanite	-	-	0.6	1.3	1.1	0.3	-	-
Sphene	0.5	0.5	1.2	2.0	-	1.0	1.2	2.3
Zircon	1.0	0.5	-	0.7	-	-	-	0.6
Rock fragments	12.7	19.4	11.8	11.3	16.0	5.9	6.8	9.0
Weathered	18.4	17.2	11.8	11.3	16.0	5.9	6.8	9.0
% Heavies	3.3	3.1	6.4	6.1	3.2	6.3	3.7	3.2
% Sand	48.5	30.7	56.0	64.4	21.7	10.5	49.7	38.4

high percentages of pyrite. Both of these samples are from canyon wall coarse layers. Sample 18-12 has an amphibole content that is considerably higher than for any of the other coarse layer samples. This sediment came from a core collected in one of the tributary valleys. The other samples, all of which came from the floor of the main canyon, have more nearly constant percentages of pyroxene (average 25.7%) and amphibole (average 21.4%).

The clinopyroxenes (mainly augite) are more prevalent than the orthopyroxenes (largely hypersthene). Ratios of clino- to ortho-pyroxene range from 0.7 to 2.5 with an average value of 1.7. The hypersthene is characterized by large numbers of inclusions, most of which appear to be magnetite. Some of the grains of hypersthene have glassy rims, indicative of a pyroclastic origin.

Of the amphibole group hornblende is by far the most abundant, varying from 5.9 to 28.8% (average 18.2%). Actinolite accounts for less than two percent of the heavy fraction. The most prevalent hornblendes are the so-called "common" hornblendes, being various shades of green and brown. Of the other types, blue-green hornblende is present in all and makes up slightly more than three percent in two of the samples. The reddish-brown basaltic hornblende occurs in small amounts in all the samples except 18-12.

Other non-opaque minerals present in all or most of the samples include apatite, chlorite, epidote group minerals (epidote and

clinozoisite), garnet, mica, monazite, olivine, and sphene. Of the opaque minerals, magnetite and/or ilmenite are present in the largest quantities with the exception of the two wall samples which contain very high percentages of pyrite (36 and 63%).

A great similarity exists between the dominant heavy mineral suites of the canyon coarse layers, adjacent shelf sands (Runge, 1966) and Columbia River sediments (Glenn, 1965 and Howell, 1966). This similarity is perhaps best expressed in Table 10 which lists the pyroxene/amphibole ratios of the various sediments mentioned. Whetten (1965, 1966) does not give percentages of individual heavy minerals, but he does indicate the importance of pyroxenes and amphiboles in the Columbia River sediments. These data strongly support the conclusions, drawn from the light fraction mineralogy, that the Columbia River has been the dominant supplier of sediments to the Astoria Canyon region.

Provenance

The evidence from the light and heavy mineral analyses indicates a close relationship between the sediments of Astoria Canyon and those making up the bed load of the Columbia River.

The dominant heavy mineral group is that of the pyroxenes. According to Glenn (1965) augite is one of the most important constituents of the Coast Range group of heavy minerals. He also

Table 10. Pyroxene/amphibole ratios for sediments from Astoria Canyon and adjacent areas.

Investigator:	Glenn (1965)	Howell (1966)	Runge (1966)		
Location:	ave. suite for Columbia River	Columbia River 1.9 mi. from mouth	Continental shelf 12 fms.	40 fms.	70 fms.
% Pyroxene	17.2	38	30	29.3	16.2
% Amphibole	25.5	14	11.9	23.8	13.5
P/A ratio	0.7	2.7	2.5	1.2	1.2

Astoria Canyon

Water depths:	930 fms.				519 fms.	460 fms.	212 fms.	845 fms.
Sample no.:	1-20	1-22	1-27	1-30	12-11	13-9	14-8	18-12
% Pyroxene	28	27.4	27	24.5	21.6	23.6	13.4	23.2
% Amphibole	21	21.5	20	21.2	23.2	10.4	5.9	29.4
P/A ratio	1.3	1.3	1.4	1.2	0.9	2.3	2.3	0.8

Willapa Canyon - Royse (1964)

Approximate Water depths:	150 fms				90 fms.	1150 fms.			1225 fms
Sample no.	29VV	29-00	29-40	29-70	39VV	48-90	48-180	48-190	50-130
% Pyroxene	12	11	7	11	12	5	8	4	13
% Amphibole	4	13	4	6	3	2	5	2	5
P/A ratio	3	0.9	1.8	1.8	2.5	2.5	1.6	2.0	2.6

considered augite together with hypersthene to be the dominant heavy minerals in the Cascade Mountain suite. The importance of these two mountain ranges as significant contributors to the sediment load of the Columbia River was shown by Whetten (1965) in a study of the composition of sediments from McNary, the Dalles, and Bonneville reservoirs. In McNary, which is fartheset upstream, hornblende is much more plentiful than pyroxene. However, at Bonneville, which is the farthest downstream, pyroxene has assumed the role of dominance.

A good share of the amphiboles, of which hornblende is the most abundant, seem to have been added to the Columbia River bed load somewhere east of the Cascade Mountains according to Whetten's data (1965). Possible sources are many, including intrusive bodies of intermediate composition in the Cascades of Central and Northern Washington, the mountains of northeastern Oregon and the Northern Rocky Mountains of Washington and Idaho. Glenn (1965) stated that hornblende is one of the important members of the Coast Range heavy mineral suite. The common (green and brown) hornblendes are the most plentiful, with subordinate amounts of blue-green and some basaltic hornblende present. He also reported significant amounts of "epidote" from the Coast Range rocks. The sediments of Astoria Canyon contain much less "epidote" than Glenn (1965) reported for the Columbia River, but this may be a function of

grain size studied. He investigated sediments having a minimum grain size of 44 microns, whereas the mineralogy of the Astoria Canyon sediments was restricted to those grains coarser than 62 microns.

Some of the minerals of the coarse layers which probably weathered from acid igneous rocks are: apatite, monazite, sphene, zircon, and, in the light fraction, potassium-rich feldspar. Sources for these minerals could be the granitic and pegmatitic Mesozoic intrusions of north central Washington, northeastern Oregon or western Idaho.

Minerals present which indicate metamorphic source rocks are actinolite, chlorite, garnet, blue-green hornblende and sillimanite. The northern Cascade region is a likely place of origin for these metamorphic minerals.

In the Columbia River drainage basin basic igneous rocks are extremely abundant. The extrusive and intrusive basic and ultrabasic rocks of the Cascade, Coast Range and Columbia Plateau regions are the most probable sources of the plagioclase feldspar, magnetite, and olivine, in addition to the dominant pyroxene minerals.

Maturity

"The maturity of a clastic sediment is the extent to which it

approaches the ultimate end product to which it is driven by the formative processes that operate upon it!' (Pettijohn, 1957, p. 508). Several measures of the maturity of the sediment of the coarse layers of Astoria Canyon are available for analysis.

The ratios of quartz/feldspar or quartz plus chert/feldspar plus rock fragments for the canyon coarse layers indicate very immature sediments. In Table 11 these ratios are compared to the maturity indices of average graywackes as listed by Pettijohn (1957).

Table 11. Maturity indices of selected coarse layers.

Sample no.	$\frac{\text{Quartz}}{\text{Feldspar}}$	$\frac{\text{Quartz + Chert}}{\text{Feldspar + rock fragments}}$
1-20	1.0	0.1
1-22	1.0	0.1
1-27	0.7	0.4
1-30	1.0	0.5
12-11	0.7	0.4
13- 9	1.1	0.5
14- 8	0.4	0.04
18-12	0.8	0.5
Average graywacke*	2.7	1.2

* After Pettijohn (1957), p. 509.

A second compositional measure of maturity involves the weathering potential of the minerals. According to Pettijohn (1957), the lower the weathering potential of a sediment, the more mature

it is considered to be. Therefore, using the order of stability of minerals based on the weathering potential index developed by Reiche (1950), which gives high values to augite and hornblende, the Astoria Canyon sands would be classed as immature.

Textural maturity of sediments can be recognized by clay content, sorting and grain roundness (Folk, 1951). Using these criteria, the coarse layer sediments would again be considered immature because of the angularity of the grains, the poor sorting, and the more than 10% clay content.

On the basis of these textural and mineralogical data, the conclusion is inescapable that these coarse layer sediments are immature. Pettijohn (1957) states emphatically that of all the processes affecting sedimentation the most fundamental factor is tectonics. The immaturity of these sediments reflects the importance of the mountain building episodes of both the Cascade and Coast Ranges on the supply of sediments to the area of study.

Clay Mineralogy

The clay mineralogy of sediments of the Astoria Canyon region has been investigated by Russell (1967). The dominant clay mineral in the Recent sediments is montmorillonite, but illite and chlorite are also present in fairly large amounts. Samples analyzed by Russell are representative of the various physiographic areas and

the different sediment types. A quantitative difference was found between the olive muds and gray clays. The relative sizes of the x-ray peaks indicate substantially more chlorite and illite in the gray clay than in the younger olive sediments. The amount of montmorillonite in the gray clays, on the other hand, is relatively less than in the overlying olive muds. He found no differences between clay minerals present in coarse layers and those of the hemipelagic muds. Russell (1967) has also x-rayed clays of the Columbia River sediments and found patterns similar to those of the olive gray clays mantling the walls and floor of Astoria Canyon. He concluded that very little diagenetic change has taken place in the clays added to Astoria Canyon by the Columbia River.

Volcanic Glass

Volcanic glass was found in the sediments in quantities ranging from over 70 to less than one percent of the coarse fraction (Appendix 3). The samples with abundant glass are primarily those from the lower end of the canyon and particularly the canyon floor. The cores in the upper part of the canyon contain small amounts of glass sprinkled throughout the core (Figure 33).

The volcanic glass occurs as angular shards, bubble shards, occasional mineral grains rimmed with glass, and as pieces of pumice. Both areal and vertical distribution of all forms seem

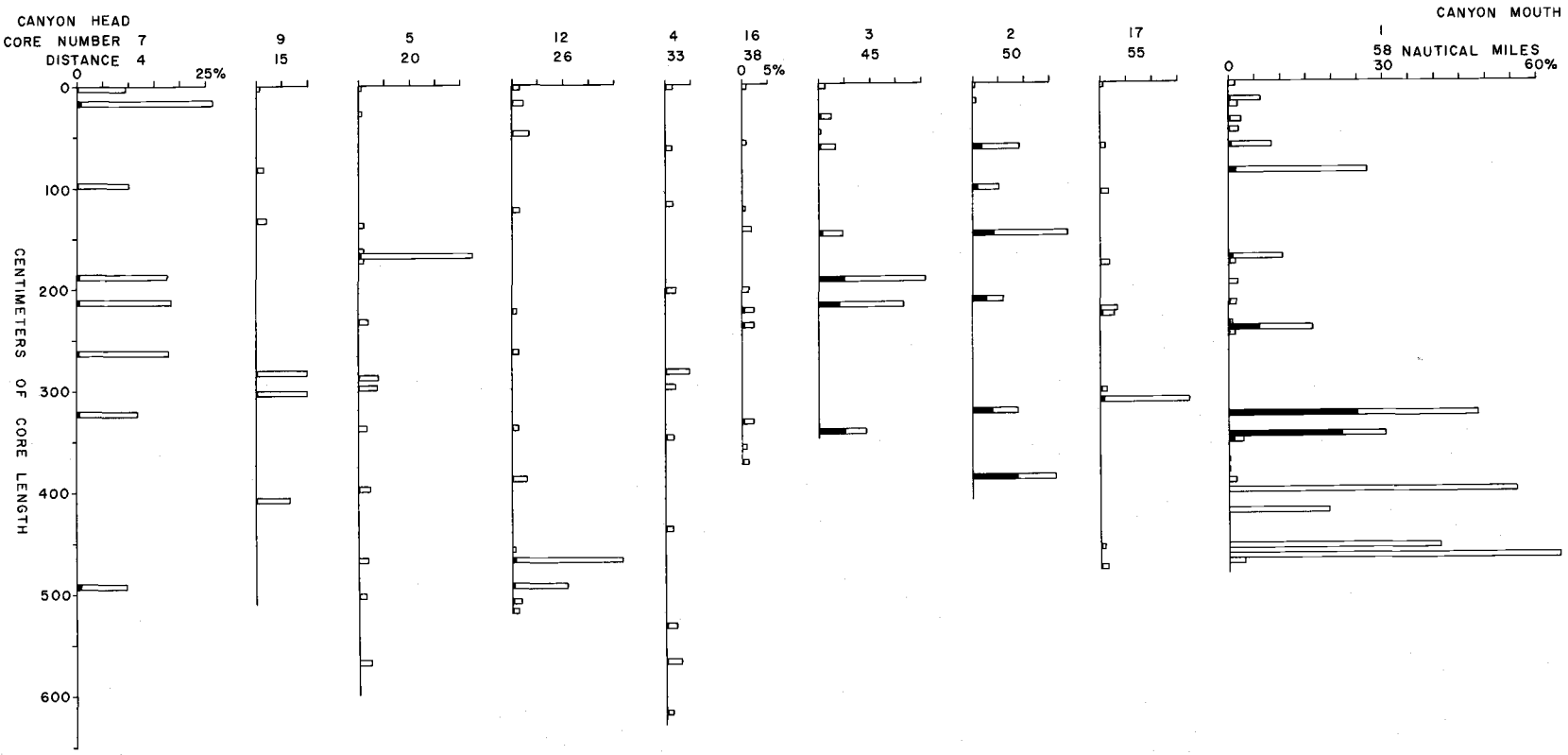

Figure 33. Volcanic glass content of canyon floor piston cores. Length of solid bar indicates proportion of volcanic glass in coarse fraction. Entire bar represents percent by weight of coarse fraction (> 62μ).

random. Nelson et al. (1967) have related the volcanic glass to the eruption of Mt. Mazama which took place approximately 6600 years ago. This relationship is based on refractive index of the glass and on C^{14} dates. The refractive index of the glass averages about 1.505. This places it in the range typical for Mt. Mazama ash (Powers and Wilcox, 1964).

Organic Carbon and Calcium Carbonate

Variations in organic carbon and calcium carbonate content were determined for nine samples selected from various environments and different core depths (Table 12). The amount of organic carbon based on dry weight of sediment varies from 1.95 to 2.57% (average 2.26%) for the olive gray sediments and ranges from 0.25 to 0.65% (average 0.43%) for the gray clays. The reverse is the case for the percentages of calcium carbonate. The olive sediments contain from 0.00 to 0.67% (average 0.17%) $CaCO_3$. The $CaCO_3$ content of the gray clay, on the other hand, ranges from 2.25 to 2.33% (average 2.30%).

The higher organic carbon in the postglacial muds than in the older gray clays is in agreement with the high percentages of plant fragments in these olive muds which form a blanket over the entire region. The gray clays of probable glacial vintage, however, contain more calcareous foraminifers than do the olive muds, thus

Table 12. Percentages of organic carbon and calcium carbonate of selected samples from canyon floor, walls and tributaries.

Core No.	Depth in Core (cm)	Organic Carbon %	$CaCO_3$ %	Physiographic Environment	Sediment Type
7	195-200	2.05	0.08	Canyon floor	olive sandy mud
9	515-520	2.11	0.00		olive mud
3	32- 37	1.97	0.17		olive mud
17	171-176	2.48	0.42		olive mud
1	475-480	0.65	2.33	(base of wall)	gray clay
11	225-230	0.25	2.25	Canyon wall	gray clay
10	195-200	2.57	0.67	Tributary valleys	olive mud
10	508-513	0.38	2.33		gray clay
18	35- 40	2.52	0.58		olive mud

higher $CaCO_3$ percentages. Gross (1965) concluded that the rapid deposition of lithogenous material serves to mask the calcareous remains of organisms in the nearshore surface sediments of Washington and Oregon.

Postglacial and Pleistocene sediments from Cascadia Abyssal Plain are similar to those of the Astoria Canyon region in relative percentages of carbonate and organic carbon (Kulm, 1967). The pre-Holocene sediments from Willapa Canyon are also lower in percent of organic carbon and higher in carbonate than are the Holocene sediments from the adjacent continental slope (Royse, 1964).

Foraminifers

Benthic foraminifers have been shown by Natland and Kuenen (1951) to be good indicators of paleo-water depths. These authors and a host of others including Phleger (1951), Ericson, Ewing and Heezen (1951) and Bandy (1964), have used displaced benthic foraminifers as evidence of turbidity current transportation and deposition. In addition to these uses, the benthic foraminifers are valuable stratigraphic markers.

Benthic foraminifers were separated from 45 samples from cores and dredge hauls of varying rock and sediment types and locations. Identifications were made with the assistance of Dr. G. A. Fowler, Oceanography Department, Oregon State University.

Foraminifers in Coarse Layers

The coarse layers of the Astoria Canyon region contain varying amounts of benthic foraminifers. In the majority of the coarse layers examined, some displaced foraminifers were found. These coarse layers contained displaced foraminifers from a variety of shelf and slope environments (Table 13). The largest number of species observed are types displaced from the inner shelf, and, of these, Buliminella elegantissima and Elphidium spp. are the most common. Some coarse layers contained benthic foraminifers displaced from only one environment. These coarse layers probably originated from a point source. However, in many instances the displaced foraminifers from a given coarse layer came from many environments ranging from inner shelf to upper slope.

Those layers containing foraminifers from a variety of environments suggest deposition by a turbidity current that started in shallow water and entrained sediment from the various environments through which it passed.

Table 13. Displaced foraminifers from coarse layers in Astoria Canyon.

Inner shelf species
Buliminella elegantissima
Buccella frigida
Cassidulina limbata
Cassidulina tortuosa
Cibicides lobatulus
Elphidiella hannai
Elphidium incertum clavatum
Elphidium incertum incertum
Elphidium magellanicum
Elphidium micrograniulosum
Elphidium sp. (fax group)
Nonionella auriculla
Quinqueloculina akneriana bellatula
Middle shelf species
Gaudryina arenaria
Nonionella basispinata
Nonionella miocenica
Outer shelf, upper slope species
Trifarina angulosa

Stratigraphic Clues Provided by Foraminifers

The foraminifers off the Oregon coast have not been studied in as much detail as those of many other parts of the country. As a result, less is known about the key stratigraphic marker species, and the Pliocene-Pleistocene and Pleistocene-postglacial boundaries are not well-defined.

Possible indicators of Pleistocene sediments are some elphidiums belonging to the fax group and abundant Elphidium incertum clavatum. The elphidiums of the fax group were obtained from gray clay dredged at sample site 103 (Figure 17) on the south wall of the canyon. According to Fowler (1967) this type of Elphidium is not found off Oregon today and could represent Pleistocene sedimentation. He suggests that the presence of abundant Elphidium incertum clavatum could signify a Pleistocene age for the sediment. Where there is a color change, the sediments above the color change contained the species Elphidium incertum incertum. In all cases this sediment is olive gray (5 Y3/2)[5] in color. Below the color change, the sediment is gray (N-4)[5]. The elphidiums from this gray clay have a much more pronounced embilical plug, and therefore compare favorably to the colder water variety Elphidium incertum clavatum. It is suggested that the olive gray to gray color change

---

[5] G.S.A. color chart, 1963.

marks the Pleistocene to postglacial change off the Oregon coast.

In two cores, number 13 from the north wall of the canyon and number one (Figure 18) from the floor at the base of the south wall, benthic foraminifers of probable Late Pliocene age were found in firm, semi-consolidated sediment. In core 13 at a depth of 120 centimeters the species Bolivina subadvena sulphurensis was found. In core number one, three species of probable Upper Pliocene foraminifers were identified from two different samples at depths of 466 and 480 centimeters. The species identified were Bolivina subadvena sulphurensis, Bolivina seminuda, and Bulimina pagoda hebespinata. Four pipe dredge hauls (numbers 101, 103, 109 and 117) from the canyon walls contained rocks in various degrees of induration, several of which exhibit marked zones of oxidation. These rocks include well-lithified siltstones and some not as well-indurated mudstones. One sample of mudstones which contained no foraminifers was riddled with well-preserved borings (Figure 34). Some of the semi-consolidated material contained specimens of Elphidium incertum clavatum which may represent the Pleistocene. The well-lithified, calcareously cemented siltstones could not be disaggregated and no foraminifers could be seen at the surface of these rocks. However, Fowler (1967) stated that lithologically these siltstones bear a resemblance to rocks of Late Tertiary age dredged from the central Oregon shelf. Possible upper Pliocene

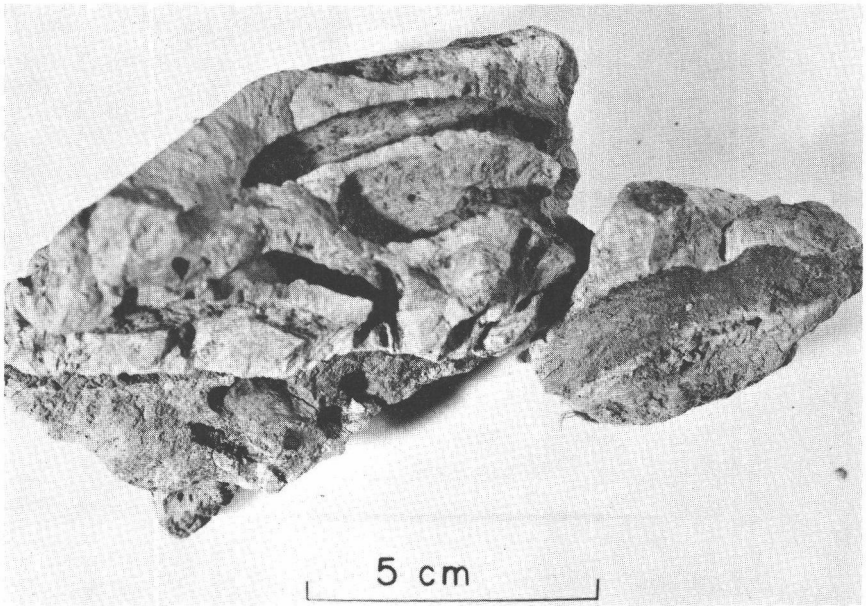

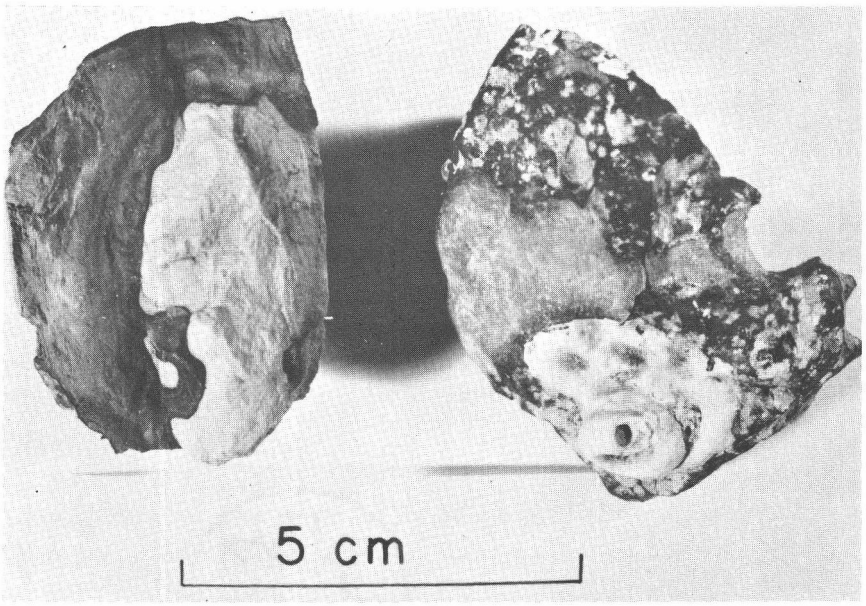

Figure 34. Rocks dredged from the walls of Astoria Submarine Canyon. Upper: sample 101, well-preserved burrows in gray siltstone. Lower: sample 103, well-lithified siltstone with encrusting organisms on outside and zones of oxidation on inside.

shale has been reported cropping out on the shelf just south of Astoria Canyon (Byrne, 1963). Pliocene siltstones were also reported to crop out on the central Oregon shelf (Byrne, 1962). Subsequent investigations (Maloney and Byrne, 1965; Fowler, 1966) have noted the occurrence of middle Miocene and younger sedimentary rock outcrops on the continental shelf and slope off central Oregon.

Paleodepths have been reported for these Miocene to Pleistocene deposits (Maloney and Byrne, 1965; Fowler, 1966). Fowler concluded from these studies that uplift as great as 580 fathoms has occurred on the central Oregon continental shelf since the Miocene. However, according to Fowler (1967), the foraminifers examined from the Astoria Canyon area do not indicate noticeable uplift.

Summary and Conclusions

A stratigraphic change occurs in the cores taken from the walls of Astoria Canyon. Varying thicknesses of postglacial olive gray mud overlie Pleistocene firm gray clay. Also found in some of the firm, semi-consolidated gray clay are foraminifers of probable Late Pliocene age. Older strata are reported from the central Oregon continental terrace sedimentary rocks. North of Astoria Canyon, Willapa Canyon cuts the continental margin. Royse (1964) has reported the occurrence of pre-Holocene foraminifers, some as

old as Early Pliocene, in the sediments of the walls of Willapa Canyon.

Displaced benthic foraminifers, largely shallow water types, are found in most of the coarse layers of Astoria Canyon. Royse (1964) reported finding displaced foraminifers in the coarse layers of Willapa Canyon. Nelson (1967) also finds numerous displaced foraminifers in the coarse layers of Astoria Fan. The presence of these displaced foraminifers implies transportation of sediment from shallow water into and through submarine canyons to the abyssal plain.

Sedimentary Structures

Sedimentary structures have been used by many investigators as aids in interpreting regimes of sedimentation (Moore and Scruton, 1957; Hulseman and Emery, 1961; Kuenen, 1964; Coleman and Galiano, 1965). Middleton (1965) stressed the importance of occurrence of structures in Recent sediments as aids in recognizing paleo environments of sedimentation. A variety of sedimentary structures have been observed in the cores collected from the Astoria Canyon area. Because of the lack of orientation of these cores and the small cross-sectional areas of the cores, no directional data could be ascertained from the structures. Nevertheless, much information regarding the conditions of deposition and transportation can be

gleaned from the various features. The sedimentary structures are grouped according to the following categories: (1) homogeneous or massive bedding, (2) thin laminae, (3) coarse layers, (4) disrupted bedding, (5) mottling.

Homogeneous or Massive Bedding

Massive homogeneous beds are the most common primary structures of the Astoria Canyon area. On the canyon floor homogeneous olive gray silty clay is dominant. In most of the piston cores taken in this environment the homogeneous olive mud makes up greater than 90% of the core. The canyon wall cores, on the other hand, average less than 30% homogeneous olive gray silty clay and in many places less than 10% of the total core length. An irregular fairly sharp contact separates this olive mud from the underlying gray silty clay. This sediment is also homogeneous and quite massive in its bedding characteristics. Figure 35 contains a photograph showing both the olive and gray homogeneous clays and the contact between them. The gray clay has been cored only on the canyon walls, or, in the case of samples one and six, at the base of the wall and on the adjacent shelf-slope area. The cores from the thalweg of the canyon have not penetrated the gray clay.

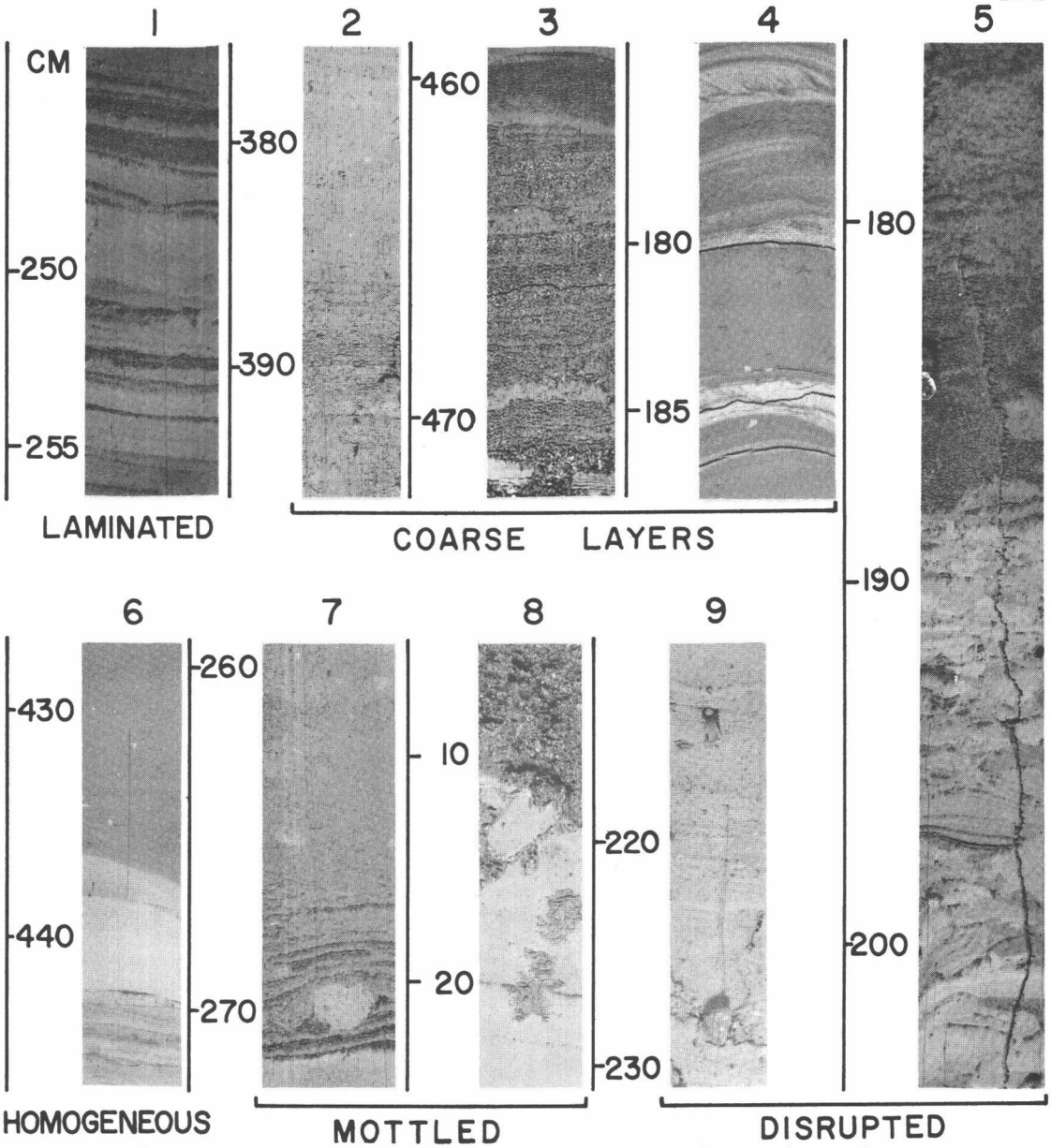

Figure 35. Sedimentary structures in cores from Astoria Canyon.

(1) Gray clayey silt, micaceous laminae, core 6;
(2) Featureless coarse layers, core 2;
(3) Graded coarse layer, core 1;
(4) Cross-laminations, core 19;
(5) Disrupted bedding, upper half irregular patchy sand and lower half slump structure, core 6;
(6) Olive gray silty clay overlying gray silty clay, core 10;
(7) Burrowed coarse layer, core 1;
(8) Burrows filled with glauconitic sediment, core 13;
(9) Patches of organic matter, core 3.

Thin Laminae

The gray clay of the canyon walls is often interspersed with numerous laminae. According to Payne (1942) the term lamination is restricted to those similar layers less than one centimeter thick. The thickness of these laminae ranges from 1.0 to 0.1 centimeter. Typical laminations (Figure 35) are for the most part composed of mica. However, in some cases they are primarily highly reduced organic concentrations.

Coarse Layers

This term is applied to those layers of visibly coarser grain size than the surrounding sediments. Great variabilities of thickness, median grain size, sorting, composition, and bedding features exist in these coarse layers. Thicknesses of the layers range from one to ten centimeters and median phi diameters from 3.1 to 7.5. All of these layers, whether the principle mode is in the sand or silt size range, are moderately to poorly sorted (Figure 27). The dominant coarse fraction composition of these layers is also highly variable. Included in the dominant compositions are mica, volcanic glass, glauconite, plant and wood fragments and detrital mineral grains and rock fragments (Figure 19). The mineral grains and rock fragments are dominant in most of the coarse layers. Bedding

features range from cross-bedded to graded-bedded coarse layers, to those that are apparently featureless. Figure 35 contains illustrations of the various types of coarse layers. The largest share of the coarse layers are featureless. Graded bedding was observed in seven of the piston cores. About 40% of the coarse layers in these cores exhibited graded bedding. Cross-bedding was noted in only two cores and only in a few of the layers. More pronounced cross-bedding, thicker, coarser and better sorted layers, and more graded bedding features were distinguished in the coarse layers of Astoria Channel (Nelson, 1967) than were found in Astoria Canyon.

Disrupted Bedding

In numerous cores bedding is disrupted in the form of slump structures (Figure 35), irregular patchy sand and silt lenses, and irregular patches of organic material. The irregular sand and silt patches and the organic patches could be the result of slumping or possibly the remnants of layers reworked by bottom dwelling organisms.

Mottling

The continuity of coarse layers is often interrupted by burrows (Figure 35). The olive gray to gray contact is found disturbed in many of the cores collected from the walls of the canyon. In some

instances, where a thin layer of glauconitic sediment overlies the gray clay, organisms have burrowed into the clay, carrying fragments of glauconite as deep as ten centimeters below the contact (Figure 35).

The homogeneous olive-gray muds found in considerable thickness on the canyon floor may owe their homogeneity at least in part to the burrowing action of organisms. One line of evidence favoring this hypothesis is the presence of numerous fecal pellets scattered throughout much of the homogeneous mud. Bouma (1964) has shown with x-ray radiography that apparently homogeneous sediments from the floor of submarine canyons off Southern California, in many instances, are almost completely reworked. Moore and Scruton (1957) reported that the activity of burrowing organisms could account for much of the patchy or irregular layers and in many instances the homogeneity of sediments.

Summary and Discussion

Massive homogeneous beds of olive gray and gray clay are the most common sedimentary structures in the study area. The olive muds are thickest on the canyon floor and in the tributaries. The gray, more compacted clays are most common in cores taken from the canyon walls. These muds represent deposition in quiet water. Interspersed in the gray clays are thin micaceous or organic laminae

which indicate a lack of burrowing activity during Pleistocene time. These are characteristic of canyon wall sediments. The laminations represent brief intermittent changes of sedimentation conditions. The interruptions may be caused by turbidity currents flowing down the axis of the canyon or short interludes of bottom current activity. The laminae of the wall sediments may represent the dilute higher parts of the density flows lapping up on the canyon walls or may have been deposited by weak bottom currents flowing down the canyon.

Turbidity currents may have originated as slumps of canyon wall material. Some evidence for slumping has been observed in the canyon cores. The coarse layers, which are best developed in the canyon floor cores, are the strongest evidence for turbidity current deposition. These layers are thickest, best graded and most numerous in the lower portions of the cores.

Evidence of much activity of bottom dwelling organisms can be seen in the cores, many of which have extensive zones of mottling. Portions of sediment not showing distinct mottling or burrowing may nonetheless have been completely homogenized by benthic organisms. In addition, many patches of sand, silt, and/or organic matter may owe their irregular shapes and orientation to the burrowing activities of mud feeders.

Comparison of Sediments of Astoria Canyon to Those of Other Submarine Canyons

Many similarities exist between Astoria Canyon and other submarine canyons of the world. Some of these features shared by many canyons have been pointed out in the section on physiography. At this point, the sediments will be compared: first, with sediments from canyons of the west coast of the United States, then with those of other canyons.

Astoria Canyon and its neighbor to the north, Willapa Canyon, have many sedimentary characteristics in common. Royse (1964) has reported the occurrence of some coarse layers on the floor of the canyon. As in the case of Astoria Canyon, coarse layers are most representative of the sediments of the outer portion of the canyon and occur in greatest numbers deep in the piston cores. They are thinner than those coarse layers found on the adjoining deep-sea fans. The composition of the coarse layers in both canyons is essentially terrigenous with a mineralogy much like that of the adjacent continental shelf sands. Displaced benthic foraminifers are characteristic of these layers. Royse also reported that the coarse layers are overlain by and interbedded with green pelagic mud which is probably the same as the olive gray silty clay discussed in this report. Similarities in wall sediments include: gray

color, fine texture, abundant pyrite, Pliocene foraminifers and greater consolidation of wall sediments than the sediments of the canyon floor.

Other west coast canyons which have been studied in detail are those off the coast of California and in the Gulf of California. Most of these canyons head in much shallower water than Astoria Canyon and therefore are quite different. Coarse layers alternate with deep water muds in canyons which empty into the southern part of San Diego Trough (Shepard and Eisele, 1962) as is the case in Astoria Canyon. In many of these southern California canyons, sands are an important part of the surface sediment (Shepard and Einsele, 1962; Bouma, 1964; Hand and Emery, 1964; Shepard, 1964; Shepard and Dill, 1966). Some of the characteristics of these coarse layers found on the floor of canyons off California and in the Gulf of California, such as graded bedding and displaced benthic foraminifers, are present in the coarse layers of Astoria Canyon. Hand and Emery (1964) reported that some of the canyons near the north end of San Diego trough have thick layers of hemipelagic clayey silt at the surface. These are underlain by thick graded coarse layers which they ascribe to turbidity currents. These canyons are more like Astoria Canyon in that they head farther from shore than do many of the California canyons. This change in sediment type was thought by Hand and Emery (1964) to be due to deactivation of the canyon head

due to drowning. The walls of many of the California canyons are different than those of Astoria Canyon. Consolidated sedimentary rocks and granitic rocks are reported cropping out on the walls of many of these canyons (Martin, 1964; Shepard, 1964; and Shepard and Dill, 1966).

The submarine canyons on the eastern coast of the United States head in water depths similar to Astoria Canyon. Many of these canyons contain sediments that are similar to those discussed in this paper. Recent greenish silts and clays which are somewhat coarser than the underlying gray to pink Pleistocene clays are characteristic of the canyons off the New England coast (Stetson, 1949). Stetson also found thicker sequences of Recent mud on the canyon floors than on the walls. No mention was made of coarse layers, but Stetson's size analyses indicate their presence in the canyons. Hudson Canyon (Ericson, Ewing and Heezen, 1951, 1952) was reported to contain numerous coarse layers with characteristics much like those reported from Astoria Canyon: graded layers, displaced shallow water foraminifers, mineralogy similar to that of the shelf sands, and numerous plant fragments. The walls, which are covered by a thin layer of Recent sediment, are made up of compacted green clay high in pyrite and containing Mio-Pliocene faunas.

There are numerous other canyons in the world which have some of the same sediment characteristics as Astoria Canyon.

The Congo Canyon area (Heezen, et al., 1964) has four sedimentary facies that resemble the sediment types found in and adjacent to Astoria Canyon. These facies are: homogeneous silty lutite (explained by the authors, p. 1133, as Congo River silt "mixed with normal pelagic particle-by-particle deposition"), crumbly silty lutite, graded silts and sands, and laminated silts. The silts and sands were thought to be deposited by turbidity currents introduced by the Congo River. These layers contain many of the same structures found in the Astoria Canyon coarse layers and the layer abundance is greater with depth in the cores.

Bourcart (1964) reports that many of the canyons of the Western Mediterranean have been incised into the hard Pleistocene mud of the continental slope. Within these canyons, the sediments range from stratified sands to muds. The upper parts of several of these canyons are partially filled with highly organic muds.

Some canyons in the Black Sea were investigated by divers. They found the walls to be made of consolidated mud with well-defined horizontal bedding. Numerous slump and slide scars were evident on the walls. The floors of these canyons were covered by several feet of semi-liquid brown mud (Kaplin, 1961).

The floor of Tokyo Canyon (Shepard, Niino and Chamberlain, 1964) has numerous thin sand layers interbedded with mud at the lower end of the canyon. These sand layers are reported to contain

shallow water foraminifers, indicating transport down the axis of the canyon. In the upper part of this canyon, long piston cores (> 400 cm) contained only dark brown mud. This is somewhat analogous to the sediment distribution in Astoria Canyon.

In this comparison of Astoria Canyon sediments with those of other canyons, threads of similarity run through the entire pattern. There are also great differences. It is, therefore, highly unlikely that all canyons are the result of the same pattern of events. However, the similarities in morphology and make-up of many of the world's great canyons indicate that certain of the same processes are in operation the world over.

It appears that one of the important limitations regarding canyon origin is the location of sea level with respect to the canyon head. In those canyons which head close to shore, sand is usually encountered at the surface of the canyon floor. However, in those canyons heading some distance offshore, the canyon floor is typically muddy at the surface. Cores of great length that have penetrated these canyon floor sediments, however, usually contain sand and/or silt layers at depth.

Therefore it seems that the presence of the head of a submarine canyon in the zone of littoral transport is an important requisite for maintaining an active canyon. As soon as local fluctuations in sea level, either eustatic or tectonic, remove the head

of the canyon from a supply of sand transported by littoral currents, the canyon scouring activity ceases and hemipelagic and pelagic sediments begin filling the canyon.

V. STRATIGRAPHY

Many problems arise when one attempts to determine the stratigraphic relationships of the sediments which make up the continental terrace. Some of these problems are: (1) inaccessibility of outcrops due to great water depths; (2) inaccuracy of sample locations; (3) uncertainty of stratigraphic positions of rocks and sediments in dredge hauls; (4) limited depth of penetration by piston corers. Submarine canyons often provide a window through which insight may be gained about the stratigraphic variations of part of the continental margin provided the canyon cuts stratigraphic horizons.

Adjacent Continental Stratigraphy

Eocene submarine lava flows and breccias intercalated with marine tuffaceous siltstones and sandstones (Tillamook volcanic series) are the oldest rocks exposed in the Oregon Coast Range (Snavely and Wagner, 1964).

Unconformably overlying the Tillamook series is a thick sequence of dominantly marine argillaceous sediment much of which is tuffaceous. Snavely and Wagner (1964) suggested that this sediment which ranges in age from late Eocene to middle Miocene is as much as 10,000 feet thick.

The youngest marine sedimentary rocks in the lower Columbia River area are those of the Astoria Formation of middle Miocene age (Weaver, 1937; Baldwin, 1964). The sandstone and siltstone of this formation are more than 1000 feet thick (Snavely and Wagner, 1964). According to Snavely and Wagner overturned folds in slump structures and textural changes of the sedimentary rocks of the Astoria formation indicate that the deepest parts of the depositional basin were west of the present day coast line. Interbedded with these marine sediments are flows of Columbia River Basalt and local pillow lavas and breccias (Baldwin, 1964).

Pliocene conglomerate (Troutdale Formation) separated from the underlying Columbia River Basalt by an unconformable contact is found cropping out along the Columbia River (Baldwin, 1966). Quartzite pebbles derived from far up the Columbia River make up a large portion of this conglomerate, indicating to Baldwin the importance of the Columbia in this area since early Pliocene. Marine sediments of Pliocene age crop out north of the Columbia River in the Grays Harbor structural embayment. Snavely and Wagner (1963) reported that these sediments indicate deeper portions of the Pliocene basin of deposition was west of the present shoreline just as in Miocene time.

The most prominent Pleistocene and Recent sediments found near the mouth of the Columbia River are those making up (1) the

lower Columbia Estuary, (2) Clatsop Plain and Spit and (3) sand dunes both north and south of the river.

Stratigraphy of the Continental Terrace

Although little is known concerning the precise sedimentary characteristics of rocks underlying the continental margin, geophysical investigations provide knowledge of the general framework of this region. Stratigraphic information is limited for the shelf in the canyon area; therefore, geophysical and lithologic data from the central Oregon shelf are used to supplement available data from the northern shelf. Seismic data suggest that the continental shelf-slope area off the central Oregon coast has the characteristics of a deep sedimentary basin (Whitcomb, 1965; Erickson, 1967). Gravity anomalies indicate the presence of north-south trending stratigraphic basins on the shelf on each side of Astoria Canyon (Couch, 1967). These basins appear to be offset, which may be interpreted as a fault crossing the shelf in the vicinity of the canyon or uplift of the shelf and Coast Range south of the canyon. It appears from the gravity data that tectonic activity may have had an influential role in the location of Astoria Canyon. Emilia, Berg and Bales (1967) have calculated depths to magnetic anomaly sources for the continental margin adjacent to Astoria Canyon. The depths to these anomalies may be an indicator of more than 30,000 feet of sediment

in this region. According to Shor et al. (1967) seismic evidence points to a crustal thickness of approximately 20 kilometers on the shelf in the vicinity of Astoria Canyon.

Rocks dredged from bank areas off the central Oregon coast have been found to contain foraminifers of Miocene to Pliocene age (Byrne, 1964; Fowler, 1966). Geophysical evidence indicates complex minor folding in some of these bank areas off central Oregon (Whitcomb, 1965). Using densities obtained from seismic velocities Whitcomb has correlated the strata on the shelf with those cropping out on shore. He reported the presence of a north-south trending syncline with an axial sediment thickness of more than 20,000 feet. Erickson (1967) has calculated dips up to 16° for some of these Tertiary strata.

Byrne (1963) reported an outcrop of upper Pliocene shale on the continental shelf south of Astoria Canyon. To the north in Willapa Canyon, lithified sediments of lower Pliocene age crop out on the canyon walls (Royse, 1964).

Samples from the walls of Astoria Canyon have yielded foramininifers as old as upper Pliocene. Most of the sediment cored, however, does not appear to be older than Pleistocene. The Plio-Pleistocene sediment is primarily a stiff, gray, micaceous, pyritic, fine silty clay. It is overlain by olive gray sediment which ranges from sand to clay; the size depends upon the water depth and distance

from shore. The thickness of this postglacial sediment ranges from at least tens of feet on the floor of Astoria Canyon to a few centimeters in some places on the canyon walls. In tributary valleys the postglacial muds are generally less than ten feet thick.

Sparker traces across the inner shelf between the mouth of the Columbia River and the head of Astoria Canyon show a series of buried channels (Berg, King and Carlson, 1966). They probably were cut by the Columbia River during the Pleistocene as it crossed the shelf to lower stands of sea level. Other sparker traces depict subsurface strata which are greatly disturbed and may represent cut and fill. The 180-240 feet of sediment covering these Pleistocene erosional features may represent the maximum thickness of Recent sediment in the Astoria Canyon area.

Stratigraphic Framework

According to seismic surveys off the northern Oregon coast the crustal thickness of the continental margin is intermediate between normal continental and oceanic thicknesses (Shor, Dehlinger and French, 1966). Chiburis (1966) using seismic dispersion methods and a Bouguer gravity anomalies reported a total crustal thickness in the Oregon Coast Range of approximately 38 kilometers. Although no sediments older than Miocene have been collected from the continental terrace off Oregon and Washington, the great

thicknesses of early Tertiary rocks on the adjacent continent plus geophysical data suggest that early Tertiary rocks are present at depth offshore.

An attempt is made in Figure 36 to portray the stratigraphic relationships between known continental formations and hypothesized strata of the continental margin. This correlation is based upon geophysical and geological evidence both continental and marine. Geological information includes: trends of sediment type, formation thicknesses and densities of the Coast Range and Coastal Plain, foraminiferal dates for shelf and slope sediments and physiographic variations. Depth calculations based on magnetic anomalies and layer thicknesses and densities based on seismic velocities are the geophysical lines of evidence used in constructing the cross-section (Table 14).

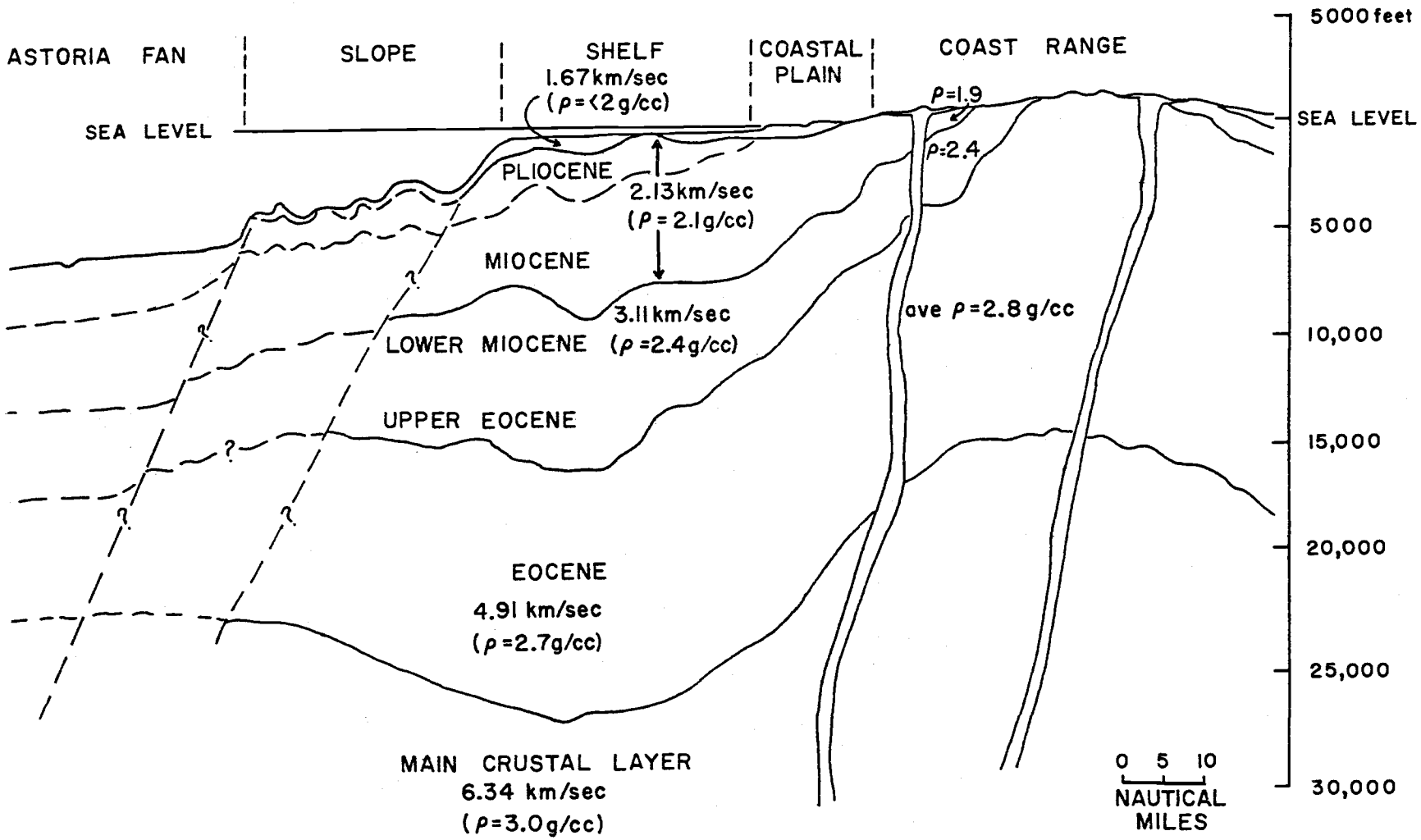

Figure 36. Hypothetical cross-section, Coast Range to abyssal plain at 46° No. latitude. Seismic velocities from Shor et al. (1967). Densities obtained from velocities using graph in Press (1966). Coast Range densities after Snavely and Wagner (1964).

Table 14. Comparisons of geophysical data for Coast Range and continental margin strata.

Coast Range*			Central Oregon Continental Shelf**			Astoria Canyon Region***		
Age	Density (gm/cc)	Thickness (feet)	Velocity (ft/sec)	Density (gm/cc)	Thickness (feet)	Velocity (ft/sec)	Density (gm/cc)	Thickness (feet)
Recent and Pleistocene			5450		250- 550	5470	2.0	330
Pliocene			6200		2400-7400			
						6970	2.1	8900
Miocene	1.9	1000	8200		4500-5000			
				2.5		10,200	2.4	8400
Oligocene	2.4	10,000						
			13,300			16,100	2.7	8000
Eocene				2.7				
	2.8	10,000						
				2.8				
						20,000	3.0	35,000

* Snavely and Wagner (1964)

** Whitcomb (1965) and Erickson (1967)

*** Shor et al. (1967); densities obtained from graph in Press (1966).

VI. SEDIMENTARY PROCESSES

Numerous sedimentary processes were and are at work continually changing Astoria Canyon. Because of the great water depths no direct observations of bottom conditions have been made. However, the various types of processes active in the past and at the present time can be inferred from core appearance, textural and compositional variations, Precision Depth Recordings, bathymetric charts and Sparker records.

Erosion

The evidence garnered from heavy and light minerals in the Astoria Canyon sediments indicates that the minerals were derived from rocks cropping out in the Columbia River drainage basin, especially from the Cascade and Coast Ranges. The abundance of unstable constituents indicates rapid erosion.

Various lines of evidence suggest that many erosional processes played important roles in the cutting of Astoria Canyon. The buried channels between the mouth of the Columbia River and the head of the canyon indicate the significance of this river during Pleistocene low stands of sea level. It is suggested that the Columbia contributed greatly to erosion of the head of the canyon during the glacial interludes.

Slumping is an important process today as it must have been in the past. Evidence of slumping as a canyon widening process can be inferred from Precision Depth Records and some piston cores (Figure 35). The importance of mass wasting in canyons off Baja and Southern California has been stressed by Shepard (1951), Chamberlain (1964) and Dill (1963). Dill on the basis of weekly observations of Southern California canyons lists three dominant types of movement as effective eroding agents. These types are: creep, slumps, and "rivers of sand."

The process of slumping is thought by many (Kuenen, 1951; Ericson, Ewing and Heezen, 1952; Gorsline and Emery, 1959, etc.) to generate turbidity currents. Coarse layers, probably deposited by turbidity currents, are most abundant in cores taken from the floor of the canyon. The coarse layers are thicker and more abundant deep in the piston cores than they are in the upper portions. The only evidence in any of the cores to show the ability of turbidity currents to erode is the truncation of pre-existing sediment layers by some of the coarse layers. It is assumed that during the Pleistocene, sediments being transported by littoral currents would become trapped in the canyon head and subsequently funneled to the abyssal plain as turbidity currents. It seems highly unlikely that the vast quantities of sand and silt present on the fan in the form of turbidity current layers (Nelson, 1967) passed through the

canyon without any erosive action.

Bottom currents also may have played a part in the cutting of the canyon. While there is no evidence for their presence in Astoria Canyon, investigators using deep submersibles have reported the presence of bottom currents from other canyons (Shepard et al., 1964; Shepard, 1965a; Von Rad and Hesse, 1966; Shepard and Dill, 1966). Von Rad and Hesse measured currents in La Jolla Canyon having a maximum velocity of up to 25 cm/sec, which is sufficient to erode medium sand. They reported that these currents pulsate and are possibly tidal. Shepard et al. (1964) suggested that these bottom currents may be due to (1) internal waves, (2) surf beat and/or (3) seaward return flow of water carried shoreward by surface swells. It was the opinion of Heezen and Hollister (1964) that deep-sea currents may be instrumental in eroding turbidity current deposits, thus making the distinction between turbidity current and bottom current deposits difficult to discern.

Burrowing organisms are deemed important agents of erosion. They weaken the canyon walls and the wall sediment responding to the pull of gravity falls to the floor of the canyon. Some of the lithified sediments dredged from the walls of Astoria Canyon are riddled with burrows (Figure 34), and cores taken from the walls of the canyon also exhibit intensive burrowing (Figure 35). First hand investigation of the walls of Scripps Canyon with the use of

SCUBA equipment led Dill (1964) to the conclusion that benthic organisms play an important role by making the rock more easily erodable by other processes.

Transportation and Deposition

The sediments once loosened by erosion are transported by many different agents to their final site of deposition. Often the agent of erosion also does the main transporting, but in many instances one process erodes and a second provides the impetus for continued transportation.

The bulk of the sediment moved toward the sea by the Columbia River is transported during the spring and summer maximum discharge period. During the winter season (time of greatest precipitation) smaller streams and rivers transport maximum amounts of sediment from the Coast Range. Sediments are also being added to the sea by wave and gravity-induced mass wasting from the beach cliffs and terraces (North and Byrne, 1965). Runge (1966) has estimated that over 21,000,000 cubic feet of sediment is added to the Oregon Continental Shelf annually as a result of coastal erosion.

The sediment carried into the sea by the Columbia River, by streams draining the west flank of the Coast Range and by land slides and wave action are transported along shore by littoral currents. The flow is south in the summer and north in the winter due

to the variations in prevailing wind directions. Ballard (1964) reported that in the vicinity of the Columbia River net sediment movement by littoral transport is in a northerly direction. Gross and Nelson (1966), in a study of radioactive bottom sediment contributed by the Columbia River, reported that the sediment moves northwest across the shelf. They obtained rates of 12 to 30 kilometers per year toward the north and 2.5 to 10 kilometers per year toward the west.

At present, with the head of Astoria Canyon approximately nine miles off shore, several years would be required for the sediment to reach the canyon. During Pleistocene times of glacial maxima, however, sea level may have been 60 to 90 fathoms lower than at present (Shepard, 1963). The canyon must have been a very effective sediment trap, intercepting the sands moved by the littoral currents in a fashion comparable to that of the canyons off Southern California today (Shepard, 1963; Hand and Emery, 1964).

Much of the sand and silt trapped in the head of the canyon eventually found its way down the canyon to abyssal depths. Proof of this are the abundant coarse layers found at depth in cores collected from the lower part of the canyon (Figure 24) and from Astoria Fan (Nelson, 1967). Questions arise over the mode of transportation of such sand and silt layers. Mass wasting processes have been favored by Dill (1964) and Chamberlain (1964). Bottom currents have

been suggested as the answer by von Rad and Hesse (1966), Hubert (1964), Kaplin (1961) and Shepard (1965a). Turbidity currents have been hypothesized as the agents of transportation by Gorsline and Emery (1959), Ericson et al. (1961), Hand and Emery (1964), Kuenen (1964), Menard (1964), Heezen, Hollister and Rudiman (1966) and Kulm and Griggs (1966). All three processes, mass wasting, bottom currents and turbidity currents, probably played a part in the transportation of sands and coarse silts into deeper water. However, based on texture, composition and structure of the coarse layers, it is suggested that turbidity currents generated by slumps at the head of the canyon were the chief transporters. One piece of textural evidence for turbidity or density current origin of the coarse layers is positive skewness which according to Ericson et al. (1961) is indicative of turbidity currents, whereas, negative skewness is typical of sediment winnowed by bottom currents. Poor to moderate sorting would be more typical of a density flow than it would be of bottom current activity for, as Hubert (1964) suggested, the winnowing action of bottom currents would result in good sorting. The similarity between C M patterns of these coarse layers and of known turbidity current deposits (Figure 28) is yet another line of textural evidence which indicates that density or turbidity currents were the agents of transportation and deposition of the sediments making up the coarse layers. Graded bedding (Figure 35) is a feature of some

of the coarse layers that is characteristic of turbidites (Kuenen and Migliorini, 1950). The presence of displaced shallow water benthic foraminifers, numerous terrigenous plant fragments and heavy mineral suites that are similar to those of the inner shelf sand (Runge, 1966) and Astoria Fan coarse layers (Nelson, 1967) reenforce the thesis that these coarse layers are composed of sediments that were transported from shallow to deep water.

On the walls of the canyon, beneath the cover of postglacial mud, laminated gray clayey silt has been cored (Figure 35). These laminae of silt sized particles are quite different than most of the coarse layers from the floor of the canyon. The very high percentages of mica in these laminae (Figure 19) suggest much lower velocities of the transporting medium than that which transported the several-centimeter-thick coarse layers found on the canyon floor. These laminated sediments seem to be similar to what Schneider and Heezen (1966) called contourites. They believed that fine laminae of clean silts found on the continental rise off the east coast of the United States were transported parallel to contours of the rise by deep ocean currents (geostrophic contour currents). Hand and Emery (1964) reported fine-grained, thin-bedded sediments to be present on the walls of submarine canyons which cut the continental margin at the north end of San Diego trough. They suggested that these sediments were transported by turbidity currents, but

represent only the more dilute higher parts of these flows. This latter explanation is favored for the laminated clayey silts of the study area because the silt laminae appear to be restricted to the Pleistocene sediments. This was a time, based on the incidence of coarse layers, of much greater turbidity current flow down Astoria Canyon than at present. Additional evidence supporting this hypothesis was provided by Shepard and Dill (1966). They mentioned that, from deep submersibles, low density, low velocity turbidity currents have been seen transporting micaceous silts deep in submarine canyons.

Homogeneous silty clay is the most plentiful of all the sediment types in the Astoria Canyon area (Table 6). The abundance of terrigenous elements in the coarse fraction of this sediment indicates a continental source for these materials. Many of these fine sediments are carried a great distance to sea by the Columbia River effluent as shown by the radionuclides measured in the surface sediment of the Astoria Canyon area (Osterberg, Kulm and Byrne, 1963). Pelagic organisms make up varying amounts of the coarse fraction of these muds; the farther from shore, the greater is the pelagic influence on the sediment content (Figure 30). Near shore the terrigenous constituents mask other material. At the present time hemipelagic and pelagic deposition is of greater importance in the canyon than it was during the Pleistocene when turbidity currents

carried much more sediment into deep water. Hemipelagic and pelagic deposits, being less affected by the variations in bathymetry than are sediments transported by slumps, turbidity currents and bottom currents, have blanketed the entire region. This blanket of sediment is of variable thickness, however, as even sediments deposited particle by particle on the walls of the canyon are subjected to mass wasting. Slumping results in greater thickness of fine grained sediment on the canyon floor than on the canyon walls.

Interspersed with some of the Pleistocene gray clays are isolated pebbles and cobbles. The occurrence of these large particles randomly dispersed among the silts and clays is best explained by ice-rafting.

Near the shelf edge, zones of slow or non-deposition are marked by authigenic deposits (Figure 29) and by relict sands (Figure 25). The authigenic material is glauconite and in some areas makes up more than 50% of the surface sediment. Some of the cores in this region reveal a thickness of glauconite-rich sediment of more than ten centimeters. Such thicknesses of this surface forming authigenic material may be due to extensive activity of burrowing organisms which serves to carry the glauconitized sediments into the substrate.

Summary

Processes currently active in Astoria Canyon and adjacent areas are quite different than those which were operative during Pleistocene and earlier time. At the present time the canyon seems to be a site of deposition rather than erosion.

During the Pleistocene Epoch erosion was the dominant process. The Columbia River played an important role in eroding, or at least altering, the head of the canyon during the glacial stages. Mass wasting, slump, and creep served to widen the canyon. Turbidity currents, which were generated by slumping of sediments deposited on the canyon walls and shelf adjacent to the canyon by littoral currents, kept the canyon scoured out and contributed the vertical cutting action necessary to erode the lower portions of the canyon.

Since the last glacial maximum the rise of sea level has moved the zone of maximum littoral current activity shoreward from the head of the canyon. The result is a lessening or possibly a cessation of turbidity current transportation down Astoria Canyon. The Columbia is still transporting vast quantities of sediment to the ocean, but most of it that reaches the canyon is suspended sediment, with the coarser material being trapped in the lower Columbia estuary. The silts and clays transported by the effluent mix with pelagic sediments to form an uneven blanket of hemipelagic mud over

practically the entire region. The exception to this is the outer shelf area where detrital deposition is practically nil as evidenced by the abundant glauconite and the patches of relict sands.

VII. RATES OF DEPOSITION

Three means are available for quantifying sedimentation rates in the Astoria Canyon area. They are:

(1) radiocarbon analyses,

(2) volcanic ash layers,

(3) radiolarian/planktonic foraminiferal ratios.

The locations of the sediments dated are shown in Figure 17.

Carbon 14

Two samples were chosen for dating by radiocarbon analysis,[6] one from the floor of the canyon and one from the floor of a tributary valley. Sample 3-7 (205-207 cm) from the canyon floor consisted of two thin layers of high magnesium carbonate surrounded by olive gray silty clay. The second sample dated was taken from core 18 in a tributary valley at a depth in the core of 205-240 cm. This sample was a gray silty clay containing a fair number of foraminifers.[7]

The sample from the canyon floor (3-7) yielded an age of

---

[6] C^{14} analyses were made on carbonate carbon for sample 3-7 and total carbon for the sample in core number 18, by Isotopes, Inc., Westwood, New Jersey.

[7] Sample 18-8, appendices 2 and 3, is representative of the sediment chosen for the radiocarbon analysis.

5,620 ± 145 years B.P. Based on this figure, a deposition rate of 36.6 cm/1000 years was calculated. From the tributary sample a date of 18,900 ± 800 years B.P. was obtained. Deposition occurred at the rate of approximately 12 cm/1000 years.

Volcanic Glass

Powers and Wilcox (1964) indicated that the eruption of Mount Mazama approximately 6600 years ago spread volcanic ash over a very wide area of the northwestern United States. They cited petrographic data which enabled them to distinguish Mazama ash from other volcanic ash. Based on the similarity of the refractive indices of Mazama ash to those of volcanic glass in layers in the sediments of Astoria Canyon and Fan, Nelson et al. (1967) correlated this glass with the Mazama event. This volcanic glass was not air fall, but was carried to the sea by the Columbia River and most likely deposited in the canyon and on the fan by turbidity currents which originated at the head of the canyon. Evidence which points to such an origin for the volcanic glass-rich layers includes:

(1) impurity of the layer: glass mixed with typical Columbia River heavy minerals,

(2) lack of areal continuity of the glass-rich coarse layers,

(3) absence of abundant volcanic glass on canyon walls and adjacent shelf-slope regions.

(4) similarity in textural parameters of the glass-rich coarse layers and the detrital coarse layers.

(5) displaced shallow water benthic foraminifers in the glass-rich coarse layers.

Although the first Mazama volcanic glass deposited in the canyon did not reach the place of final deposition at the same time that the wind-blown ash was laid down on the continent there must not have been too great a time lag. Fryxell (1965) reported a minimum area of fallout for Mazama ash of about 900,000 square kilometers. The debris thrown out by the Mt. Mazama eruption (Figure 37) must have blanketed the Columbia River drainage system. Possibly as soon after the eruption as the next major spring thaw this ash was transported by streams and rivers to the Columbia River and hence into the ocean.

Most of the cores contain volcanic glass, but in those near the mouth of Astoria Canyon the glass is most abundant. In core number one, a volcanic glass-rich coarse layer 351 cm deep in the core(1-22) evidently marks the first introduction of Mazama ash into the canyon. This two centimeter-thick layer is a sandy silt. The coarse fraction consists of 72% volcanic glass which has an average refractive index of 1.505. The rate of deposition based on a date of 6600 years B.P. is 53.2 cm/1000 years. Cores farther up the canyon (numbers 2 and 3) also contain large quantities of volcanic glass

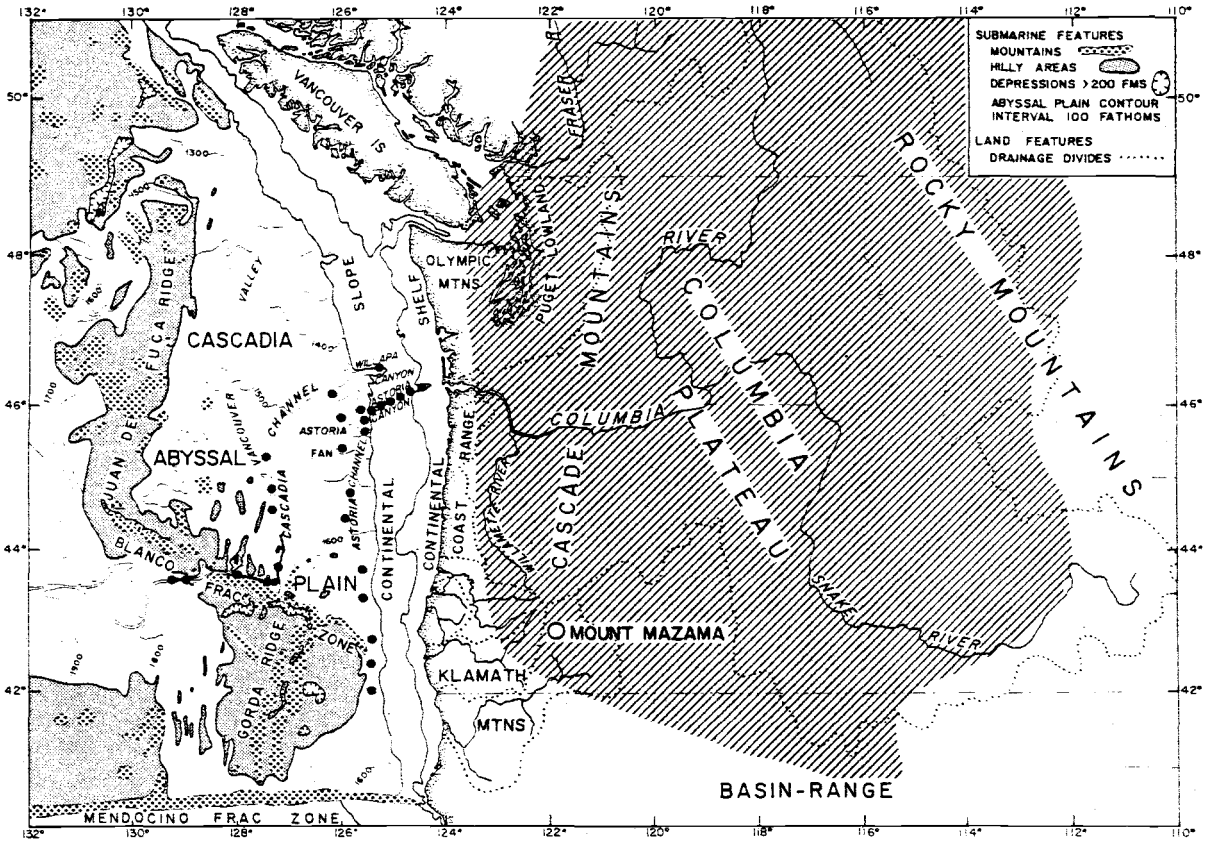

Figure 37. Mazama ash occurrence in the Pacific Northwest and on the sea floor of the northeast Pacific Ocean. Continental limits (shown by slanted line pattern) taken from Fryxell (1965). Sea floor locations (solid black dots represent areas where ash has been found): Willapa Canyon, Royse (1964); Astoria Fan and Channel, Nelson (1967); Cascadia Channel, Kulm (1967), Griggs (1967); and southeastern portion of Cascadia Abyssal Plain, Duncan (1967).

with a similar refractive index, but the layers are not as distinct. In both of these cores, the glass percentages increase to the bottom of the core (Figure 33) indicating that the cores, although both greater than 350 cm in length, may not have penetrated sediment older than 6600 years B. P. Calculations of deposition rates, assuming the bottoms of these cores to represent the first influx of ash, give values similar to or greater than the rate from core one. In core number two 60 cm/1000 years represents a minimum rate. On the floor in the upper end of the canyon Mazama volcanic glass is found scattered throughout the sediment, from the surface down to a depth of at least 500 cm. The low percentages are due to the masking effect of the detrital grains. However, the presence of the ash indicates that these sediments have been deposited since the eruption of Mt. Mazama. Therefore a minimum rate of deposition at the upper end of the canyon would seem to be near 78 cm/1000 years.

An almost pure layer of volcanic glass was cored in one of the tributaries of Astoria Canyon (no. 18, Figure 18). The purity of the layer and its location in a tributary valley rather than in the main canyon suggests that this ash layer may have been part of the suspended load rather than bottom load. As the main influx of Mazama volcanic glass was swept down the canyon, possibly as a turbidity current, the flow very likely covered at least the entire floor of the canyon. Some ponding of the suspended load may have

occurred with the resulting deposition of a glass-rich layer in tributary valleys such as that from which core number 18 was obtained. This layer of an estimated 80% volcanic glass was found 125 cm deep in the core. The refractive indices of these glass shards also average 1.505 which indicates the eruption of Mt. Mazama (6600 years B. P.) was the source of this glass. On the basis of this date the rate of deposition in this tributary valley is 19 cm/1000 years.

Radiolarian-Foraminifer Break

Several hundred miles offshore in the northeast Pacific Ocean, Nayudu (1964) found a change in the dominant planktonic organisms at depth in the pelagic sediment. He suggested that this increase in globigerinids encountered a few centimeters deep in the core represents a paleoclimatic change and placed the time at approximately 12,000 years B. P. Duncan (1967) has expanded and refined this concept showing that a change from dominant radiolarians in the surface few centimeters to dominant planktonic foraminifers represents a significant stratigraphic marker in the deep-sea sediments off Oregon. Based on radiocarbon analyses, he established a date of 12,000 years B. P. for this change in planktonic organisms.

Two cores in the study area (18 and 19, Figure 17) show similar radiolarian to foraminifer relationships (Figure 38). In core 18

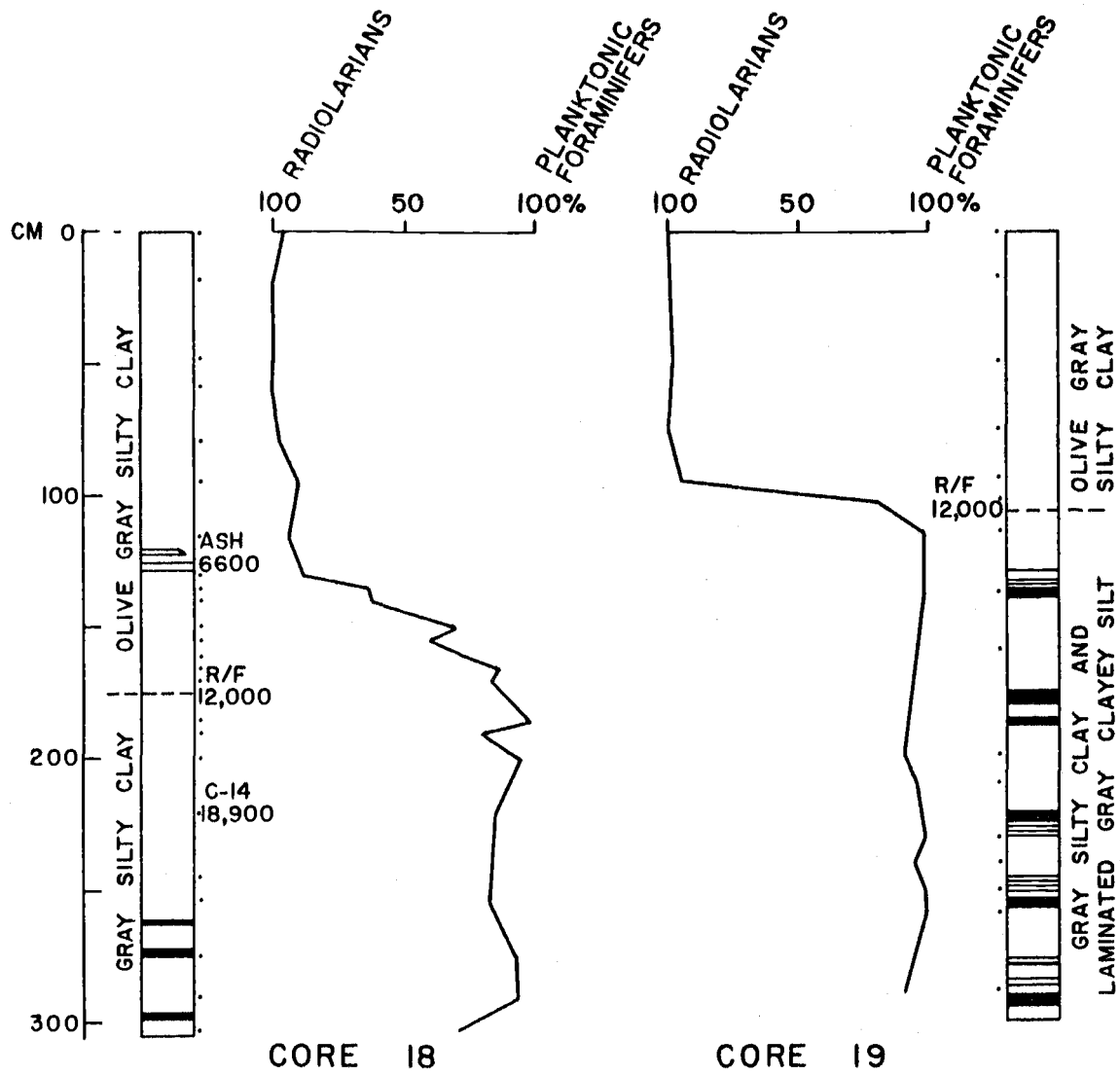

Figure 38. Radiolarian/foraminifer distribution and lithologies of cores 18 and 19. Dots adjacent to cores represent sample positions.

the break is at 175 cm and in core 19 at 103 cm. In both cases the transition coincides quite closely with the change in sediment type from the overlying olive gray silty clay to gray silty clay. Closer to the continent the radiolarians and planktonic foraminifers are less abundant than at the lower end of the canyon. Nevertheless, they are present in sufficient numbers in core 10 (Figure 17) taken from a tributary valley near the shelf-slope break to show the same relationship as that found on the lower slope and abyssal plain. In core 10 the transition from radiolarians to planktonic foraminifers coincides with the olive to gray color change in the sediment at 435 cm.

Calculations based on 12,000 years B.P. as the time of the change yield a sedimentation rate of 15 cm/1000 years in the case of the tributary core number 18 and 36.2 cm/1000 years for tributary core number 10. For core 19 taken from the levee at the mouth of the canyon, the rate of deposition is approximately 9 cm/1000 years.

Summary and Comparison

Astoria Canyon

The rates of deposition in the Astoria Canyon area range from less than 10 cm/1000 years to more than 75 cm/1000 years

(Figure 39). This great range in rates is influenced primarily by physiographic location and to a lesser degree by distance from shore.

On the floor of the canyon near the mouth the rate of deposition based on the first occurrence of Mazama volcanic glass is 53.2 cm/1000 years. Rates of up to 78 cm/1000 years have been estimated for sediments further up the canyon.

In core number three, rates of sedimentation have been computed using two different dates. A radiocarbon date indicates 36.6 cm/1000 years for the upper 200 cm. The rate for the entire core based on the volcanic glass maximum at the base of the core yields a rate of 53 cm/1000 years. This difference suggests that the depositional rate for the lower 150 cm of the core sediment was three times greater (150 cm/1000 years) than for the upper 200 cm. This hypothesis is consistent with the increased thickness and number of coarse layers with depth in the cores taken from the canyon floor (Figure 34).

Core number 18 from the canyon tributary was dated using all three methods. The rates of deposition based on the three different methods are:

(1) C^{14}	12 cm/1000 years
(2) Mazama glass	19 cm/1000 years
(3) Radiolarian-foraminifer break	15 cm/1000 years

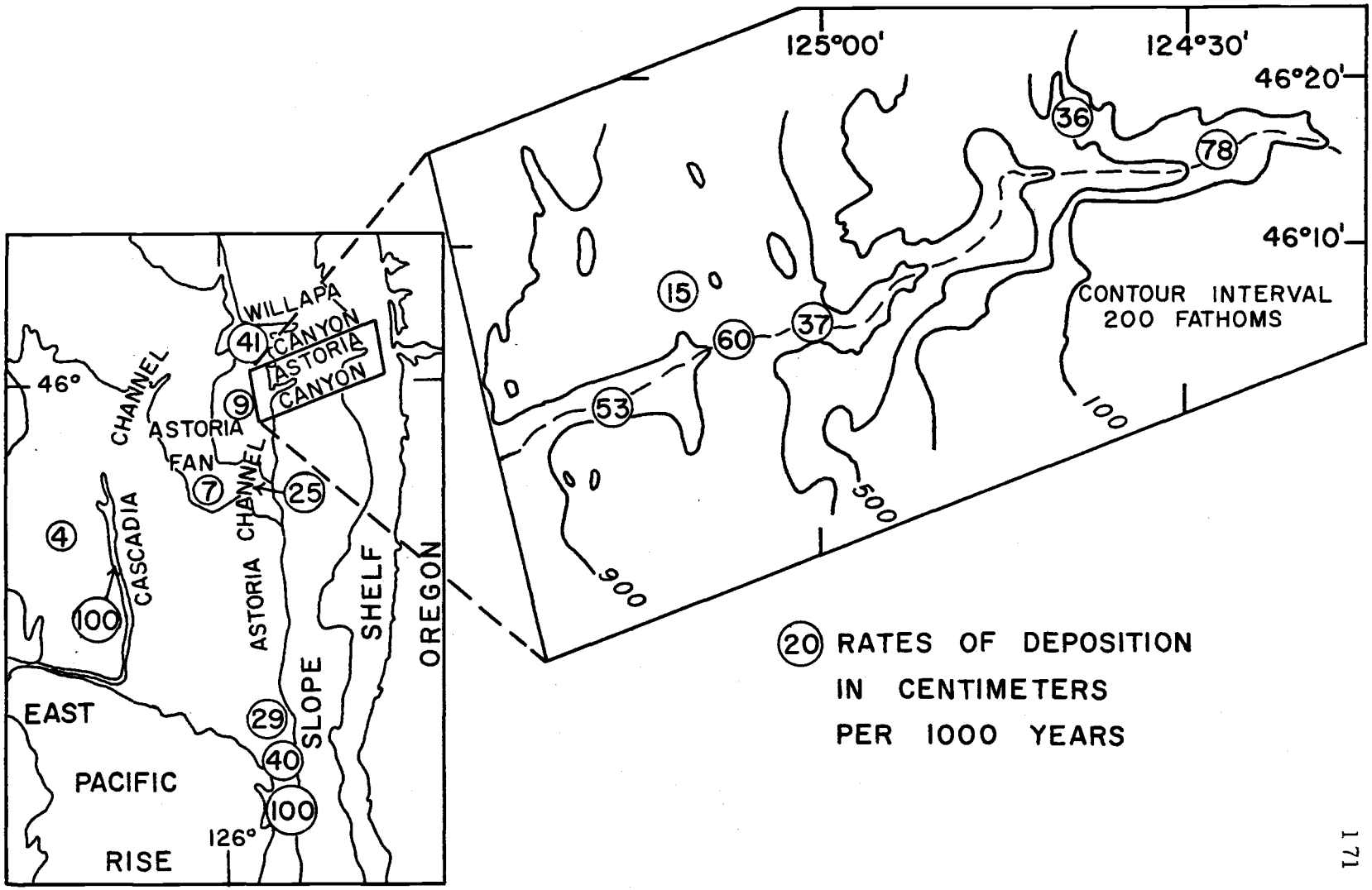

Figure 39. Map of postglacial deposition rates in Astoria Canyon and nearby areas.

The relative positions of the dates and the lithologic variations of the core (Figure 38) show a much slower and more uniform rate of deposition than in the canyon floor sediments.

Astoria Fan

On the north levee at the mouth of the canyon the rate of deposition is approximately 9 cm/1000 years based on the radiolarian-foraminifer change. This rate is consistent with rates calculated by Nelson (1967) for sediments of the inner part of Astoria Fan. However, for sediments from the outer fan Nelson has calculated rates of deposition of less than 5 cm/1000 years using first occurrence of Mazama volcanic glass and the radiolarian-foraminifer change as dating horizons. In Astoria Channel Nelson has calculated rates greater than 25 cm/1000 years based on first occurrences of Mt. Mazama volcanic glass.

Deposition Rates in the Northeast Pacific Ocean

Sedimentation rates in Cascadia Channel (Figure 39) range from 15 to more than 100 cm/1000 years (Kulm and Griggs, 1966). These rates are based on the occurrence of Mazama glass and substantiated by radiocarbon dates.

West of Cascadia Channel on Cascadia Abyssal Plain, Kulm

and Nelson (1967) reported a change in the rate of deposition from glacial to postglacial times. These rates are based on the C^{14} date which supports the radiolarian-planktonic foraminiferal transition as a marker of the change from glacial to postglacial sedimentation conditions at 12,000 years B. P. According to Kulm and Nelson the most rapid deposition in this area west of the channel took place during the Pleistocene with rates calculated to be greater than 170 cm/1000 years. However, using the radiolarian-foraminifer break as the beginning of postglacial sedimentation yields approximately 4 cm/1000 years for the present rate of deposition (Kulm, 1967).

Off the southern Oregon Coast at the eastern edge of Cascadia Abyssal Plain, Duncan (1967) has calculated postglacial rates of deposition ranging from 29 cm/1000 years to 100 cm/1000 years (Figure 39). These calculations are based on both radiolarian-foraminifer changes and occurrence of Mazama volcanic glass.

On the upper slope in the Willapa Canyon region the sedimentation rate corresponds well with rates in the Astoria Canyon area. Based on the occurrence of Mazama ash and on C^{14} dates Royse (1964) calculated a rate of 41 cm/1000 years in the lower end of the canyon.

Maximum rates of deposition in the northeast Pacific occur on deep-sea channel floors, in places reaching more than 100 cm/1000 yrs. These high rates are believed to be due in large measure to

turbidity current deposition. Far from the continent and away from the channels, however, rates of deposition are less than 5 cm/1000 yrs. These sediments are primarily pelagic. In protected areas on the continental slope, the closeness to the continent results in an increase of hemipelagic deposition. In these areas the rate rises to above 10 cm/1000 years. The rate of deposition on the floor of Astoria Canyon ranges from about 50 cm/1000 yrs near the mouth to more than 75 cm/1000 yrs near the head.

VIII. GEOLOGIC HISTORY OF ASTORIA CANYON

Interpretation of the history of Astoria Submarine Canyon is based upon sedimentary and bathymetric data. These data are supplemented by other geological and geophysical information, both marine and continental, in order to obtain some insight into the development of the continental terrace.

Continental Terrace

Since early Tertiary time a north-south trending eugeosyncline has occupied western Oregon and Washington extending from the western edge of the Cascades to "some miles west of the present coast line" (Snavely and Wagner, 1963, p. 1). Gravity data have indicated the probable presence of north-south trending stratigraphic basins on the shelf in the Astoria Canyon area (Couch, 1967). On the slope in the vicinity of the canyon, Emilia, Berg and Bales (1967) reported depths to sources of magnetic anomalies which may indicate sediment thickness of more than 30,000 feet.

Based on the outcrops of Tertiary sediments in the Coast Range and along the coastal plain, Snavely and Wagner (1963) concluded that the shoreline moved progressively westward. By Miocene time it occupied much the same position as the present-day shoreline, except for a broad downwarping in the Columbia River region. Into

this depression the ancestral Columbia River has carried the arkosic and lithic sands which make up a large part of the Astoria Formation. Foraminifers from the type section of the Astoria Formation indicate that bathyal water depths occurred in this embayment during the middle Miocene (Carlson, 1965).

The Miocene Epoch was also the time of great outpouring of Columbia Plateau Basalt. In northwestern Oregon submarine lavas have been found intertonguing with Astoria marine sediments (Baldwin, 1964). Outcrops of laterized Miocene basalt led Lowry and Baldwin (1952) to the conclusion that the Columbia River had a low gradient during much of the Miocene. Regional uplift of the Coast Range in late Miocene time resulted in the withdrawal of the sea from the Astoria embayment (Snavely and Wagner, 1963). They located the Pliocene shoreline approximately five miles west of the present day mouth of the Columbia River.

The Coast Range was uplifted to its modern day elevation in the late Pliocene and at the same time volcanism in the Cascade area was building the platform on which the Quaternary andesitic cones were to form (Snavely and Wagner, 1963). As the Cascade Mountains were attaining their present elevation in Pliocene-Pleistocene time, the Columbia River kept pace with the uplift by scouring out the scenic gorge it now occupies (Mackin and Cary, 1965). One result of this uplift and consequent erosion by the Columbia and its

tributaries was the deposition of a sizeable thickness of sediment in the area of the present continental shelf and slope (Table 14, Figure 36).

At the same time the continental morphology was being changed, great changes were also taking place in the deep sea. Sometime during the Early Tertiary (Menard, 1964) or Late Cretaceous (Vine, 1966), the East Pacific Rise had its inception. This rise, a zone of high heat flow, is thought to be the surface manifestation of the upwelled limb of convection cells which are the mechanisms called upon by Hess (1962) to maintain sea floor spreading. Vine (1966) through the use of paleomagnetic anomalies assigned a spreading rate of 2.9 cm/yr for the last 5.5 million years to the Juan de Fuca Ridge[8] (Figure 1). He suggested that prior to that time the rate may have been as high as 5 cm/yr. Vine speculated that the spreading direction changed from east-west to northwest-southeast at the same time as the rate changed. He is of the opinion that the more recent geologic structures of the western United States are due to the westward drifting continent overriding the eastward spreading limb of the East Pacific Rise. In the Southwestern United States this has progressed to such a degree that the crest of the rise has been

---

[8]Name applied to a segment of the East Pacific Rise off the Oregon and Washington coasts.

"overriden and damped out" (Vine, 1966, p. 1411). In the Pacific Northwest, however, he indicated that only the east flank of the rise has been overriden by the continent.

A result of impingement of the spreading sea floor on the continental terrace is expressed in a series of north-northwest trending ridges and troughs which make up the slope in the study area (Figure 2). Other lines of evidence of the compressional effect of the sea floor spreading from the East Pacific Rise have been reported from the central Oregon shelf. Sparker records show complex minor folding and possible faulting superimposed on a synclinal structure (Whitcomb, 1965). Dips up to 16 degrees have been determined by Erickson (1967) for some of the shelf strata. Byrne, Fowler and Maloney (1966) reported that Miocene and Pliocene rocks from the central Oregon shelf and slope have been uplifted as much as 1000 meters since their deposition. This uplift they attribute to compressional forces acting normal to the continental margin. Byrne et al. further suggested that there has been an average maximum of 16 km of horizontal accretion of sedimentary rock since their deposition during the Pliocene.

Siltstones and mudstones bearing well-preserved burrows and some oxidized zones have been dredged from the walls of Astoria Canyon (Figure 34). Although no foraminifers were obtained from these rocks, the high degree of induration, the well-preserved

burrows, the presence of oxidized zones and the similarity to Late Tertiary rocks dredged from the central Oregon shelf by Maloney (1965) point to a possible late Tertiary age for these rocks cropping out on the walls of Astoria Canyon. Foraminiferal evidence indicates that Pliocene semi-consolidated sediments crop out on the walls of the canyon, but the paleodepths of these fossils generally correspond to present day water depths (Fowler, 1967). Therefore, it appears that the last significant uplift of the continental shelf and slope in the study area may have occurred during the Pliocene. Any tectonism since that time has not been of sufficient magnitude in the Astoria Canyon region to be distinguished on the basis of the faunal record. Marine terrace heights along the Oregon coast bear out this conclusion. These Plio-Pleistocene terraces (Baldwin, 1964) which are present in varying numbers all along the Oregon coast are much more pronounced along the southern than the northern coast. Going from north to south along the coast these discontinuous terraces generally are found at increasingly higher elevations. In the southern coastal areas the uppermost of the several marine terraces have been identified at elevations of 1500-1600 feet above sea level (Baldwin, 1964).

Events of Pliocene-Pleistocene time which affected the development of Astoria Canyon included:

(1) glacial advances and retreats and the accompanying fall and

rise of sea level,

(2) local and regional uplifts and downwarpings of adjacent continental areas,

(3) damming of rivers, particularly the Columbia River, by ice sheets with resulting catastrophic floods after breakup of the ice dams,

(4) volcanism resulting in the formation of the andesitic composite volcanoes of the Cascade Range.

Canyon Cutting

The origin of submarine canyons has been debated for many decades. During the last half of the nineteenth century many ideas about these mysterious canyons were published. After a hiatus in the debate about canyon origins during the first quarter of the twentieth century, a rash of publications began appearing in the early 1930's. Johnson (1939) and Shepard and Dill (1966) have thoroughly reviewed these early hypotheses. The arguments over the past 30 years have revolved around the relative merits of turbidity current versus subaerial erosion of the canyons. There has been a gradual evolution of these theories (Shepard, 1952; Kuenen, 1953) as more and more field evidence has been collected. Some of the newer evidence, based on direct observations made possible by the advent of Scuba equipment and deep submersibles, stresses the importance

of marine processes such as creep and slump (Dill, 1964; Chamberlain, 1954) and bottom currents (Pérès, Picard and Ruivo, 1957; Shepard et al., 1964; Shepard, 1964; von Rad and Hesse, 1966). However, in spite of all the sediment cores, dredge hauls, deep-sea photographs and direct observations, in the words of Shepard and Dill (1966), "The origin of canyons on the sea floor is today almost as puzzling as it was to the early investigators."

The volume of sediments making up Astoria Fan indicate that incision of the canyon may have begun in late Pliocene or early Pleistocene time. During the early Pleistocene as the first glacial lobes advanced, sea level dropped, exposing extensive areas of the continental margin to subaerial erosion. At this time the Columbia River flowed across the shelf and deposited its load of sediments on the continental slope. According to Curray (1965) during the times of lowest stands of sea level, practically all marine deposition occurred on the upper slope where rivers discharged their sediment load at the shelf edge. The lower base level permitted the river to cut a sizeable channel into the shelf sediments. The river also scoured its present channel much deeper. Excavations in the channel for the footings of the bridge spanning the Columbia River near Astoria had not reached bedrock at a depth of 250 feet (Glenn, 1966). The greatest amounts of erosion may have taken place when the huge ice dams which created glacial Lake Missoula

failed. According to Richmond et al. (1965) this occurred at least three times, the last approximately 18,000 years ago. The eroded sediment from the shelf was also transported to the sea and deposited on the continental slope. This time of downcutting was probably repeated numerous times during the Pleistocene. In between glacial ages, the higher stands of sea level resulted in the filling of these shelf channels (Figure 14).

At the same time the Columbia River was eroding a channel across the shelf, and possibly even earlier, marine processes such as slumps and turbidity currents were cutting into the continental slope. Some of the sediment carried to the sea by the river was probably deposited on the slope during the glacial ages. Slumping resulted in large masses of sediment being moved down the slope to the abyssal plain. As these slump blocks moved downslope, the sediment would mix with the overlying water resulting in turbidity or density flows. The turbidity current moved down the slope eroding and thus incorporating more sediment from the slope. This sediment was deposited on the abyssal plain and now remains as part of Astoria Deep-Sea Fan.

Once a gully was started on the slope, it acted as a funnel to the abyssal plain. The sediment which was funneled down this embryonic canyon came not only from the muddy waters of the Columbia, but also from the littoral drift. As the canyon increased in size it

was able to trap even more littoral current transported sand which in turn was moved down the canyon. Although one turbidity current probably would not be sufficient to carve even a small canyon, this process repeated over many hundreds of thousands of years must have resulted in significant erosion. Heezen et al. (1964) estimated, on the basis of cable breaks, that the Congo Submarine Canyon is presently experiencing turbidity currents at the rate of 50 per century. If we assume, as they do, that this rate would compare favorably to, or may be even less than, that experienced by canyons off Pleistocene rivers, more than 200,000 turbidity currents would have occurred in Astoria Canyon. This figure is based only on the length of the glacial ages (424,000 years out of a total of 1.5 million years for the entire Pleistocene according to Ericson and Wollin, 1964). Probably additional thousands of turbidity currents moved down the canyon during interglacial times when the glaciers were receding, but sea level had not reached its present day high position.

The route taken by these slumps and turbidity currents must have varied somewhat depending upon the initial relief, the position of the Columbia River as it flowed across the shelf, the angle of storm wave approach, and the direction of longshore current movement to name some of the variables. However, it is suggested here that underlying structure may have played an important part in determining the path of the canyon. This hypothesis is based on the

step-like offsets of the canyon axis (Figure 5) and the offsets of the sedimentary basins north and south of the canyon as defined by gravity contours (Couch, 1967). Also the north-northwest trends of the ridges and valleys suggest significant structural influence on the continental slope.

The river flowing across the shelf and the turbidity currents flowing down the slope resulted in downcutting of the canyon. As Kuenen (1953) pointed out, however, canyon widening is accomplished by slumping from the canyon walls. In Astoria Canyon slumping may have occurred as a result of: burrowing and boring activities of organisms; earthquakes; oversteepening of the walls due to downcutting on the canyon floor; agitation by storm waves and tsunamis; and deposition of large amounts of sediment in or near the canyon head by the Columbia River during flood stage and by littoral currents.

The volume of sediment removed from the shelf and slope to form Astoria Submarine Canyon is approximately 400 cu km (67 cu nautical mi). The volume of the fan, however, is estimated at approximately 27,500 cu km (4300 cu nautical mi) (Nelson, 1967). This amount which does not include the underlying Cascadia Abyssal Plain deposits, is approximately 70 times greater than the volume of sediments eroded to make Astoria Canyon. If the assumption is made that Willapa Canyon was formed by removal of the same

amount of sediment as Astoria Canyon, the volume of the fan is 35 times greater than the volume of the two canyons. The additional sediment was contributed by the Columbia River and by littoral currents. Present day sediment contribution of the Columbia River to the lower estuary is approximately 12.2 million cu m/yr (.0122 cu km/yr) (16 million cu yds/yr): (bottom load 1.78 million cu yds/yr (Lockett, 1965b); suspended load 14.5 million cu yds/yr (U.S. Army Engineers, 1962)). Although much of this sediment does not reach the ocean but is trapped in the estuary, it is assumed that at least 12 million cubic meters of sediment must have been added annually during the Pleistocene. During the time of the gigantic floods which carved the channeled scablands of Washington, even more sediment than the suggested annual volume was probably funneled down Astoria Canyon to the fan. The littoral current contribution is estimated to be about 3.1 million cu m/yr (.0031 cu km/yr).[9]

Addition of the average annual volume of sediments contributed by the Columbia River and by littoral drift gives a volume of .0153 cu km/yr. At this rate Astoria Fan could be built in 4,000,000 years assuming a compaction to 45% of the original volume. The compaction factor is taken from a table compiled by Hamilton (1959). This calculation assumes an average fan sediment thickness of 1.4 km

---

[9] Based on computations made in regional geology section, p. 12.

(Nelson, 1967). Also inherent in this calculation is the assumption that all of the sediment contributed by the Columbia and by littoral drift goes into the formation of Astoria Fan. Even if we add to this the volume of sediments removed to form Astoria and Willapa Canyons, the time would be only slightly reduced. This four million years indicates that the fan and canyon system originated during the Pliocene. However, if the volume of sediments carried by the Columbia River was much greater during the Pleistocene than it is now, the number of years needed to form the canyon and fan system would be reduced. If we assume a volume three times greater than the present sediment load of the Columbia River, which seems justifiable based on the postglacial and glacial differences in rates of deposition of Astoria Fan sediments (Nelson, 1967), 1.36 million years would be needed to build the fan. This would bring the time of origin to within Pleistocene time.

By way of comparison, Menard (1960, p. 1278) has arrived at a pre-Pleistocene "possibly even pre-Pliocene" date for the time of origin of the Monterey Canyon and Fan system. Martin (1964) concluded that Monterey Canyon was cut as early as late Pliocene time. Wilde (1965) suggested that Monterey Fan may have been forming as early as Oligocene time. On the other hand, the canyons cutting the continental margin of the eastern United States are believed by many investigators to have been cut during the Pleistocene (Stetson,

1949; Ericson, Ewing and Heezen, 1951; Ericson et al., 1961).

Canyon Filling

Although many canyons are presently acting as sediment supply routes to the abyssal depths, others such as Astoria Canyon no longer appear to be serving in such a capacity. Instead this canyon appears to be filling. Various lines of evidence bolster such a hypothesis:

(1) buried channels between the head of the canyon and the mouth of the Columbia River,

(2) thick accumulations of sediment in the canyon dating back to Mt. Mazama eruption (6600 yrs B.P.),

(3) lack of coarse layers in the surface parts of piston cores from the canyon and the fan.

The last glacial episode in the Pacific Northwest (Fraser), according to Crandell (1965), took place between 25,000 and 10,000 years ago. With the final retreat of the glaciers and resulting rise in sea level, the large volume of sediments being carried by the Columbia River began to fill the shelf channels and the present day estuary. These channels became buried as the zones of wave base and effective littoral current transport were moved progressively eastward to their present position by the rising sea level. When the canyon no longer was able to intercept the sediments moved by longshore currents, the canyon-cleaning turbidity currents were

not generated. Lacking these scouring density currents the canyon began to fill with hemipelagic sediments.

Even after the canyon began to fill, however, some turbidity currents continued to flow down the canyon. Evidence for these currents are coarse layers found in cores taken from the lower end of the canyon. These last flows were probably emplaced before sea level reached its present position. Some of these sediments apparently came directly down the Columbia River, across the shelf and down the canyon to a place of deposition near the mouth of the canyon. Coarse layers, in core no. one (Figures 18 and 33) made up largely of volcanic glass from the eruption of Mount Mazama (6600 yrs B. P.), are evidence of such a route. Radionuclides in the surface sediments of the canyon (Osterberg, Kulm and Byrne, 1963) also indicate that sediment is being added to the canyon at the present time. The fine nature of these surface sediments, however, suggests that the sediment is carried primarily in suspension rather than as bottom load. Precision depth recordings seem to indicate that slumping has occurred on the canyon walls, adding to the canyon fill.

Based on the various rates of deposition calculated by several means, a timetable for complete filling of the canyon may be set up (Table 15). Implicit in such estimations is the unlikely assumption that the filling would continue at a constant rate.

Table 15. Timetable for the filling of Astoria Canyon.

Core number and location	Type of date	Rate cm/1000 yrs	Minimum relief (fms)	Years needed to fill completely	
				no compaction	compaction*
Canyon floor					
1-22 near mouth	volcanic ash	53.2	260	895,000	2,560,000
3-7 mid-canyon	C^{14}	36.6	240	1,200,000	4,200,000
12 upper canyon	volcanic ash	78.3	200	468,000	1,340,000
Tributaries					
18-3 lower cont. slope; north wall of canyon	volcanic ash	19.0	180	1,730,000	4,950,000
18	Radiolarians Plank. forams	14.7	180	2,240,000	6,390,000
18	C^{14}	11.9	180	2,770,000	7,900,000
10 shelf-slope area; north wall of canyon	Radiolarians Plank. forams	36.2	200	1,010,000	2,890,000

* Assuming final gravity compaction to 35% of their original thickness (Emery and Bray, 1962).

Summary

Astoria Submarine Canyon which was probably cut during late Pliocene-Pleistocene time is not the result of only one erosional process but a combination of several. During the glacial ages, the Columbia River cut channels across the exposed continental shelf. Thus subaerial erosion was responsible for the cutting or at least modifying the head of Astoria Canyon. During low stands of sea level sands moved by longshore currents were intercepted by the head of the canyon. These sands and sediments carried by the river were moved down the canyon and out on the fan by turbidity currents which provided the scouring necessary to cut vertically. The canyon increased in size laterally by mass-wasting processes active on the walls of the canyon. These slumps and slides may have been influenced by numerous agents including burrowing organisms, earthquakes, tsunamis, and severe storms. Erosion of the canyon possibly was made easier because of tectonic activity. The morphologic character of the canyon indicates that it may have been cut along a zone of structural weakness.

Astoria Canyon is currently being filled by hemipelagic sediments. This filling began after the effective zone of littoral drift was moved shoreward of the present day head of the canyon, and the shelf channels began to fill. When this happened, at least 6600 years

ago, the incidence of canyon scouring turbidity currents was greatly curtailed. Other factors that possibly contributed to the cessation of turbidity currents in Astoria Canyon may have been a decrease in runoff and a decrease in the amount of sediment load contributed by the Columbia River. Presently the estuary is filling, thus cutting off much of the coarser sediments that were probably supplied to the canyon during Pleistocene glacial ages.

The rates of deposition of these canyon filling sediments range from 12 cm/1000 yrs in a tributary to more than 78 cm/1000 yrs in the main canyon. At these rates the length of time needed for the canyon to become filled varies from less than two million to almost eight million years.

IX. GEOLOGICAL SIGNIFICANCE OF SUBMARINE CANYONS

The study of modern submarine canyons can be a real aid to the recognition of ancient submarine canyons.

Canyons are currently incised into the margins of all continents. These incisions provide opportunity to sample pre-Holocene sediments and, thereby, shed additional light on the history of the continental margin.

Submarine canyons act as funnels through which sediments pour from the continent to abyssal depths. Because of the transitional relationships of these physiographic features, the sediments on the floors of submarine canyons are sources of information about modes of emplacement and provenance of coarse sediments found at abyssal depths.

Investigations of widely diverse canyons in various stages of development are necessary to obtain a complete picture of the origin and subsequent filling of submarine canyons. Many studies of the marine environment have included some discussion of the role of submarine canyons as a part of a larger study. Other investigations have been centered on some facet of one or more canyons. Very few studies, however, have concentrated on characteristics of modern day canyons which will aid in the detection of "fossil" canyons. Most of the canyons studied in greatest detail, those off

Southern California, serve as active routes of sediment movement. The transport of sediments down these canyons, whatever the process, keeps the canyons scoured out. Astoria Canyon, on the other hand, is a canyon that is currently being filled. As such it provides an excellent opportunity to study in a Recent environment differences in characteristics of canyon sediments.

Summary of Characteristics of Astoria Canyon

Geometry of the Canyon

Astoria Canyon has a sinuous axial pattern with an average gradient of one degree. The transverse profiles of the canyon vary from U to V shape. The slope of the walls varies from 2° to 17° with an average of 6°. The width of the canyon averages approximately four miles from rim to rim and slightly more than one mile across the floor. The relief of the canyon in the shelf area ranges from less than 60 to 310 fathoms. In the slope portion of the canyon the relief varies from 80 to 520 fathoms.

Astoria Canyon has numerous tributaries entering from each side and channels located at both ends. On the shelf near the head of the canyon, channels which probably served to connect the Columbia River to the head of the canyon are buried by postglacial sediments. Several deep-sea channels radiate from the lower end

of Astoria Canyon onto Astoria Fan.

Sedimentary Characteristics

Diagnostic features of sediments of the canyon can be categorized in terms of texture, composition and sedimentary structures.

The sediments which are currently being deposited in the canyon range from sandy clayey silt at the upper end to silty clay at the lower end. These sediments are poorly sorted and both positively and negatively skewed. At depth in this fill, moderately to poorly sorted coarser layers of very fine sand to medium silt (modal size) are interbedded with the silty clay. These coarse layers contain considerable feldspar and rock fragments and are thus considered as arkosic, lithic and volcanic wackes (classification system of Williams, Turner and Gilbert, 1958). Sand-shale ratios for piston cores collected from the canyon floor range from 1:2 to 1:27 (Table 16). The number of sand layers increases with depth in the sediment, indicating a greater influx of turbidity currents during glacial than has occurred in postglacial time. In general, the sand-shale ratio of the cores increases slightly with distance down the canyon. This trend continues into Astoria Channel where Nelson (1967) has measured sand-shale ratios which range from 2:1 to 4:1.

Upon lithification these sediments which make up the canyon fill will most likely be classified as mudstones and shales. The

Table 16. Sand-shale ratios for piston cores from the floor of Astoria Submarine Canyon. Cores are arranged in descending order from canyon head to mouth. Calculations are based on the assumption that compaction of mud to shale is approximately 35% of the former thickness (Emery and Bray, 1962).

Core number	Number of coarse layers				Total cm of coarse layers	Sand: shale
	Total	cm increments in core				
		0-100	100-200	> 200		
9	12	0	3	9	25	1:7
5	8	0	1	7	10	1:20
12	8	1	2	5	35	1:5
4	9	0	4	5	20	1:11
16	9	1	4	4	25	1:15
3	8	1	3	4	49	1:3
2	25	1	10	14	71	1:2
17	6	1	1	4	6	1:27
1	26	2	9	15	68	1:2

lower portion of the fill will probably be classified as mudstone or shale with numerous sandy partings and sand lenses.

The most diagnostic compositional elements of the canyon fill are plant fragments, radiolarians, diatoms, displaced shallow water benthic foraminifers, and volcanic glass. Plant fragments are abundant in sediments filling the upper end of the canyon, diatoms are the dominant biogenic constituents in mid-canyon, and radiolarians predominate over other planktonic organisms in sediments of the lower canyon. Shallow water benthic foraminifers are present in most of the coarse layers whereas the surrounding muds contain benthic foraminifers representative of deeper environments. Although the volcanic glass found in the sediments filling Astoria Canyon would not be diagnostic of all canyons, it represents a new source of materials suddenly injected into the environment. Any such material supplied from an outside source and essentially confined to the canyon would provide identifying horizons and enable the investigator to delineate the canyon from the surrounding sedimentary facies.

Slumping of sediments from the canyon walls is a common phenomenon which may contribute to creation of intraformational breccias in the sediments of the canyon fill. Mottling also is plentiful in the sediments of the canyon fill, indicating the presence of abundant burrowing organisms. The coarse layers often contain internal structures such as graded bedding and cross-bedding.

Additional structures not found in the coarse layers of Astoria Canyon, but reported from other canyons, include parallel and current-ripple laminations (Bouma, 1965).

Unconsolidated to semi-consolidated Plio-Pleistocene sediments which have been cored on the walls of Astoria Canyon are somewhat finer grained than those sediments currently filling the canyon. These poorly sorted Plio-Pleistocene sediments are primarily silty clays and laminated clayey silts. All of the gray wall sediments are positively skewed in contrast to the sediments of the canyon floor. Lithification of these sediments will produce shale and laminated silty shale.

These facies cored on the canyon walls are characterized by abundant mica and pyrite. Mica is the chief constituent of the laminations. However, some of the laminations are composed largely of pyrite and others primarily of black, soft, paste-like, organic matter. Although the microfossil populations are quite sparse, there is a significant difference in the dominant planktonic organisms in this sediment and the younger canyon fill. Planktonic foraminifers are most plentiful in the Pleistocene sediments and the radiolarians are very rare. The reverse is the situation in the postglacial sediments filling the canyon. Also the fauna of the canyon walls is older than the fauna of the canyon fill sediments.

Aside from the micaceous and organic laminations, the only

other sedimentary structures observed in the Plio-Pleistocene wall sediments are a few thin sand and/or silt lenses and massive-bedded silty clays.

Fossil Canyons

Although some ancient submarine canyons and valleys have been reported from the geologic record, it is likely that many more exist unrecognized. Many of the fossil canyons and channels reported in the literature are in California (Starke, 1956; Bruce, 1959; Frick, Harding and Marianos, 1959; Sullwold, 1960; Martin, 1963 and 1964; Barstow, 1966). Ancient buried submarine canyons and channels also have been found in the Gulf of Mexico area (Bornhouser, 1948; Hoyt, 1959), England (Whitaker, 1962; Walker, 1966), Israel (Neev, 1960) and the French Maritime Alps (Stanley and Bouma, 1964). These fossil canyons and channels which range in age from Silurian (Whitaker, 1962) to Pliocene (Bartow, 1966) are tied very closely to ancient deposits referred to as turbidites. Many other clastic deposits, when investigated in more detail, will probably be interpreted in a similar manner.

The importance of proper paleographic interpretation of these sediments cannot be too highly stressed. Frick, Harding and Marianos (1959) reported the presence of natural gas in the sediments filling an Eocene canyon in the northern part of the Sacramento

Valley. They also stated that the canyon fill has trapped gas in the Cretaceous sediments truncated by the canyon. Also in California, many oil bearing turbidite sands have been discovered. In the Los Angeles basin, which has produced almost five billion barrels of oil, nearly all the oil sands are turbidites interpreted as deep-sea fan deposits which formed at the mouths of submarine canyons (Sullwold, 1961). Because of these discoveries the economic importance of marine physiographic features such as submarine canyons and adjacent fans has become very evident.

Many of the characteristics of the geometry and the sediments of these fossil canyons and channels are similar to those of Astoria Canyon. Stanley (1966) has mapped fossil canyons in the Maritime Alps that have winding paths, steep walls and tributaries. Frick, Harding and Marianos (1959) reported that subsurface evidence reveals the existence of a narrow, sinuous 40 mile long submarine canyon which truncates Cretaceous sediments in the northern Sacramento Valley. An axial gradient of 4° and wall slopes of 19-40° are reported by Martin (1963) for Rosedale Channel, a Late Miocene submarine canyon located in the Great Valley of California. He also has found displaced foraminifers in the poorly sorted siltstone and sandstone layers of the canyon fill. These coarse layers show some grading and are interbedded with shales. In England Whitaker (1962) found features he described as the heads

of submarine canyons. The canyon fills include slump sheets, finely laminated siltstones, and near the base of the fill, cobble and boulder beds. He also suggested that tributary channels have been preserved.

In another locality in England, Walker (1966) recorded the existence of deep-sea fan channels. Sediment was supplied to these laterally migrating fans by feeder channels. These feeder channels seem to bear a close resemblance to the distributary channels radiating out across Astoria Fan from the terminal end of Astoria Canyon. Stanley and Bouma (1964) reported the occurrence of poorly sorted, lithic and feldspar-rich sands in the fill of an ancient submarine canyon or channel exposed in an outcrop in the Maritime Alps. At the mouth of this fossil canyon, they reported the existence of a fan-shaped deposit. Bartow (1966) suggested that poorly sorted feldspathic sandstone which makes up part of the fill of a Miocene-Pliocene submarine fan channel in Southern California came from a nearby submarine canyon. Current directions in the sediments of the Miocene age Tarzana Fan of Southern California led Sullwold (1960) to the conclusion that the fine to very fine sands of the fan had a point source. He suggested that this source was a submarine canyon some 14 miles long having an axial slope of four degrees. Sullwold described these turbidite deposits as graded, poorly sorted arkosic wackes having from 13 to 35% silt and clay.

He reported sand-shale ratios of 1:1, 1:4 and 1:12 from wells near the apex of Tarzana Fan. Sullwold hypothesized that the 1:1 ratio may be from ancient canyon fill.

Based on the characteristics of Astoria Canyon and the buried ancient submarine canyons, the following features are suggested as a model of fossil canyons (Figure 40).

(1) The deposit is elongate and sinuous with a bottom axial gradient of only a few degrees.

(2) U- to V-shaped cross profiles truncate subjacent strata.

(3) There is a variable dip of the contact between the fill and the walls which ranges from less than five degrees to vertical and possibly even overhanging.

(4) Numerous tributaries enter the main canyon.

(5) A large fan-shaped turbidite sequence is present at the lower end of the canyon.

(6) Channels radiate from the terminal end of the canyon deposit out across the fan.

(7) The age of this sinuous deposit is younger than the juxtaposed strata.

(8) The deposit consists of graded, poorly sorted coarse layers interbedded with shale or mudstone.

(9) Sand and silt coarse layers are more plentiful and thicker at the base of the deposit than at the top.

SUBMARINE CANYON MODEL

	SIZE	SORTING	COMPOSITION	SEDIMENTARY STRUCTURES	LITHOLOGY	GEOMETRY
CANYON FLOOR Coarse layers head ↓ mouth	medium ↓ coarse	poor ↓ moderate	graywacke sands displaced shallow water organisms	graded bedding sole marks	sandstone and siltstone layers interbedded with shale and mudstone	
Hemipelagic head ↓ mouth	fine ↑ very fine	poor ↑ very poor	terrigenous plant fragments planktonics	homogeneous burrows slump structure		
CANYON WALLS head ↓ mouth	fine ↓ very fine	very poor	mica ↓ authigenics	thin horizontal laminae cross-laminations	sandy mudstone ↓ shale	
ADJACENT SHELF ↓ SLOPE	medium ↑ very fine	moderate ↑ very poor	terrigenous glauconite planktonics	homogeneous burrows	sandstone ↓ shale or mudstone	

Figure 40. Characteristics of submarine canyon model.

(10) Sand-shale ratios increase with distance down the canyon. Values near the mouth of the canyon might be 1:2 or greater.

(11) The coarse layers are positively skewed.

(12) Sorting of the coarse layer constituents increases slightly with distance down the canyon.

(13) Coarse layers are characterized by abundant feldspar, rock fragments and matrix; most of this immature sediment will become graywacke upon lithification.

(14) Mica, which is most plentiful in thin laminae or in the upper portion of the coarse layers, increases in abundance with distance down the canyon.

(15) Displaced shallow water benthic foraminifers are present in most coarse layers.

(16) The prospective shale or mudstone becomes more poorly sorted and the median particle size decreases with distance down the canyon.

(17) Plant fragments are numerous in the canyon fill and decrease in abundance with distance down the canyon.

(18) Diatoms make up a significant percentage of the coarse fraction of the mudstones in the outer-shelf, upper-slope region.

(19) Radiolarians and/or planktonic foraminifers constitute the most important biogenic constituents of the mudstones and shales in the lower portion of the canyon.

(20) Glauconite is most abundant in the canyon axis near the shelf-slope break where it accumulates as a result of slumping from its place of formation in the area of the outer-shelf and upper-slope.

(21) Slump structures may be associated with canyon deposits.

(22) Directional features such as sole marks if present would indicate current directions parallel to the axis of the deposit.

BIBLIOGRAPHY

Allison, Ira S. 1962. Landforms. In: Atlas of the Pacific Northwest resources and development, ed. by Richard M. Highsmith, Jr. 3d ed. Corvallis, Oregon State University Press. p. 27-30.

American Society for Testing Materials. 1964. Standard method for grain-size analysis of soils. In: 1965 Book of ASTM Standards, Part 11. Philadelphia. p. 193-204. (ASTM designation: D422-63)

Bailey, E. H. and R. E. Stevens. 1960. Selective staining of K-feldspar and plagioclase on rock slabs and thin sections. The American Mineralogist 45:1020-1025.

Baldwin, Ewart M. 1964. Geology of Oregon. 2d ed. Eugene, University of Oregon Cooperative Book Store. 165 p.

Baldwin, Ewart M. 1966. Geology of the Columbia River Gorge. Northwest Science 40:121-128.

Ballard, R. L. 1964. Distribution of beach sediments near the mouth of the Columbia River. Seattle. 81 p. (Washington. University. Department of Oceanography. Technical report 98)

Bandy, Orville L. 1964. Foraminiferal trends associated with deep-water sands, San Pedro and Santa Monica Basins, California. Journal of Paleontology 38(1):138-148.

Bartow, J. A. 1966. Deep submarine channel in Upper Miocene rocks, Orange County, California. Journal of Sedimentary Petrology 36:700-705.

Berg, Joseph W., John M. King and Paul R. Carlson. 1966. Seismic reflection studies of buried channels off the Columbia River. Ore Bin 28:145-150.

Bornhauser, Max. 1948. Possible ancient submarine canyon in southwestern Louisiana. Bulletin of the American Association of Petroleum Geologists 32:2287-2294.

Bouma, A. H. 1964. Turbidites. In: Turbidites, ed. by A. H. Bouma and A. Brouwer. Amsterdam, Elsevier Publishing Co. p. 247-256.

Bouma, A. H. 1965. Sedimentary characteristics of samples collected from some submarine canyons. Marine Geology 3:291-320.

Bourcart, Jacques. 1964. Les sables profonds de la Mediterranée occidentale. In: Turbidites, ed. by A. H. Bouma and A. Brouwer. Amsterdam, Elsevier Publishing Co. p. 247-256.

Bretz, J. Harlan, H. T. V. Smith and George E. Neff. 1956. Bretz's flood hypothesis. Bulletin of the Geological Society of America 67:957-1050.

Bruce, Donald D. 1959. Princeton gas field. California Division of Oil and Gas, California Oil Fields 45:23-26.

Buffington, E. C. 1964. Structural control and precision bathymetry of LaJolla Submarine Canyon, California. Marine Geology 1: 44-58.

Burt, Wayne V. and Bruce Wyatt. 1964. Drift bottle observations of the Davidson Current off Oregon. In: Studies on oceanography, a collection of papers dedicated to Kaji Hidaka. Seattle, University of Washington Press. p. 156-165.

Byrne, John V. 1962. Geomorphology of the continental terrace off the central coast of Oregon. Ore Bin 24:65-74.

Byrne, John V. 1963. Geomorphology of the continental terrace off the northern coast of Oregon. Ore Bin 25:201-209.

Byrne, John V. 1964. Evidence for a Tertiary sedimentary basin off the Oregon coast. (Abstract) Special Paper of the Geological Society of America 76:193.

Byrne, John V. 1966. Effect of the East Pacific Rise on the geomorphology of the continental margin off Oregon. (Abstract) In: Program of the 79th Annual Meeting of the Geological Society of America, San Francisco, 1966. p. 33-34.

Byrne, John V., Gerald A. Fowler and Neil J. Maloney. 1966. Uplift of the continental margin and possible continental accretion off Oregon. Science 154: 1654-1656.

Byrne, John V., L. D. Kulm and Neil J. Maloney. 1966. Textural trends of Recent sediments from river to abyssal plain off Oregon. (Abstract) Bulletin of the American Association of Petroleum Geologists 50:645-646.

Carlson, Paul R. 1965. Unpublished research on microfauna of the Astoria Formation. Corvallis, Oregon State University, Department of Oceanography.

Chamberlain, T. K. 1964. Mass transport of sediment in the heads of Scripps Submarine Canyon, California. In: Progress in marine geology, ed. by R. L. Miller, New York, Macmillan. p. 42-64.

Chiburis, Edward F. 1966. Crustal structure in the Pacific Northwest states from phase-velocity dispersion of seismic surface waves. Ph. D. thesis. Corvallis, Oregon State University. 170 numb. leaves.

Cloud, Preston. 1955. Physical limits of glauconite formation. Bulletin of the American Association of Petroleum Geologists 39:484-492.

Coleman, James M. and Sherwood M. Gagliano. 1965. Sedimentary structures: Mississippi River deltaic plain. In: Primary sedimentary structures and their hydrodynamic interpretation, ed. by Gerald V. Middleton, Tulsa, Oklahoma, Society of Economic Paleontologists and Mineralogists. p. 133-148.

Collins, Curtis A., H. Clayton Creech and June G. Pattullo. 1966. A compilation of observations from moored current meters and thermographs. Corvallis. 39 numb. leaves. (Oregon State University. Department of Oceanography. Data report no. 23 on National Science Foundation Grant GP 4472)

Couch, Richard. 1967. Instructor, Oregon State University, Department of Oceanography. Personal communication. Corvallis, Oregon.

Crandell, Dwight R. 1965. The glacial history of western Washington and Oregon. In: The Quaternary of the United States, ed. by H. E. Wright, Jr. and D. G. Frey. Princeton, New Jersey, Princeton University Press. p. 341-353.

Curl, Herbert, Jr. 1962. Analysis of carbon in marine plankton organisms. Journal of Marine Research 20:181-188.

Curray, Joseph R. 1965. Late Quaternary history, continental shelves of the United States. In: The Quaternary of the United States, ed. by H. E. Wright, Jr. and D. G. Frey. Princeton, New Jersey, Princeton University Press. p. 723-735.

Dill, Robert F. 1963. Contemporary erosion in the heads of submarine canyons. Special Paper of the Geological Society of America 76:45.

Dill, Robert F. 1964. Sedimentation and erosion in Scripps Submarine Canyon Head. In: Papers in marine geology, ed. by R. L. Miller. New York, MacMillan. p. 23-41.

Dodimead, A. J., F. Favorite and T. Hirano. 1963. Salmon of the North Pacific Ocean. Part II: Review of oceanography of the subarctic Pacific region. Bulletin of the International North Pacific Fisheries Commission 13:1-195.

Duane, D. B. 1964. Significance of skewness in Recent sediments. Journal of Sedimentary Petrology 34:864-874.

Duncan, John R., Jr. 1967. Oregon State University, Department of Oceanography. Personal communication. Corvallis, Oregon.

Duxbury, Alyn C. 1965. The union of the Columbia River and the Pacific Ocean--general features. In: Ocean Science and Ocean Engineering; Transactions of the Joint Conference of the Marine Technology Society and American Society of Limnology and Oceanography, Washington, D. C., June 1965. p. 914-922.

Emery, K. O. 1938. Rapid method of mechanical analysis of sand. Journal of Sedimentary Petrology 8:105-111.

Emery, K. O. 1960. The sea off southern California. New York, Wiley. 366 p.

Emery, K. O. and E. E. Bray. 1962. Radiocarbon dating of California basin sediments. Bulletin of the American Association of Petroleum Geologists 46:1839-1856.

Emilia, David A., Joseph W. Berg, Jr. and William E. Bales. 1967. Magnetic anomalies off the Pacific Northwest coast. (To be submitted to the Bulletin of the Geological Society of America)

Erickson, Barrett H. 1967. Marine seismic studies near Newport, Oregon. Master's thesis. Corvallis, Oregon State University. 39 numb. leaves.

Ericson, D. B., Maurice Ewing and Bruce C. Heezen. 1951. Deep-sea sands and submarine canyons. Bulletin of the Geological Society of America 62:961-966.

Ericson, D. B., Maurice Ewing and Bruce C. Heezen. 1952. Turbidity currents and sediments in North Atlantic. Bulletin of the American Association of Petroleum Geologists 36:489-511.

Ericson, David B. and Goesta Wollin. 1964. The deep and the past. New York, Knopf. 292 p.

Ericson, David B., Maurice Ewing, Goesta Wollin and Bruce C. Heezen. 1961. Atlantic deep-sea sediment cores. Bulletin of the Geological Society of America 72:193-286.

Ewing, John, Xavier Le Pichon and Maurice Ewing. 1963. Upper stratification of Hudson Apron region. Journal of Geophysical Research 68:6303-6316.

Fenneman, N. M. 1931. Physiography of western United States. New York, McGraw-Hill. 534 p.

Fessenden, Franklin W. 1959. Removal of heavy liquid separates from glass centrifuge tubes. Journal of Sedimentary Petrology 29: 621.

Folk, Robert L. 1951. Stages of textural maturity in sedimentary rocks. Journal of Sedimentary Petrology 21:127-130.

Folk, Robert L. 1966. A review of grain-size parameters. Sedimentology 6:73-93.

Folk, R. L. and W. C. Ward. 1957. Brazos River bar: a study in the significance of grain-size parameters. Journal of Sedimentary Petrology 27:3-26.

Fowler, Gerald A. 1966. Notes on Late Tertiary foraminifera from off the central coast of Oregon. Ore Bin 28:53-60.

Fowler, Gerald A. 1967. Assistant Professor, Oregon State University, Department of Oceanography. Personal communication. Corvallis, Oregon.

Frick, J. D., T. D. Harding and A. W. Marianos. 1959. Eocene Gorge in Northern Sacramento Valley. (Abstract) Bulletin of the American Association of Petroleum Geologists 43:255.

Fryxell, Roald. 1965. Mazama and Glacier Peak volcanic ash layers: relative ages. Science 147:1288-1290.

Geological Society of America. 1963. Rock color chart. New York, Geological Society of America. 6 p.

Glenn, Jerry L. 1965. Late Quaternary sedimentation and geologic history of the North Willamette Valley, Oregon. Ph. D. thesis. Corvallis, Oregon State University. 231 numb. leaves.

Glenn, Jerry L. 1966. Hydrologist, U.S. Geological Survey, Water Resources Division. Personal communication. Portland, Oregon.

Gorsline, D. S. and K. O. Emery. 1959. Turbidity current deposits in San Pedro and Santa Monica Basins off Southern California. Bulletin of the Geological Society of America 70:279-290.

Greene, Herbert G. and Bert L. Conrey. 1966. Seismic investigation of Eel Submarine Canyon, Humboldt County, California. (Abstract) Bulletin of the American Association of Petroleum Geologists 50:648.

Griggs, Gary B. 1967. Oregon State University, Department of Oceanography. Personal communication. Corvallis, Oregon.

Gross, M. Grant. 1965. The carbonate content of surface sediments from the northeast Pacific Ocean. Northwest Science 39:85-92.

Gross, M. Grant. 1966. Distribution of radioactive marine sediments derived from the Columbia River. Journal of Geophysical Research 71:2017-2021.

Gross, M. Grant and Jack L. Nelson. 1966. Sediment movement on the continental shelf near Washington and Oregon. Science 154:879-881.

Hamilton, Edwin L. 1959. Thickness and consolidation of deep-sea sediments. Bulletin of the Geological Society of America 70: 1399-1424.

Hand, B. M. and K. O. Emery. 1964. Turbidites and topography of north end of San Diego Trough, California. Journal of Geology 72:526-542.

Heezen, Bruce C. and Charles Hollister. 1964. Deep-sea current evidence from abyssal sediments. Marine Geology 1: 141-174.

Heezen, Bruce C., Charles Hollister and W. F. Ruddiman. 1966. Shaping of the continental rise by deep geostrophic contour currents. Science 152:502-508.

Heezen, Bruce C., Marie Tharp and Maurice Ewing. 1959. The floors of the oceans. New York. 122 p. (Geological Society of America. Special paper 65)

Heezen, B. C., R. J. Menzies, E. D. Schneider, W. M. Ewing and N. C. L. Granelli. 1964. Congo Submarine Canyon. Bulletin of the American Association of Petroleum Geologists 48:1126-1149.

Hersey, J. B. 1965. Sedimentary basins of the Mediterranean Sea. In: Submarine geology and geophysics, ed. by W. F. Whittard and R. Bradshaw. London, Butterworth, p. 75-89.

Hess, H. H. 1962. History of ocean basins. In: Petrologic studies: a volume in honor of A. F. Buddington, ed. by A. E. J. Engel, Harold L. James and B. F. Leonard. New York, Geological Society of America. p. 599-620.

Highsmith, Richard M., Jr. 1962. Water. In: Atlas of the Pacific Northwest resources and development, ed. by Richard M. Highsmith, Jr. 3d ed. Corvallis, Oregon State University Press. p. 38-42.

Howell, Paul. 1966. Geologist, U. S. Army Engineers. Personal communication. Portland, Oregon.

Hoyt, William V. 1959. Erosional channel in the middle Wilcox near Yoakum, Lavaca County, Texas. Transactions of the Gulf Coast Association Geological Society 9:41-50.

Hubert, J. F. 1964. Textural evidence for deposition of many western North Atlantic deep-sea sands by ocean bottom currents rather than turbidity currents. Journal of Geology 72: 757-785.

Hulsemann, Jobst and K. O. Emery. 1961. Stratification in Recent sediments of Santa Barbara Basin as controlled by organisms and water content. Journal of Geology 69:279-290.

Hurley, Robert J. 1960. The geomorphology of abyssal plains in the Northeast Pacific Ocean. San Diego, Calif. 105 numb. leaves. Scripps Institute of Oceanography. Marine Physical Laboratory. SIO Reference 60-7)

Inman, D. L. 1952. Measures for describing the size distribution of sediments. Journal of Sedimentary Petrology 22:125-145.

Inman, D. L. and T. K. Chamberlain. 1955. Particle-size distribution in nearshore sediments. In: Finding ancient shorelines, ed. by J. L. Hough and H. W. Menard. Tulsa, Oklahoma. p. 106-129. (Society of Economic Paleontologists and Mineralogists. Special publication no. 3)

Johnson, D. W. 1939. The origin of submarine canyons. New York, Columbia University Press. 122 p.

Kaplin, P. A. 1961. Diver studies of the heads of submarine canyons. Deep-Sea Research 10:764-767. (Translated from Okeanologiya 1:1034-1038)

Kerr, Paul D. 1959. Optical mineralogy. 3d ed. New York. McGraw-Hill. 442 p.

Krumbein, W. C. and F. J. Pettijohn. 1938. Manual of sedimentary petrography, New York, D. Appleton-Century. 549 p.

Kuenen, Ph. H. 1951. Properties of turbidity currents of high density. In: Turbidity currents and the transportation of coarse sediments to deep water, Tulsa, Oklahoma. p. 14-33. (Society of Economic Paleontologists and Mineralogists. Special publication no. 2)

Kuenen, Ph. H. 1953. Origin and classification of submarine canyons. Bulletin of the Geological Society of America 64:1295-1314.

Kuenen, Ph. H. 1964. Deep-sea sands and ancient turbidites. In: Turbidites, ed. by A. H. Bouma and A. Brouwer. Amsterdam, Holland, Elsevier. p. 3-33.

Kuenen, Ph. H. and C. I. Migliorini. 1950. Turbidity currents as a cause of graded bedding. Journal of Geology 58:91-127.

Kulm, L. D. 1967. Assistant Professor, Oregon State University, Department of Oceanography. Personal communication. Corvallis, Oregon.

Kulm, L. D. and Gary B. Griggs. 1966. Sedimentation in Cascadia Deep-Sea Channel. (Abstract) In: Program of the 79th Annual Meeting of the Geological Society of America, San Francisco, 1966. p. 116.

Kulm, L. D. and C. Hans Nelson. 1967. Comparison of deep-sea channel and interchannel deposits off Oregon. (Abstract) Bulletin of the American Association of Petroleum Geologists. 51:472.

Lane, Robert K. 1965. Climate and heat exchange in the oceanic region adjacent to Oregon. Ph. D. thesis. Corvallis, Oregon State University. 115 numb. leaves.

Le Conte, Joseph. 1891. Tertiary and post-Tertiary changes of the Atlantic and Pacific coasts. Bulletin of the Geological Society of America 2:323-330.

Livingston, John G. 1964. Manual of techniques for study of textural and compositional variation in beach sand. Corvallis, Oregon State University, Department of Geology. 51 p.

Livingston, John G. 1967. Geologist. Personal communication. Auburn, California. January 13, 1967.

Lockett, John B. 1965a. Phenomena affecting improvement of the lower Columbia estuary and entrance. In: Federal Inter-Agency Sedimentation Conference, Jackson, Mississippi, 1963 Proceedings, Symposium 3: Sedimentation in estuaries, harbors and coastal areas. p. 626-669. (U.S. Department of Agriculture. Miscellaneous publication 970)

Lockett, John B. 1965b. Some indications of sediment transport and diffusion in the vicinity of the Columbia Estuary and

and Entrance, Oregon and Washington. Presented before the International Association for Hydraulic Research. Portland, U.S. Army Engineer Division, North Pacific. 7 numb. leaves.

Lowry, W. D. and E. Baldwin. 1952. Late Cenozoic geology of the Lower Columbia River Valley, Oregon and Washington. Bulletin of the Geological Society of America 63:1-24.

Mackin, J. Hoover and Allen S. Cary. 1965. Origin of Cascade landscapes. Olympia. 35 p. (Washington State Division of Mines and Geology. Information circular no. 41)

Malde, Harold E. 1965. Snake River Plain. In: The Quaternary of the United States, ed. by H. E. Wright, Jr. and D. G. Frey. Princeton, New Jersey, Princeton University Press. p. 255-263.

Maloney, Neil J. 1965. Geology of the continental terrace off the central coast of Oregon. Ph. D. thesis. Corvallis, Oregon State University. 233 numb. leaves.

Maloney, Neil J. and John V. Byrne. 1965. Offshore Oregon: some notes on petrography and geologic history. (Abstract) Bulletin of the American Association of Petroleum Geologists 49:1764.

Martin, Bruce D. 1963. Rosedale Channel - Evidence for Late Miocene submarine erosion in Great Valley of California. Bulletin of the American Association of Petroleum Geologists 47:441-456.

Martin, Bruce D. 1964. Monterey Submarine Canyon, California: genesis and relationship to continental geology. 273 numb. leaves. (Abstracted in Dissertation Abstracts 25:5213-5214. 1965)

Maughan, Paul M. 1963. Observations and analysis of ocean currents above 250 meters off the Oregon coast. Master's thesis. Corvallis, Oregon State University. 49 numb. leaves.

McManus, Dean A. 1964. Major bathymetric features near the coast of Oregon, Washington and Vancouver Island. Northwest Science 38:65-82.

McManus, Dean A. 1965. A study of maximum load for small-diameter sieves. Journal of Sedimentary Petrology 35:792-796.

Menard, H. W. 1955. Deep-sea channels topography, and sedimentation. Bulletin of the American Association of Petroleum Geologists 39:236-255.

Menard, H. W. 1960. Possible pre-Pleistocene deep-sea fans off central California. Bulletin of the Geological Society of America 71:1271-1278.

Menard, H. W. 1964. Marine geology of the Pacific. New York, McGraw-Hill. 271 p.

Middleton, G. V. 1965. Introduction. In: Primary sedimentary structures and their hydrodynamic interpretation, ed. by Gerald V. Middleton. Tulsa, Oklahoma. p. 1-4. (Society of Economic Paleontologists and Mineralogists. Special publication no. 12)

Mooers, C. N. K. 1967. Oregon State University, Department of Oceanography. Personal communication. Corvallis, Oregon.

Moore, D. G. and P. C. Scruton. 1957. Minor internal structure of some Recent unconsolidated sediments. Bulletin of the American Association of Petroleum Geologists 41:2723-2751.

Morse, Betty-Ann and Noel McGary. 1965. Graphic representation of the salinity distribution near the Columbia River mouth. In: Ocean Science and Ocean Engineering; Transactions of the Joint Conference of the Marine Technology Society and American Society of Limnology and Oceanography, Washington, D. C., June, 1965. p. 923-942.

Natland, M. L. and Ph. H. Kuenen. 1951. Sedimentary history of the Ventura Basin, California, and the action of turbidity currents. In: Turbidity currents and the transportation of coarse sediments to deep water. Tulsa, Oklahoma. p. 76-107. (Society of Economic Paleontologists and Mineralogists. Special publication no. 2)

National Marine Consultants, Inc. 1961. Wave statistics for three deep water stations along the Oregon-Washington Coast. Santa Barbara, Calif. 17 numb. leaves. (Prepared for U. S. Army Engineers District, Portland, Oregon)

Nayudu, Y. R. 1964. Carbonate deposits and paleoclimatic implications in the northeast Pacific Ocean. Science 146:515-517.

Neev, D. 1960. A pre-Neogene erosion channel in the southern coastal plain of Israel. Israel Ministry of Development, Geological Survey Bulletin 25, Oil Division Paper 7. p. 1-20. (Cited in: Emery, K.O., B. C. Heezen and T. D. Allan. 1966. Bathymetry of the eastern Mediterranean Sea. Deep-Sea Research 13:173-192)

Nelson, C. Hans. 1967. Oregon State University, Department of Oceanography. Personal communication. Corvallis, Oregon.

Nelson, Hans, L. D. Kulm, Paul R. Carlson and John R. Duncan, Jr. 1967. Mazama volcanic ash: recognition and distribution in northeastern Pacific sediments. (To be submitted to Science)

North, William B. and John V. Byrne. 1965. Coastal landslides of northern Oregon. Ore Bin 27:217-241.

Osterberg, C., N. Cutshall and J. Cronin. 1965. Chromium-51 as a radioactive tracer of Columbia River water at sea. Science 150:1585-1587.

Osterberg, C., L. D. Kulm and J. V. Byrne. 1963. Gamma emitters in marine sediments near the Columbia River. Science 139:916-917.

Park, Kilho, June G. Pattullo and Bruce Wyatt. 1962. Chemical properties as indicators of upwelling along the Oregon coast. Limnology and Oceanography 7:435-437.

Passega, R. 1957. Texture as characteristic of clastic deposition. Bulletin of the American Association of Petroleum Geologists 41:1952-1984.

Passega, R. 1964. Grain size representation by CM patterns as a geological tool. Journal of Sedimentary Petrology 34:830-847.

Pattullo, J. G. and W. V. Burt. 1962. The Pacific Ocean. In: Atlas of the Pacific Northwest resources and development, ed. by Richard M. Highsmith, Jr. 3d ed. Corvallis, Oregon State University Press. p. 93-95.

Pattullo, J. G. and W. Denner. 1965. Processes affecting sea water characteristics along the Oregon coast. Limnology and Oceanography 10:443-450.

Pattullo, J. G. and W. B. McAlister. 1962. Evidence for oceanic frontogenesis off Oregon. Science 135:106-107.

Payne, T. G. 1942. Stratigraphical analysis and environmental reconstruction. Bulletin of the American Association of Petroleum Geologists 26:1697-1770.

Péres, J. M., J. Piccard and M. Ruivo. 1957. Resultats de la Campagne de Recherches du Bathyscaphe F. N. R. S. III. Bulletin of the Institute of Oceanography at Monaco 1092:1-29.

Pettijohn, F. J. 1957. Sedimentary rocks. 2d ed. New York, Harper. 718 p.

Phleger, Fred B. 1951. Displaced foraminifera faunas. In: Turbidity currents and the transportation of coarse sediments to deep water. Tulsa, Oklahoma. p. 66-75. (Society of Economic Paleontologists and Mineralogists. Special publication no. 2)

Poole, David M. 1957. Size analysis of sand by a sedimentation technique. Journal of Sedimentary Petrology 27:460-468.

Powers, Howard A. and Ray E. Wilcox. 1964. Volcanic ash from Mount Mazama (Crater Lake) and from Glacier Peak. Science 144:1334-1336.

Pratt, W. L. 1963. Glauconite from the sea floor off southern California. In: Essays in marine geology in honor of K. O. Emery, ed. by Thomas Clements. Los Angeles. University of Southern California Press, p. 97-119.

Press, Frank. 1966. Seismic velocities. In: Handbook of physical constants, ed. by Sydney P. Clark, Jr. New York. p. 196-218. (Geological Society of America. Memoir 97)

Reiche, Parry. 1950. A survey of weathering processes and products. Albuquerque. 95 p. (New Mexico. University. University of New Mexico Publications in geology no. 3)

Richmond, Gerald M., Roald Fryxell, George E. Neff and Paul L. Weis. 1965. The Cordilleran ice sheet of the northern Rocky Mountains and related quaternary history of the Columbia Plateau. In: The Quaternary of the United States, ed. by H. E. Wright, Jr. and David G. Frey. Princeton, New Jersey, Princeton University Press. p. 231-242.

Roberson, M. L. 1964. Continuous seismic profiler survey of Oceanographer, Gilbert and Lydonia Submarine Canyons, Georges Bank. Journal of Geophysical Research 69:4779-4789.

Rosenberg, Donald H. 1962. Characteristics and distribution of water masses off the Oregon coast. Master's thesis. Corvallis, Oregon State University. 45 numb. leaves.

Royse, Chester F. 1964. Sediments of Willapa Submarine Canyon. Seattle. 62 p. (Washington. University. Department of Oceanography. Technical report no. 111)

Runge, Erwin J., Jr. 1966. Continental shelf sediments. Columbia River to Cape Blanco, Oregon. Ph. D. thesis. Corvallis, Oregon State University. 143 numb. leaves.

Rusnak, Gene A. 1960. Sediments of Laguna Madre, Texas. In: Recent sediments, Northwest Gulf of Mexico, ed. by Francis P. Shepard, Fred B Phleger and Tjeerd H. van Andel. Tulsa, Oklahoma. American Association of Petroleum Geologists. p. 153-196.

Russell, Kenneth L. 1967. Clay mineral origin and distribution on Astoria Fan. Master's thesis. Corvallis, Oregon State University. 47 numb. leaves.

Schatz, Clifford E. 1965. Source and characteristics of the tsunami observed along the coast of the Pacific Northwest on March 28, 1964. Master's thesis. Corvallis, Oregon State University. 39 numb. leaves.

Schneider, E. D. and Bruce C. Heezen. 1966. Processes of abyssal sedimentation and their effect on sediment facies and bottom morphology in the Western North Atlantic. (Abstract) In: Program of the 79th Annual Meeting of the Geological Society of America, San Francisco, 1966. p. 191-192.

Shepard, Francis P. 1933. Submarine valleys. Geographical Review 23:77-89.

Shepard, F. P. 1951. Mass movements in submarine canyon heads. Transactions of the American Geophysical Union 32:405-418.

Shepard, Francis P. 1952. Composite origin of submarine canyons. Journal of Geology 60:84-96.

Shepard, F. P. 1954. Nomenclature based on sand-silt-clay ratios. Journal of Sedimentary Petrology 24:151-158.

Shepard, Francis P. 1963. Submarine geology. 2d ed. New York, Harper. 557 p.

Shepard, Francis P. 1964. Sea-floor valleys of Gulf of California. In: Marine geology of the Gulf of California, ed. by Tjeerd H. van Andel and George G. Shor, Jr., Tulsa, Oklahoma. p. 157-192. (American Association of Petroleum Geologists. Memoir 3)

Shepard, Francis P. 1965a. Submarine canyons explored by Cousteau's diving saucer. In: Proceedings of the 17th Symposium of the Colston Research Society, ed. by W. F. Whittard and R. Bradshaw. London, Butterworths. p. 303-311.

Shepard, Francis P. 1965b. Types of submarine valleys. Bulletin of the American Association of Petroleum Geologists 49:304-310.

Shepard, Francis P. and C. N. Beard. 1938. Submarine canyons: distribution and longitudinal profiles. Geographical Review 28:439-451.

Shepard, Francis P. and Robert F. Dill. 1966. Submarine canyons and other sea valleys. Chicago, Rand McNally. 381 p.

Shepard, Francis P. and G. Einsele. 1962. Sedimentation in San Diego Trough and contributing submarine canyons. Sedimentology 1:81-133.

Shepard, Francis P. and David G. Moore. 1960. Bays of central Texas coast. In: Recent sediments, Northwest Gulf of Mexico, ed. by Francis P. Shepard, Fred B Phleger and Tjeerd H van Andel. Tulsa, Oklahoma, American Association of Petroleum Geologists. p. 117-152.

Shepard, Francis P., H. Niino and T. K. Chamberlain. 1964. Submarine canyons and Sagami Trough, east central Hanshu, Japan. Bulletin of the Geological Society of America 75:1117-1130.

Shepard, F. P., J. R. Curray, D. L. Inman, E. A. Murray, E. L. Winterer and R. F. Dill. 1964. Submarine geology by diving saucer. Science 145:1042-1046.

Shor, George C., Jr., Peter Dehlinger and William S. French. 1966. Seismic-refraction studies off Oregon and Northern California. (Abstract) In: Program of the 62nd Annual Meeting of the Geological Society of America, Cordilleran Section, Reno. p. 66.

Shor, G. G., Jr., P. Dehlinger, H. Kirk and W. S. French. 1967. Seismic refraction studies off Oregon and northern California. (To be submitted to the Journal of Geophysical Research)

Smith, Robert L., June G. Pattullo and Robert K. Lane. 1966. An investigation of the early stage of upwelling along the Oregon coast. Journal of Geophysical Research 71:1135-1140.

Snavely, Parke D., Jr. and Holly C. Wagner. 1963. Tertiary geologic history of Western Oregon and Washington. Olympia. 25 p. (Washington. State Division of Mines and Geology. Report of Investigations no. 22)

Snavely, Parke D., Jr. and Holly C. Wagner. 1964. Geologic sketch of Northwestern Oregon. Bulletin of the United States Geological Survey 1181-M:1-17.

Stanley, Daniel J. 1966. Associate Curator, Smithsonian Institution, Division of Sedimentology. Personal communication. Washington, D. C. December 2, 1966.

Stanley, Daniel J. and Arnold H. Bouma. 1964. Methodology and paleogeographic interpretation of flysch formations: a summary of studies in the Maritime Alps. In: Turbidites, ed. by A. H. Bouma and A. Brouwer. Amsterdam, Elsevier. p. 34-64.

Starke, G. W. 1956. Genesis and geologic antiquity of the Monterey Submarine Canyon. (Abstract) Bulletin of the Geological Society of America 67:1783.

Stetson, H. C. 1949. The sediments and stratigraphy of the East Coast continental margin, Georges Bank to Norfolk Canyon. Papers in Physical Oceanography and Meteorology 11:1-60.

Stevenson, Merritt R. 1966. Subsurface currents off the Oregon Coast. Ph. D. thesis. Corvallis, Oregon State University. 140 numb. leaves.

Sullwold, H. H., Jr. 1960. Tarzana Fan, deep submarine fan of late Miocene age, Los Angeles County, California. Bulletin of the American Association of Petroleum Geologists 44:433-457.

Sullwold, H. H., Jr. 1961. Turbidites in oil exploration. In: Geometry of sandstone bodies, ed. by J. A. Peterson and J. C. Osmund. Tulsa, Oklahoma, American Association of Petroleum Geologists. p. 63-81.

Sundborg, Åke. 1956. The river Klarälven, a study of fluvial processes. Geografiska Annalar 38:127-316.

Sverdrup, H. U., M. W. Johnson and R. H. Fleming. 1942. The oceans: their physics, chemistry and general biology. New York, Prentice Hall. 1087 p.

Trask, P. D. 1932. Origin and environment of source sediments of petroleum. Houston, Gulf Publishing Company. 67 p.

Triplehorn, D. M. 1966. Glauconite provides good oil search data. World Oil 162:94-97.

Turner, F. J. and J. Verhoogen. 1951. Igneous and metamorphic petrology. New York, McGraw-Hill. 602 p.

U. S. Army Engineers. 1961. Sedimentation investigation: lower Columbia and lower Willamette Rivers, July 1959 - August 1960. Portland, Oregon. 17 p.

U.S. Army Engineers. 1962. Reservoir regulations manual - Bonneville Dam, Columbia River, Washington and Oregon. Portland, Oregon. 12 p.

U.S. Board on Geographical Names. 1938. Decisions rendered between July 1, 1937 and June 30, 1938. Washington, D.C., U. S. Government Printing Office. 63 p.

van Andel, Tjeerd H. 1964. Recent marine sediments of Gulf of California. In: Marine geology of the Gulf of California, ed. by Tjeerd H. van Andel and George C. Shor, Jr. Tulsa,

Oklahoma, p. 216-310. (American Association of Petroleum Geologists. Memoir 3)

Vine, F. J. 1966. Spreading of the ocean floor: new evidence. Science 154:1405-1415.

von Rad, Ulrich and Reinhard Hesse. 1966. Possible non-turbidite origin of deep-sea sands in Cretaceous flysch (Bavarian Alps, Germany) and Recent San Diego Trough (California). (Abstract) Bulletin of the American Association of Petroleum Geologists 50:632-633.

Walker, Roger G. 1966. Shale grit and Grindslow Shales: transition from turbidite to shallow water sediments in the Upper Carboniferous of Northern England. Journal of Sedimentary Petrology 36:90-114.

Waters, A. C. 1961. Stratigraphic and lithologic variations in the Columbia River Basalt. American Journal of Science 259: 583-611.

Weaver, Charles E. 1937. Tertiary stratigraphy of western Washington and northwestern Oregon. Seattle, University of Washington Press. 266 p.

Whetten, J. T. 1965. Mineral and chemical composition of lower Columbia River reservoir sediments. (Abstract) Special Paper of the Geological Society of America 76:182.

Whetten, John T. 1966. Sediments from the Lower Columbia River and origin of graywacke. Science 152:1057-1058.

Whitaker, J. H. McD. 1962. The geology of the area around Leintwardine, Herefordshire. Quarterly Journal of the Geological Society of London 118:319-351.

Whitcomb, James H. 1965. Marine geophysical studies of offshore - Newport, Oregon. Master's thesis. Corvallis, Oregon State University. 51 numb. leaves.

Wilde, Pat. 1965. Recent sediments of the Monterey Deep-Sea Fan. Berkeley. 155 numb. leaves. (California. University. Hydraulic Engineering Laboratory. Technical report HEL-2-13)

Williams, H., F. J. Turner and C. M. Gilbert. 1958. Petrography. San Francisco, Freeman. 406 p.

APPENDICES

APPENDIX 1. SAMPLE LOCATIONS AND DEPTHS

No.*	OSU Sample number	Latitude	Longitude	Water depth (fms)	Depth in core (cm)
1- 1	6502-PC01-01	45°58.7'	125°17.0'	930	3
1- 2	6502-PC01-02				14
1- 3	6502-PC01-03				19
1- 4	6502-PC01-04				36
1- 5	6502-PC01-05				41
1- 6	6502-PC01-06				43
1- 7	6502-PC01-07				44
1- 8	6502-PC01-08				60
1- 9	6502-PC01-09				88
1-10	6502-PC01-10				120
1-11	6502-PC01-11				168
1-12	6502-PC01-12				172
1-13	6502-PC01-13				195
1-14	6502-PC01-14				197
1-15	6502-PC01-15				215
1-16	6502-PC01-16				229
1-17	6502-PC01-17				259
1-18	6502-PC01-18				264
1-19	6502-PC01-19				269
1-20	6502-PC01-20				323
1-21	6502-PC01-21				344
1-22	6502-PC01-22				347
1-23	6502-PC01-23				351
1-24	6502-PC01-24				371
1-25	6502-PC01-25				379
1-26	6502-PC01-26				391
1-27	6502-PC01-27				400
1-28	6502-PC01-28				420
1-29	6502-PC01-29				457
1-30	6502-PC01-30				466
1-31	6502-PC01-31				471
2- 1	6502-PC02-01	46°04.7'	125°07.7'	880	3
2- 2	6502-PC02-02				15
2- 3	6502-PC02-03				17
2- 4	6502-PC02-04				59
2- 5	6502-PC02-05				100
2- 6	6502-PC02-06				145

* The first number represents the core number, the second represents the sediment sample taken from that core.

APPENDIX 1 (Continued)

No.	OSU Sample number	Latitude	Longitude	Water depth (fms)	Depth in core(cm)
2- 7	6502-PC02-07	46°04.7'	125°07.7'	880	210
2- 8	6502-PC02-08				265
2- 9	6502-PC02-09				318
2-10	6502-PC02-10				387
3- 1	6502-PC03-01	46°05.2'	125°00.7'	815	2
3- 2	6502-PC03-02				32
3- 3	6502-PC03-03				43
3- 4	6502-PC03-04				60
3- 5	6502-PC03-05				145
3- 6	6502-PC03-06				190
3- 7	6502-PC03-07				204
3- 8	6502-PC03-08				213
3- 9	6502-PC03-09				340
4- 1	6502-PC04-01	46°10.1'	124°46.0'	570	3
4- 2	6502-PC04-02				60
4- 3	6502-PC04-03				117
4- 4	6502-PC04-04				149
4- 5	6502-PC04-05				200
4- 6	6502-PC04-06				280
4- 7	6502-PC04-07				345
4- 8	6502-PC04-08				435
4- 9	6502-PC04-09				528
4-10	6502-PC04-10				565
4-11	6502-PC04-11				617
5- 1	6502-PC05-01	46°15.1'	124°37.7'	455	2
5- 2	6502-PC05-02				23
5- 3	6502-PC05-03				133
5- 4	6502-PC05-04				162
5- 5	6502-PC05-05				168
5- 6	6502-PC05-06				170
5- 7	6502-PC05-07				230
5- 8	6502-PC05-08				285
5- 9	6502-PC05-09				295
5-10	6502-PC05-10				335
5-11	6502-PC05-11				395
5-12	6502-PC05-12				465
5-13	6502-PC05-13				500
5-14	6502-PC05-14				565
6- 1	6502-PC06-01	46°14.3'	124°25.0'	225	5

APPENDIX 1. (Continued)

No.	OSU Sample number	Latitude	Longitude	Water depth (fms)	Depth in core(cm)
6- 2	6502-PC06-02	46°14.3'	124°25.0'	225	30
6- 3	6502-PC06-03				60
6- 4	6502-PC06-04				102
6- 5	6502-PC06-05				115
6- 6	6502-PC06-06				145
6- 7	6502-PC06-07				156
6- 8	6502-PC06-08				183
6- 9	6502-PC06-09				190
6-10	6502-PC06-10				215
6-11	6502-PC06-11				239
6-12	6502-PC06-12				280
6-13	6502-PC06-13				317
6-14	6502-PC06-14				332
6-15	6502-PC06-15				345
6-16	6502-PC06-16				355
6-17	6502-PC06-17				405
7- 1	6508-PC07-01	46°16.0'	124°20.0'	100	14
7- 2	6508-PC07-02				95
7- 3	6508-PC07-03				185
7- 4	6508-PC07-04				210
7- 5	6508-PC07-05				260
7- 6	6508-PC07-06				319
7- 7	6508-PC07-07				410
7- 8	6508-PC07-08				490
8- 1	6508-PC08-01	46°14.4'	124°32.0'	236	0
9- 1	6508-PC09-01	46°14.0'	124°33.0'	390	25
9- 2	6508-PC09-02				80
9- 3	6508-PC09-03				130
9- 4	6508-PC09-04				168
9- 5	6508-PC09-05				210
9- 6	6508-PC09-06				226
9- 7	6508-PC09-07				278
9- 8	6508-PC09-08				300
9- 9	6508-PC09-09				355
9-10	6508-PC09-10				405
9-11	6508-PC09-11				441
9-12	6508-PC09-12				445
9-13	6508-PC09-13				515
10- 1	6508-PC10-01	46°16.2'	124°40.0'	415	10

APPENDIX 1. (Continued)

No.	OSU Sample number	Latitude	Longitude	Water depth (fms)	Depth in core (cm)
10- 2	6508-PC10-02	46°16.2'	124°40.0'	415	34
10- 3	6508-PC10-03				100
10- 4	6508-PC10-04				152
10- 5	6508-PC10-05				235
10- 6	6508-PC10-06				330
10- 7	6508-PC10-07				396
10- 8	6508-PC10-08				425
10- 9	6508-PC10-09				440
10-10	6508-PC10-10				450
10-11	6508-PC10-11				470
10-12	6508-PC10-12				480
10-13	6508-PC10-13				490
10-14	6508-PC10-14				503
10-15	6508-PC10-15				196
11- 1	6508-PC11-01	46°16.0'	124°43.0'	438	0
11- 2	6508-PC11-02				78
11- 3	6508-PC11-03				97
11- 4	6508-PC11-04				110
11- 5	6508-PC11-05				140
11- 6	6508-PC11-06				170
11- 7	6508-PC11-07				210
12- 1	6508-PC12-01	46°12.8'	124°42.8'	519	8
12- 2	6508-PC12-02				15
12- 3	6508-PC12-03				45
12- 4	6508-PC12-04				120
12- 5	6508-PC12-05				180
12- 6	6508-PC12-06				220
12- 7	6508-PC12-07				260
12- 8	6508-PC12-08				335
12- 9	6508-PC12-09				382
12-10	6508-PC12-10				455
12-11	6508-PC12-11				462
12-12	6508-PC12-12				482
12-13	6508-PC12-13				490
12-14	6508-PC12-14				505
12-15	6508-PC12-15				516
13- 1	6508-PC13-01	46°13.8'	124°46.7'	460	0
13- 2	6508-PC13-02				5
13- 3	6508-PC13-03				22

APPENDIX 1. (Continued)

No.	OSU Sample number	Latitude	Longitude	Water depth (fms)	Depth in core (cm)
13- 4	6508-PC13-04	46°13.8'	124°46.7'	460	30
13- 5	6508-PC13-05				53
13- 6	6508-PC13-06				75
13- 7	6508-PC13-07				112
13- 8	6508-PC13-08				120
13- 9	6508-PC13-09				157
13-10	6508-PC13-10				171
13-11	6508-PC13-11				185
13-12	6508-PC13-12				190
14- 1	6508-PC14-01	46°03.2'	124°45.7'	212	0
14- 2	6508-PC14-02				25
14- 3	6508-PC14-03				30
14- 4	6508-PC14-04				55
14- 5	6508-PC14-05				70
14- 6	6508-PC14-06				80
14- 7	6508-PC14-07				87
14- 8	6508-PC14-08				93
14- 9	6508-PC14-09				113
14- 9a	6508-PC14-09a				146
14-10	6508-PC14-10				150
14-11	6508-PC14-11				156
14-11a	6508-PC14-11a				159
14-12	6508-PC14-12				161
14-12a	6508-PC14-12a				165
14-13	6508-PC14-13				167
14-14	6508-PC14-14				183
14-15	6508-PC14-15				211
14-16	6508-PC14-16				223
14-17	6508-PC14-17				224
14-18	6508-PC14-18				217
15- 1	6508-PC15-01	46°03.0'	124°53.0'	480	5
15- 2	6508-PC15-02				35
15- 3	6508-PC15-03				80
15- 4	6508-PC15-04				130
15- 5	6508-PC15-05				195
15- 6	6508-PC15-06				230
15- 7	6508-PC15-07				295
15- 8	6508-PC15-08				375
15- 9	6508-PC15-09				410

APPENDIX 1. (Continued)

No.	OSU Sample	Latitude	Longitude	Water depth (fms)	Depth in core (cm)
15-10	6508-PC15-10	46°03.0'	124°53.0'	480	431
15-11	6508-PC15-11				433
16- 1	6508-PC16-01	46°08.5'	124°51.4'	655	8
16- 2	6508-PC16-02				55
16- 3	6508-PC16-03				120
16- 4	6508-PC16-04				140
16- 5	6508-PC16-05				197
16- 6	6508-PC16-06				219
16- 7	6508-PC16-07				235
16- 8	6508-PC16-08				245
16- 9	6508-PC16-09				330
16-10	6508-PC16-10				355
16-11	6508-PC16-11				370
17- 1	6508-PC17-01	46°01.9'	125°14.2'	952	11
17- 2	6508-PC17-02				60
17- 3	6508-PC17-03				105
17- 4	6508-PC17-04				175
17- 5	6508-PC17-05				220
17- 6	6508-PC17-06				226
17- 7	6508-PC17-07				300
17- 8	6508-PC17-08				400
17- 9	6508-PC17-09				409
17-10	6508-PC17-10				455
17-11	6508-PC17-11				473
18- 0	6508-PC18-00	46°06.4'	125°14.2'	845	0
18- 1	6508-PC18-01				35
18- 2	6508-PC18-02				95
18- 3	6508-PC18-03				125
18- 4	6508-PC18-04				145
18- 5	6508-PC18-05				160
18- 6	6508-PC18-06				175
18- 7	6508-PC18-07				190
18- 8	6508-PC18-08				220
18- 9	6508-PC18-09				271
18-10	6508-PC18-10				284
18-11	6508-PC18-11				287
18-12	6508-PC18-12				298
18-13	6508-PC18-13				302
19- 1	6408-PCA1-01	45°51.0'	125°39.5'	1180	10

APPENDIX 1. (Continued)

No.	OSU Sample number	Latitude	Longitude	Water depth (fms)	Depth in core (cm)
19- 2	6408-PCA1-02	45°51.0'	125°39.5'	1180	92
19- 3	6408-PCA1-03				103
19- 4	6408-PCA1-04				127
19- 5	6408-PCA1-05				132
19- 6	6408-PCA1-06				137
19- 7	6408-PCA1-07				173
19- 8	6408-PCA1-08				248
19- 9	6408-PCA1-09				253
19-10	6408-PCA1-10				258
19-11	6408-PCA1-11				291
‡T 1- 1	6502-PT01-01	45°58.7'	125°17.0'	930	0
T 2- 1	6502-PT02-01	46°04.7'	125°07.7'	880	0
T 2- 2	6502-PT02-02				18
T 2- 3	6502-PT02-03				23
T 3- 1	6502-PT03-01	46°05.2'	125°00.7'	815	0
T 4- 1	6502-PT04-01	46°10.1'	124°46.0'	570	0
T 5- 1	6502-PT05-01	46°15.1	124°37.7'	455	0
T 6- 1	6502-PT06-01	46°14.3'	124°25.0'	225	0
T 6- 2	6502-PT06-02				27
T 7- 1	6508-PT07-01	46°16.0'	124°20.0'	100	0
T 8- 1	6508-PT08-01	46°14.4'	124°32.0'	236	0
T 9- 1	6508-PT09-01	46°14.0'	124°33.0'	390	0
T 11- 1	6508-PT11-01	46°16.0'	124°43.0'	438	0
T 11- 2	6508-PT11-02				15
T 11- 3	6508-PT11-03				35
T 12- 1	6508-PT12-01	46°12.8'	124°42.8'	519	0
T 12- 2	6508-PT12-02				30
T 13- 1	6508-PT13-01	46°13.8'	124°46.7'	460	0
T 13- 2	6508-PT13-02				10
T 14- 1	6508-PT14-01	46°03.2'	124°45.7'	212	0
T 14- 2	6508-PT14-02				11
T 15- 1	6508-PT15-01	46°03.0'	124°53.0'	480	0
T 16- 1	6508-PT16-01	46°08.5'	124°51.4'	655	0
T 17- 1	6508-PT17-01	46°01.9'	125°14.2'	952	0
T 18- 1	6508-PT18-01	46°06.4'	125°14.2'	845	0
T 19- 1	6408-PT19-01	45°51.0'	125°39.5'	1180	0
20- 1	6407-STDC-01	46°14.0'	124°27.5'	302	75**

‡ T indicates trigger weight gravity core.

** Depth in feet below sediment water interface.

APPENDIX 1. (Continued)

No.	OSU Sample number	Latitude	Longitude	Water depth (fms)	Depth in core (cm)
20- 2	6407-STDC-02	46°14.0'	124°27.5'	302	135**
20- 3	6407-STDC-03				195**
20- 4	6407-STDC-04				255**
20- 5	6407-STDC-05				315**
20- 6	6407-STDC-06				370**
20- 7	6407-STDC-07				435**
21- 1	6208-KG01-01	46°19.9'	124°24.0'	71	2
22- 1	6208-KG02-01	46°19.2'	124°18.0'	41	2
23- 1	6208-KG03-01	46°16.5'	124°17.8'	51	2
24- 1	6208-KG04-01	46°16.3'	124°13.3'	30	2
25- 1	6208-KG05-01	46°15.5'	124°20.0'	65	2
26- 1	6208-KG06-01	46°13.3'	124°13.3'	35	2
27- 1	6208-KG07-01	46°13.6'	124°17.9'	48	2
28- 1	6208-KG08-01	46°12.4'	124°20.6'	56	2
29- 1	6208-KG09-01	46°12.0'	124°23.5'	62	2
30- 1	6208-KG10-01	46°14.0'	124°24.3'	84	0
31- 1	6208-KG11-01	46°15.1'	124°25.0'	235	2
32- 1	6208-KG12-01	46°17.7'	124°26.7'	112	0
33- 1	6208-KG13-01	46°19.1'	124°32.4'	68	0
34- 1	6208-KG14-01	46°18.3'	124°28.8'	115	0
35- 1	6208-KG15-01	46°16.3'	124°31.3'	240	0
36- 1	6208-KG16-01	46°12.7'	124°29.9'	75	0
37- 1	6208-KG17-01	46°11.2'	124°29.5'	72	2
38- 1	6208-KG18-01	46°10.9'	124°32.9'	72	2
38- 2	6208-KG18-02				11
38- 3	6208-KG18-03				32
39- 1	6208-KG19-01	46°07.9'	124°36.8'	84	2
40- 1	6208-KG20-01	46°13.0'	124°38.6'	110	7
40- 2	6208-KG20-02				11
41- 1	6208-KG21-01	46°14.8'	124°38.2'	438	2
42- 1	6208-KG22-01	46°15.6'	124°38.4'	300	2
43- 1	6208-KG23-01	46°19.4'	124°39.3'	103	0
44- 1	6208-KG24-01	46°19.1'	124°44.0'	370	19
44- 2	6208-KG24-02				29
45- 1	6208-KG25-01	46°15.6'	124°45.2'	515	2
46- 1	6208-KG26-01	46°11.6'	124°44.8'	548	2
47- 1	6208-KG27-01	46°07.2'	124°44.5'	230	0
48- 1	6208-KG28-01	46°01.7'	124°44.0'	157	0
48- 2	6208-KG28-02				8

APPENDIX 1. (Continued)

No.	OSU Sample number	Latitude	Longitude	Water depth (fms)	Depth in core (cm)
49- 1	6208-KG29-01	46°01.5'	124°49.5'	260	0
49- 2	6208-KG29-02				8
49- 3	6208-KG29-03				9
50- 1	6208-KG30-01	46°06.7'	124°49.5'	345	0
50- 2	6208-KG30-02				4
51- 1	6208-KG31-01	46°09.1'	124°49.9'	640	2
52- 1	6208-KG32-01	46°11.6'	124°50.0'	460	0
53- 1	6208-KG33-01	46°13.7'	124°50.3'	378	0
53- 2	6208-KG33-02				10
54- 1	6208-KG34-01	46°17.2'	124°50.0'	394	2
54- 2	6208-KG34-02				8
55- 1	6208-KG35-01	46°17.3'	124°55.1'	480	2
56- 1	6208-KG36-01	46°11.1'	124°55.0'	450	2
57- 1	6208-KG37-01	46°09.0'	124°55.0'	640	2
58- 1	6208-KG38-01	46°04.5'	124°54.7'	605	2
59- 1	6208-KG39-01	46°01.4'	124°54.7'	510	2
60- 1	6412-RC01-01	46°01.7'	124°19.0'	900	0
60- 2	6412-RC01-02				83
61- 1	6412-RC02-01	45°59.5'	125°20.0'	920	0
61- 2	6412-RC02-02				23
61- 3	6412-RC02-03				49
62- 1	6412-RC03-01	46°00.0'	125°13.0'	900	0
63- 1	6412-RC04-0'	46°04.1'	125°13.4'	777	0
63- 2	6412-RC04-02				53
64- 1	6412-RC05-01	46°06.0'	125°08.5'	792	0
64- 2	6412-RC05-02				4
64- 3	6412-RC05-03				12
64- 4	6412-RC05-04				20
64- 5	6412-RC05-05				45
65- 1	6412-RC06-01	46°03.3'	125°08.5'	800	0
65- 2	6412-RC06-02				22
65- 3	6412-RC06-03				45
65- 4	6412-RC06-04				55
66- 1	6412-RC07-01	46°03.3'	125°03.3'	690	0
67- 1	6412-PH7A-01	46°04.3'	125°02.8'	795	0
67- 2	6412-PH7A-02				25
68- 1	6412-PH08-01	46°06.4'	125°04.3'	755	0
69- 1	6412-PH09-01	46°06.4'	124°58.0'	745	0
70- 1	6412-PH10-01	46°04.2'	124°57.6'	745	0

APPENDIX 1. (Continued)

No.	OSU Sample number	Latitude	Longitude	Water depth (fms)	Depth in core (cm)
70- 2	6412-PH10-02	46°04.2'	124°57.6'	745	36
71- 1	6412-PH11-01	46°07.0'	124°52.7'	630	0
71- 2	6412-PH11-02				2
71- 3	6412-PH11-03				27
72- 1	6412-PH12-01	46°10.0'	124°55.0'	550	0
72- 2	6412-PH12-02				15
73- 1	6412-PH13-01	46°10.4'	124°49.3'	515	0
73- 2	6412-PH13-02				17
74- 1	6412-PH14-01	46°08.3'	124°41.7'	230	0
75- 1	6412-PH15-01	46°11.7'	124°41.2'	450	0
75- 2	6412-PH15-02				25
76- 1	6501-RC16-01	46°12.6'	124°45.4'	520	3
76- 2	6501-RC16-02				76
76- 3	6501-RC16-03				98
77- 1	6501-RC17-01	46°17.0'	124°39.5'	330	0
77- 2	6501-RC17-02				20
78- 1	6501-RC18-01	46°13.5	124°39.4'	361	1
78- 2	6501-RC18-02				67
79- 1	6501-RC19A-1	46°13.2'	124°36.4	225	0
80- 1	6502-RC19-01	46°13.7'	124°38.0'	335	0
80- 2	6502-RC19-02				54
80- 3	6502-RC19-03				63
81- 1	6502-RC20-01	46°17.6'	124°36.8'	220	1
81- 2	6502-RC20-02				11
81- 3	6502-RC20-03				44
81- 4	6502-RC20-04				71
82- 1	6502-RC21-01	46°15.7'	124°30.0'	230	5
82- 2	6502-RC21-02				70
83- 1	6502-RC22-01	46°13.2'	124°30.0'	100	0
83- 2	6502-RC22-02				12
83- 3	6502-RC22-03				19
83- 4	6502-RC22-04				31
84- 1	6502-RC23-01	46°14.8'	124°25.4'	144	0
84- 2	6502-RC23-02				39
84- 3	6502-RC23-02				61
84- 4	6502-RC23-04				77
84- 5	6502-RC23-05				95
85- 1	6502-RC24-01	46°17.4'	124°26.4'	150	2
85- 2	6502-RC24-02				60

APPENDIX 1. (Continued)

No.	OSU Sample number	Latitude	Longitude	Water depth (fms)	Depth in core (cm)
86- 1	6502-RC25-01	46°16.5'	124°22.0'	100	2
86- 2	6502-RC25-02				22
86- 3	6502-RC25-03				42
86- 4	6502-RC25-04				63
87- 1	6502-RC26-01	46°15.6'	124°21.5'	58	0
87- 2	6502-RC26-02				10
87- 3	6502-RC26-03				17
88- 1	6502-RC27-01	46°18.3'	124°24.4'	85	0
88- 2	6502-RC27-02				52
88- 3	6502-RC27-03				82
89- 1	6502-RC28-01	46°18.8'	124°18.8'	50	3
89- 2	6502-RC28-02				22
90- 1	6502-RC29-01	46°16.2	124°19.7'	73	0
90- 2	6502-RC29-02				58
90- 3	6502-RC29-03				87
91- 1	6508-RG01-01	46°10.0'	124°36.6'	86	0
92- 1	6508-RG02-01	46°10.0'	124°25.1'	75	0
93- 1	6508-RG03-01	46°18.5'	124°32.0'	75	0
94- 1	6508-RG04-01	46°03.2'	124°48.5'	150	0
95- 1	6508-RG05-01	46°13.9'	124°50.1'	375	0
95- 2	6508-RG05-02				12
96- 1	6508-RG06-01	45°59.4'	124°57.2'	260	0
97- 1	6508-RG07-01	46°08.0'	125°08.8'	725	0
97- 2	6508-RG07-02				10
97- 3	6508-RG07-03				17
98- 1	6508-RG08-01	46°08.6'	125°19.3'	685	0
98- 2	6508-RG08-02				4
99- 1	6508-RG09-01	45°55.6'	125°18.9'	670	0
100- 1	6508-RG10-01	46°02.2	125°22.0'	800	0
100- 2	6508-RG10-02				10
101- 1	6502-PD02-01	46°12.0'	124°38.5'	200	0
102- 1	6502-PD03-01	46°15.5'	124°38.8'	375	0
103- 1	6502-PD04-01	46°13.0'	124°30.0'	150	0
104- 1	6412-PD05-01	46°06.4'	125°09.5'	705	0
105- 1	6412-PD06-01	46°03.5'	125°08.0'	780	0
106- 1	6412-PD07-01	46°12.2'	124°44.0'	500	0
107- 1	6502-PD08-01	46°15.2'	124°31.8'	140	0
108- 1	6508-PD09-01	46°15.0'	124°20.6'	100	0
109- 1	6508-PD10-01	46°12.8'	125°25.5'	150	0

APPENDIX 1. (Continued)

No.	OSU Sample number	Latitude	Longitude	Water depth (fms)	Depth in core (cm)
110- 1	6508-PD11-01	46°16.2'	124°29.5'	175	0
111- 1	6508-PD12-01	46°14.6'	124°35.3'	253	0
112- 1	6508-PD13-01	46°05.3'	124°42.8'	200	0
113- 1	6508-PD14-01	46°04.0'	124°48.5'	450	0
114- 1	6508-PD15-01	46°10.0'	124°51.0'	550	0
115- 1	6508-PD16-01	46°08.5'	124°57.6'	552	0
116- 1	6508-PD18-01	46°02.0'	125°03.0'	600	0
117- 1	6508-PD21-01	45°55.3'	125°18.2'	830	0

APPENDIX 2. TEXTURAL ANALYSES OF SEDIMENT SAMPLES

No.	Inman Statistics*						Percents		
	Mdϕ	Mϕ	$\sigma\phi$	$\alpha\phi$	$\alpha_2\phi$	$\beta\phi$	Sand	Silt	Clay
1- 1	8.6	9.1	2.4	.2	-.0	.6	1.2	40.9	57.9
1- 2	7.6	7.6	3.2	-.0	.1	.2	6.1	48.7	45.2
1- 3	8.6	8.7	2.3	.0	-.3	.7	1.8	38.3	59.8
1- 4	8.0	8.6	2.9	.2	.1	.5	2.4	47.5	50.1
1- 7	8.6	8.6	2.5	-.0	-.3	.6	2.0	39.8	58.2
1- 8	7.4	7.5	3.2	.0	.1	.2	8.3	48.0	43.7
1- 9	5.2	6.8	3.2	.5	.7	.3	27.0	43.4	29.6
1-11	7.6	7.5	3.2	-.0	.0	.3	11.4	43.9	44,7
1-12	8.8	8.9	2.2	.0	-.3	.7	1.3	35.9	62.9
1-14	8.7	8.7	2.4	-.0	-.2	.5	1.8	37.4	60.8
1-15	8.2	8.3	2.3	.0	-.2	.5	1.7	44.8	53.6
1-17	8.3	8.5	2.6	.1	-.0	.5	.8	44.5	53.7
1-18	6.2	7.1	3.1	.3	.4	.4	16.4	50.5	33.2
1-19	8.8	8.8	2.4	.0	-.3	.7	1.2	37.0	61.8
1-20	4.0	5.2	2.3	.5	1.2	.9	48.5	37.7	13.8
1-22	4.3	5.1	1.8	.4	1.1	1.1	30.7	57.3	12.0
1-23	7.9	8.3	2.3	.2	.0	.5	2.9	47.9	49.2
1-24	8.1	8.5	2.4	.2	.2	.4	.2	48.5	51.3
1-25	8.3	8.5	2.1	.1	.0	.5	.2	45.7	54.2
1-26	8.0	8.3	2.4	.2	.1	.5	1.4	48.8	49.9
1-27	3.8	4.5	1.4	.5	1.9	1.6	56.0	33.8	10.2
1-28	4.9	6.5	2.9	.5	.9	.5	24.4	52.6	23.0
1-29	4.2	4.9	1.9	.4	1.2	1.1	41.0	48.7	10.3
1-30	3.2	5.3	2.9	.7	1.0	.6	64.4	18.6	17.0
1-31	8.5	9.1	3.9	.2	.2	.3	3.0	42.9	54.2
2- 1	8.4	8.4	1.8	.0	-.4	.8	.6	41.0	58.4
2- 3	8.8	8.9	2.3	.0	-.3	.6	.7	36.6	62.6
2- 4	7.9	7.7	3.1	-.1	-.2	.4	9.1	41.5	49.4
2- 5	8.1	8.0	3.2	-.0	-.0	.3	5.1	43.2	51.8
2- 6	6.8	7.1	3.6	.1	.2	.3	18.7	43.5	37.7
2- 7	7.5	7.9	3.1	.1	.2	.3	6.0	50.2	43.8
2- 9	7.2	7.5	3.1	.1	.1	.4	8.9	49.7	41.4
2-10	6.7	7.1	3.2	.2	.2	.4	16.1	50.6	33.3
3- 1	8.0	8.2	2.5	.1	-.0	.4	1.4	48.0	50.6
3- 2	8.2	8.3	2.7	.1	-.0	.4	2.6	44.9	52.5
3- 3	8.5	8.7	2.2	.1	-.3	.7	.3	42.4	57.3
3- 4	7.9	8.3	2.8	.2	.1	.5	3.4	47.8	48.8

* Inman statistics (Inman, 1952) based on Phi size (ϕ) = $-\text{Log}_2$(mm.). Mdϕ = Median; Mϕ = Mean; $\sigma\phi$ = Sorting; $\alpha\phi$ = Skewness; $\alpha_2\phi$ = Second Skewness; $\beta\phi$ = Kurtosis.

APPENDIX 2. (Continued)

No.	Inman Statistics						Percents		
	Mdϕ	Mϕ	$\sigma\phi$	$\alpha\phi$	$\alpha_2\phi$	$\beta\phi$	Sand	Silt	Clay
3- 5	7.7	7.8	2.9	.0	.1	.3	4.7	48.6	46.7
3- 6	6.6	6.9	3.5	.1	.2	.3	20.7	45.5	33.8
3- 8	7.1	7.3	3.5	.1	.1	.3	16.5	43.7	39.7
3- 9	7.2	7.7	3.2	.2	.2	.4	9.1	52.2	38.7
4- 1	8.3	8.2	2.4	-.0	-.3	.5	1.5	43.0	55.6
4- 2	8.2	8.0	2.7	-.1	-.2	.4	1.3	46.2	52.5
4- 3	8.0	8.4	2.4	.2	.0	.5	1.4	47.8	50.8
4- 5	8.2	8.2	2.5	.0	-.1	.5	2.0	45.5	52.5
4- 6	7.8	7.9	3.0	.0	.0	.3	4.8	46.9	48.3
4- 7	8.3	8.2	2.3	-.0	-.2	.5	1.6	43.9	54.5
4- 8	8.1	8.2	2.6	.0	-.1	.5	1.5	46.5	52.0
4- 9	8.2	8.6	2.3	.2	-.1	.7	2.1	45.0	52.9
4-10	7.9	8.1	2.5	.1	-.0	.5	3.0	47.5	49.5
4-11	8.3	8.8	2.5	.2	-.1	.6	1.3	44.3	54.4
5- 1	8.8	8.8	2.4	-.0	-.3	.6	.5	37.1	62.4
5- 2	8.8	8.6	3.5	-.1	-.0	.3	.7	41.1	58.3
5- 3	8.7	9.0	2.4	.1	-.2	.7	1.0	39.8	59.2
5- 4	8.7	8.6	2.8	-.0	-.2	.5	1.0	40.0	59.0
5- 5	5.8	7.7	4.0	.5	.6	.3	22.3	40.7	37.0
5- 6	8.4	8.7	2.7	.1	-.0	.5	1.5	44.2	54.3
5- 7	8.8	8.8	2.7	.0	-.2	.5	2.0	38.1	59.9
5- 8	8.3	8.3	2.9	.0	-.1	.4	4.0	42.2	53.8
5- 9	8.4	8.7	2.9	.1	-.0	.5	3.8	42.1	54.1
5-10	8.5	8.5	2.4	.0	-.2	.6	1.9	41.0	57.1
5-11	8.5	8.7	2.8	.1	-.1	.5	2.4	41.0	56.7
5-12	8.7	8.3	2.7	.1	-.2	.4	2.0	37.8	60.2
5-13	8.5	8.6	2.7	.0	-.1	.5	1.3	42.2	56.5
5-14	8.4	8.3	2.8	-.0	-.1	.4	2.4	42.7	54.9
6- 1	8.4	8.2	3.0	-.1	-.1	.3	3.8	40.6	55.6
6- 2	7.9	7.9	3.5	.0	.0	.3	11.6	39.3	49.1
6- 3	7.9	7.9	3.5	.0	.0	.3	11.9	39.2	49.0
6- 5	7.2	7.7	3.2	.2	.2	.4	13.3	44.6	42.2
6- 6	5.6	6.8	3.3	.4	.6	.3	30.3	39.8	30.0
6- 8	4.4	6.1	2.9	.6	1.1	.7	38.2	42.6	19.2
6- 9	6.9	8.2	4.4	.3	.4	.3	18.4	42.0	39.5
6-10	8.9	10.0	5.5	.2	.3	.3	6.5	38.6	54.8
6-11	5.6	7.1	3.4	.4	.7	.4	24.0	49.3	26.7
6-12	6.0	7.4	3.6	.4	.6	.3	21.3	45.8	32.9
6-13	9.1	9.2	2.7	.0	-.1	.5	.7	35.2	64.1
6-15	9.7	9.8	3.3	.0	-.1	.5	.8	31.7	67.5

APPENDIX 2. (Continued)

No.	Inman Statistics						Percents		
	Mdϕ	Mϕ	σϕ	αϕ	$\alpha_2\phi$	βϕ	Sand	Silt	Clay
6-16	7.3	7.6	3.4	.1	.1	.3	10.8	44.6	44.5
6-17	7.7	7.7	3.3	.0	.1	.3	8.2	45.3	46.5
7- 1	6.0	7.1	3.9	.3	.5	.3	26.5	41.7	31.8
7- 2	6.7	7.5	3.3	.2	.4	.3	10.1	51.3	38.6
7- 3	6.5	7.0	3.2	.2	.3	.4	17.5	50.7	31.8
7- 4	6.5	7.1	3.3	.2	.3	.3	18.3	46.4	35.3
7- 5	6.5	6.9	3.2	.1	.2	.4	17.8	49.2	33.0
7- 6	6.7	7.1	3.3	.1	.2	.3	16.9	48.2	34.9
7- 8	6.7	7.1	3.5	.1	.2	.3	19.8	43.0	37.2
8- 1	8.6	9.2	2.7	.2	-.0	.6	1.7	41.4	56.8
9- 2	8.5	8.4	2.7	-.0	-.2	.5	1.4	41.9	56.7
9- 3	8.1	8.2	2.6	.1	-.1	.5	2.0	46.6	51.4
9- 7	7.5	7.8	3.6	.1	.2	.3	10.0	46.2	43.8
9- 8	7.7	7.9	3.6	.1	.1	.3	10.8	41.5	47.7
9- 9	7.6	7.8	3.3	.1	.2	.3	4.9	49.1	46.0
9-10	7.6	7.8	3.1	.1	.1	.3	6.7	48.4	44.9
10- 1	8.9	8.8	8.8	-.1	-.2	.4	.7	37.6	61.6
10- 2	8.6	9.0	2.9	.1	-.0	.5	1.3	41.9	56.8
10- 4	8.6	8.6	2.6	-.0	-.2	.5	1.2	40.1	58.7
10- 5	8.0	8.7	3.0	.2	.1	.5	1.4	47.9	50.7
10- 6	8.3	8.7	2.8	.1	.1	.5	1.5	44.7	53.8
10- 7	8.0	8.6	3.1	.2	.2	.4	3.0	46.8	50.2
10- 8	8.2	8.9	3.0	.2	.2	.5	1.2	46.4	52.3
10- 9	9.4	9.6	3.3	.1	.0	.4	.9	35.8	63.3
10-10	9.8	9.9	3.3	.0	-.1	.4	.8	31.3	67.9
10-11	10.1	10.1	3.1	.0	-.1	.4	.1	27.5	72.4
10-12	9.8	9.8	3.0	-.0	-.1	.4	.3	28.6	71.1
10-13	9.8	9.7	3.0	-.0	-.1	.4	.6	28.2	71.3
10-14	9.1	9.4	3.1	.1	.0	.4	1.4	37.8	60.8
10-15	8.4	8.8	2.8	.1	.0	.5	1.3	44.4	54.3
11- 1	9.2	9.7	3.7	.1	.1	.4	1.1	38.8	60.1
11- 2	7.3	8.5	3.0	.4	.5	.4	1.5	56.7	41.8
11- 3	6.7	7.6	2.3	.4	.5	.5	1.1	68.2	30.7
11- 5	9.4	9.5	3.0	.0	-.0	.4	.3	34.4	65.3
11- 7	9.1	9.2	2.4	.1	-.0	.4	.1	35.3	64.7
12- 1	8.4	8.4	3.8	.0	.1	.3	1.3	45.2	53.5
12- 2	8.7	8.6	3.1	-.0	-.1	.4	2.3	39.3	58.4
12- 3	8.5	8.3	3.1	-.1	-.1	.4	3.3	40.3	56.4
12- 4	8.4	8.7	2.9	.1	-.0	.5	1.6	44.1	54.4
12- 6	8.6	8.8	2.9	.1	-.1	.4	1.0	41.6	57.4

APPENDIX 2, (Continued)

No.	Inman Statistics						Percents		
	Mdϕ	Mϕ	$\sigma\phi$	$\alpha\phi$	$\alpha_2\phi$	$\beta\phi$	Sand	Silt	Clay
12- 7	8.2	9.4	3.3	.4	.3	.5	1.4	46.7	51.9
12- 8	8.6	8.7	2.4	.0	-.2	.6	1.3	40.3	58.4
12- 9	8.3	8.4	2.8	.1	-.1	.4	3.0	43.5	53.6
12-10	8.5	8.8	2.8	.1	-.1	.5	.6	43.5	56.0
12-11	6.5	7.2	3.5	.2	.3	.3	21.7	41.0	37.3
12-13	7.6	7.7	3.4	.0	-.1	.4	11.9	41.6	46.5
12-14	8.3	8.5	2.8	.1	-.0	.5	1.9	44.5	54.6
12-15	8.6	8.8	3.1	.1	-.0	.5	1.2	42.6	56.1
13- 1	8.3	7.9	3.1	-.1	-.5	.7	8.9	36.7	54.5
13- 3	9.0	9.1	2.5	.1	-.2	.6	1.0	36.4	62.7
13- 4	8.6	8.8	2.7	.1	-.0	.4	.1	42.6	57.3
13- 5	6.8	7.8	2.5	.4	.5	.4	1.0	63.4	35.6
13- 6	8.4	8.7	2.6	.1	-.0	.5	.9	43.5	55.6
13- 7	9.2	9.3	2.6	.0	-.2	.6	.4	33.8	65.8
13- 8	9.1	9.3	2.5	.1	-.1	.5	.3	39.7	65.1
13- 9	7.5	7.6	3.0	.0	-.0	.4	10.5	46.0	43.5
13-11	7.3	7.9	2.6	.2	.3	.4	.5	59.6	39.9
14- 1	3.3	3.5	.8	.3	3.7	4.0	76.3	15.3	8.4
14- 4	7.1	8.1	2.5	.4	.4	.5	2.6	60.2	37.1
14- 5	7.0	7.5	3.1	.1	.1	.5	12.1	51.1	36.7
14- 6	4.3	5.8	3.8	.4	.5	.3	47.1	26.2	26.7
14- 8	2.5	2.8	3.1	.1	.1	.7	49.7	14.4	15.7
14- 9	7.4	7.8	2.4	.1	.1	.4	1.9	56.1	42.0
14-10	5.7	6.6	2.7	.3	.5	.3	19.2	54.5	26.3
14-11	7.3	5.8	3.8	-.4	-1.3	1.1	12.2	38.1	38.7
14-13	7.2	7.6	3.3	.1	.2	.2	5.0	52.2	42.8
14-15	7.9	8.2	2.2	.1	.0	.4	.2	50.4	49.4
14-18	7.2	7.8	2.5	.2	.2	.5	3.1	56.9	40.0
15- 1	9.1	9.1	2.6	-.0	-.3	.6	1.7	33.8	64.5
15- 2	8.5	8.5	2.8	.0	-.1	.4	1.7	41.8	56.6
15- 3	7.9	7.7	3.7	-.1	-.1	.4	16.1	34.5	49.4
15- 4	8.5	8.3	2.4	-.1	-.3	.5	3.6	37.5	58.8
15- 5	8.2	8.2	3.0	-.0	-.0	.4	3.3	43.8	52.9
15- 6	7.8	7.9	3.5	.0	.1	.2	7.0	44.4	48.7
15- 7	8.0	8.3	3.4	.1	.2	.3	2.4	47.6	49.9
15- 8	7.9	8.3	3.3	.1	.1	.3	5.8	44.7	49.4
15- 9	7.8	8.3	3.4	.1	.2	.3	3.3	48.1	48.6
16- 1	8.9	9.2	2.6	.1	-.2	.6	.8	38.5	60.7
16- 2	8.6	8.9	2.9	.1	-.1	.5	.9	41.7	57.4
16- 3	8.4	8.5	2.4	.0	-.1	.5	.6	43.5	55.9

APPENDIX 2. (Continued)

No.	Inman Statistics						Percents		
	Mdϕ	Mϕ	$\sigma\phi$	$\alpha\phi$	$\alpha_2\phi$	$\beta\phi$	Sand	Silt	Clay
16- 4	8.3	8.8	2.8	.2	.1	.5	1.9	44.9	53.2
16- 5	8.3	8.4	2.5	.1	-.1	.5	1.2	44.5	54.3
16- 6	8.3	9.1	3.1	.2	.1	.5	2.2	44.5	53.3
16- 7	8.3	8.6	2.9	.1	.0	.5	2.4	44.4	53.2
16- 8	8.3	8.9	2.9	.2	.1	.5	2.0	44.2	53.8
16- 9	8.2	8.5	2.9	.1	.1	.4	2.2	45.8	52.1
16-10	8.6	8.8	2.8	.1	-.1	.5	.9	41.5	57.6
16-11	8.5	9.0	2.8	.2	.0	.5	1.2	42.7	56.1
17- 1	8.7	8.8	2.6	.0	-.1	.5	.7	40.8	58.6
17- 2	8.5	8.9	3.0	.1	.0	.5	1.0	43.8	55.3
17- 3	8.4	8.5	2.8	.0	-.1	.4	1.6	43.4	55.0
17- 4	8.3	8.5	3.0	.1	.0	.4	1.8	44.9	53.3
17- 5	7.9	8.1	3.0	.1	.1	.3	3.3	47.8	48.8
17- 6	7.9	8.1	3.2	.1	.1	.3	2.9	48.2	48.9
17- 7	8.4	8.5	2.6	.1	-.1	.5	1.2	43.8	55.1
17- 8	8.1	8.3	2.7	.1	.0	.4	2.4	45.9	51.7
17- 9	6.9	7.3	3.5	.1	.1	.3	17.3	41.6	41.2
17-10	8.4	8.8	2.9	.1	.0	.5	.9	44.3	54.9
17-11	8.3	9.0	3.1	.2	.2	.5	1.4	45.6	53.0
18- 0	9.0	9.0	2.0	.0	-.4	.7	.3	32.8	66.9
18- 2	9.2	9.2	2.4	.0	-.2	.6	.5	33.0	66.5
18- 4	9.1	9.1	2.6	.0	-.2	.5	.6	34.2	65.2
18- 6	9.5	9.8	3.1	.1	-.1	.5	.4	34.5	65.1
18- 7	8.8	9.0	2.8	.1	-.0	.4	.3	40.3	59.3
18- 8	9.5	9.6	2.6	.0	-.2	.6	.8	30.1	69.1
18-13	8.5	8.9	2.3	.2	.1	.5	.1	43.2	56.7
19- 1	9.0	9.0	2.1	.0	-.4	.8	1.3	31.8	66.9
19- 2	8.5	8.4	2.5	-.0	-.2	.5	2.3	40.2	57.5
19- 3	7.8	8.2	2.3	.2	.1	.5	.1	52.8	47.1
19- 4	7.3	7.9	2.3	.3	.3	.4	.1	59.3	40.6
19- 5	5.0	5.4	1.2	.3	1.9	2.0	9.5	79.3	11.3
19- 6	8.6	8.9	2.3	.1	.0	.4	.1	41.1	58.8
19- 7	5.3	6.0	1.7	.4	1.7	1.6	8.8	76.4	14.8
19- 8	7.7	8.3	2.5	.3	.3	.4	.1	54.8	45.1
19- 9	5.2	5.9	1.6	.4	1.4	1.3	8.2	77.8	14.1
19-10	8.3	8.6	2.4	.1	.1	.4	.0	45.2	54.7
19-11	5.1	5.9	1.6	.5	1.8	1.4	5.0	80.8	14.3
T1- 1	8.7	8.9	2.4	.0	-.2	.6	.8	38.4	60.8
T2- 1	8.9	9.1	2.4	.1	-.0	.4	.4	36.2	63.4
T3- 1	8.7	8.8	2.3	.1	-.2	.6	.3	40.1	59.5

APPENDIX 2. (Continued)

No.	Inman Statistics						Percents		
	Mdϕ	Mϕ	σϕ	$\alpha\phi$	$\alpha_2\phi$	βϕ	Sand	Silt	Clay
T 4- 1	8.4	8.6	2.6	.1	-.1	.5	1.7	42.9	55.4
T 5- 1	9.0	9.1	2.7	.1	-.1	.6	.8	37.6	61.6
T 6- 1	8.2	8.4	2.8	.1	.0	.4	3.6	44.2	52.3
T 7- 1	7.3	7.9	3.4	.2	.2	.4	9.3	49.8	40.9
T 8- 1	8.5	8.8	2.7	.1	-.0	.5	1.7	42.2	56.1
T 9- 1	8.7	9.2	2.8	.2	-.0	.6	.7	41.5	57.9
T11- 1	8.6	8.6	2.7	.0	-.1	.5	3.2	39.6	57.1
T11- 2	9.6	9.9	3.6	.1	.1	.4	.4	36.0	63.6
T12- 1	8.4	8.8	3.0	.1	.0	.4	1.5	43.6	54.9
T13- 1	7.6	6.9	3.7	-.2	-.3	.4	17.6	36.3	45.3
T14- 1	3.6	5.5	2.5	.8	1.4	.8	62.6	21.4	16.1
T15- 1	8.5	8.6	2.8	.0	-.1	.4	1.8	42.2	56.1
T16- 1	8.7	8.7	2.5	.0	-.2	.5	.7	39.7	59.6
T17- 1	8.7	8.9	2.7	.1	-.1	.5	.6	40.9	58.6
T18- 1	8.9	9.0	2.0	.0	-.4	.8	.6	33.2	66.2
T19- 1	9.1	9.1	2.4	.0	.3	.6	1.0	32.4	66.6
20- 1	7.9	8.5	2.2	.3	.3	.4	.6	49.9	49.6
20- 2	7.8	8.4	2.3	.2	.2	.5	1.4	50.5	48.1
20- 3	7.9	8.4	2.2	.2	.2	.4	.8	50.2	48.9
20- 4	7.7	8.3	2.2	.3	.2	.4	.5	53.4	46.1
20- 5	8.9	9.2	2.0	.2	-.1	.6	.4	35.4	64.1
20- 6	7.2	7.6	2.8	.1	.2	.4	7.9	53.6	38.5
20- 7	8.3	8.7	2.2	.2	-.6	1.1	7.0	38.1	55.0
21- 1	4.0	5.8	3.1	.1	1.1	.5	49.7	31.0	19.3
22- 1	5.5	6.1	3.2	.2	.5	.4	26.3	51.4	22.3
23- 1	4.0	5.7	3.0	.6	1.0	.5	49.3	31.8	18.8
24- 1	4.5	5.7	2.5	.5	1.2	.8	34.2	49.0	16.8
25- 1	3.7	5.7	3.0	.7	1.1	.5	53.1	28.1	18.8
26- 1	3.0	5.1	2.6	.8	1.6	.9	61.9	23.2	14.9
27- 1	5.2	6.0	2.4	.3	.8	.8	22.0	60.3	17.7
28- 1	3.2	5.3	2.6	.8	1.4	.8	60.8	23.3	15.9
29- 1	2.9	3.7	1.1	.7	3.0	2.5	76.9	12.9	10.2
30- 1	8.2	8.6	2.8	.1	.1	.4	1.6	46.0	52.4
31- 1	8.2	8.5	2.8	.1	.0	.4	1.6	46.1	52.3
32- 1	7.6	8.1	3.3	.1	.2	.3	6.1	47.6	46.3
33- 1	2.0	3.1	1.6	.7	2.1	1.7	80.1	11.1	8.7
34- 1	7.6	7.8	3.4	.1	.1	.3	9.8	45.0	45.2
35- 1	8.3	8.7	2.5	.2	.0	.5	.9	45.0	54.1
37- 1	3.1	3.5	.8	.6	3.9	3.7	77.5	13.6	8.9
38- 1	3.4	6.1	3.3	.8	1.1	.4	58.4	19.1	22.5

APPENDIX 2. (Continued)

No.	Inman Statistics						Percents		
	Mdϕ	Mϕ	$\sigma\phi$	$\alpha\phi$	$\alpha_2\phi$	$\beta\phi$	Sand	Silt	Clay
38- 2	8.7	8.9	2.4	.1	.0	.4	.2	39.8	59.9
38- 3	7.6	8.2	2.8	.2	.3	.4	.3	54.9	44.9
39- 1	6.5	7.0	3.6	.1	.3	.3	22.5	43.1	34.4
40- 2	7.6	7.6	3.1	.1	.1	.1	8.0	48.1	43.8
41- 1	8.9	9.1	2.6	.1	-.1	.5	.9	38.1	61.0
42- 1	7.8	8.3	2.6	.2	.2	.5	2.0	51.0	47.0
43- 1	7.6	8.0	2.6	.2	.1	.5	4.4	52.0	43.5
44- 1	2.8	5.2	3.4	.7	1.0	.4	64.3	16.9	18.9
45- 1	8.6	8.6	2.7	.0	-.1	.5	.9	41.7	57.4
46- 1	8.7	8.9	2.7	.0	-.1	.5	.7	40.0	59.3
47- 1	3.9	5.8	2.9	.7	2.3	1.8	53.8	29.4	16.8
48- 1	4.2	6.5	3.4	.7	1.0	.5	41.5	35.2	23.3
48- 2	8.0	8.5	3.4	.1	.2	.3	4.2	45.2	50.7
50- 2	8.6	8.9	2.8	.1	-.0	.5	1.6	41.2	57.3
51- 1	8.3	8.5	2.6	.1	-.1	.5	1.8	43.9	54.2
52- 1	8.4	8.2	2.9	-.1	-.1	.4	3.7	40.8	55.4
53- 1	4.3	6.7	4.0	.6	.8	.4	42.9	27.8	29.3
53- 2	9.0	9.3	2.6	.1	.0	.4	.5	37.6	61.9
55- 1	8.7	8.9	2.9	.1	-.1	.5	2.9	39.2	57.9
56- 1	8.6	8.7	2.9	.1	-.1	.5	1.8	41.3	56.9
57- 1	8.7	9.0	2.6	.1	.0	.4	.3	40.3	59.4
58- 1	6.5	5.1	4.7	-.3	-.3	.3	29.8	34.3	31.9
59- 1	8.1	8.0	3.5	-.0	-.0	.3	7.5	40.7	51.8
60- 1	8.8	8.8	2.7	.0	-.2	.5	1.7	38.3	60.1
60- 2	7.6	8.0	3.2	.1	.2	.3	4.0	49.9	46.1
61- 1	9.3	9.6	3.3	.1	-.0	.4	2.6	34.7	62.7
61- 2	9.4	9.5	2.9	.0	-.0	.4	.3	33.5	66.2
61- 3	6.9	7.9	2.8	.4	.5	.4	1.5	61.3	37.2
62- 1	4.6	5.9	3.1	.4	.7	.6	34.1	45.8	20.1
63- 1	9.1	9.6	3.7	.2	.1	.4	2.6	38.7	58.7
63- 2	8.7	9.1	3.0	.1	.0	.4	1.4	40.7	57.9
64- 1	8.5	8.9	2.4	.2	-.0	.6	.2	43.9	55.9
64- 5	8.6	8.8	2.5	.1	-.1	.6	.8	41.6	57.6
67- 1	9.0	9.1	2.5	.0	-.2	.6	.7	36.1	63.2
67- 2	8.6	8.8	2.5	.1	-.1	.6	.7	41.9	57.4
69- 1	7.8	8.4	2.2	.2	.3	.4	.3	52.6	47.0
70- 1	8.8	8.9	2.4	.0	-.2	.6	.6	37.8	61.5
70- 2	8.4	8.8	2.6	.1	-.1	.6	1.0	43.6	55.4
71- 2	9.4	9.6	2.5	.0	-.1	.5	.2	30.5	69.3
71- 3	9.2	9.3	2.6	.0	-.1	.5	.3	33.8	65.9

APPENDIX 2. (Continued)

No.	Inman Statistics						Percents		
	Mdϕ	Mϕ	σϕ	$\alpha_1\phi$	$\alpha_2\phi$	βϕ	Sand	Silt	Clay
72- 1	8.3	8.2	2.7	-.0	-.1	.4	4.3	41.5	54.2
72- 2	8.4	8.5	2.7	.1	-.1	.5	2.6	42.6	54.8
73- 1	8.2	8.3	2.5	.1	-.1	.5	2.5	44.7	52.8
73- 2	8.4	8.8	3.1	.1	.1	.4	3.1	43.2	53.7
74- 1	7.6	8.3	2.5	.2	.2	.5	3.7	50.8	45.5
75- 1	7.3	7.6	3.5	.1	.2	.3	11.9	46.4	41.7
75- 2	6.5	7.3	3.2	.2	.3	.4	15.5	48.8	35.7
76- 1	8.6	8.6	2.5	.0	-.2	.5	1.0	40.4	58.7
76- 2	8.3	8.5	2.6	.1	-.1	.5	3.3	42.0	54.7
76- 3	8.4	8.5	2.6	.0	-.1	.5	2.4	41.7	55.9
77- 1	7.6	8.1	2.4	.2	.1	.5	4.6	52.3	43.0
77- 2	8.2	8.6	2.0	.2	.1	.4	.0	45.7	54.2
78- 1	6.9	7.5	3.3	.2	.3	.2	6.8	53.7	39.5
78- 2	7.1	7.9	3.6	.2	.4	.3	6.4	51.9	41.7
80- 1	7.7	7.6	3.2	-.0	.0	.2	7.1	45.4	47.5
80- 2	6.2	6.8	3.7	.2	.2	.4	25.5	41.5	33.0
80- 3	6.8	7.6	2.8	.3	.4	.4	4.4	60.7	34.9
81- 1	7.5	8.1	2.4	.3	.3	.4	.8	56.9	42.3
81- 2	5.6	6.8	2.4	.5	.8	.6	6.8	70.5	22.7
81- 3	6.8	7.6	2.3	.4	.5	.4	1.0	65.5	33.6
82- 1	8.3	8.6	2.4	.1	-.1	.5	1.3	43.8	54.9
82- 2	8.2	8.7	2.8	.2	.1	.4	1.9	45.3	52.8
83- 1	6.1	5.0	4.4	-.3	-.4	.5	11.9	49.5	25.4
83- 3	4.7	3.1	5.3	-.1	-.4	.5	14.7	47.3	17.8
83- 4	8.0	8.5	1.9	.3	.3	.4	.3	49.4	50.3
84- 1	4.3	6.3	3.5	.6	.8	.3	43.4	31.1	25.5
84- 3	4.7	6.2	3.3	.5	.8	.4	37.7	38.7	23.6
84- 4	7.2	7.4	3.5	.1	.1	.3	16.7	42.9	40.3
84- 5	5.8	6.8	3.6	.3	.5	.3	29.5	40.4	30.0
85- 1	8.1	8.5	2.6	.2	.1	.5	1.8	47.2	51.1
85- 2	8.2	8.7	2.8	.2	.1	.5	1.5	46.3	52.2
86- 1	7.0	7.3	3.3	.1	.1	.4	16.0	45.7	38.3
86- 2	3.9	6.0	3.2	.7	1.0	.5	51.2	27.7	21.1
86- 3	3.4	5.2	2.5	.7	1.3	.8	60.3	24.5	15.3
86- 4	3.0	4.4	2.3	.6	1.3	1.3	70.8	17.2	12.0
87- 1	2.6	3.5	3.7	.2	.5	.7	59.4	16.7	13.2
87- 2	4.0	4.6	3.7	.2	.2	.7	41.1	32.6	17.7
87- 3	4.5	6.3	3.0	.6	.9	.5	36.5	40.9	22.6
88- 1	7.5	7.8	3.3	.1	.2	.3	8.1	47.7	44.2
88- 2	3.6	5.4	2.5	.7	1.4	.8	58.2	25.9	15.9
88- 3	4.8	6.6	3.5	.5	.8	.4	34.1	40.0	25.9

APPENDIX 2. (Continued)

No.	Inman Statistics						Percents		
	Mdϕ	Mϕ	$\sigma\phi$	$\alpha\phi$	$\alpha_2\phi$	$\beta\phi$	Sand	Silt	Clay
89- 1	4.9	6.2	3.5	.4	.7	.4	37.0	38.7	24.3
89- 2	3.4	5.8	3.1	.8	1.2	.5	56.9	23.7	19.4
90- 1	6.8	7.5	3.2	.2	.3	.4	12.4	51.5	36.2
90- 2	3.6	5.2	2.3	.7	1.5	.9	56.5	29.4	14.1
90- 3	3.9	6.1	3.2	.7	1.1	.5	51.8	27.7	20.6
95- 1	4.4	6.6	3.6	.6	.7	.4	39.2	31.3	29.5
95- 2	9.5	9.5	2.8	-.0	-.2	.5	.5	30.8	68.7
97- 1	8.9	8.7	2.7	-.1	-.3	.5	2.7	34.6	62.7
97- 2	9.3	9.4	2.5	.1	-.2	.6	1.0	32.0	67.0
97- 3	9.8	9.8	3.0	.0	-.1	.5	.4	29.4	70.2
98- 2	6.3	7.2	2.9	.3	.5	.4	9.9	59.1	31.0
99- 1	8.2	8.5	2.3	.1	-.0	.6	3.6	43.4	53.0
100- 1	4.2	5.6	2.4	.6	1.2	.8	42.3	41.4	16.3
101- 1	7.4	6.9	3.7	-.1	-.2	.4	18.3	39.1	42.6
102- 1	8.3	8.3	2.6	-.0	-.2	.5	2.1	43.1	54.8
103- 1	7.7	7.9	3.5	.1	.1	.4	12.3	40.6	47.1
104- 1	8.8	8.9	2.5	.1	.3	.7	1.0	38.6	60.4
105- 1	8.9	8.9	2.6	.0	-.2	.5	1.1	36.9	62.0
107- 1	9.7	9.7	2.2	.0	-.5	.8	3.0	20.7	76.3
109- 1	7.5	8.3	2.4	.3	.3	.5	2.9	54.5	42.6
111- 1	8.8	8.8	2.8	.0	-.2	.5	2.9	37.5	59.7

APPENDIX 3. COMPOSITION OF SAND FRACTIONS (Values given as percent of sand fraction)

No.[a]	% Sand	Terrigenous[b]						Authogenous[c]			Biogenous[d]							Grains counted
		Q	H	M	RX	V	Total	G	Py	Total	P	B	D	R	F	O	Total	
1- 1	1.2	15	1	9	17	7	49	2		2	Tr	1	11	22	8	7	50	359
1- 2	6.1	17	2	11	32	3	65	4		4	Tr	3	4	9	11	5	31	394
1- 3	1.8	28	3	9	25	1	67	2		2		1	8	15	6	2	31	376
1- 4	2.4	16	1	8	24	5	54	2		2	Tr	2	13	8	11	8	43	374
1- 7	2.0	9	1	10	14	3	37	1		1		1	27	17	18	10	62	433
1- 8	8.3	29	2	11	25	5	72	7		7		1	7	2	8	3	21	394
1- 9	27.0	44	4	6	24	5	82	5		5		4	2	4	3	2	14	347
1-11	11.4	38	4	8	22	7	79	5		5		2	2	5	6	1	16	371
1-12	1.3	27	3	12	14	5	61	2	Tr	2		5	8	19	4	2	37	342
1-14	1.8	43	5	10	18	4	81	2	Tr	2	Tr	2	4	8	3	2	18	338
1-15	1.7	41	4	10	18	7	81	1	1	2	1	2	3	5	4	2	17	389
1-17	.8	22	3	15	8	27	75	1	1	1	Tr	1	3	2	10	8	24	393
1-18	16.4	19	2	11	8	36	75	Tr		Tr		1	2	2	18	2	25	405
1-19	1.2	35	2	8	13	10	67	1	2	3	1	3	8	14	3	1	30	365
1-20	48.5	26	5	3	12	52	98	1		1		Tr		Tr	Tr	Tr	1	350

a The number consists of two parts; the first number is the station location number and the second is the sample number.

b Terrigenous: Q = Quartz and Feldspar, H = Ferromagnesians, M = Mica, RX = Rock fragments, V = Volcanic glass.

c Authogenous; G = Glauconite, Py = Pyrite.

d Biogenous: P = Planktonic foraminifers, B = Benthonic foraminifers, D = Diatoms, R = Radiolarians, F = Plant fragments, O = Other (includes Spicules, Shell fragments, Pollen and Statoliths).

APPENDIX 3. (Continued)

No.	% Sand	Terrigenous						Authogenous			Biogenous							Grains counted
		Q	H	M	RX	V	Total	G	Py	Total	P	B	D	R	F	O	Total	
1-22	30.7	16	3	3	5	72	98	1	Tr	1					2		2	312
1-23	2.9	21	5	13	17	35	91	1		1	1	2	1	1	3	1	8	331
1-24	.2	34	3	36	9	7	89	2	Tr	3	1	Tr		Tr	6	Tr	8	359
1-25	.2	13	1	45	12	10	80	1	2	3	1	1	Tr	1	13	1	17	375
1-26	1.4	39	3	30	11		82	1	1	3	3	2	3	2	5	1	16	377
1-27	56.0	65	7	5	17	Tr	94	4		4	Tr	1			2	Tr	3	338
1-28	24.4	58	7	10	16	Tr	91		Tr	Tr	1	2		1	6	Tr	9	335
1-29	41.0	55	4	12	14	1	86	1	Tr	1	Tr	2	1	Tr	7	2	13	358
1-30	64.4	62	8	5	20		94	2	1	3		1			2		3	322
1-31	3.0	63	5	13	12	Tr	92				Tr	1	Tr	Tr	5	1	8	327
2- 1	.6	12	1	11	11	3	37	Tr		Tr		1	23	12	10	17	63	332
2- 3	.7	9	Tr	8	6	3	27	1		1		3	33	18	9	10	72	361
2- 4	9.1	27	3	7	10	18	65	4		4		1	7	1	19	3	31	372
2- 5	5.1	30	2	6	11	18	66	3	Tr	4	Tr	2	11	3	12	2	30	327
2- 6	18.7	31	5	6	14	21	76	3		3		Tr	4	1	15	1	21	376
2- 7	6.0	23	5	3	12	46	88	1		1		1	1	Tr	6	3	11	319
2- 9	8.9	32	5	2	9	42	90	2		2		Tr	2		5	1	8	337
2-10	16.1	10		3	8	54	75	Tr		Tr			2		22	1	25	333
3- 1	1.4	15	1	6	5	4	31	1		1			24	6	32	6	68	377
3- 2	2.6	19	1	3	6	10	39	2		2		6	18	1	26	8	59	410
3- 3	.3	2		3	3	1	9				Tr	3	29	24	22	13	91	403
3- 4	3.4	38	4	10	14	13	79	1		1	Tr	1	7	1	8	2	20	295
3- 5	4.7	12	1	4	6	12	35	1		1		1	28	1	29	7	65	384
3- 6	20.7	34	2	4	16	26	83	2		2			2		13	1	15	328
3- 8	16.6	33	3	10	11	24	81	2		2		1	1	Tr	14	Tr	17	347

APPENDIX 3. (Continued)

No.	% Sand	Terrigenous						Authogenous			Biogenous							Grains counted
		Q	H	M	RX	V	Total	G	Py	Total	P	B	D	R	F	O	Total	
3- 9	9.1	16	3	4	8	56	86	1		1		Tr	1	1	11	Tr	13	400
4- 1	1.5	15	2	6	7	2	32	2		2		2	27	6	25	6	67	337
4- 2	1.3	36	2	9	12	1	59	9		9		2	6	4	13	7	32	322
4- 3	1.4	30	2	4	9	1	46	4		4		1	20	2	22	6	51	420
4- 5	2.0	49	2	14	20	5	90	10		10								170
4- 6	4.8	28	1	8	12	3	52	3	Tr	4			19	2	18	5	44	334
4- 7	1.6	14	2	5	17	2	39	3		3		5	25	2	20	6	58	393
4- 8	1.5	10	Tr	2	11	2	24	2	Tr	2		3	30	3	28	10	74	336
4- 9	2.1	11	1	6	7	3	27	2		2	Tr	5	38	3	20	5	70	380
4-10	3.0	6	1	7	2	2	18	1		1		1	24	2	53	2	82	417
4-11	1.4	15	2	9	14	3	43	3		3	Tr	3	17	5	18	11	54	392
5- 1	.5	14	1	12	15	1	44	4	Tr	4		2	21	3	16	11	53	399
5- 2	.7	5	Tr	10	4	2	21	4		4		1	21	3	38	13	75	364
5- 3	1.0	11	1	6	4	1	23	2		2	1	2	26	4	13	28	74	330
5- 4	1.0	32	2	3	13	Tr	51	4	Tr	5	Tr	1	19	2	12	10	45	384
5- 5	22.3	64	3	2	21	1	91	3		3		1	2	Tr	2	1	6	337
5- 6	1.5	23	1	9	24	1	58	4		4		7	11	1	16	4	39	382
5- 7	2.0	14	Tr	5	16	1	36	3		3		3	20	2	24	13	62	360
5- 8	4.0	30	3	4	16	1	54	9		9		3	15	Tr	14	4	37	276
5- 9	3.8	26	2	3	13	1	44	5		5		2	23	1	11	13	51	345
5-10	1.9	9	Tr	4	13	1	26	2		2		3	34	3	22	11	72	394
5-11	2.4	23	1	6	18	1	49	3		3		3	15	1	21	9	49	408
5-12	2.0	17	2	3	10	Tr	32	3		3	Tr	3	26	1	16	19	65	576
5-13	1.3	22	1	6	17	1	46	4		4		3	17	1	24	6	50	360
5-14	2.4	20	1	3	18		42	1		1		1	30		11	15	57	414

APPENDIX 3. (Continued)

No.	% Sand	Terrigenous						Authogenous			Biogenous							Grains counted
		Q	H	M	RX	V	Total	G	Py	Total	P	B	D	R	F	O	Total	
6- 1	3.8	39	3	6	23	9	80	4	Tr	4		Tr	3	1	10	1	16	385
6- 2	11.6	39	4	5	18	13	80	6	Tr	7		Tr	2		11	1	14	335
6- 3	11.9	49	8	8	21	Tr	86	4		4		Tr	4	Tr	6	2	11	348
6- 5	13.2	64	6	5	17		93	Tr	1	1	Tr	1	1	Tr	4	1	6	333
6- 6	30.0	69	5	6	20		99	Tr		Tr		Tr			1		1	331
6- 8	38.2	66	9	9	12	Tr	96	1		1		Tr			3		3	329
6- 9	18.4	51	5	14	17	Tr	88	Tr	Tr	1		Tr			11		11	340
6-10	6.5	54	5	12	16	1	88	Tr	1	1	Tr	Tr	Tr		10	Tr	11	346
6-11	24.0	67	5	9	15	1	97	Tr		Tr					3		3	313
6-12	21.3	66	4	11	13	1	95								6		6	382
6-13	.7	62	4	11	20	Tr	97		1	1		Tr			2		2	310
6-15	.8	55	5	15	16	1	92	1	1	2	Tr	2	Tr		3	Tr	6	320
6-16	10.8	56	5	4	22	2	88	4		4		Tr	1		6	1	8	342
6-17	8.2	52	3	5	17	2	79	3	Tr	4		1	1	1	15	Tr	17	351
7- 1	26.5	56	5	2	25	3	91	2		2	Tr		1	Tr	7		8	344
7- 2	10.1	55	3	2	27	3	89	3		3			2		6		8	326
7- 3	17.5	45	3	4	16	1	69	2		2			2		28		30	321
7- 4	18.3	53	4	5	25	3	89	1		1	Tr		2		7	1	10	374
7- 5	17.8	48	5	8	23	2	85	2		2			2		11	Tr	13	326
7- 6	16.9	42	3	6	27	3	80	3		3			4	1	12	2	18	392
7- 8	19.8	48	4	10	20	4	86	3		3			5		5	2	12	319
8- 1	1.7	31	4	6	24	1	65				Tr	4	8	2	19	3	35	471
9- 2	1.4	5		13	6	4	28	1		1		3	14	1	49	5	72	431
9- 3	2.0	28	2	6	23	2	62	2		2		6	16	1	11	4	37	476
9- 7	10.0	48	4	5	20	1	78	1		1		Tr	13	Tr	7	1	21	507

APPENDIX 3. (Continued)

No.	% Sand	Terrigenous						Authogenous			Biogenous							Grains counted
		Q	H	M	RX	V	Total	G	Py	Total	P	B	D	R	F	O	Total	
9- 8	10.8	44	5	6	23	1	79					1	5	1	13	1	21	377
9- 9	4.9	31	3	14	17	1	65	1		1			6	Tr	26	2	34	361
9-10	6.7	25	3	5	18		51	Tr		Tr	Tr	Tr	15		31	2	49	439
10- 1	.7	39	2	10	14	1	57	6		6		4	12	5	10	7	38	435
10- 2	1.3	21	2	8	13	1	45	9		9		6	17	2	15	8	46	388
10- 3	1.3	36	2	7	14	2	61	9		9		4	9	2	12	4	31	343
10- 4	1.6	5	1	5	9	1	21	6		6	1	7	32	4	25	5	74	376
10-15	1.3	12	1	8	4	Tr	26	3		3		3	28	4	22	15	72	379
10- 5	1.4	27	2	12	16	3	59	10		10		3	4	3	17	3	30	479
10- 6	1.5	31	4	8	9	6	57	8		8		5	9	5	13	4	35	330
10- 7	3.0	32	2	7	14	7	62	9		9		1	4	3	12	9	28	355
10- 8	1.2	31	3	6	8	4	52	11	Tr	11		7	7	6	12	7	37	509
10- 9	.9	53	3	16	12		89		5	5		2	1		4	Tr	7	336
10-10	.8	36	5	20	28		89	1	Tr	2	1	1	1	Tr	6		9	337
10-11	.1	12	1	37	6		56	1	5	6	4	6	2	1	24	3	39	427
10-12	.3	14	3	20	50		87	1		1	1	1	1	1	6	2	12	350
10-13	.6	21	2	21	36		80	4	Tr	5	1	3	1	1	8	1	15	362
10-14	1.4	27	4	11	48		90	2		2	1	1	1	1	3	2	8	335
11- 1	1.1	44	4	8	20	1	76	9	6	15	Tr	5	Tr	1	3	Tr	9	365
11- 2	1.5	47	3	21	16	2	89	Tr	5	5	Tr	Tr	3	Tr	3	Tr	5	430
11- 3	1.1	37	1	42	5	2	87					1			12	1	13	356
11- 5	.3	39	4	25	12	2	82	1	2	3	1	2	1	Tr	11	1	16	374
11- 7	.1	16	1	28	15	3	62	3	5	8	5	13	1	1	8	1	29	388
12- 1	1.3	41	2	7	12	1	64	16		16	Tr	2	3	3	8	5	21	347
12- 2	2.3	43	5	7	13	2	69	10		10		5	3	4	7	2	21	386

APPENDIX 3. (Continued)

No.	% Sand	Terrigenous						Authogenous			Biogenous							counted
		Q	H	M	RX	V	Total	G	Py	Total	P	B	D	R	F	O	Total	
12- 3	3.3	39	2	5	16	2	64	10		10		1	7	2	12	4	26	349
12- 4	1.6	25	6	14	14	4	61	7		7	Tr	3	4	8	9	7	32	346
12- 6	1.0	31	1	7	11	3	53	8		8	Tr	2	7	3	22	5	39	496
12- 7	1.4	29	2	8	14	3	55	5		5		4	12	3	16	6	40	392
12- 8	1.3	34	3	9	19	3	66	11		11		1	10	1	6	5	23	378
12- 9	3.0	30	1	4	11	1	47	8	Tr	8		4	23	3	10	5	45	449
12-10	.6	4		3	1		7	Tr	Tr	1		Tr	45	1	33	12	92	446
12-11	21.7	56	5	5	21	2	88	8		8		2			1	1	4	324
12-13	11.9	46	3	4	14	3	69	8		8	Tr	9	2	Tr	7	4	23	374
12-14	1.9	33	1	7	18	5	66	9	Tr	10		1	12	Tr	8	4	24	373
12-15	1.2	30	2	10	10	3	54	9	Tr	9		1	10	3	16	8	38	379
13- 1	8.9	23	2	2	62	Tr	90	5		5			2	1	2	1	5	364
13- 3	1.0	17	5	5	22	6	55	5	36	41	Tr	1		Tr	1	Tr	3	331
13- 4	.1	26	3	49	10	1	90		2	2	1	2			5	Tr	8	352
13- 5	1.0	52	3	33	8	1	97		1	1		1			1		2	363
13- 6	.9	39	5	33	12	1	91		2	2	Tr	1		Tr	4	2	7	327
13- 7	.4	28	4	13	5	1	52		42	42	3	2			2		6	330
13- 8	.3	19	2	5	4	Tr	30		63	63	2	2			3	1	7	405
13- 9	10.5	61	7	7	21	Tr	96		1	1	1	1	Tr		1		3	409
13-11	.5	26	1	63	3	1	93		Tr	Tr	2	2			2	1	7	329
14- 1	76.3	51	6	2	19	1	79	21		21					Tr	1	1	344
14- 4	2.6	13	1	22	7	1	44	7	4	12	14	20	1	1	7	2	44	364
14- 5	12.1	20	2	5	9	1	41	27	4	31	16	11		Tr	2	4	29	491
14- 6	47.1	7	1	1	3		12	62	6	68	9	8			1	3	20	358
14- 8	49.7	5	Tr	1	4		11	84	2	86	Tr	1			Tr	2	3	316

APPENDIX 3. (Continued)

No.	% Sand	Terrigenous						Authogenous			Biogenous							Grains counted
		Q	H	M	RX	V	Total	G	Py	Total	P	B	D	R	F	O	Total	
14- 9	1.9	18	1	23	15		57	36	2	38	Tr	1			5	Tr	6	333
14-10	19.2	66	9	10	12	2	98		1	1					1		1	320
14-11	12.2	28	3	7	59		96		3	3	Tr	Tr			1		1	324
14-13	5.0	56	3	12	17	1	89		1	1	1	2		Tr	7	Tr	10	329
14-15	.2	25	3	23	16	3	69	Tr	8	9					22		22	433
14-18	3.1	28	2	7	9	2	48	42	5	47	1	1			3	Tr	5	321
15- 1	1.7	34	3	10	30	1	78	5		5	1	5	1	4	4	4	18	379
15- 2	1.7	29	4	4	20	1	58	3		3		5	5	12	13	6	40	478
15- 3	16.1	34	7	3	24	1	70	22		22	Tr	3	1	2	2		8	340
15- 4	3.6	36	1	7	26	1	70	8		8		6	5	4	1	5	22	445
15- 5	3.3	12	1	3	13	1	29	4		4		20	15	15	10	6	67	228
15- 6	7.0	31	4	9	26	2	72	9	Tr	9		3	1	6	5	5	19	346
15- 7	2.5	27	2	13	20	5	68	3	Tr	3		1	2	10	10	7	29	343
15- 8	5.8	50	2	7	17	3	79	8	1	9		3	1	3	2	5	13	325
15- 9	3.3	23	2	14	19	9	67	2	Tr	2		3	1	9	12	6	31	509
16- 1	.8	5	1	6	5	1	17	2		2		1	9	14	39	18	81	439
16- 2	.9	22	2	7	9	1	42	4		4		4	17	9	13	12	54	415
16- 3	.6	6	1	6	5	1	18	2		2		1	32	6	26	15	80	430
16- 4	1.9	8	1	4	8	1	21	1		1	Tr	12	34	4	24	4	78	398
16- 5	1.2	28	2	6	11		47	1		1		5	20	2	19	6	52	420
16- 6	2.2	20	1	16	8	7	51	3	1	3		3	8	1	25	8	46	434
16- 7	2.4	32	2	11	16	12	73	3	1	4		1	1	1	16	4	23	352
16- 8	2.0	41	4	11	16	3	74	3		3		4	5	1	12	2	23	354
16- 9	2.2	40	4	5	20	8	78	2	1	3	Tr	2	5	Tr	10	1	19	610
16-10	.9	17	1	11	12	3	43	2	2	4		5	10	13	13	12	53	416

APPENDIX 3. (Continued)

No.	% Sand	Terrigenous						Authogenous			Biogenous							Grains counted
		Q	H	M	RX	V	Total	G	Py	Total	P	B	D	R	F	O	Total	
16-11	1.2	23	3	10	17	6	59	3		3		4	10	4	11	10	38	338
17- 1	.7	4	1	6	5	1	18	1		1	Tr	1	27	15	27	12	82	416
17- 2	1.0	12	2	11	17	3	44	4		4		1	14	6	27	4	53	423
17- 3	1.6	23	2	12	30	3	70	3		3		1	6	5	12	4	27	399
17- 4	1.8	40	3	10	24	1	77	6		6		2	4	3	5	3	17	416
17- 5	3.4	37	6	6	21	2	71	3		3		1	4	3	17	3	27	403
17- 6	2.9	44	7	7	16	5	79	2		2		3	3	6	5	3	19	392
17- 7	1.2	27	2	15	22	8	74	4		4		Tr	3	3	12	5	23	372
17- 8	2.4	18	1	12	16	6	52	4		4		1	7	8	21	8	44	537
17- 9	17.3	46	5	7	26	4	87	3		3		1	1	2	4	3	10	454
17-10	.9	29	2	12	21	8	71	5		5	Tr	1	4	3	12	4	24	468
17-11	1.4	17	1	10	33	4	65	2		2		1	9	4	14	6	33	516
18- 0	.3	14	4	5	28	3	54	1		1	1	Tr	7	31	4	2	45	368
18- 2	.5	13	1	13	13	15	54		5	5	2	4	6	22	3	3	45	388
18- 4	.6	4	1	7	11	Tr	24		3	3	27	14	6	22	Tr	3	74	447
18- 6	.4	35	4	15	10	1	65		1	1	10	11	1	6	5	3	34	604
18- 7	.3	35	5	29	9	1	78		2	2	8	4	Tr	2	5		20	355
18- 8	.9	21	6	6	15	Tr	80		1	1	12	4		2	1	Tr	19	482
18-13	.1	4	1	9	2		16		20		20	32	2	8	1	2	65	516
19- 1	1.3	23	2	6	22	4	57	7		7	Tr	1	5	26	1	3	35	339
19- 2	2.3	27	2	4	43	15	90	1		1	Tr	2	2	5	1	Tr	9	342
19- 3	.1	13	2	55	17	Tr	86				6	2		1	5		14	344
19- 4	.1	2	1	86	2	Tr	92				Tr		1		8		9	329
19- 5	9.5	47	5	30	17		98					Tr			1		2	313
19- 6	.1	15	2	19	24	1	60				29	4	Tr	1	5	1	40	341

APPENDIX 3. (Continued)

No.	% Sand	Terrigenous						Authogenous			Biogenous							Grains counted
		Q	H	M	RX	V	Total	G	Py	Total	P	B	D	R	F	O	Total	
19- 7	8.8	52	2	33	12		99				Tr	Tr				Tr	1	338
19- 8	.1	4	1	77	6		87				5				9		13	340
19- 9	8.2	47	2	36	15		99								1		1	316
19-10	.1	6	1	29	28		63		Tr		33	1	Tr	1	2		37	325
19-11	5.0	48	3	36	13	1	100											318
T1- 1	.8	25	3	15	16	3	63	1		1		Tr	5	15	11	5	37	408
T2- 1	.4	20	5	8	16	4	52	3	Tr	3	1	7	7	18	6	5	45	470
T3- 1	.3	21	3	11	14	2	51	4		4		1	11	14	7	12	45	397
T4- 1	1.7	24	4	8	20	1	58					Tr	18	5	13	6	42	374
T5- 1	.8	42	2	4	10	1	30	3		3			18	3	19	28	67	347
T6- 1	3.6	23	4	10	21	12	70	2		2			9		17	2	27	399
T7- 1	9.3	30	5	11	14	3	62	1		1		1	4	1	29	2	37	322
T8- 1	1.7	16	2	8	15	2	42	4		4		6	10	1	29	7	53	307
T9- 1	.7	14	2	6	8	2	33	4		4		2	20	2	30	7	62	360
T11-1	3.2	14	3	9	17	2	44	4		4		5	10	5	21	11	52	372
T11-2	.4	20	4	24	13	Tr	61	1	22	23	Tr	4	1		10	2	17	327
T12-1	1.5	43	6	8	20	1	78	10		10		2		1	5	4	13	315
T13-1	17.6	21	4	2	39	2	68	29	1	30		Tr	1	1	1		2	331
T14-1	62.6	50	9	2	14	1	75	24		24								342
T15-1	1.8	48	9	6	14	Tr	77	9	1	9		3	2	4	3	3	14	352
T16-1	.7	15	3	11	10	1	41			2	Tr	5	14	10	17	12	58	364
T17-1	.6	10	3	7	5	1	26	1		1		2	28	12	26	5	73	480
T18-1	.6	9	1	6	21	2	39	1		1		3	24	27	3	3	60	378
T19-1	1.0	22	2	7	8	4	44	4	Tr	5		1	12	33	3	3	51	370
20- 1	.6	30	13	38	12		92	Tr		Tr	1	2	1		4		8	344

APPENDIX 3. (Continued)

No.	% Sand	Terrigenous						Authogenous			Biogenous							Grains counted
		Q	H	M	RX	V	Total	G	Py	Total	P	B	D	R	F	O	Total	
20- 2	1.4	34	17	18	21		89	1	Tr	1	2	3	Tr		5	Tr	10	340
20- 3	.8	35	12	21	25		93	1		1	1	1	2		2	1	6	348
20- 4	.5	35	9	42	9		91	1			Tr	1	1		8		9	316
20- 5	.5	29	15	39	10		94	Tr		Tr	Tr	2			4	Tr	6	337
20- 6	7.9	53	12	26	9		100								Tr		Tr	310
20- 7	7.0	51	10	29	8		98	Tr		Tr		Tr			1	Tr	2	319
21- 1	49.7	51	11	3	29	1	96	3		3					1		1	364
22- 1	26.3	40	8	3	23	5	79	2	Tr	2					19	Tr	19	349
23- 1	49.3	37	5	9	22	5	78	1		1			1	Tr	19	1	20	338
24- 1	34.2	37	5	10	18	9	79	Tr		Tr					20	1	21	353
25- 1	53.1	45	12	4	29	3	93	5		5					2	1	3	326
26- 1	61.9	46	15	3	27	1	91	1		1					8		8	338
27- 1	22.0	51	6	15	3	3	89	1		1					11		11	375
28- 1	60.8	45	17	2	31		95	1		1					2	1	3	370
29- 1	76.9	54	8	1	30	1	94	5		5					1	1	1	403
30- 1	1.6	46	6	11	26	1	90	2		2		1	1		6		8	426
31- 1	1.6	17	2	8	16	1	43	1		1		3	12	1	37	3	56	407
32- 1	6.1	40	5	5	17	2	69	3		3		Tr	2	1	25	1	29	305
33- 1	80.1	41	7	4	42	Tr	94	5		5					1		1	319
34- 1	9.8	48	4	7	19	1	79	4	Tr	5			1	1	14	1	17	399
35- 1	.9	16	2	4	11	1	32	2		2	Tr	3	18	1	36	7	66	401
37- 1	77.5	51	8	2	24	Tr	86	14		14								347
38- 1	58.4	50	8	3	18	1	79	20		20					1		1	322
38- 2	.2	25	4	42	13	1	86	8		8		1			5		6	347
38- 3	.3	16	2	53	4	17	91				1	Tr			8	Tr	8	425

APPENDIX 3. (Continued)

No.	% Sand	Terrigenous						Authogenous			Biogenous							Grains counted
		Q	H	M	RX	V	Total	G	Py	Total	P	B	D	R	F	O	Total	
39- 1	22.5	44	5	7	10	1	68	30		30		1			1		2	354
40- 1	8.0	30	8	6	29	Tr	72	12	1	13	4	8	Tr	Tr	2	1	15	540
41- 1	.9	10	2	8	8	1	30	3		3		3	18	6	29	12	67	385
42- 1	2.0	31	6	13	25	1	75	3	4	7		Tr	Tr	1	15	2	18	424
43- 1	4.4	39	4	20	20		83	6		6	6	4			2	Tr	11	421
44- 1	64.3	51	11	3	27		90	9		9		Tr					Tr	321
45- 1	.9	26	4	11	14	1	55	4		4		4	8	8	15	8	42	512
46- 1	.7	15	4	8	8	Tr	35	3		3		2	13	9	26	11	62	393
47- 1	53.8	35	8	5	7	Tr	55	43		43						2	2	342
48- 1	41.5	41	4	1	7	Tr	54	44		44				Tr	1	1	2	293
48- 2	4.2	43	9	12	16	Tr	80	3	3	6		4	Tr	Tr	9	1	14	460
50- 2	1.6	43	8	5	21	1	77	5	8	13			1	4	4	2	12	353
51- 1	1.8	11	2	5	3		20	2		2			36	3	31	9	78	381
52- 1	3.7	46	7	5	18		77	7	Tr	7			2	5	7	2	16	380
53- 1	42.9	47	10	3	28		90	9		9			Tr				Tr	438
53- 2	.5	38	5	12	21	Tr	76	1		1	1	3	4	1	12	2	23	329
55- 1	2.9	31	4	9	17		62	2		2		1	6	12	12	6	36	374
56- 1	1.8	29	5	8	18		60	2		2	Tr	1	3	13	10	10	38	362
57- 1	.3	15	2	10	7	1	35	1		1	Tr	4	19	10	14	18	64	461
58- 1	29.8	24	7	5	51	1	88	2		2			1	4	3	1	10	393
59- 1	7.5	53	8	6	17	1	85	1		1	Tr	Tr	3	3	3	4	14	419
60- 1	1.7	24	4	10	8	1	47	4		4	Tr	1	23	16	2	7	49	501
60- 2	4.0	23	4	9	6	49	91	1		1	Tr	Tr	1	3	3	1	8	416
61- 1	2.6	61	11	5	11	1	90	Tr	7	7	1	2		Tr	Tr	1	4	333
61- 2	.3	55	6	12	7	1	82				5	9	1	Tr	3	1	18	375

APPENDIX 3. (Continued)

No.	% Sand	Terrigenous						Authogenous			Biogenous							Grains counted
		Q	H	M	RX	V	Total	G	Py	Total	P	B	D	R	F	O	Total	
61- 3	1.5	54	6	28	7		95				Tr	Tr			4	Tr	5	358
62- 1	34.1	63	11	11	11		97				Tr	Tr			3		3	314
63- 1	2.6	63	10	7	7	Tr	87	Tr	Tr	1	3	5		1	2	1	12	356
63- 2	1.4	52	11	14	8	1	86	Tr	1	2	2	2	1	3	4	Tr	11	373
64- 1	.2	28	6	11	33	1	79		4	4	3	4	1	2	6	2	17	722
64- 5	.8	42	7	10	12	1	72	2		2	1	2	7	10	4	2	26	462
67- 1	.7	27	6	7	15	3	59	3		3		3	8	19	5	3	38	514
67- 2	.7	27	4	5	15	3	54	3		3		4	9	17	8	5	43	362
69- 1	.3	26	4	35	33	1	98				Tr			Tr	1		2	390
70- 1	.6	22	3	10	16	2	52	2		2		2	6	18	14	8	47	475
70- 2	1.0	20	4	9	15	3	50	2		2		2	15	18	7	8	48	585
71- 2	.2	26	4	15	22	1	67	3		3	4	2	3	4	16	2	30	346
71- 3	.3	17	3	30	13		63	1		1	4	3	7	2	16	5	36	373
72- 1	4.3	19	5	5	40	1	70	5		5	1	5	10	6	3	2	26	379
72- 2	2.6	25	4	7	20	2	58	5		5	Tr	5	10	8	8	7	38	348
73- 1	2.5	21	4	8	13	1	48	8		8		2	15	10	10	7	44	455
74- 1	3.7	18	5	20	36	1	80	6	4	10	1	1	1	1	5	2	10	381
75- 1	11.9	43	8	4	27	Tr	83	15	Tr	15			1	1	Tr		2	321
75- 2	15.5	33	8	7	32	6	84	8		8		Tr		1	3	4	8	348
76- 1	1.0	7	2	6	9		23	1		1	Tr	4	23	9	12	23	76	433
76- 2	3.3	21	4	6	10	Tr	41	3	Tr	4	Tr	4	46	1	13	7	56	373
76- 3	2.4	14	2	3	6		25	2		2		1	48	2	6	18	74	509
77- 1	4.6	31	6	15	28		80	3		3	Tr	4	4	2	5	3	17	385
77- 2	.1	6	2	69	24		90				2		1	1	6	2	10	405
78- 1	6.8	39	8	11	18	1	76	8		8		1	5	3	4	4	16	366

APPENDIX 3. (Continued)

No.	% Sand	Terrigenous						Authogenous			Biogenous							Grains counted
		Q	H	M	RX	V	Total	G	Py	Total	P	B	D	R	F	O	Total	
78- 2	6.4	36	6	8	16	1	67	5	Tr	5		1	11	4	5	7	28	429
80- 1	7.1	44	8	7	18		76	2	Tr	3		2	9	2	3	5	22	494
80- 2	25.5	45	10	6	34		94	2	1	3		2	1	Tr		1	4	328
80- 3	4.4	55	7	25	9	Tr	96	1		1	Tr	1	Tr	Tr	1	Tr	3	318
81- 1	.8	34	3	46	7		90	1	6	8	1	1			1	Tr	3	603
81- 2	6.8	55	10	28	4	1	97	1	Tr	1	Tr	2			Tr		2	408
81- 3	1.0	28	6	53	5		92	Tr	1	1	Tr	1	Tr		3	2	7	366
82- 1	1.3	24	8	8	9		50	2		2		2	22	2	15	8	48	375
82- 2	1.9	25	2	7	7	Tr	42	2	Tr	2			38	Tr	15	6	56	352
83- 1	11.9	42	13	9	26	1	91	2		2	Tr		1		2	4	8	353
83- 3	14.7	60	16	6	17		98	1		1		Tr			1		1	311
83- 4	.3	22	3	48	18	Tr	91	1		1	3	1	Tr	Tr	3	1	7	904
84- 1	43.4	65	9	6	17		97	Tr		Tr		Tr	1		2		3	341
84- 3	37.7	66	13	5	14	1	99					Tr	Tr		1		2	336
84- 4	16.7	60	10	9	15		94				Tr	1	1		4	1	6	341
84- 5	29.5	60	12	8	17		97	Tr		Tr		1	Tr	Tr	2		3	324
85- 1	1.8	33	9	9	13		63	1		1	1	Tr	18	1	11	3	33	422
85- 2	1.5	25	4	8	9	Tr	47						27	1	16	9	53	417
86- 1	16.0	60	10	4	18	Tr	92	Tr		Tr			3		4	1	8	469
86- 2	51.2	60	10	6	21	1	97	1		1					2		2	321
86- 3	60.3	54	9	4	19	2	88	3		3	Tr		Tr		8	1	9	422
86- 4	70.8	64	13	2	17		95	2		2			Tr		2	Tr	3	395
87- 1	59.4	62	10	6	20	Tr	98	1		1		Tr		Tr	1		2	340
87- 2	41.1	64	10	6	17		97	1		1				Tr	2		2	343
87- 3	36.5	64	14	8	13		99								Tr	Tr	1	739

APPENDIX 3. (Continued)

No.	% Sand	Terrigenous						Authogenous			Biogenous							Grains counted
		Q	H	M	RX	V	Total	G	Py	Total	P	B	D	R	F	O	Total	
88- 1	8.1	49	8	8	16		82	Tr		Tr			8	Tr	8	2	18	369
88- 2	58.2	63	12	3	19	Tr	97	1		1			Tr		1	1	2	460
88- 3	34.1	59	10	6	17	1	94	1		1			1	Tr	4	Tr	6	369
89- 1	37.0	52	10	5	15	1	82	1		1			Tr		17		17	356
89- 2	56.9	37	10	8	7	Tr	63								37		37	317
90- 1	12.4	53	12	9	13	Tr	88	Tr		Tr			4		7	1	12	364
90- 2	56.5	59	16	4	16	Tr	95	Tr		Tr					5		5	403
90- 3	51.8	54	15	4	19	2	94	2		2					4	Tr	4	331
95- 1	39.2	41	10	4	36	2	92	7		7				1			1	328
95- 2	.5	20	4	12	23	2	60	5	2	7	5	8	2	4	13	Tr	33	424
97- 1	2.7	21	4	5	31	23	84	2		2	1	Tr	1	12	1	Tr	15	322
97- 2	1.0	12	2	6	20	11	51	1		1	18	19	1	8	3	1	48	407
97- 3	.4	3	2	6	5	2	18	1		1	10	50	Tr	14	5	3	82	371
98- 2	9.9	54	5	12	23	1	95	1		1	2	1		Tr	2		5	346
99- 1	3.6	37	4	3	20		64	26	7	33	2	1	Tr	Tr			3	364
100- 1	42.3	56	9	9	22	1	97	1		1	1	1		1		Tr	2	414

APPENDIX 4. PROCEDURES OF SEDIMENT ANALYSES

Some of the following procedures are modifications of techniques already described in the literature (Table 1).

Coarse Fraction Analysis

The sample was wet-sieved through a 62μ screen and the sand size material retained on the screen was washed into a small beaker. The coarse fraction was stirred vigorously and a very small aliquot of the sample was taken with a controlled-intake dropper. This split of the sample was then spread evenly over a gum tragacanth-coated micropaleontological slide. After the slide dried, a binocular dissecting microscope was used to obtain a 300 grain count.

Heavy Mineral Separations

Tetrabromethane (S. G. 2.96) was used to separate the sand size grains into light and heavy mineral fractions. The samples were stirred and centrifuged in pyrex test tubes for ten minutes at 1200 rpm. Then the bottom of the tube was placed in dry ice until that portion of the liquid covering the heavy fraction became frozen. The light mineral fraction was poured out and then the heavy fraction was thawed out and removed from the test tube.

Magnetic Separator

Glauconite is a common constituent of many of the sediments in the Astoria Canyon area. However, it occurs in such a wide variation of forms that its identification is sometimes difficult. The glauconitic nature of the sedimentary rock fragments was checked using a Frantz magnetic separator. The types of glauconite were all most effectively separated from the other sand grains using the following settings: forward slope 25°, side slope 10°, amperage .35 to .50.